



Best Available Copy

PATENT  
Attorney Docket No. 077/US/PCT2/US  
00537/187002

IN THE UNITED STATES PATENT AND TRADEMARK OFFICE

Applicant : Dong, Zheng Xin <i>et al.</i>	Examiner : BORIN, Michael L.
Serial No. : 09/856,676	Art Unit : 1631
Filed : July 16, 2001	
Title : GLP-1 ANALOGUES	

Commissioner for Patents  
P.O. Box 1450  
Alexandria, VA 22313-1450

**DECLARATION OF DR. ZHENG XIN DONG**  
**UNDER 37 C.F.R. §1.132**

I, Dr. Zheng Xin Dong, hereby declare and state that:

1. I am familiar with the subject matter claimed in the above-identified patent application, U.S. Serial No. 09/856,676.
2. I have a Ph.D. in Organic Chemistry and I serve as Senior Director of Chemistry at Biomeasure, Incorporated, 27 Maple Street, Milford, MA 01757-3650.
3. I understand that, with respect to the above-identified patent application, the Examiner issued the decision of rejection on May 26, 2006, rejecting the application as being obvious over certain prior art references cited by the Examiner. Specifically, the Examiner stated in the decision that:

Within the context of chemistry, unsubstituted compounds are similar to their homologue, lower alkyl (e.g., methyl) substituted compounds in the physical properties, and, because of their structural similarity, it is generally predictive that their chemical properties will be similar. Because the adjacent homologs, lower alkyl compounds -N(lower alkyl)-, would be expected to have similar physical and chemical properties as unsubstituted (-NH-) compounds, a high degree of predictability in producing a compound having the same physical and chemical properties would be expected when substituting H for lower alkyl group in a large compound. Therefore, it would have been obvious to one having

ordinary skill in the art at the time the invention was made to modify the preferred Ala<sup>8</sup> or Gly<sup>8</sup> GLP-1 analogs of Buckley or Galloway such that NH- group is replaced by N-Me group. Since one of ordinary skill in the art of pharmaceutical chemistry would have expected that such modification would not change the properties of a compound in a significant way, one of ordinary skill in the art would have been motivated to make such a modification so as to obtain another preferred compound with the activity disclosed in Buckley and Galloway.

4. I make this declaration to show that, with respect to the compounds of the formulae [N-Me-Ala<sup>8</sup>]hGLP-1(7-36)-NH<sub>2</sub>, [N-Me-D-Ala<sup>8</sup>]hGLP-1(7-36)-NH<sub>2</sub> and [N-Me-Gly<sup>8</sup>]hGLP-1(7-36)-NH<sub>2</sub>, as claimed in pending Claim 8, the fact that these compounds have been modified to include an N-methylated amino acid is significant in that, the N-methyl amino acids can (1) impose conformational constraint on peptide backbone, (2) block hydrogen bonding sites and (3) potentially protect the peptide bonds against enzymatic cleavage.
5. In addition, in conjunction with what is commonly known by those skilled in the art in the field of medicinal chemistry, to produce polypeptide and protein analogs and derivatives which have better biological properties, sometimes incorporation of unnatural amino acid residues into specific positions inside the polypeptides and proteins is required. Such analogs and derivatives could have improved stability, increased enzymatic stability, prolonged duration of action *in vivo*, and enhanced biological activities. One class of such unnatural amino acids is the N-methyl amino acids.
6. As such, although one can state *as a general matter* that structural similarity is *generally* predictive of similar physical and chemical properties, in the field of medicinal chemistry, the differences between N-Me derivatives of Ala<sup>8</sup>-hGLP-1(7-36)-NH<sub>2</sub>, D-Ala<sup>8</sup>-hGLP-1(7-36)-NH<sub>2</sub>, and Gly<sup>8</sup>-hGLP-1(7-36)-NH<sub>2</sub>, as instantly claimed, and their unsubstituted (-NH-) counterparts, in terms of their respective biological, enzymatic properties, are very significant. Due to such significant differences in their biological, enzymatic properties, it is my belief that their structural differences – *i.e.*, the fact that the claimed compounds are N-methylated at position 8 – are also very significant.

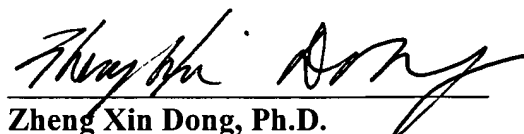
7. The following scientific papers, copies of which are attached hereto, render ample support to the above statements by the declarant:

- F. Haviv *et al.*, "Effect of N-Methyl Substitution of the Peptide Bonds in Luteinizing Hormone-Releasing Hormone Agonists," *J. Med. Chem.*, Vol. 36, 363-369 (1993);
- D. P. Failie *et al.*, "Macrocyclic Peptidomimetics – Forcing Peptides into Bioactive Conformations," *Curr. Med. Chem.*, Vol. 2, 654-686 (1995);
- R. Schmidt *et al.*, "Structure-activity relationships of dermorphin analogues containing N-substituted amino acids in the 2-position of the peptide sequence," *Int. J. Pept. Protein Res.*, Vol. 46, 47-55 (1995);
- W. L. Cody *et al.*, *J. Med. Chem.*, "Design of a Potent Combined Pseudopeptide Endothelin-A/Endothelin-B Receptor Antagonist, Ac-D<sup>16</sup>Bhg<sup>16</sup>-Leu-Ile-[NMe]Ile-Trp<sup>21</sup> (PD 156252): Examination of Its Pharmacokinetic and Spectral Properties," Vol. 40, 2228-2240 (1997). Copies of these references are attached herewith for the Examiner's convenience.
- J. M. Ostresh *et al.*, "Libraries from libraries: Chemical transformation of combinatorial libraries to extend the range and repertoire of chemical diversity," *Proc. Natl. Acad. Sci. USA*, Vol. 91, 11138-11142 (1994);
- S. M. Miller *et al.*, "Comparison of the Proteolytic Susceptibilities of Homologous L-Amino Acid, D-Amino Acid, and N-Substituted Glycine Peptide and Peptoid Oligomers," *Drug Dev. Res.*, Vol. 35, 20-32 (1995); and
- Y. Takeuchi *et al.*, "Conformational Analysis of Reverse-Turn Constraints by N-Methylation and N-Hydroxylation of Amide Bonds in Peptides and Non-Peptide Mimetics.

8. I further declare that all statements made herein of my own knowledge are true and that statements made upon information and belief are believed to be true and further that false statements and the like so made are punishable by fine or imprisonment or both under Section 1001 of Title 18 of the United States Code, and that such willful false statements may jeopardize the validity of the above-identified application or by any patent issuing thereon.

Oct. 26, 2006

Date

  
Zheng Xin Dong, Ph.D.

## Effect of *N*-Methyl Substitution of the Peptide Bonds in Luteinizing Hormone-Releasing Hormone Agonists<sup>1</sup>

Fortuna Haviv,\* Timothy D. Fitzpatrick, Rolf E. Swenson, Charles J. Nichols, Nicholas A. Mort, Eugene N. Bush, Gilbert Diaz, Gary Bammert, A. Nguyen, Neal S. Rhutasel, Hugh N. Nellans, Daniel J. Hoffman, Edwin S. Johnson, and Jonathan Greer

Pharmaceutical Products Division, Abbott Laboratories, Abbott Park, Illinois 60064

Received September 11, 1992

Each peptide bond in leuprolide (1), deslorelin (13), and nafarelin (24) was separately substituted with *N*-methyl. The synthesized compounds were tested for in vitro receptor binding, LH release, and stability against chymotrypsin and intestinal degradation. The NMe-Ser<sup>4</sup> (30), NMe-Leu<sup>7</sup> (33), and Sar<sup>10</sup> (35) analogues of nafarelin had *p*D<sub>2</sub> values 2-, 20-, 9-fold higher than their respective parent. All the other *N*-methyl agonists were less active. For the first time, conversion of LHRH agonists to antagonists was observed as a result of *N*-methyl substitution in the peptide backbone. [NMe-Phe<sup>3</sup>,DLeu<sup>6</sup>,Pro<sup>9</sup>NHET]*LHRH* (4), [NMe-1Nal<sup>3</sup>,DLeu<sup>6</sup>,Pro<sup>9</sup>NHET]*LHRH* (6), [NMe-His<sup>2</sup>,DTrp<sup>6</sup>,Pro<sup>9</sup>NHET]*LHRH* (14), [NMe-Phe<sup>3</sup>,DNaI<sup>7</sup>]*LHRH* (27), and [D2Nal<sup>3</sup>,NMe-Arg<sup>9</sup>]*LHRH* (34) exhibited antagonist responses. Substitutions of NMe-1Nal<sup>3</sup>, NMe-Ser<sup>4</sup>, or NMe-Tyr<sup>5</sup> in leuprolide rendered the 3-4 peptide bond in these compounds completely stable to chymotrypsin. Examination of the three-dimensional structure of leuprolide when bound to the active site of chymotrypsin, reveals the NH's of residues 3 and 5 are involved in hydrogen bond interactions with the enzyme. *N*-Methylation at these positions is not only disrupting the hydrogen bond interactions, but is also sterically preventing the substrate from fitting in the enzyme's active site. All the compounds in the leuprolide series were also tested against intestinal degradation using an in vitro rat jejunum sac assay. In this model the pattern of stabilization was similar, but not identical, to that against chymotrypsin. The pharmacokinetics of all the analogues in the leuprolide series and of several others in the deslorelin and nafarelin series were determined. The clearance values of all the three NMe-Tyr<sup>5</sup> analogues 8, 20, and 31 were lower than their respective parents. These slower clearances suggest lower rates of metabolism.

### Introduction

Several agonists of luteinizing hormone-releasing hormone (LHRH), pGlu-His-Trp-Ser-Tyr-Gly-Leu-Arg-Pro-GlyNH<sub>2</sub>, are currently used in the treatment of prostate cancer, endometriosis, precocious puberty, and other indications which are testosterone or estrogen dependent.<sup>1-4</sup> All of them are administered either subcutaneously, nasally, or as depot.<sup>5,6</sup> As an initial step toward the development of an orally active agonist, we tried to stabilize the leuprolide<sup>4</sup> (1) molecule against enzymatic degradation. We previously reported the stabilization of several LHRH agonists against chymotrypsin and intestinal degradation by structural modification of positions 1, 2, and 3.<sup>7,8</sup> We also demonstrated that substitution of NMe-Ser<sup>4</sup> in leuprolide (1) stabilized the peptide bond Trp<sup>3</sup>-Ser<sup>4</sup> against enzymatic digestion.<sup>7,8</sup> Stimulated by these findings we pursued the effect of *N*-methyl substitution at each position of three LHRH agonists: leuprolide (1), deslorelin<sup>9,10</sup> (13), and nafarelin<sup>11,12</sup> (24). The synthesized analogues were tested in vitro for LHRH receptor binding, LH release, and stability to chymotrypsin and intestinal

degradation. We also measured the in vivo pharmacokinetics of the peptides.

### Peptide Synthesis

All the peptides were synthesized using solid phase peptide synthesis (SPPS) techniques.<sup>13</sup> The appropriate Boc-protected amino acids, Boc-Pro-Merrifield resin for leuprolide and deslorelin analogues, and Boc-Gly-4-methylbenzhydrylamine resin for nafarelin analogues were used. The synthesis protocol, cleavage of the peptide from resin, removal of the protecting groups, workup, and HPLC purification were analogous to those extensively described in our recent publication.<sup>8,14</sup> No difficulties were encountered in coupling the Boc-*N*-methyl amino acids to the peptide resin.<sup>8</sup> The same activator and the same coupling time, which were applied for regular Boc-amino acids, were used for the Boc-*N*-methyl amino acids.<sup>8</sup> All the peptides were characterized by analytical HPLC, FAB mass spectrometry (FABMS), and amino acid analysis (AAA). Boc-NMe-Ser(OBzl) was synthesized according to D. H. Rich et al.<sup>15</sup> Boc-NMe-His(Tos) was synthesized by *N*-methylation of Boc-His(Tos).<sup>16</sup> Analogous syntheses were used for Boc-NMe-1-Nal and Boc-NMe-D-2Nal.

### Bioassays

Peptides were tested in vitro for rat pituitary LHRH receptor binding and for LH release from cultured rat pituitary cells.<sup>14</sup> The binding affinities are reported as *p*K<sub>1</sub>. The LH release potencies for agonists are reported as *p*D<sub>2</sub>, those for antagonist as *p*A<sub>2</sub> (for definitions of *p*K<sub>1</sub>, *p*D<sub>2</sub>, and *p*A<sub>2</sub> see footnotes of Table I). The stability of peptides against chymotrypsin degradation was deter-

<sup>1</sup> Part of this work was presented as a poster at the 74th Annual Meeting of the Endocrine Society, San Antonio, TX, June 24-27, 1992. Abstr. No. 178.

<sup>2</sup> Abbreviations: The abbreviations for the amino acids are in accordance with the recommendations of the IUPAC-IUB Joint Commission on Biochemical Nomenclature (*Eur. J. Biochem.* 1984, 138, 9-37). The symbols represent the *L*-isomer except when indicated otherwise. Additional abbreviations: D2Nal, D-3-(2-naphthyl)alanine; 1Nal, 3-(1-naphthyl)alanine; NMe-1Nal, *N*-α-methyl-3-(1-naphthyl)alanine; HPLC, high-pressure liquid chromatography; LH, luteinizing hormone; sc, subcutaneous; FABMS, fast atom bombardment mass spectrum; AAA, amino acid analysis.

mined using a reported assay.<sup>8</sup> To determine in vitro intestinal stability of peptides we used the rat jejunum sac model, which we previously described.<sup>8</sup> To measure pharmacokinetics, the compounds were administered to rats by iv bolus. The serum levels of the compounds, were determined by a RIA using an antibody to an LHRH analogue which recognizes the C-terminal residues Leu-Arg-Pro-NH<sub>2</sub> or Leu-Arg-Pro-GlyNH<sub>2</sub>.<sup>17</sup> The pharmacokinetics are reported as values of the whole body clearance, which is defined as the volume of plasma cleared of compound per unit time expressed in units of mL/min per kg, and calculated as the dose divided by the area under the curve of blood concentration of compound as a function of time.

## Results and Discussion

**Effect of *N*-Methyl Substitution on in Vitro Potency.** In our previous publication we reported<sup>8</sup> several LHRH agonists which derived from NAc-Sar<sup>1</sup>, NMe-Phe<sup>2</sup>, 1NaI<sup>3</sup>, and NMe-Ser<sup>4</sup> substitutions in leuprolide (1), deslorelin (13), and nafarelin (24). To complete the studies of positions 2 and 3 we substituted NMe-His<sup>2</sup> and NMe-1NaI<sup>3</sup> in the three parent agonists. For completeness and comparison purposes we have included in Table I some of the compounds from our previous studies.<sup>8</sup>

**Leuprolide Series (1–12).** *N*-Methylation of each residue separately in leuprolide caused significant losses in in vitro potency (Table I). Losses in binding affinity ranging from 10- to 295-fold were observed in this series with NMe-DLeu<sup>6</sup> (9) and NMe-His<sup>2</sup> (2) compounds at the extremes. Likewise, 10- to 1860-fold reductions in *pD*<sub>2</sub> values were obtained, with the NMe-DLeu<sup>6</sup> (9) and NMe-Arg<sup>8</sup> (11) analogues being most and least potent, respectively. In two cases, the NMe-Phe<sup>2</sup> (4) and NMe-1NaI<sup>3</sup> (6), the biological responses changed to antagonists, having very modest *pA*<sub>2</sub> values (7.53 and 6.59, respectively). This is the first time that an agonist was converted to an antagonist just by *N*-methylation of position 2 or 3. We previously reported<sup>14</sup> in the (4–9) reduced size LHRH analogues a similar switch of biological responses from agonist to antagonist effected by varying the size or the shape of the substituent at position 3 or 6.

**Deslorelin Series (13–23).** The analogous *N*-methyl substitutions, described above, were performed on deslorelin. In the receptor binding assay the affinities were again lower, ranging from 6-, for NMe-Leu<sup>7</sup> (21), to 140-fold for NMe-His<sup>2</sup> (14). The *pD*<sub>2</sub> values were decreased from 4-, for the NMe-Leu<sup>7</sup> (21), to 1000-fold for the NMe-1NaI<sup>3</sup> (18) compounds. In this series, unlike the previous leuprolide series, only the NMe-His<sup>2</sup> analogue (14) was an antagonist. These findings suggest that there is a feedback between position 6 and 2 which is capable of influencing the agonist to antagonist conversion as a result of *N*-methylation at position 2.

**Nafarelin Series (24–35).** This series, unlike the previous two, is a decapeptide rather than a nonapeptide. The analogous *N*-methyl backbone substituents reduced the receptor binding affinities ranging from 3- to 2884-fold, with the NMe-Tyr<sup>5</sup> (31) and the NMe-Arg<sup>8</sup> (34) analogues at the extremes. The *pD*<sub>2</sub> values for NMeSer<sup>4</sup> (30), NMe-Leu<sup>7</sup> (33), and Sar<sup>10</sup> (35) derivatives were, for the first time, higher by 2-, 20-, and 9-fold, respectively, than the parent. The *pD*<sub>2</sub> for the NMe-Tyr<sup>5</sup> analogue (31) was in the range of nafarelin. The NMe-Phe<sup>2</sup> (27)

and NMe-Arg<sup>8</sup> (34) peptides were antagonists. Again, this is the first time that agonist to antagonist conversion was observed by substitution of *N*-methyl at position 8 of a decapeptide LHRH agonist.

A number of groups, applying theoretical methods to both agonists<sup>18,19</sup> and antagonists,<sup>20</sup> have indicated the presence of a type II'  $\beta$ -turn extending from residues 5 to 8 in the bioactive conformation of LHRH analogues when bound to their receptor (Figure 1). Experimental NMR studies<sup>21,22</sup> have confirmed the presence of this  $\beta$ -turn in cyclic antagonists. The introduction of a *N*-methyl group in the peptide's backbone at position 5 would have the effect of interfering with the  $\beta$ -turn conformation and especially the hydrogen bond formed from the main chain NH of Tyr<sup>5</sup> to the C=O of residue Arg<sup>8</sup> (Figure 1). It is surprising therefore, that for the NMe-Tyr<sup>5</sup> agonists reported here (8, 20, and 31), the binding affinity and in vitro potency is quite close to that of the parent, losing only 10-fold or less in the three agonist series. Similar studies have been performed with antagonists where *N*-methylation of Tyr<sup>5</sup> resulted in retention or even increase in binding affinity and in vitro potency.<sup>23,24</sup> This suggests that in these agonists, as well as in the antagonists, the  $\beta$ -turn in the bioactive conformation does not have a classic type II' conformation.

In examining the conformation of the  $\beta$ -turn (Figure 1), *N*-methylation of the amide at position 8 should be even more disruptive. Position 8 is one of the central residues of the  $\beta$ -turn and *N*-methylation should greatly destabilize a  $\beta$ -turn and prevent hydrogen bond formation between the main chain NH of Arg<sup>8</sup> and the C=O of Tyr<sup>5</sup>. Indeed, the NMe-Arg<sup>8</sup> analogues (11 and 34) show greater losses, and are the worst compounds of the leuprolide and nafarelin series, with binding affinity reductions of 1800- and 2900-fold, respectively. However, the NMe-Arg<sup>8</sup> analogue in the deslorelin series (22) is surprisingly good, with reduction in binding affinity of only 30-fold relative to the parent, giving a compound that is better than LHRH (36). Thus, it is clear that the actual conformation of LHRH analogues in the receptor is not a simple type II'  $\beta$ -turn and appears to vary from series to series based on the detailed interactions of the various side chains with the receptor.

**Stability against Enzymatic Degradation.** All the *N*-methyl analogues in the leuprolide series and several from the deslorelin and nafarelin series were tested for enzymatic stability. Two model systems were used: purified chymotrypsin (*t*<sub>1/2</sub>) and the intestinal rat jejunum sac (*T*<sub>1/2</sub>).<sup>8</sup> Leuprolide is highly labile to chymotrypsin under the testing conditions, with a half-life of 1 min (Table I and Figure 2). *N*-Methylation at positions 3, 4, and 5 effectively blocked chymotrypsin cleavage giving half-lives of over 60 min (5 and 1 versus 6, 7, and 8). The same modification at position 2, whether the residue is His or Phe, increased the half-life by 7- and 6-fold, respectively (1 and 3 versus 2 and 4). *N*-Methylation at the remaining positions 6, 7, 8, or 10 had no influence whatsoever (1 versus 9, 10, 11, and 12). Chymotrypsin has been shown to cleave the Trp<sup>6</sup>-Ser<sup>4</sup> bond in leuprolide.<sup>8</sup> Therefore, *N*-methylation of Ser<sup>4</sup> (7) was clearly expected to stabilize this peptide bond to cleavage, since it blocks the mechanism of action of the enzyme as we already reported.<sup>7,8</sup> More unexpected, though, was that *N*-methylation of the peptide bond preceding or following the 3-4 bond also stabilized it against cleavage by chymotrypsin, as dem-

Table I. In Vitro Biological Activity, Enzymatic Stability, and Pharmacokinetics of LHRH Agonists  
pGlu-His-Trp-Ser-Tyr-DLeu-Leu-Arg-Pro-NHEt

compd	substitution	MH <sup>a</sup>	t <sub>R</sub> <sup>b</sup>	pK <sub>i</sub> <sup>c</sup>	pD <sub>2</sub> <sup>d</sup>	pA <sub>2</sub> <sup>e</sup>	t <sub>1/2</sub> <sup>f</sup>	T <sub>1/2</sub> <sup>g</sup>	clearance <sup>h</sup>
1 (leuprolide) <sup>i</sup>				9.73 (±0.04)	10.69 (±0.04)		1.0	4.0 (2.5-9.5)	9.0 (±0.8)
2	NMeHis <sup>1</sup>	1223	18.46	7.48 (±0.07)	8.22 (±0.06)		7.0	48.0 (34-78)	7.16 (±0.39)
3	Phe <sup>2</sup>			8.68 (±0.06)	9.81 (±0.05)			2.2 (1.1-4.9)	25.4 (±5.5)
4	NMePhe <sup>2</sup>	1233	26.65	7.92 (±0.01)		7.53 (±0.00)	6.0	18 (15-21)	30.96 (±7.42)
5	1Na1 <sup>3</sup>			10.03 (±0.18)	10.35 (±0.45)		>15.0	25.0 (15.5-65)	28.4 (±4.7)
6	NMe1Na1 <sup>3</sup>	1234	18.70	8.49 (±0.57)		6.59 (±0.00)	>80.0	44.0 (32-74)	14.45 (±2.9)
7	NMeSer <sup>4</sup>			8.85 (±0.09)	9.42 (±0.18)		>80.0	>90.0	18.9 (±0.8)
8	NMeTyr <sup>5</sup>	1223	13.20	8.80 (±0.07)	9.57 (±0.18)		>80.0	42 (24-147)	8.2 (±0.5)
9	NMeDLeu <sup>6</sup>	1223	35.18	8.42 (±0.08)	9.81 (±0.16)		1.0	54 (51-58)	21.0 (±1.3)
10	NMeLeu <sup>7</sup>	1223	32.90	9.80 (±0.00)	10.45 (±0.05)		1.0	4.1 (2.0-9.1)	8.3 (±0.68)
11	NMeArg <sup>8</sup>	1223	30.35	8.48 (±0.10)	7.00 (±0.10)		1.0	6.8 (6.2-6.9)	
12	Ser <sup>10</sup> NH <sub>2</sub>	1252	17.90	7.99 (±0.05)	8.73 (±0.15)		1.0	8.4 (7.1-10)	9.77 (±1.88)
13	DTrp <sup>6</sup> (deslorelin)			11.00 (±0.17)	11.33 (±0.14)				34.3 (±5.48)
14	NMeHis <sup>2</sup> DTrp <sup>6</sup>	1296	18.85	8.85 (±0.09)		8.26 (±0.26)			16.4 (±1.07)
15	Phe <sup>2</sup> DTrp <sup>6</sup>			10.61 (±0.05)	10.81 (±0.13)			10.8 (8.9-26)	28.8 (±2.4)
16	NMePhe <sup>2</sup> DTrp <sup>6</sup>			9.68 (±0.07)	8.40 (±0.15)		3.7	44.4 (29-133)	44.5 (±4.41)
17	1Na1 <sup>3</sup> DTrp <sup>6</sup>	1283	18.40	10.71 (±0.12)	11.49 (±0.00)				
18	NMe1Na1 <sup>3</sup> DTrp <sup>6</sup>	1307	33.40	9.00 (±0.19)	8.35 (±0.05)				15.14 (±1.08)
19	NMeSer <sup>4</sup> DTrp <sup>6</sup>			10.11 (±0.06)	10.10 (±0.40)			39.1 (25-91)	19.9 (±1.2)
20	NMeTyr <sup>5</sup> DTrp <sup>6</sup>	1296	25.15	10.07 (±0.15)	10.55 (±0.45)				11.1 (±0.43)
21	DTrp <sup>6</sup> NMeLeu <sup>7</sup>	1296	34.38	10.24 (±0.27)	10.70 (±0.10)				19.5 (±0.14)
22	DTrp <sup>6</sup> NMeArg <sup>8</sup>	1296	17.90	9.51 (±0.01)	9.35 (±0.53)				25.0 (±2.4)
23	DTrp <sup>6</sup> Ser <sup>10</sup> NH <sub>2</sub>	1325	20.15	9.50 (±0.02)	10.05 (±0.05)				4.32 (±0.16)
24	D2Na1 <sup>6</sup> Gly <sup>10</sup> NH <sub>2</sub> (nafarelin)			11.01 (±0.28)	11.05 (±0.45)		0.5	28 (18-63)	5.50 (±0.60)
25	NMeHis <sup>2</sup> D2Na1 <sup>6</sup> Gly <sup>10</sup> NH <sub>2</sub>	1336	26.13	8.85 (±0.12)	8.18 (±0.14)				4.13 (±0.19)
26	Phe <sup>2</sup> D2Na1 <sup>6</sup> Gly <sup>10</sup> NH <sub>2</sub>	1832	42.56	10.13 (±0.04)	10.23 (±0.22)				
27	NMePhe <sup>2</sup> D2Na1 <sup>6</sup> Gly <sup>10</sup> NH <sub>2</sub>	1346	30.93	9.53 (±0.09)		8.80 (±0.02)			
28	1Na1 <sup>3</sup> D2Na1 <sup>6</sup> Gly <sup>10</sup> NH <sub>2</sub>	1333	37.20	10.57 (±0.15)	11.55 (±0.18)				
29	NMe1Na1 <sup>3</sup> D2Na1 <sup>6</sup> Gly <sup>10</sup> NH <sub>2</sub>	1347	22.70	9.13 (±0.02)	8.70 (±0.30)				
30	NMeSer <sup>4</sup> D2Na1 <sup>6</sup> Gly <sup>10</sup> NH <sub>2</sub>			10.37 (±0.14)	11.30 (±0.20)		>60.0	47.0 (38-78)	27.55 (±2.25)
31	NMeTyr <sup>5</sup> D2Na1 <sup>6</sup> Gly <sup>10</sup> NH <sub>2</sub>	1336	23.88	10.51 (±0.00)	10.85 (±0.15)		>60.0	33 (25-45)	3.40 (±0.34)
32	NMeD2Na1 <sup>6</sup> Gly <sup>10</sup> NH <sub>2</sub>	1336	24.88	8.57 (±0.19)	8.30 (±0.20)				
33	D2Na1 <sup>6</sup> NMeLeu <sup>7</sup> Gly <sup>10</sup> NH <sub>2</sub>	1336	28.10	10.50 (±0.14)	12.35 (±0.05)				
34	D2Na1 <sup>6</sup> NMeArg <sup>8</sup> Gly <sup>10</sup> NH <sub>2</sub>	1336	35.60	7.55 (±0.13)		7.95 (±0.38)			3.87 (±0.22)
35	D2Na1 <sup>6</sup> Ser <sup>10</sup> NH <sub>2</sub>	1336	25.45	10.49 (±0.03)	11.87 (±1.02)				3.55 (±0.21)
36	LHRH			8.90 (±0.05)	9.27 (±0.18)				

<sup>a</sup> Values determined by FAB/MS. <sup>b</sup> t<sub>R</sub> = HPLC retention time in min. <sup>c</sup> pK<sub>i</sub> = the negative logarithm of the equilibrium dissociation constant in the rat pituitary receptor binding assay. <sup>d</sup> pD<sub>2</sub> = the negative logarithm of the concentration of agonist that produces 50% of the maximum release of LH from cultured rat pituitary cells in response to the test compound. <sup>e</sup> pA<sub>2</sub> = the negative logarithm of the concentration of antagonist that requires 2-fold higher concentration of agonist to release LH from cultured rat pituitary cells. <sup>f</sup> t<sub>1/2</sub> = chymotrypsin degradation half-life in min. <sup>g</sup> T<sub>1/2</sub> = the time, in min, required for the luminal concentration of compound in the rat sac jejunal to decrease by 50%. <sup>h</sup> Clearance of compound after iv administration in the rat, expressed as the dose divided by the area under the curve of the concentration of compound as a function of time, units are mL/min per kg. <sup>i</sup> Compound reported in ref 8.

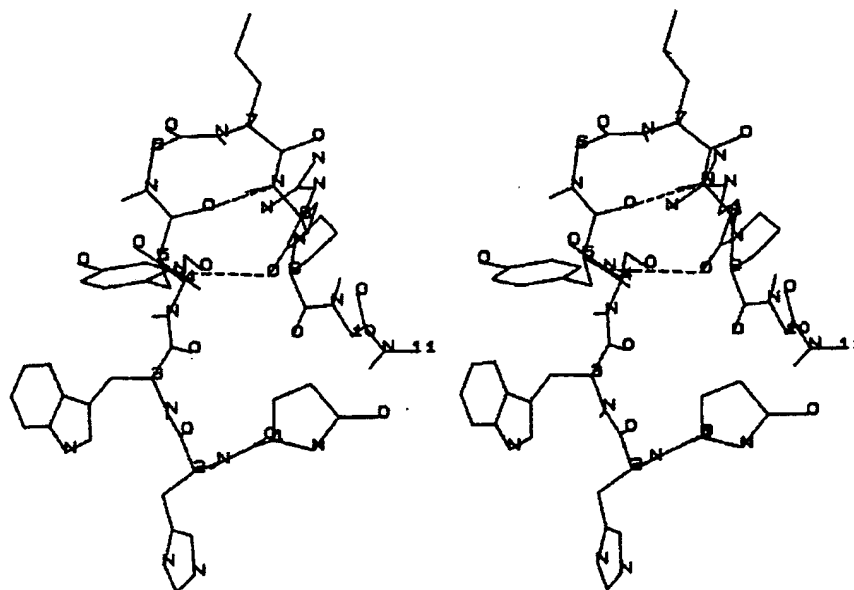


Figure 1. Stereo presentation of the three-dimensional structure of LHRH as calculated by Momany.<sup>18,19</sup> This structure depicts Momany's C conformation. The dotted lines show the possible hydrogen bonds that occur between the NH of Arg<sup>5</sup> and the C=O of Tyr<sup>3</sup> and between the NH of Tyr<sup>5</sup> and the C=O of Arg<sup>8</sup>. Both of these hydrogen bonds and the main chain conformation would be disrupted by N-methylation at the 5 and especially at the 8 positions.

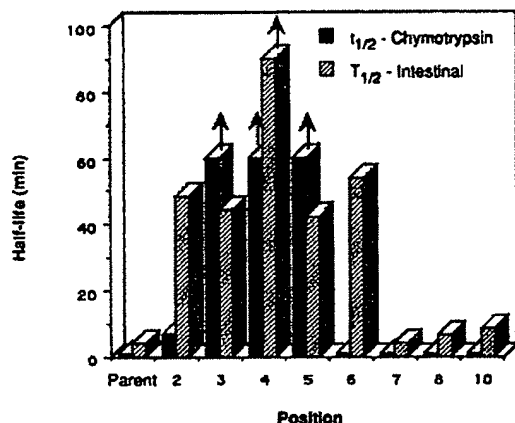


Figure 2. Bar graph of the digestion data for leuprolide (1) and its *N*-methyl analogues 2 and 6-12 in the chymotrypsin ( $t_{1/2}$ ) and the in vitro rat intestinal jejunum ( $T_{1/2}$ ) models. The arrows represent values greater than that shown. For the chymotrypsin digestion, *N*-methylation at positions 3, 4, and 5 stabilizes the molecule. For the intestinal model, *N*-methylation at positions 2 (with the His substitution), 3, 4, 5, and 6 stabilizes the peptide. Thus, the two patterns appear similar but are different in detail.

onstrated by the half-life values of compounds 6 and 8. To understand the molecular basis for this protection, we examined the three-dimensional structure of chymotrypsin<sup>25</sup> and a model structure for the conformation of a substrate peptide bound in the active site<sup>26</sup> to see how it was affected when the peptide bonds prior to and following the scissile bond, i.e. positions 3 and 5, are *N*-methylated. Figure 3 shows the active site of chymotrypsin with leuprolide bound in the substrate binding site in position to be cleaved between residues 3 and 4. The side chain of Trp<sup>3</sup> sits in the primary specificity pocket. There are a number of hydrogen bonds between the substrate, leuprolide, and the enzyme. Both main chain

NH's of residues 3 and 5 are involved in hydrogen bond interactions with the enzyme, with the main chain carbonyls of Ser 214 and Phe 41, respectively. Substitution of the amide hydrogen with *N*-methyl will disrupt the hydrogen bond, and steric hindrance of the larger methyl group forces a distortion in the conformation of the substrate on the enzyme. One would therefore expect that these compounds are significantly poorer substrates of chymotrypsin thereby stabilizing the molecules against cleavage between residues 3 and 4.

When the compounds were tested in the in vitro rat jejunum sac model, *N*-methylation at position 4 was the most stabilizing with a half-life of over 90 min relative to 4 min for the parent leuprolide (7 versus 1). *N*-Methyl substitutions at positions 2, 3, 5, and 6 gave intermediate increases in half-life ranging from 42 to 64 min (2, 6, 8, and 9). Interestingly, unlike with chymotrypsin, the degree of stabilization was different for the two different residues at position 2, with *N*Me-Phe<sup>2</sup> much less stable than *N*Me-His<sup>2</sup>, 18 versus 48 min, in the leuprolide series (4 versus 2). However, the *N*Me-Phe<sup>2</sup> substitution in the deslorelin (16) series had a half-life (44 min) longer than its parent, and similar to the *N*Me-His<sup>2</sup> in leuprolide (2). *N*-Methyl substitution at position 7, 8, or 10 had no significant influence on the half-life of the compounds. Overall, the pattern of stabilization in the intestinal model is rather similar to that found for chymotrypsin (Figure 2). However, an interesting difference is that the *N*Me-His<sup>2</sup> and *N*Me-DLeu<sup>6</sup> analogues (3 and 9) showed a large increase in stability in the intestinal model but were as labile as the parent leuprolide to chymotrypsin (Table I and Figure 2). This result suggests that chymotrypsin is not the major proteolytic enzyme in the rat intestinal model.

**Pharmacokinetics.** The clearance values for all the analogues in the leuprolide series, except compound 11 for which we do not have an antibody, were determined using our previous method.<sup>17</sup> The pharmacokinetics of several analogues in the deslorelin and nafarelin series

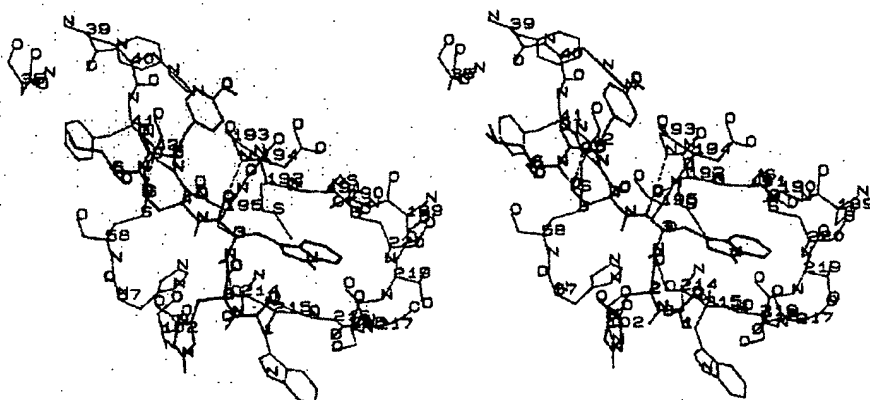


**Figure 3.** Three-dimensional structure of the active site region of chymotrypsin<sup>25</sup> (red) with leuprolide (blue) placed in the active site so that Trp<sup>5</sup> is in the primary specificity pocket and the 3-4 peptide bond is positioned for cleavage. It is clear that N-methylation of the Ser<sup>4</sup> of leuprolide would block cleavage of the Trp-Ser scissile bond. The main chain NHs of residues 3 and 5 of leuprolide form hydrogen bonds (green dashed lines) with the enzyme, to the main chain carbonyl oxygens of Ser 214 and Phe 41, respectively. Substitution of the amide hydrogens with methyls will block hydrogen bond formation and the increased bulk of the methyl groups sterically prevent the peptide from binding to the active site making these analogues poor substrates of chymotrypsin.

were also determined (Table I). The low value obtained for the clearance of nafarelin agrees with the previous report that this agonist extensively binds to plasma protein.<sup>27</sup> The pattern of clearance values in the three series does not reflect a clear correlation between in vitro enzymatic stabilization and in vivo clearance. This finding can be rationalized since clearance is constituted from three major components, distribution, metabolism, and elimination; the physicochemical properties of the compounds may have a significant effect on in vivo elimination.<sup>17</sup> In spite of this, the NMe-Tyr<sup>5</sup> substitution in the three series consistently gave lower clearance values, suggesting that metabolic stabilization of the 4-5 peptide bond, independently of the substituent at position 6 or 10, has a significant effect on the peptides' clearance rates. These findings agree with previous metabolism studies of leuprolide which indicated the presence of a (5-9) fragment as a metabolite.<sup>28</sup> Recently we have reported the effect on NMe-Tyr<sup>6</sup> substitution in LHRH antagonists on in vitro and in vivo potency.<sup>23,24</sup>

## Conclusions

The structure-activity relationships of the receptor binding affinities and the in vitro LH release activities of the N-methyl analogues in the leuprolide, deslorelin, and nafarelin series were quite subtle and varied with the substitutions at positions 6 and 10. With the exception of compounds 30, 33, and 35, which were more potent than nafarelin, all the N-methylated analogues were less active than the respective parents. In five cases (compounds 4, 6, 14, 27, and 34) for the first time the agonist response was converted to antagonist upon N-methylation of the peptide bond. The agonist/antagonist switch was influenced by a combination of the site of N-methylation and the substituents at positions 6 and 10. Cleavage of leuprolide by chymotrypsin was blocked not only by the N-methylation of the 3-4 scissile bond, but also by N-methylation of the adjacent 2-3 or 4-5 peptide bonds. These findings were rationalized by examining the three-dimensional structure of the substrate bound to the enzyme's active site. The lower clearance values for the NMe-Tyr<sup>5</sup> analogues 8, 20, and 31 suggest slower rates of metabolism.

## Experimental Section

All the peptides were synthesized using a Milligen-Bioscience Model 9500 automated peptide synthesizer (Milligen-Bioscience, Division of Millipore, Burlington, MA). The HF-reaction apparatus, Type 1B, was from Peninsula Laboratories, Inc., Belmont, CA. Peptide purification was performed with a Rainin/Gilson Ternary HPLC system. FAB/MS were run using a Finnigan MAT, MAT90 double focusing magnetic sector (BE) mass spectrometer, xenon FAB ionization, and (1:1) glycerol/thioglycerol matrix. Amino acid analyses were performed on a Beckman Model 6300 Amino Acid Analyzer, using ninhydrin derivatization. The peptides were hydrolyzed with 6 N HCl containing 0.5% phenol at 150 °C for 2 h. If the peptide contained Trp, 0.5% phenol was replaced with 5% thioglycolic acid. The data handling system was PE Nelson ACCESS CHROM. For calibration, Beckman standards were used. The values for the Ser, His and Trp were generally low because of partial decomposition. The values for Arg were high because of interference of the ethylamide residue and were corrected accordingly. The content of Glu, Phe, Tyr, Leu, Pro, Gly, and Ser were within  $\pm 10\%$ . We did not look for the presence of any unnatural amino acid (except NMe-Tyr, NMe-Phe, NMe-His). That was confirmed by FAB/MS.

All the Boc-protected amino acids, Boc-Pro, Boc-Sar, Boc-Arg(Tos), Boc-Leu, Boc-NMe-Leu, Boc-D-Leu, Boc-D-Trp, Boc-D2Nal, Boc-Tyr(O-2-Br-Cbz), Boc-NMe-Tyr(O-2,6-Cl-Bzl), Boc-Ser(O-Bzl), Boc-Trp(N-ind-formyl), Boc-His(N-im-Cbz), Boc-Phe, Boc-NMe-Phe, and Cbz-p-Glu were purchased from Bachem Inc. (Torrance, CA). Boc-Pro-Merrifield resin (with a substitution varying from 0.4 to 0.7 mmol/g) was obtained from the same company. Boc-Gly-4-methylbenzhydrylamine resin (with a substitution varying from 0.4 to 0.7 mmol/g) was obtained from Peninsula Laboratories, Inc., (Belmont, CA). Boc-NMe-Arg(Tos) was purchased from Bachem Bioscience Inc. (Philadelphia, PA). TFA was obtained from Kali-Chemie Co. Inc. (Greenwich, CT). All the solvents were purchased from Fisher Scientific Co. (Fairlawn, NJ). HF gas cylinders were purchased from AGA Gas Inc., (Cleveland, OH). All other chemicals were obtained from Aldrich Chemical Co., Inc. (Milwaukee, WI).

**General Procedure for the Synthesis of N-(tert-Butoxycarbonyl)-N-methyl-D-3-(2-naphthyl)alanine (37) and N-(tert-Butoxycarbonyl)-N-methyl-3-(1-naphthyl)alanine (38).** Sodium hydride (60% dispersion in oil, 2.5 g, 63 mmol) was washed with anhydrous pentane (3  $\times$  15 mL) to remove oil, and then suspended in dry THF (25 mL) and cooled, with stirring, to 0 °C in an ice-bath. A solution of the Boc-amino acid (5 g, 16 mmol) in THF (25 mL) was added via cannula, followed by the portionwise addition of methyl iodide (7.9 mL, 126 mmol) over 10 min. The reaction mixture was allowed to warm to room temperature and stirring was continued for 24 h. The reaction

was slowly added to a cold 1 N sodium hydrogen sulfate (80 mL) solution with rapid stirring. The resulting mixture was extracted with ethyl acetate (3 × 75 mL), washed with 1 N sodium thiosulfate (50 mL) and brine (50 mL), dried ( $\text{Na}_2\text{SO}_4$ ), and concentrated in vacuo. The sticky crystals obtained were triturated with anhydrous hexane overnight, filtered, and dried to yield a white powder.

Compound 37 was isolated in 93% yield (4.90 g): mp 136–137 °C;  $[\alpha]_D^{25}$ : +62.2° (EtOH,  $c = 1$ );  $^1\text{H}$  NMR ( $\text{CDCl}_3$ , 3:2 mixture of rotamers)  $\delta$  1.81, 1.38 (s, 9 H), 2.67, 2.78 (s, 3 H), 3.22, 3.35 (dd, 1 H,  $J = 14.35, 10.83$  Hz), 3.48 (dd, 1 H,  $J = 14.35, 5.14$  Hz), 4.75, 4.87 (dd,  $J = 10.83, 5.14$  Hz), 7.30 (m, 1 H), 7.45 (m, 2 H), 7.65 (s, 1 H), 7.79 (m, 3 H); IR ( $\text{CDCl}_3$ )  $\nu_{\text{max}}$  ( $\text{cm}^{-1}$ ) 2975 (m), 1715 (s), 1685 (s), 1390 (m), 1370 (m), 1170 (m), 1155 (s), 1145 (s); MS ( $M + \text{H}^+$ ) 330. Anal. ( $\text{C}_{19}\text{H}_{23}\text{NO}_4$ ) C, H, N.

Compound 38 was isolated in 92.6% yield (4.82 g): mp 42–46 °C;  $[\alpha]_D^{25}$ : -141.6° (EtOH,  $c = 1$ );  $^1\text{H}$  NMR ( $\text{CDCl}_3$ , 3:2 mixture of rotamers)  $\delta$  1.05, 1.44 (s, 9 H), 2.50, 2.78 (s, 3 H), 3.35, 3.69 (dd, 1 H,  $J = 14.16, 6.94$  Hz), 3.82, 3.93 (dd, 1 H,  $J = 14.16, 0.98$  Hz), 4.64, 4.95 (dd, 1 H,  $J = 6.84, 0.98$  Hz), 7.31 (m, 1 H), 7.39 (m, 1 H), 7.53 (m, 2 H), 7.77 (m, 1 H), 7.88 (m, 1H), 8.07 (m, 1H); IR (KBr)  $\nu_{\text{max}}$  ( $\text{cm}^{-1}$ ), 2980 (m), 1740 (s), 1700 (s) 1390 (m), 1365 (m), 1170 (s), 1155 (s). MS, ( $M + \text{H}^+$ ) 330. Anal. ( $\text{C}_{19}\text{H}_{23}\text{NO}_4$ )  $1/2(\text{H}_2\text{O})$  C, H, N.

**General Synthesis and Purification of Peptides 2, 4, 6, 8–14, 17, 18, 20–23.** All the peptides were synthesized using the solid phase peptide synthesis (SPPS) techniques<sup>18</sup> analogously to our previously reported syntheses for LHRH agonists.<sup>14,14</sup> The crude peptides were purified by HPLC using a  $\text{C}_{18}$  reversed-phase column. Analytical HPLC separation was achieved with a  $\text{C}_{18}$  Dynamax column (0.46 × 25 cm, 300-Å pore size, 5-mm particle size) fitted with a guard column of the same material (0.46 × 1.5 cm). The solvent system was 0.1% TFA in water/acetonitrile, and the gradient was 20–45% acetonitrile over 40 min. The UV detector was set at 254 nm. Preparative HPLC separation was accomplished with a  $\text{C}_{18}$  Dynamax column using analogous conditions to those previously reported.<sup>8</sup> The purity of the final compounds was over 95% on the basis of analytical HPLC, FABMS, and AAA.

**Biological Assays.** We previously reported the receptor binding and LH release assays.<sup>14</sup>

**Rat Jejunum Sac Assay.** This test was described in our recent publication.<sup>8</sup>

**Pharmacokinetics Determination.** Each compound was administered iv to castrate male rats at a dose of 100  $\mu\text{g}/\text{kg}$ . Blood samples were drawn over a 6-h period, using EDTA as anticoagulant. The plasma concentration of each compound was determined by RIAs using a LHRH analogue antibody that recognizes the C-terminal residues Leu-Arg-Pro-NH<sub>2</sub> or Leu-Arg-Pro-GlyNH<sub>2</sub>. The antiserum and tracer used for leuprolide and deslorelin analogues were rabbit antiserum C-402 and [<sup>125</sup>I-Tyr<sup>5</sup>]leuprolide. The RIAs for nafarelin analogues and for Sar<sup>10</sup>-substituted leuprolide and deslorelin analogues used rabbit antiserum 5328W and [<sup>125</sup>I-Tyr<sup>5</sup>, D-Lys<sup>6</sup>]LHRH as reagents. Both rabbit antisera were obtained from Dr. P. Michael Conn of the University of Iowa. The area under the plasma concentration versus time curve was calculated via the trapezoidal rule. The whole body clearance was determined from the ratio of the dose divided by the area under the curve and is expressed in units of mL/min per kg.

**Chymotrypsin Cleavage Assay.** We previously reported our method for measuring the resistance of LHRH agonists to chymotrypsin.<sup>9</sup>

**Acknowledgment.** We are indebted to Dr. P. Michael Conn of the University of Iowa for providing the anti-rat-LH and anti-LHRH analogue antibodies.

## References

- (1) Karten, M. J.; Rivier, J. E. Gonadotropin-Releasing Hormone Analogs Design, Structure-Function Studies Toward the Development of Agonist and Antagonists: Rationale and Perspective. *Endocr. Rev.* 1986, 7, 44–66.
- (2) Dutta, A. S. Luteinizing Hormone-Releasing Hormone (LHRH) Agonists. *Drugs Future* 1988, 13, 43–67.
- (3) Friedman, A. J. The Biochemistry, Physiology, and Pharmacology of Gonadotropin Releasing Hormone (GnRH) and GnRH Analogs. In *Gonadotropin Releasing Hormone Analogs: Applications in Gynecology*; Barbieri, R. L.; Friedmann, A. J., Eds.; Elsevier: New York-Amsterdam-London, 1990; pp 1–15.
- (4) Garnick, M. B.; Glode, M. The Leuprolide Study Group. Leuprolide versus diethylstilbestrol for metastatic prostate cancer. *N. Engl. J. Med.* 1984, 311, 1281–1286.
- (5) Filicori, M.; Flamigni, C. GnRH Agonists and Antagonists Current Clinical Status. *Drugs* 1988, 35, 69–82.
- (6) Dlugi, M. A.; Miller, J. D.; Knittle, J.; Lupron Study Group. Lupron depot (leuprolide acetate for depot suspension) in the treatment of endometriosis: a randomized, placebo-controlled double-blind study. *Fertil. Steril.* 1990, 54, 419–427.
- (7) Haviv, F.; Fitzpatrick, T. D.; Nichols, C. J.; Bush, E. N.; Diaz, G.; Nellans, H. N.; Hoffman, D. J.; Ghanbari, H.; Johnson, E. S.; Love, S.; Cybulski, V.; Nguyen, A.; Greer, J. Metabolically stabilized agonists of luteinizing hormone-releasing hormone (LHRH). In *Peptides, Chemistry and Biology. Proceedings of the Twelfth American Peptide Symposium*; Smith, J. A., Rivier, J. E., Eds.; ESCOM: Leiden, 1992; pp 54–58.
- (8) Haviv, F.; Fitzpatrick, T. D.; Nichols, C. J.; Swenson, R. E.; Bush, E. N.; Diaz, G.; Nguyen, A. T.; Nellans, H. N.; Hoffman, D. J.; Ghanbari, H.; Johnson, E. S.; Love, S.; Cybulski, V. A.; Greer, J. Stabilization of the N-Terminal Residues of Luteinizing Hormone-Releasing Hormone Agonists and the Effect on Pharmacokinetics. *J. Med. Chem.* 1992, 35, 3890–3894.
- (9) Coy, D. H.; Labrie, F.; Savary, M.; Coy, E. J.; Schally, A. V. LH-Releasing Activity of Potent LH-RH Analogs in vitro. *Biochem. Biophys. Res. Commun.* 1975, 67, 576–582.
- (10) Rivier, C.; Vals, W.; Rivier, J. Effects of gonadotropin releasing agonists and antagonists on reproductive functions. *J. Med. Chem.* 1983, 26, 1545–1550.
- (11) Nestor, J. J. Jr.; Ho, T. L.; Simpson, R. A.; Horner, B. L.; Jones, G. H.; McRae, G. L.; Vickery, B. H. Synthesis and biological activity of some very hydrophobic superagonist analogues of LHRH. *J. Med. Chem.* 1982, 25, 795–801.
- (12) Nestor, J. J. Jr.; Horner, B. L.; Ho, T. L.; Jones, G. H.; McRae, G. L.; Vickery, B. H. Synthesis of a novel class of heteroaromatic amino acids and their use in the preparation of analogues of LHRH. *J. Med. Chem.* 1984, 27, 320–325.
- (13) Stewart, J. M. *Solid Phase Peptide Synthesis*; Pierce Chemical Co.: Rockford, IL, 1984; pp 71–89.
- (14) Haviv, F.; Palabrica, C. A.; Bush, E. N.; Diaz, G.; Johnson, E. S.; Love, S.; Greer, J. Active Reduced Size Hexapeptide Analogues of Luteinizing Hormone-Releasing Hormone. *J. Med. Chem.* 1989, 32, 2340–2344.
- (15) Rich, D. H.; Dharm, M. K.; Dunlap, B.; Miller, S. P. F. Synthesis and Antimitogenic Activities of Four Analogues of Cyclosporin A Modified in the 1-Position. *J. Med. Chem.* 1986, 29, 978–984.
- (16) Thairivongsa, S.; Fala, D. T.; Harris, D. W.; Katim, W. M.; Turner, S. R. Design and Synthesis of a Potent and Specific Renin Inhibitor with a Prolonged Duration of Action in Vivo. *J. Med. Chem.* 1984, 27, 320–325.
- (17) Haviv, F.; Fitzpatrick, T. D.; Bush, E. N.; Diaz, G.; Johnson, E. S.; Love, S.; Greer, J. Structure-activity relationships, pharmacokinetics, and bioavailability studies of reduced size analogs of gonadotropin-releasing hormone (GnRH). In *Peptides, Chemistry and Biology. Proceedings of the Eleventh American Peptide Symposium*; Rivier, J. E., Marshall, G. R., Eds.; ESCOM: Leiden, 1990; pp 192–194.
- (18) Momany, F. A. Conformational Energy Analysis of the Molecule, Luteinizing Hormone-Releasing Hormone. 1. Native Decapeptide. *J. Am. Chem. Soc.* 1976, 98, 2990–2995.
- (19) Momany, F. A. Conformational Energy Analysis of the Molecule, Luteinizing Hormone-Releasing Hormone. 2. Tetrapeptide and Decapeptide Analogues. *J. Am. Chem. Soc.* 1976, 98, 2996–3000.
- (20) Struthers, R. S.; Tanaka, G.; Koerber, S. C.; Solmajer, T.; Baniak, E. L.; Gierasch, L. M.; Vals, W.; Rivier, J.; Hagler, A. T. Design of Biologically Active, Conformationally Constrained GnRH Antagonists. *Protein: Struct. Funct. Genet.* 1990, 8, 295–304.
- (21) Baniak, E. L.; Rivier, J. E.; Struthers, R. S.; Hagler, A. T.; Gierasch, L. M. Nuclear Magnetic Resonance Analysis and Conformational Characterization of a Cyclic Decapeptide Antagonist of Gonadotropin-Releasing Hormone. *Biochemistry* 1987, 26, 2842–2856.
- (22) Riso, J.; Koerber, S. C.; Binstock, J. R.; Rivier, J.; Hagler, A. T.; Gierasch, L. M. Conformational Analysis of a Highly Potent, Constrained Gonadotropin-Releasing Hormone Antagonist. 1. Nuclear Magnetic Resonance. *J. Am. Chem. Soc.* 1992, 114, 2852–2859.
- (23) Haviv, F.; Fitzpatrick, T. D.; Nichols, C. J.; Swenson, R. E.; Mort, N. A.; Bush, E. N.; Diaz, G. J.; Nguyen, A.; Love, S. K.; Milusa, J.; Leal, J. A.; Cybulski, V.; Dodge, P. W.; Johnson, E.; Knittle, J.; Greer, J. A-75998: A Potent and Safe Antagonist of Gonadotropin-Releasing Hormone (GnRH). 74th Annual Meeting of the Endocrine Society, San Antonio, TX, 1992; Abstr. No. 178.

*Peptide Bond N-Methyl Substitution in LHRH Agonists*

- (24) Haviv, F.; Fitzpatrick, T. D.; Nichols, C. J.; Swenson, R. E.; Mort, N. A.; Bush, E. N.; Dias, G.; Nguyen, A. T.; Holst, M. R.; Cybulski, V. A.; Leal, J. A.; Bammert, G.; Rhutasel, N. S.; Dodge, P. W.; Johnson, E. S.; Cannon, J. B.; Knittle, J.; Greer, J. The Effect of NMeTyr<sup>6</sup> Substitution in Luteinizing Hormone-Releasing Hormone Antagonists. *J. Med. Chem.*, submitted for publication.
- (25) Birktoft, J. J.; Blow, D. M. Structure of crystalline  $\alpha$ -chymotrypsin. V. The atomic structure of tosyl  $\alpha$ -chymotrypsin at 2 Å resolution. *J. Mol. Biol.* 1972, 68, 187-240.

*Journal of Medicinal Chemistry, 1993, Vol. 36, No. 3 369*

- (26) Greer, J. Model of a specific interaction: salt bridges form between prothrombin and its activating enzyme blood clotting factor Xa. *J. Mol. Biol.* 1981, 153, 1043-1053.
- (27) Chan, R. L.; Chaplin, M. D.; Plasma Binding of LHRH and Nafarelin Acetate. *Biochem. Biophys. Res. Commun.* 1985, 127, 679-679.
- (28) Naeeshiro, I.; Kondo, T.; Mitani, M.; Kimura, K.; Shimomura, H.; Tanayama, S. Metabolic Fate of TAP-144, an LH-RH Agonist, in Rats and Dogs. *Jpn. Pharmacol. Ther.* 1990, 18 (Suppl 8), 545-568.

# Conformational Analysis of Reverse-Turn Constraints by N-Methylation and N-Hydroxylation of Amide Bonds in Peptides and Non-Peptide Mimetics

Yasuo Takeuchi and Garland R. Marshall\*

Contribution from the Center for Molecular Design, Washington University, St. Louis, Missouri 63110

Received March 17, 1997. Revised Manuscript Received March 30, 1998

**Abstract:** Several non-peptide systems have been designed to mimic different types of reverse turns. The incorporation of some of these mimetics into biologically active peptides has led to peptidomimetics with enhanced activity or metabolic stability. This paper reports the conformational analysis of tetrapeptides containing several bicyclic mimetics, sequences containing proline, other *N*-methyl and *N*-hydroxy amino acids, and pipecolic acid at residue *i* + 2 of the turn, and control peptide sequences using the Monte Carlo/stochastic dynamics simulation with the new set of AMBER\* parameters for proline-containing peptides in water as implicitly represented by the GB/SA solvation model. Simple *N*-methylation (Pro-D-NMeAA and D-Pro-NMeAA) and *N*-hydroxylation of the amide bond between residues *i* + 1 and *i* + 2 or inclusion of the larger ring homolog pipecolic acid (D-Pro-Pip) in the third position (*i* + 2) causes significant nucleation of reverse-turn structures. Spirotricyclic analogs restrict three of the four torsion angles that characterize the type II  $\beta$ -turn. Spirolactam analogs also restrict two of the four torsion angles as effective  $\beta$ -turn constraints. However, the geometry of a turn induced by indolizidinone and BTB differs significantly from that of an ideal  $\beta$ -turn and (*S*)-indolizidinone is more effective as a reverse turn than as a  $\beta$ -turn mimetic. These systems provide useful conformational constraints when incorporated into the structure of selected bioactive peptides. Such analogs can scan receptors for biological recognition of  $\beta$ -turn scaffolds with oriented side chains through combinatorial libraries to efficiently develop three-dimensional structure–activity relationships.

## Introduction

Reverse turns play an important structural role in the compact globular architecture of native folded proteins<sup>1–3</sup> and have often been implicated as recognition elements in intermolecular interactions.<sup>3–5</sup> High-resolution examples of turns as recognition motifs can be found in crystal structures of antibody–peptide complexes.<sup>4,6,7</sup> These complexes are entirely consistent with the receptor recognition of turn motifs deduced from structure–activity studies of the peptide hormones, angiotensin II,<sup>8,9</sup> bradykinin,<sup>10–12</sup> GnRH (gonadotrophin releasing hor-

none),<sup>13,14</sup> somatostatin,<sup>15,16</sup> RGD (Arg-Gly-Asp) sequence,<sup>17,18</sup> repeated NPNA (Asn-Pro-Asn-Ala) tetrapeptide,<sup>19</sup> and many others. One of the most common reverse turns is the  $\beta$ -turn. A  $\beta$ -turn consists of four residues, which are designated as *i*, *i* + 1, *i* + 2, and *i* + 3, where the chain changes direction by almost 180°. Several different types of  $\beta$ -turns are possible depending upon the  $\Phi$  and  $\Psi$  torsion angles of the *i* + 1 and *i* + 2 residues.<sup>2,3</sup> In addition, these turns may (classic  $\beta$ -turn) or may not (open  $\beta$ -turn) be stabilized by an intramolecular hydrogen bond between the carbonyl oxygen of the first residue (*i*) and the amide hydrogen of the fourth residue (*i* + 3),<sup>3</sup> although the classical and more stringent definition of a  $\beta$ -turn requires the hydrogen bond. An alternative method of characterizing reverse turns, which focuses on the topography of the side chains, has been suggested by Ball et al.<sup>20</sup>

\* To whom correspondence should be addressed.

(1) Chou, P. Y.; Fasman, G. D. *J. Mol. Biol.* **1977**, *115*, 135–175.

(2) Smith, J. A.; Pease, L. G. *CRC Crit. Rev. Biochem.* **1980**, *8*, 315–399.

(3) Rose, G. D.; Gierasch, L. M.; Smith, J. A. *Adv. Protein Chem.* **1985**, *37*, 1–109.

(4) Stanfield, R. L.; Fieser, T. M.; Lerner, R. A.; Wilson, I. A. *Science* **1990**, *248*, 712–719.

(5) Marshall, G. R. *Curr. Opin. Struct. Biol.* **1992**, *2*, 904–919.

(6) Rini, J. M.; Schulze-Gahmen, U.; Wilson, I. A. *Science* **1992**, *255*, 959–965.

(7) Garcia, K. C.; Ronco, P. M.; Veroust, P. J.; Brunger, A. T.; Amzel, L. M. *Science* **1992**, *257*, 502–507.

(8) Plucinska, K.; Kataoka, T.; Yodo, M.; Cody, W. L.; He, J. X.; Humblet, C.; Lu, G. H.; Lunney, E.; Major, T. C. *J. Med. Chem.* **1993**, *36*, 1902–1913.

(9) Nikiforovich, G. V.; Marshall, G. R. *Biochem. Biophys. Res. Commun.* **1993**, *195*, 222–228.

(10) Kaczmarek, K.; Li, K.-M.; Skeean, R.; Dooley, D.; Humblet, C.; Lunney, E.; Marshall, G. R. In *Peptides: Proceedings of the 13th American Peptide Symposium*; Hodges, R., Smith, J. A., Eds.; ESCOM Scientific Publishers: Leiden, 1994; pp 687–689.

(11) Kyle, D. J.; Blake, P. R.; Smithwick, D.; Green, L. M.; Martin, J. A. *J. Med. Chem.* **1993**, *36*, 1450–1460.

(12) Thureau, C.; Félétou, M.; Hennig, P.; Raimbaud, E.; Canet, E.; Fauchère, J.-L. *J. Med. Chem.* **1996**, *39*, 2095–2101.

(13) Nikiforovich, G.; Marshall, G. R. *Int. J. Pept. Protein Res.* **1993**, *42*, 171–180.

(14) Nikiforovich, G. V.; Marshall, G. R. *Int. J. Pept. Protein Res.* **1993**, *42*, 181–193.

(15) Nutt, R. F.; Veber, D. F.; Saperstein, R. *J. Am. Chem. Soc.* **1980**, *102*, 6539–6545.

(16) Brady, S. F.; Paleveda, W. J., Jr.; Arison, B. H.; Saperstein, R.; Brady, E. J.; Raynor, K.; Reisine, T.; Veber, D. F.; Freidinger, R. M. *Tetrahedron* **1993**, *49*, 3449–3466.

(17) Bach, A. C., II; Espina, J. R.; Jackson, S. A.; Stouten, P. F. W.; Duke, J. L.; Mousa, S. A.; DeGrado, W. F. *J. Am. Chem. Soc.* **1996**, *118*, 293–294.

(18) Haubner, R.; Schmitt, W.; Holzemann, G.; Goodman, S. L.; Jonczyk, A.; Kessler, H. *J. Am. Chem. Soc.* **1996**, *118*, 7881–7891.

(19) Bisang, C.; Weber, C.; Inglis, J.; Schiffer, C. A.; Gunsteren, W. F. v.; Jelesarov, I.; Bosshard, H. R.; Robinson, J. A. *J. Am. Chem. Soc.* **1995**, *117*, 7904–7915.

Several non-peptide systems have been designed to mimic the different types of  $\beta$ -turns.<sup>21–29</sup> The incorporation of some of these mimics into biologically active peptides has led to peptidomimetics with enhanced activity or metabolic stability.<sup>30–34</sup> Examples of modifications which enhance reverse-turn propensity are the dipeptide lactam,<sup>35</sup> the bicyclic dipeptide BTDD<sup>25</sup> and similar proline derivatives,<sup>36</sup> spirolactam bicyclic and tricyclic systems based on proline,<sup>28,37–39</sup> substitution by  $\alpha$ , $\alpha$ -dialkyl amino acids,<sup>28,40–42</sup> *N*-aminoproline,<sup>43</sup> functionalized dibenzofurans,<sup>44–46</sup> and substitution by dehydroamino acids.<sup>47–50</sup> Other efforts have focused on stabilizing Type VI  $\beta$ -turns by stabilizing a *cis*-amide bond through disulfide bonds,<sup>16,51</sup>

incorporating of tetrazole rings as *cis*-amide bond surrogates,<sup>52–54</sup> or incorporating certain sequences into cyclic peptides.<sup>55</sup> In other turn mimetics, hydrogen bonding groups stabilizing the turn are replaced by covalent bonds.<sup>56–63</sup> Benzodiazepines have also been used as turn mimetics.<sup>64–66</sup>

Chalmers et al.<sup>67</sup> reported the conformational analysis of tetrapeptides containing several bicyclic mimetics, sequences containing proline and other *N*-methyl amino acids in the residues *i* + 1 and *i* + 2 of the turn, and control peptide sequences using a Monte Carlo conformational search followed by molecular dynamics simulation in water as implicitly represented by the GB/SA solvation model. Stimulated by the discrepancy in the calculated and experimentally observed conformation of c[Pro-D-Pro-Pro-D-Pro] reported by Chalmers et al.,<sup>67</sup> McDonald et al.<sup>68</sup> recently reported a reparametrization of the AMBER\* force field in MacroModel for proline-containing peptides based on the results of high-level *ab initio* calculations for *N*-acetylproline methylamide. In addition, the conformational search—molecular dynamics protocol<sup>67</sup> used previously does not give a true Boltzmann sample of conformers which would be desirable to make the statistical comparisons equitably, while the newer combined Monte Carlo/stochastic dynamics protocol of Guarnieri and Still<sup>69</sup> produces a true Boltzmann distribution.

In this paper we report the conformational analysis of model blocked tetrapeptides of the type Ac-Ala-Pro-Pro-Ala-NHMe using Monte Carlo searches<sup>70</sup> in water as implicitly represented by the GB/SA solvation model.<sup>71</sup> We compare the results on the differences in free energy between minima on the potential

(20) Ball, J. B.; Hughes, R. A.; Alewood, P. F.; Andrews, P. R. *Tetrahedron* **1993**, *49*, 3467–3478.

(21) Ball, J. B.; Alewood, P. F. *J. Mol. Recognit.* **1990**, *3*, 55–64.

(22) Freidinger, R. M.; Veber, D. F.; Hirschmann, R.; Paegle, L. M. *J. Pept. Protein Res.* **1980**, *16*, 464–470.

(23) Freidinger, R. M. In *Peptides: Synthesis-Structure-Function*; Rich, D. H., Gross, E., Eds.; Pierce Chemical Company: Rockford, IL, 1981; pp 673–683.

(24) Krstenansky, J. L.; Baranowsky, R. L.; Currie, B. C. *Biochem. Biophys. Res. Commun.* **1982**, *109*, 1368–1374.

(25) Nagai, U.; Sato, K. *Tetrahedron Lett.* **1985**, *26*, 647–650. Nagai, U.; Sato, K.; Nakamura, R.; Kato, R. *Tetrahedron Lett.* **1993**, *49*, 3577–3592.

(26) Kemp, D. S.; Stites, W. E. *Tetrahedron Lett.* **1988**, *29*, 5057–5060.

(27) Kahn, M.; Wilke, S.; Chen, B.; Fujita, K.; Lee, Y.-H.; Johnson, M. *J. Mol. Recognit.* **1988**, *1*, 75–79.

(28) Hinds, M. G.; Richards, N. G. J.; Robinson, J. A. *J. Chem. Soc., Chem. Commun.* **1988**, 1447–1449.

(29) Olson, G. L.; Voss, M. E.; Hill, D. E.; Kahn, M.; Madison, V. S.; Cook, C. M. *J. Am. Chem. Soc.* **1990**, *112*, 323–333.

(30) Freidinger, R. M.; Veber, D. F.; Perlow, D. S.; Brooks, J. R.; Saperstein, R. *Science* **1980**, *210*, 656–658.

(31) Sato, K.; Nagai, U. *J. Chem. Soc., Perkin Trans. 1* **1986**, 1231–1234.

(32) Casceri, M. A.; Chicchi, C. G.; Freidinger, R. M.; Colton, C. D.; Perlow, D. S.; Williams, B.; Curtis, N. R.; McKnight, A. T.; Maguire, J. J.; Veber, D. F.; Liang, T. *Mol. Pharmacol.* **1986**, *29*, 34–38.

(33) Yu, K.-L.; Rajakumar, G.; Srivastava, L. K.; Mishra, R. K.; Johnson, R. L. *J. Med. Chem.* **1988**, *31*, 1430–1436.

(34) Douglas, A. J.; Mulholland, G.; Walker, B.; Guthrie, D. J. S.; Elmore, D. T.; Murphy, R. F. *Biochem. Soc. Trans.* **1988**, *16*, 175–176.

(35) Freidinger, R. M.; Perlow, D. S.; Veber, D. F. *J. Org. Chem.* **1982**, *47*, 104–109.

(36) Lombart, H.-G.; Lumbell, W. D. *J. Org. Chem.* **1994**, *59*, 6147–6149.

(37) Hinds, M. G.; Welsh, J. H.; Brennand, D. M.; Fisher, J.; Glennie, M. J.; Richards, N. G. J.; Turner, D. L.; Robinson, J. A. *J. Med. Chem.* **1991**, *34*, 1777–1789.

(38) Genin, M. J.; Johnson, R. L. *J. Am. Chem. Soc.* **1992**, *114*, 8778–8783.

(39) Ward, P.; Ewan, G. B.; Jordan, C. C.; Ireland, S. J.; Hagan, R. M.; Brown, J. R. *J. Med. Chem.* **1990**, *33*, 1848–1851.

(40) Toniolo, C.; Bonora, G. M.; Bavoso, A.; Benedetti, E.; Blasio, B. D.; Pavone, V.; Pedone, C. *Biopolymers* **1983**, *22*, 205–215.

(41) Valle, G.; Crisma, M.; Toniolo, C.; Sudhanand; Rao, R. B.; Sukumar, M.; Balam, P. *Int. J. Pept. Protein Res.* **1991**, *38*, 511–518.

(42) Welsh, J. H.; Zerbe, O.; von Philipsborn, W.; Robinson, J. A. *FEBS Lett.* **1992**, *297*, 216–220.

(43) Zerkout, S.; Dupont, V.; Aubry, A.; Vidal, J.; Collet, A.; Vicherat, A.; Marraud, M. *Int. J. Peptide Protein Res.* **1994**, *44*, 378–384.

(44) Diaz, H.; Espina, J. R.; Kelly, J. W. *J. Am. Chem. Soc.* **1992**, *114*, 8316–8318.

(45) Diaz, H.; Tsang, K. Y.; Choo, D.; Kelly, J. W. *Tetrahedron* **1993**, *49*, 3533–3545.

(46) Tsang, K. Y.; Diaz, H.; Graciani, N.; Kelly, J. W. *J. Am. Chem. Soc.* **1994**, *116*, 3988–4005.

(47) Bach, A. C., II; Gierasch, L. M. *J. Am. Chem. Soc.* **1985**, *107*, 3349–3350.

(48) Bach, A. C., II; Gierasch, L. M. *Biopolymers* **1986**, *25*, S175–S191.

(49) Chauhan, V. S.; Sharma, A. K.; Uma, K.; Paul, P. K. C.; Balam, P. *Int. J. Pept. Protein Res.* **1987**, *29*, 126–133.

(50) Palmer, D. E.; Pattaroni, C.; Nunami, K.; Chadha, R. K.; Goodman, M.; Wakamiya, T. *J. Am. Chem. Soc.* **1992**, *114*, 5634–5642.

(51) Sukumaran, D. K.; Prorok, M.; Lawrence, D. S. *J. Am. Chem. Soc.* **1991**, *113*, 706–707.

(52) Zabrocki, J.; Smith, G. D.; Dunbar, J. B., Jr.; Iijima, H.; Marshall, G. R. *J. Am. Chem. Soc.* **1988**, *110*, 5875–5880.

(53) Smith, G. D.; Zabrocki, J.; Flak, T. A.; Marshall, G. R. *Int. J. Pept. Protein Res.* **1991**, *37*, 191–197.

(54) Zabrocki, J.; Dunbar, J. B., Jr.; Marshall, K. W.; Toth, M. V.; Marshall, G. R. *J. Org. Chem.* **1992**, *57*, 202–209.

(55) Muller, G.; Gurrath, M.; Kurz, M.; Kessler, H. *Proteins: Struct. Funct. Genet.* **1993**, *15*, 235–251.

(56) Kahn, M.; Nakanishi, H.; Chrusciel, R. A.; Fitzpatrick, D.; Johnson, M. E. *J. Med. Chem.* **1991**, *34*, 3395–3399.

(57) Nakanishi, H.; Chrusciel, R. A.; Shen, R.; Bertenshaw, S.; Johnston, M. E.; Rydel, T. J.; Tulinsky, A.; Kahn, M. *Proc. Natl. Acad. Sci. U.S.A.* **1992**, *89*, 1705–1709.

(58) Chen, S.; Chrusciel, R. A.; Nakanishi, H.; Raktabutr, A.; Johnson, M. E.; Sato, A.; Weiner, D.; Hoxie, J.; Saragovi, H. U.; Greene, M. I.; Kahn, M. *Proc. Natl. Acad. Sci. U.S.A.* **1992**, *89*, 5872–5876.

(59) Gardner, B.; Nakanishi, H.; Kahn, M. *Tetrahedron* **1993**, *49*, 3433–3448.

(60) Arrhenius, T.; Satterthwait, A. C. In *Peptides: Chemistry, Structure and Biology*; Rivier, J. E., Marshall, G. R., Eds.; ESCOM Scientific Publishers: Leiden, 1990; pp 870–872.

(61) Callahan, J. F.; Newlander, K. A.; Burgess, J. L.; Eggleston, D. S.; Nichols, A.; Wong, A.; Huffman, W. F. *Tetrahedron* **1993**, *49*, 3479–3488.

(62) Hermkens, P. H. H.; v. Dinther, T. G.; Joukema, C. W.; Wagenaars, G. N.; Ottenheijm, H. C. J. *Tetrahedron Lett.* **1994**, *35*, 9271–9274.

(63) Virgilio, A. A.; Ellman, J. A. *J. Am. Chem. Soc.* **1994**, *116*, 11580–11581.

(64) Ripka, W. C.; DeLucca, G. V.; Bach, A. C., II; Pottorf, R. S.; Blaney, J. M. *Tetrahedron* **1993**, *49*, 3593–3608.

(65) Ripka, W. C.; Lucca, G. V. D.; Bach, A. C., II; Pottorf, R. S.; Blaney, J. M. *Tetrahedron* **1993**, *49*, 3609–3628.

(66) Ku, T. W.; Ali, F. E.; Barton, L. S.; Bean, J. W.; Bondinell, W. E.; Burgess, J. L.; Callahan, J. F.; Calvo, R. R.; Chen, L.; Eggleston, D. S.; Gleason, J. S.; Huffman, W. F.; Hwang, S. M.; Jakas, D. R.; Karash, C. B.; Keenan, R. M.; Kopple, K. D.; Miller, W. H.; Newlander, K. A.; Nichols, A.; Parker, M. F.; Peishoff, C. E.; Samanen, J. M.; Uzinskas, I.; Venslavsky, J. W. *J. Am. Chem. Soc.* **1993**, *115*, 8861–8862.

(67) Chalmers, D. K.; Marshall, G. R. *J. Am. Chem. Soc.* **1995**, *117*, 5927–5937.

(68) McDonald, D. Q.; Still, W. C. *J. Org. Chem.* **1996**, *61*, 1385–1391.

(69) Guarnieri, F.; Still, W. C. *J. Comput. Chem.* **1994**, *15*, 1302–1310.

(70) Goodman, J. M.; Still, W. C. *J. Comput. Chem.* **1991**, *12*, 1110–1117.

surface of the original AMBER\* force field parameters<sup>72,73</sup> in MacroModel 4.5<sup>74</sup> with those of the modified AMBER\* force field parameters<sup>68</sup> in MacroModel 5.5 and other force fields. Improved conformational analysis was also performed of tetrapeptides containing several bicyclic mimetics, sequences containing proline, other *N*-methyl and *N*-hydroxy amino acids, and pipecolic acid (Pip) at residue *i* + 2 of the turn, and control peptide sequences using the Monte Carlo/stochastic dynamics simulation with the new set of AMBER\* parameters for proline-containing peptides in the GB/SA solvation water model.

## Methods

Conformational searches and molecular dynamics were performed with MacroModel<sup>74</sup> version 4.5 and 5.5 on Silicon Graphics Iris Indigo R4000 and Indigo Impact R10000 workstations. The MacroModel implementations of either the AMBER all-atom force field,<sup>72</sup> MM2,<sup>75</sup> MM3,<sup>76</sup> the Merck Molecular Force Field (MMFF),<sup>77–81</sup> or the AMBER/OPLS united-atom force fields<sup>82</sup> were used (respectively denoted AMBER\*, MM2\*, MM3\*, MMFF\*, and AMBER/OPLS\*). For solution-phase calculations, the GB/SA continuum models for water or chloroform were used.<sup>71</sup>

Amide bonds were required to be *trans*, i.e. structures containing non-proline *cis*-amide bonds were discarded as energetically improbable except in the case of *N,N*-dialkyl amino acids (Pro, Pip, NMeAla, etc.) whose imide bonds were purposefully sampled and accepted with either *cis* or *trans* geometry in the conformational searches.

**Conformational Searches.** Conformational searches were performed with use of the systematic Monte Carlo method of Goodman and Still.<sup>70</sup> For each search, 5000 starting structures were generated and minimized until the gradient was less than 0.05 (kJ/mol)/Å<sup>-1</sup>, using the truncated Newton-Raphson method implemented in MacroModel. Duplicate conformations and those with an energy greater than 50 kJ/mol above the global minimum were discarded.

**Monte Carlo/Stochastic Dynamics.** All simulations were performed at 300 K with use of the recently described Monte Carlo/stochastic dynamics (MC/SD) hybrid simulation algorithm<sup>69</sup> with the new AMBER\* all-atom force field in MacroModel 5.5. A time step of 1.5 fs was used for the stochastic dynamics (SD) part of the algorithm. The MC part of the algorithm used random torsional rotations between ±60° and ±180° that were applied to all rotatable bonds except the proline amide C–N bond where the random rotations were between ±90° and ±180°. No torsion rotations were applied to bonds in the pyrrolidine ring of proline as the barriers are low enough to permit adequate sampling from the SD part of the simulation. The total simulation time was 1000 ps and samples were taken at 1 ps intervals, yielding 1000 conformations for analysis.

## Results and Discussion

**Conformational Searches.** Monte Carlo searches were performed on model blocked tetrapeptides of the type Ac-Ala-

**Table 1.** Energy Differences between the Minimum Energy Proline  $\omega_{12}$  and  $\omega_{23}$  *trans*- and *cis*-Conformers for Tetrapeptides of the Type Ac-Ala- $\omega_{12}$ -Xxx- $\omega_{23}$ -Yyy-Ala-NHMe Using the Systematic Monte Carlo Searches with Original AMBER/OPLS\*, Original AMBER\* All-Atom, New AMBER/OPLS\*, New AMBER\* All-Atom, and MMFF\* All-Atom

Xxx-Yyy	original		v5.5 new		v5.5 MMFF* all-atom
	AMBER/ OPLS*	AMBER* all-atom	AMBER/ OPLS*	AMBER* all-atom	
$\Delta E(\omega_{12} \text{ cis-trans})$ (kJ/mol)					
Pro-Pro	8.5	5.0	6.7	2.6	9.6
Pro-D-Pro	12.5	6.2	10.9	1.5	9.1
D-Pro-Pro	15.2	16.5	12.9	10.4	9.8
D-Pro-D-Pro	17.7	4.7	14.1	7.1	10.1
$\Delta E(\omega_{23} \text{ cis-trans})$ (kJ/mol)					
Pro-Pro	-6.3 <sup>a</sup>	-0.1 <sup>a</sup>	-6.7 <sup>a</sup>	-3.6 <sup>a</sup>	5.8
Pro-D-Pro	25.2	8.5	22.4	1.7	10.5
D-Pro-Pro	12.8	13.0	11.1	5.8	16.3
D-Pro-D-Pro	3.7	-0.9 <sup>a</sup>	1.5	5.8	5.6

<sup>a</sup>  $\omega_{23}$  is *cis* in the minimum energy structure.

Pro-Pro-Ala-NHMe with use of the GB/SA solvation water model. The results of the comparison with the original AMBER\* force field parameters<sup>72,73</sup> in MacroModel 4.5 and the new AMBER\* force field parameters<sup>68</sup> in MacroModel 5.5 are summarized in Table 1.

To increase the speed of calculation, the normal amide bonds such as those of alanine were required to be *trans* due to the improbable occurrence of *cis*-amides in low energy structures. The united-atom force field, AMBER/OPLS\*, the AMBER\* all-atom force field, and the MMFF\* all-atom force field were also investigated to make sure that the differences observed were not due to parametrization.

As can be seen from Table 1, both the united-atom force field, AMBER/OPLS\*  $\Delta E$ , and the AMBER\* all-atom  $\Delta E$  for relative *cis-trans* stability of all tetrapeptides with the new AMBER\* parameters were lower than those with the original AMBER\* parameters. The AMBER\* all-atom  $\Delta E$  for relative  $\omega_{12}$  *cis-trans* stability of all tetrapeptides with the new AMBER\* parameters were lower than the united-atom force field, AMBER/OPLS\*  $\Delta E$  with the new AMBER\* parameters. The united-atom force field, AMBER/OPLS\* provides more rapid conformational searching. However, the energetic results, particularly for imide *cis-trans* isomerism in Ac-Ala-Pro-D-Pro-Ala-NHMe, were substantially different (9–21 kJ/mol) from those of the AMBER\* all-atom force field. The energetic results with the MMFF\* all-atom force field, particularly for imide *cis-trans* isomerism in Ac-Ala-Pro-Pro-Ala-NHMe and Ac-Ala-Pro-D-Pro-Ala-NHMe, were substantially different (7–9 kJ/mol) from those of the AMBER\* all-atom force field. The stabilization of the *cis* conformer (−4 kJ/mol) for  $\omega_{23}$  in Ac-Ala-Pro-Pro-Ala-NHMe was found with the new AMBER\* all-atom parameters. Upon inversion of chirality of the first proline  $\alpha$ -carbons, the stabilization of the *trans* conformation (10 kJ/mol) of the imide ( $\omega_{12}$ ) in Ac-Ala-D-Pro-Pro-Ala-NHMe was found with the new AMBER\* all-atom parameters. The hydrogen bonding between the carbonyl oxygen of residue 1 (*i*) and the NH of residue 4 (*i* + 3) plays an important part in stabilizing the  $\beta$ -turn in the model tetrapeptides.<sup>67</sup>

**Monte Carlo/Stochastic Dynamics.** A summary of the results from the Monte Carlo/stochastic dynamics simulations is given in Table 2. Three parameters were used as measures of reverse-turn forming ability: (1) Reverse turns can be identified by using the criterion that the C $\alpha$ 1–C $\alpha$ 4 distance is less than 7 Å.<sup>3,20</sup> (2) The virtual torsion angle,  $\beta$ , is defined by the atoms C $\alpha$ 1, C $\alpha$ 2, C $\alpha$ 3, and N4 (Figure 1).<sup>20,21</sup> The range

(71) Still, W. C.; Tempczyk, A.; Hawley, R. C.; Hendrickson, T. J. *Am. Chem. Soc.* **1990**, *112*, 6127–6129.

(72) Weiner, S. J.; Kollman, P. A.; Nguyen, D. T.; Case, D. A. *J. Comput. Chem.* **1986**, *7*, 230–252.

(73) Weiner, S. J.; Kollman, P. A.; Case, D. A.; Singh, U. C.; Ghio, C.; Alagona, G.; Profeta, S.; Weiner, P. *J. Am. Chem. Soc.* **1984**, *106*, 765–784.

(74) Mohamadi, F.; Richards, N. G. J.; Guida, W. C.; Liskamp, R.; Lipton, M.; Caufield, C.; Chang, G.; Hendrickson, T.; Still, W. C. *J. Comput. Chem.* **1990**, *11*, 440–467.

(75) Allinger, N. L. *J. Am. Chem. Soc.* **1977**, *99*, 8127–8134.

(76) Lii, J.-H.; Allinger, N. L. *J. Comput. Chem.* **1991**, *12*, 186–199.

(77) Halgren, T. A. *J. Comput. Chem.* **1996**, *17*, 490–519.

(78) Halgren, T. A. *J. Comput. Chem.* **1996**, *17*, 520–552.

(79) Halgren, T. A. *J. Comput. Chem.* **1996**, *17*, 553–586.

(80) Halgren, T. A.; Nachbar, R. B. *J. Comput. Chem.* **1996**, *17*, 587–615.

(81) Halgren, T. A. *J. Comput. Chem.* **1996**, *17*, 616–641.

(82) Tirado-Rives, J.; Jorgensen, W. L. *J. Am. Chem. Soc.* **1990**, *112*, 2773–2781.

(83) Lewis, P. N.; Momany, F. A.; Scheraga, H. A. *Biochim. Biophys. Acta* **1973**, *303*, 211.

**Table 2.** Percentage of Tetrapeptide Conformers of Blocked Tetrapeptides Ac-Ala-Xxx-Yyy-Ala-NHMe and BILD1263 which Exhibit Characteristics of a Reverse Turn from 1000 ps, 300 K MC/SD Simulations Using New All-Atom AMBER\* Parameters and GB/SA Water in MacroModel 5.5

Xxx-Yyy	% $ \beta  < 30^\circ$	% $d < 7 \text{ \AA}$	% $d(\text{C=O} \cdots \text{H-N})$	
			$< 4 \text{ \AA}$	$< 2.5 \text{ \AA}$
Pro-Pro	32	40	35	4
Pro-D-Pro	18	34	23	4
D-Pro-Pro	26	35	31	9
D-Pro-D-Pro	13	18	16	2
Pro-D-NMeAla	44	64	34	13
D-Pro-NMeAla	49	61	41	6
D-Pro-Pip	62	74	47	7
Pro $\psi$ [CN <sub>4</sub> ]-Ala	26	40	15	5
Pro-NOHAla	41	78	48	23
Pro-D-NOHAla	0	7	4	1
D-Pro-NOHAla	2	2	2	0
D-Pro-D-NOHAla	25	72	40	14
BTD	69	33	0	0
(S)-spiro lactam	48	48	47	16
spiro tricycle	76	71	57	27
(R)-indolizidinone	78	58	1	0
(S)-indolizidinone	77	85	0	0
BILD1263	9	6	0	0

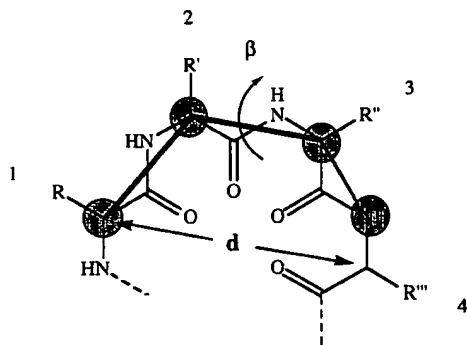


**Figure 1.** Schematic of tetrapeptide showing the virtual torsion  $\beta$ <sup>82</sup> and the distance  $d$  from C $\alpha$ 1 to C $\alpha$ 4 used to characterize reverse turns.

$0 \pm 30^\circ$  was taken to indicate a tight reverse turn. (3) The distance between the carbonyl oxygen of residue  $i$  and the amide hydrogen of residue  $i + 3$  indicates an appropriate hydrogen bond characteristic of a  $\beta$ -turn. A distance of less than  $4 \text{ \AA}$  was taken to indicate significant interaction between these groups.<sup>67</sup> A distance less than  $2.5 \text{ \AA}$  may imply a hydrogen bond between residues  $i$  and  $i + 3$ , which characterizes some types of  $\beta$ -turn.<sup>84</sup>

**Ac-Ala-Pro-D-Pro-Ala-NHMe and Ac-Ala-D-Pro-Pro-Ala-NHMe.** A plot of the distances between the carbonyl oxygen of residue  $i$  and the amide hydrogen of residue  $i + 3$  against  $\omega_{23}$  (Figure 2a) of the tetrapeptide Ac-Ala-Pro-D-Pro-Ala-NHMe shows that  $\omega_{23}$  of most conformers where distances are less than  $4 \text{ \AA}$  is *trans*. Table 2 shows that  $|\beta|$  is less than  $30^\circ$  in 18% of the structures,  $d$  is less than  $7 \text{ \AA}$  in 34%, the distance between the amide hydrogen and carbonyl oxygen is less than  $4 \text{ \AA}$  for 23%, and the distance is less than  $2.5 \text{ \AA}$  for 4% of the time. These percentages of conformers which can be classified as turns with use of the new AMBER\* force field parameters in MacroModel 5.5 were lower than those<sup>67</sup> with use of the original AMBER\* force field parameters in MacroModel 4.5 due to the smaller  $\Delta E$  (Table 1) for relative *cis*–*trans* stability with the new AMBER\* force field parameters.

(84) Constantine, K. L.; Mueller, L.; Andersen, N. H.; Tong, H.; Wandler, C. F.; Friedrichs, M. S.; Brucoleri, R. E. *J. Am. Chem. Soc.* 1995, 117, 10841–10854.

As a result of swapping the chirality of residues  $i + 2$  and  $i + 3$  to give Ac-Ala-D-Pro-Pro-NHMe,  $\omega_{23}$  of all conformers where distances between the carbonyl oxygen of residue  $i$  and the amide hydrogen of residue  $i + 3$  are less than  $4 \text{ \AA}$  is also *trans* (Figure 2b). A plot of the distances between the carbonyl oxygen of residue  $i$  and the amide hydrogen of residue  $i + 3$  against  $\omega_{12}$  (Figure 2c) shows that both  $\omega_{12}$  and  $\omega_{23}$  of all conformers where distances are less than  $4 \text{ \AA}$  are *trans*.  $\omega_{12}$  and  $\omega_{23}$  of most conformers where distances between the carbonyl oxygen and the amide hydrogen are between  $4$  and  $6.5 \text{ \AA}$  are *trans* and *cis*, respectively. Both  $\omega_{12}$  and  $\omega_{23}$  of most conformers where distances between the carbonyl oxygen and the amide hydrogen are between  $6.5$  and  $8 \text{ \AA}$  are *cis*. Table 2 shows that the percentage of conformers with  $|\beta| < 30^\circ$  and  $d < 7 \text{ \AA}$  has risen to 26% and 35%, respectively. The carbonyl oxygen and amide hydrogen of residues  $i$  and  $i + 3$  are less than  $4$  and  $2.5 \text{ \AA}$  apart in 31% and 9% of the sampled structures, respectively.

**Ac-Ala-Pro-Pro-Ala-NHMe and Ac-Ala-D-Pro-D-Pro-Ala-NHMe.** A plot of the distances between the carbonyl oxygen of residue  $i$  and the amide hydrogen of residue  $i + 3$  against  $\omega_{23}$  (Figure 2d) of the tetrapeptide Ac-Ala-Pro-Pro-Ala-NHMe shows that  $\omega_{23}$  of most conformers where distances are less than  $4 \text{ \AA}$  is *cis*. Table 2 shows that  $|\beta|$  is less than  $30^\circ$  in 32% of the structures,  $d$  is less than  $7 \text{ \AA}$  in 40%, the distance between the amide hydrogen and carbonyl oxygen is less than  $4 \text{ \AA}$  for 35%, and the distance is less than  $2.5 \text{ \AA}$  for 4% of the time. These percentages of conformers which can be classified as type VIa  $\beta$ -turns by using the new AMBER\* force field parameters in MacroModel 5.5 were considerably higher than those<sup>67</sup> with use of the original AMBER\* force field parameters in MacroModel 4.5 due to the stabilization of the *cis* conformer ( $-4 \text{ kJ/mol}$ ) for  $\omega_{23}$  (Table 1) with the new AMBER\* force field parameters.

The corresponding sequence with D-amino acids in positions  $i + 2$  and  $i + 3$  had lower values for the percentage of hydrogen bonded conformers (16%, 2%) and with  $d$  under  $7 \text{ \AA}$  (18%) and  $|\beta|$  under  $30^\circ$  (13%) (Table 2). Some reduction of turn induction was due to the stabilization of the *trans* conformer ( $6 \text{ kJ/mol}$ ) for  $\omega_{23}$  (Table 1) with use of the new AMBER\* force field parameters.

**Ac-Ala-Pro-D-NMeAla-Ala-NHMe and Ac-Ala-D-Pro-NMeAla-Ala-NHMe.** Because the torsion angle ( $\Phi_3$ ) associated with the proline ring was not ideal for a  $\beta$ -turn and whether an *N*-methyl-substituted amino acid was sufficient for turn induction, we investigated tetrapeptides containing NMeAla at position  $i + 2$ . Ac-Ala-Pro-D-NMeAla-Ala-NHMe proved to be an extremely efficient turn promoter. During the MC/SD simulation the carbonyl oxygen of residue  $i$  and the amide hydrogen of residue  $i + 3$  were less than  $4$  and  $2.5 \text{ \AA}$  apart in 34% and 13% of the sampled conformers, respectively (Table 2).  $|\beta|$  is less than  $30^\circ$  in 44% of the MC/SD structures and 64% have a C $\alpha$ 1–C $\alpha$ 4 distance of less than  $7 \text{ \AA}$ , higher values than the two proline compounds. Figure 2e shows that  $\omega_{23}$  of all conformers where distances between the carbonyl oxygen of residue  $i$  and the amide hydrogen of residue  $i + 3$  are less than  $4 \text{ \AA}$  is *trans*.

The corresponding sequence with a D-amino acid in position  $i + 1$  and an L-amino acid in position  $i + 2$  also had higher values for the percentage of hydrogen bonded conformers (41%, 6%) and with  $d$  under  $7 \text{ \AA}$  (61%) and  $|\beta|$  under  $30^\circ$  (49%). Figure 2f shows that  $\omega_{23}$  of all conformers where distances between the carbonyl oxygen of residue  $i$  and the amide hydrogen of residue  $i + 3$  are less than  $4 \text{ \AA}$  is *trans*. The

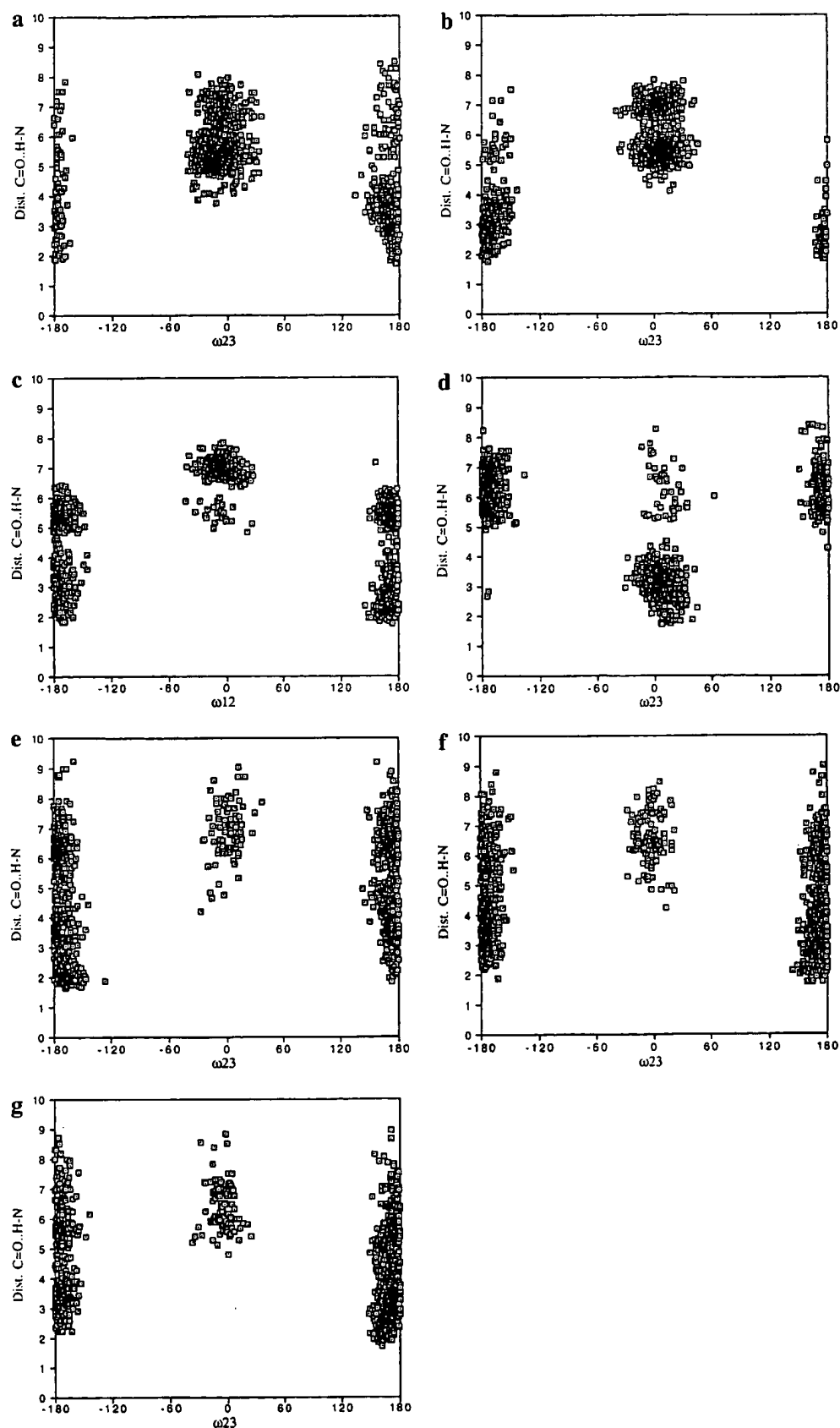


**Figure 2.** Distance  $d$  (Å) between the carbonyl oxygen of residue 1 and the amide hydrogen of residue 4 versus  $\omega_{23}$  or  $\omega_{12}$  for selected tetrapeptides: Ac-Ala-Pro-D-Pro-Ala-NMe (a), Ac-Ala-D-Pro-Pro-Ala-NMe (b, c), Ac-Ala-Pro-Pro-Ala-NMe (d), Ac-Ala-Pro-D-NMeAla-Ala-NMe (e), Ac-Ala-D-Pro-NMeAla-Ala-NMe (f), Ac-Ala-D-Pro-Pip-Ala-NMe (g). In each case samples were taken at 1 ps intervals during 1000 ps of the Monte Carlo/stochastic dynamics simulations in GB/SA water.

conformational restrictions caused by this sequence are clear in plots of  $\Phi$  versus  $\Psi$  for residues  $i + 1$  and  $i + 2$  (Figure 3, a and b, respectively), indicating the enhanced propensity of this sequence for the type II'  $\beta$ -turn. Figure 3b shows the decreased restrictions for  $\Phi_3$  versus  $\Psi_3$  with the new AMBER\* all-atom parameters compared to the result<sup>66</sup> with the original AMBER\* all-atom parameters. Figure 4a shows a plot of the distance  $d$  versus potential energy for this tetrapeptide. The distance  $d$  is restricted to be under 7 Å. Figure 5a shows the restriction of  $\beta$  in the D-Pro-NMeAla sequence. Figure 6a shows that the hydrogen bond between residues  $i$  and  $i + 3$  of a  $\beta$ -turn is present in the lower energy conformers obtained from the D-Pro-NMeAla simulation.

Clearly from these results, the presence of proline at position  $i + 2$  is not necessary for the induction of tight  $\beta$ -turns. In fact, the enhanced  $\beta$ -turn propensity of these sequences reflects the fact that the angles  $\Phi_3$  and  $\Psi_3$  are less restricted than in proline and can assume values closer to those of an ideal Type II or II' turn.

**Ac-Ala-D-Pro-Pip-Ala-NHMe.** To see if increasing the ring size of residue  $i + 2$  would allow conformations more compatible with  $\beta$ -turns by allowing a wider variation in  $\Phi_3$  and  $\Psi_3$ , we examined the effect of replacing proline by pipercolic acid (Pip, homoproline), which contains a 6-membered ring. Ac-Ala-D-Pro-Pip-Ala-NHMe showed better stabilization by all three criteria compared to the two proline model compounds and D-Pro-NMeAla sequence. Table 2 shows that the percentage of conformers for Ac-Ala-D-Pro-Pip-Ala-NHMe where  $|\beta| < 30^\circ$  is 62% and the percentage with  $d$  less than 7 Å is 74%; the percentage of conformers with hydrogen bonding between residues 1 and 4 has risen to 47% and 7%. Figure 2g shows that  $\omega_{23}$  of all conformers where distances are less than 4 Å is *trans*. In contrast to Ac-Ala-D-Pro-Pro-Ala-NHMe (Figure 2b),  $\omega_{23}$  of most conformers where distances are more than 4 Å is also *trans*.

**Ac-Ala-Pro $\psi$ [CN<sub>4</sub>]-Ala-Ala-NHMe.** Marshall *et al.* showed that the tetrazole ring system, when incorporated into peptides, mimics a *cis* amide bond by X-ray crystal structure of Z-Pro $\psi$ -[CN<sub>4</sub>]-Ala-OBzl.<sup>52,53</sup> We investigated the sequence Ac-Ala-Pro $\psi$ [CN<sub>4</sub>]-Ala-Ala-NHMe containing the tetrazole ring (Figure 8). Table 2 shows that  $|\beta|$  is less than  $30^\circ$  in 26% of the MC/SD structures and 40% have a C $\alpha$ 1–C $\alpha$ 4 distance of less than 7 Å. The amide hydrogen and carbonyl oxygen are less than 4 and 2.5 Å apart in 15% and 5% of the sampled structures, respectively. These values for the percentage of three criteria are between the Pro-Pro sequence where the *cis*-amide conformer for  $\omega_{23}$  is stable and the D-Pro-D-Pro sequence where the *trans*-amide conformer is stable (Table 1).

**Ac-Ala-Pro-D-NOHAla-Ala-NHMe and Ac-Ala-D-Pro-NOHAla-Ala-NHMe.** To investigate whether an *N*-hydroxy-substituted amino acid (NOHAA) was sufficient for turn induction, we investigated tetrapeptides containing NOHAla. These studies were stimulated by the experimental work of the Marraud group.<sup>85</sup> Ac-Ala-Pro-D-NOHAla-Ala-NHMe had lower values for the percentage of hydrogen-bonded conformers (4%, 1%) and conformers with  $d$  under 7 Å (7%) and with  $|\beta|$  under  $30^\circ$  (0%) compared to Ac-Ala-Pro-D-NMeAla-Ala-NHMe (Table 2). A plot of  $\omega_{23}$  against  $\omega_{12}$  (Figure 7) shows that  $\omega_{23}$  of most conformers is *cis*. Some reduction of turn induction was due to the stabilization of the *cis* conformer for  $\omega_{23}$ . For Ac-Ala-D-Pro-NOHAla-Ala-NHMe,  $|\beta|$  is less than  $30^\circ$  in only 2% of the MC/SD structures and  $d$  is less than 7 Å in 2%. The

percentages of conformers with the characteristic hydrogen bond are also only 2% and 0%.

**Ac-Ala-Pro-NOHAla-Ala-NHMe and Ac-Ala-D-Pro-D-NOHAla-Ala-NHMe.** It was found that, in the case of Ac-Ala-Pro-NOHAla-Ala-NHMe and Ac-Ala-D-Pro-D-NOHAla-Ala-NHMe, there was significant turn stabilization. Table 2 shows that, for Ac-Ala-Pro-NOHAla-Ala-NHMe,  $|\beta|$  is less than  $30^\circ$  in 41% of the MC/SD structures and 78% have a C $\alpha$ 1–C $\alpha$ 4 distance of less than 7 Å. During the MC/SD simulation the carbonyl oxygen of residue  $i$  and the amide hydrogen of residue  $i + 3$  were less than 4 and 2.5 Å apart in 48% and 23% of the sampled conformers, respectively, the higher value for other tetrapeptides. Swapping the chirality of residues  $i + 1$  and  $i + 2$  to give Ac-Ala-D-Pro-D-NOHAla-Ala-NHMe had lower values for the percentage of hydrogen-bonded conformers (40%, 14%), conformers with  $d$  under 7 Å (72%), and conformers with  $|\beta| < 30^\circ$  (25%), but still appears to be a highly effective turn inducer.

**Piv-Pro-NOHGly-NHiPr.** The stabilization of the *cis* conformer for  $\omega_{23}$  in the tetrapeptides containing NOHAla is not consistent with the X-ray and NMR studies of Dupont *et al.*, who found that *N*-hydroxylation or *N*-amination of an amide bond within RCO-Pro-Gly-NHiPr seems to have no tendency to induce a *cis* conformation of the modified peptide bond.<sup>85</sup> The relevant structural data of the *N*-hydroxy amide were obtained by searching the Cambridge Structural Database (CSD).<sup>86,87</sup> Among 23 *N*-hydroxy amide analogues in CSD, there were only two structures<sup>88,89</sup> which have the *cis* amide bond.

We investigated several force fields for the *N*-hydroxy analogue of RCO-Pro-Gly-NHiPr (Me<sub>3</sub>CCO-Pro-NOHGly-NHiPr). There are no parameters for *N*-hydroxy amide in either the MM2\* force field or the MM3\* force field. As shown in Table 3, the results (98% *trans* in water and 91% *trans* in CHCl<sub>3</sub>) from only the MMFF\* force field for *cis*–*trans* isomerism of the amide bond ( $\omega_{23}$ ) are consistent with the X-ray result<sup>85</sup> due to the high-quality parameters for the *N*-hydroxy amide group in the MMFF\* force field.<sup>77–81</sup> There are no specific parameters for the *N*-hydroxy amide in either the AMBER\* all-atom force field or the AMBER/OPLS\* united-atom force field. The AMBER\* all-atom force field in CHCl<sub>3</sub> had higher values for the percentage of hydrogen-bonded conformers (82%) and conformers with  $d$  under 7 Å (80%) compared to those of the AMBER\* all-atom force field in water (Table 3).

### Comparison with Other Reverse-Turn Peptidomimetics

**BTD dipeptide.** The dipeptide mimetic BTD (Figure 8) designed and prepared by Nagai *et al.*<sup>25</sup> has been incorporated at positions thought to require a reverse turn for recognition in a number of biologically active peptides with varying success. This 6,5-bicyclic ring system is composed of a six-membered ring annulated onto thioproline. The percentage of conformers for Ac-Ala-BTD-Ala-NHMe in which  $|\beta|$  is less than  $30^\circ$  is 69%, a higher value than those of other tetrapeptides. The percentage where  $d$  is less than 7 Å is 33%. Importantly, no

(86) Allen, F. H.; Bellard, S.; Brice, M. D.; Cartwright, B. A.; Doubleday, A.; Higgs, H.; Hummelink, T.; Hummelink-Peters, B. G.; Kennard, O.; Motherwell, W. D. S.; Rodgers, J. R.; Watson, D. G. *Acta Crystallogr.* 1979, B35, 2331.

(87) Allen, F. H.; Kennard, O.; Taylor, R. *Acc. Chem. Res.* 1983, 16, 146.

(88) Nishio, T.; Tanaka, N.; Hirotake, J.; Katsube, Y.; Ishida, Y.; Oda, J. *J. Am. Chem. Soc.* 1988, 110, 8733–8734.

(89) Obodovskaya, A. E.; Starikova, Z. A.; Eliseeva, L. N.; Pokrovskaya, I. E. *Kristallografiya* 1993, 38, 236.

(85) Dupont, V.; Lecoq, A.; Mangeot, J.-P.; Aubry, A.; Boussard, G.; Marraud, M. *J. Am. Chem. Soc.* 1993, 115, 8898–8906.

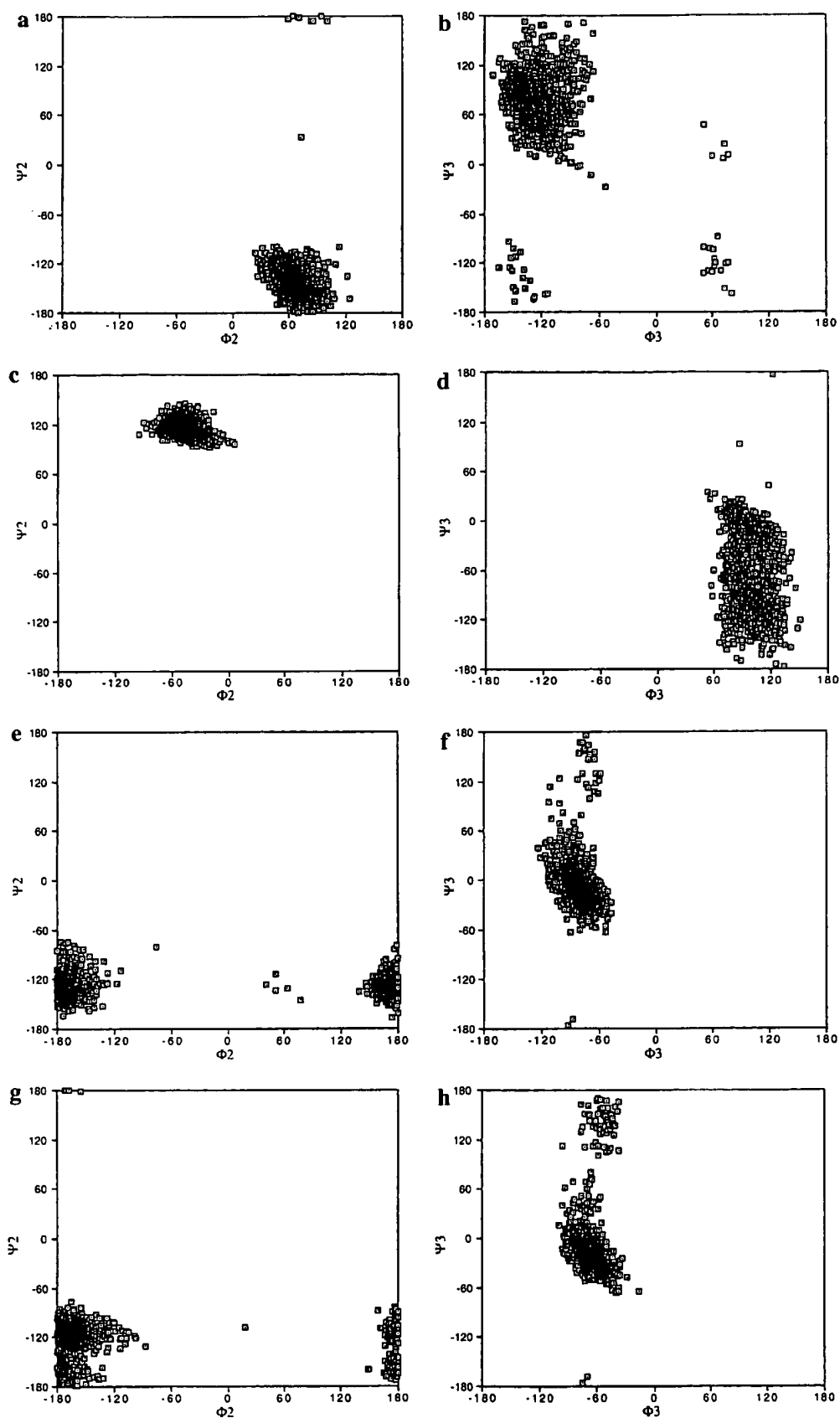


**Figure 3.** Plots of the backbone torsion angle  $\Phi_2$  versus  $\Psi_2$  and  $\Phi_3$  versus  $\Psi_3$  during the Monte Carlo/stochastic dynamics simulation for selected tetrapeptides: Ac-Ala-D-Pro-NMeAla-Ala-NMe (a, b), Ac-Ala-spirotricyclic-Ala-NMe (c, d), Ac-Ala-(R)-indolizidinone-Ala-NMe (e, f), and Ac-Ala-(S)-indolizidinone-Ala-NMe (g, h).

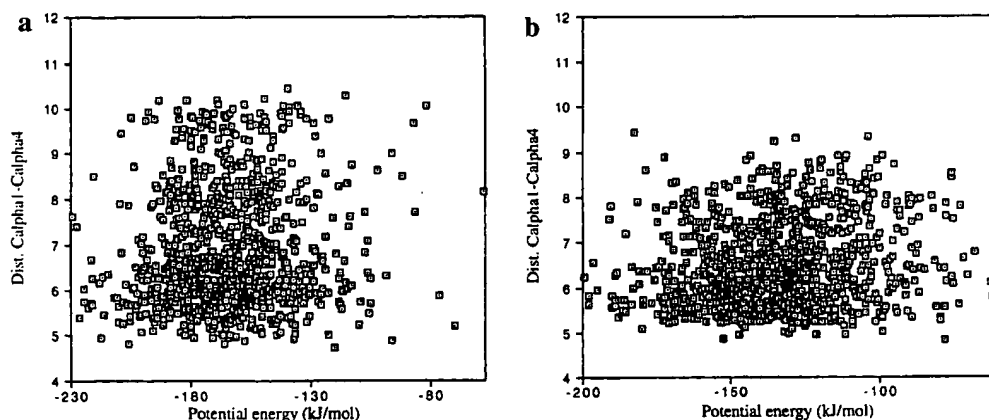


**Figure 4.** Plots of the distance between C $\alpha$ 1 and C $\alpha$ 4 versus potential energy during the Monte Carlo/stochastic dynamics simulation for (a) the restricted tetrapeptide Ac-Ala-D-Pro-NMeAla-Ala-NMe and (b) Ac-Ala-spirotricyclic-Ala-NMe which contains a rigid peptidomimetic.

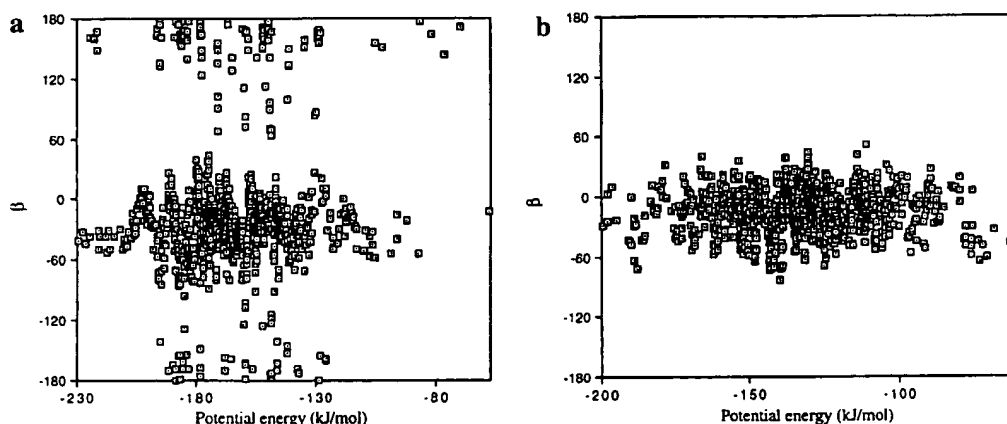


**Figure 5.** Plots of the  $\beta$ -turn parameter  $\beta^{22}$  versus potential energy during the Monte Carlo/stochastic dynamics simulation for (a) Ac-Ala-D-Pro-NMeAla-Ala-NMe and (b) Ac-Ala-spirotricyclic-Ala-NMe which are tightly constrained to adopt turn-like conformations.

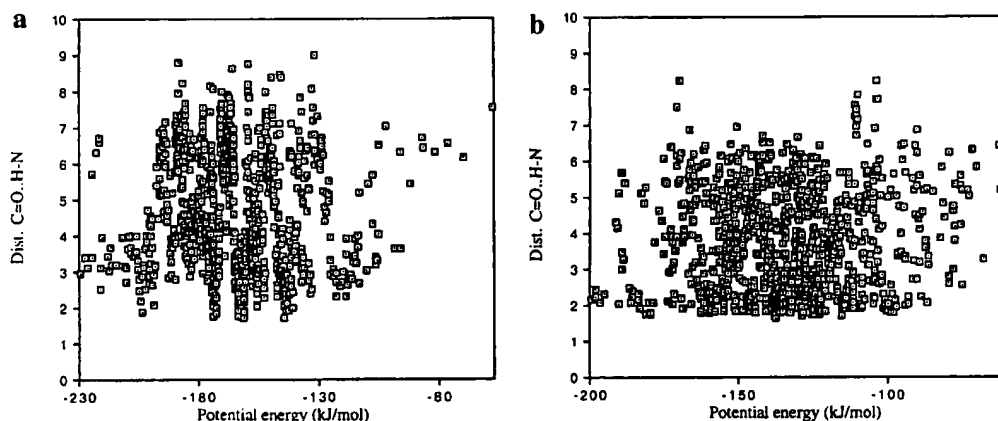


**Figure 6.** Plots of the distance  $d$  (Å) between the carbonyl oxygen of residue 1 and the amide hydrogen of residue 4 versus potential energy during the Monte Carlo/stochastic dynamics simulation for (a) Ac-Ala-D-Pro-NMeAla-Ala-NMe and (b) Ac-Ala-spirotricyclic-Ala-NMe.

interaction was observed between the carbonyl oxygen of residue  $i$  and the amide hydrogen of residue  $i + 3$ . The percentage of conformers where  $d_{O-H}$  is less than 4 Å is 0% (Table 2). These results suggest that the geometry of a turn induced by BTD differs significantly from that of an ideal  $\beta$ -turn. It would be inappropriate, therefore, to utilize BTD to initiate a  $\beta$ -hairpin peptide conformation.

**S-Spirolactam Compound.** These spiro lactam bicyclic proline derivatives (Figure 8) in which an  $\alpha$ -alkyl substituent on the pyrrolidine ring is cyclized to the amide nitrogen of the adjacent amino acid can be considered chimeras of the cyclic lactam of Freidinger et al.<sup>35</sup> and  $\alpha$ -methyl-Pro.<sup>37,42</sup> This bicyclic

constraint restricts both  $\Phi$  and  $\Psi$  of the spiro derivative. Table 2 shows that for Ac-Ala-S-spirolactam-Ala-NHMe, 48% of conformers had  $|\beta|$  less than 30° and 48% had values of  $d$  lower than 7 Å. The percentages of conformers with an appropriate distance for the hydrogen bond characteristic of the  $\beta$ -turn are 47% and 16%, which are higher values than those for other tetrapeptides. These results are consistent with the NMR studies in DMSO of the cyclic pseudopentapeptide (c(Arg-Gly-Asp-spiro)).<sup>18</sup>

**Spirotricyclic Compound.** Genin and Johnson<sup>38,90</sup> have combined the spiro lactam constraint with annulation of a

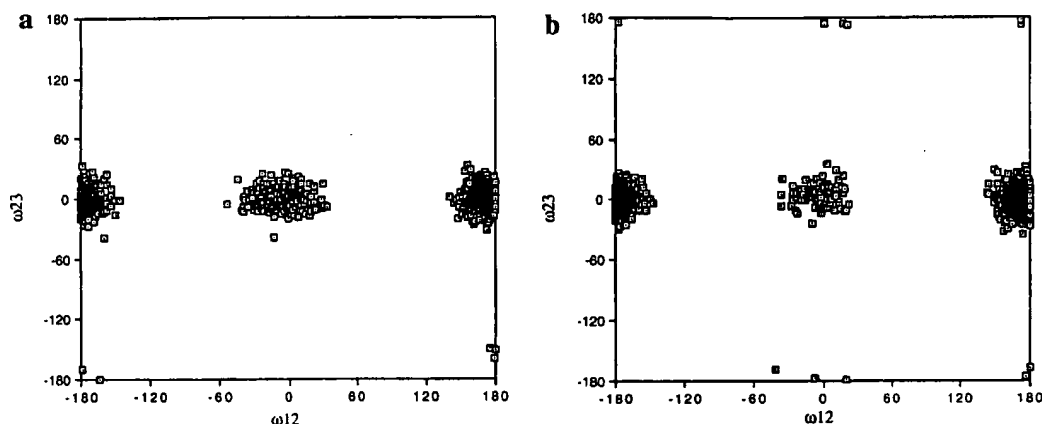


Figure 7. Plot of the backbone torsion angle  $\omega_{12}$  versus  $\omega_{23}$  during the Monte Carlo/stochastic dynamics simulation for Ac-Ala-Pro-D-NOHAla-Ala-NMe.

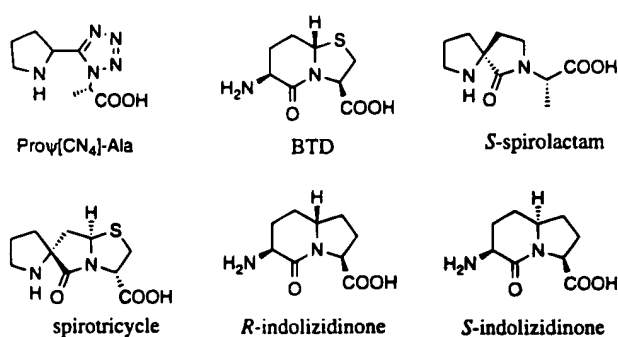


Figure 8. Structures of nonpeptidic reverse turn mimetics.

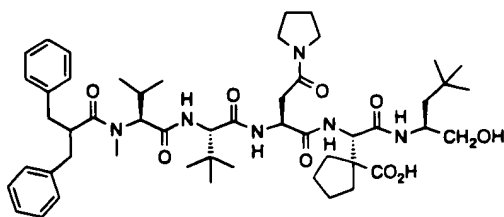


Figure 9. Structure of BILD 1263.

Table 3. Percentage of Conformers of Me<sub>3</sub>CCO-Pro- $\omega$ -NOHGly-NHiPr Which Exhibit Characteristics of a Reverse Turn and  $\omega$  *trans* Form During 1000 ps MC/SD Simulations Using MacroModel 5.5

	% $ \beta $ < 30°	% $d$ < 7 Å	% $d$ (C=O...H-N) < 4 Å	% $\omega$ <i>trans</i> form
in water				
AMBER* all-atom	19	30	25	0
MMFF*	9	6	8	98
in CHCl <sub>3</sub>				
AMBER* all-atom	69	80	82	12
AMBER/OPLS*	27	25	21	0
MMFF*	29	34	25	91

thioalkyl ring similar to BTD, generating a spirotricyclic ring system (Figure 8) that restricts  $\Phi_2$ ,  $\Psi_2$ , and  $\Phi_3$ . Plots of  $\Phi_2$  versus  $\Psi_2$  and  $\Phi_3$  versus  $\Psi_3$  for the MC/SD simulation of Ac-Ala-spirotricyclic-Ala-NHMe are shown in Figure 3, plots c and d. These figures show that the spirotricyclic tightly constrains all the backbone angles except  $\Psi_3$ . A plot of the distance between C $\alpha$ 1 and C $\alpha$ 4 versus potential energy for the MC/SD simulation (Figure 4b) shows that mimetic effectively constrains

this parameter ( $d < 7$  Å, 71%). Figure 5 shows the dramatic restriction of  $\beta$  in the spirotricyclic mimetic (plot b,  $|\beta| < 30^\circ$ , 76%) compared to the D-Pro-NMeAla tetrapeptide (plot a). These may be due to the highest percentage (Table 2) of hydrogen-bonded conformers ( $d < 4$  Å, 57%,  $d < 2.5$  Å, 27%, Figure 6b) for any of the model compounds, implying an excellent  $\beta$ -turn mimetic. These results are consistent with the modeling studies and NMR studies in CDCl<sub>3</sub> of the spirotricyclic analog<sup>38</sup> due to three restrictions ( $\Phi_2$ ,  $\Psi_2$ , and  $\Phi_3$ ) of the four torsion angles that characterize the type II  $\beta$ -turn.

**Indolizidinone Compounds.** Lombart and Lubell<sup>36</sup> prepared bicyclic turn mimetics containing the indolizidinone ring system (Figure 8). Plots e and f in Figure 3 show Ac-Ala-(*R*)-indolizidinone-Ala-NHMe has only rigidified  $\Psi_2$  and  $\Phi_3$ , while the spirotricyclic constrains all the backbone angles except  $\Psi_3$  shown in Figure 3, plots c and d. The percentage (Table 2) of conformers in which  $|\beta|$  is less than 30° is 78%, the highest value for any of the model compounds. The percentage of conformers with the distance C $\alpha$ 1–C $\alpha$ 4 less than 7 Å was also high (58%). However, like BTD (Table 3) the percentage of conformers with the *i* to *i* + 3 hydrogen bond is very low (1%, 0%).

Modifying the chirality of this compound gave more significant results. Plots g and h in Figure 3 show Ac-Ala-(*S*)-indolizidinone-Ala-NHMe has only rigidified  $\Psi_2$  and  $\Phi_3$ . The percentage (Table 2) of conformers in which  $|\beta|$  was less than 30° was 77% and the percentage with  $d$  under 7 Å was 85%, which was the highest value for any of the model compounds. No interaction was observed between the carbonyl oxygen of residue *i* and the amide hydrogen of residue *i* + 3 (0%, 0%).

However, the hydrogen bond between the amide hydrogen of residue *i* + 1 and the carbonyl oxygen of residue *i* + 3 was found in the lowest energy conformation. These results are consistent with the NMR studies in DMSO of the cyclic pseudopentapeptide (c(Arg-Gly-Asp-BTD)).<sup>18</sup> These results suggest that the geometry of a turn induced by BTD and indolizidinone differs significantly from that of an ideal  $\beta$ -turn and that (*S*)-indolizidinone is more effective as a reverse turn than other  $\beta$ -turn mimetics.

**BILD1263.** Moss et al.<sup>91</sup> have reported a new class of peptidomimetic inhibitor, BILD 1263 (Figure 9), effective against herpes simplex virus (HSV) *in vitro* and *in vivo*. To investigate whether the Monte Carlo/stochastic dynamics simulations roughly represent the conformers present in aqueous

(90) Genin, M. J.; Mishra, R. K.; Johnson, R. L. *J. Med. Chem.* **1993**, *36*, 3481–3483.

(91) Moss, N.; Beaulieu, P.; Duceppe, J.-S.; Ferland, J.-M.; Gauthier, J.; Ghio, E.; Goulet, S.; Grenier, L.; Llinas-Brunet, M.; Plante, R.; Wernic, D.; Déziel, R. *J. Med. Chem.* **1995**, *38*, 3617–3623.

solution, the simulation using the GB/SA water model was performed on BILD 1263. Table 2 shows that, for BILD 1263,  $|\beta|$  is less than  $30^\circ$  in only 9% of the MC/SD structures and only 6% have a C $\alpha$ 1–C $\alpha$ 4 distance of less than 7 Å. No interaction was observed between the carbonyl oxygen of residue  $i$  and the amide hydrogen of residue  $i + 3$  (0%, 0%). These three measures of reverse-turn propensity reflect predominately extended structures. The distance between the amide hydrogen of *tert*-butyl in residue 2 and the  $\alpha$ -hydrogen of valine in residue 1 is 1.9 Å in the lowest energy conformation. The *N*-methyl hydrogen of valine in residue 1 is 2.1 Å apart from the  $\beta$ -hydrogen of valine in residue 1 and the  $\alpha$ -hydrogen of *N*-terminal dibenzylacetyl. These results are consistent with NOE data of the NMR studies of Moss et al.<sup>90</sup> It was found that the distance between the *N*-methyl hydrogen of valine in residue 1 and the  $\alpha$ -hydrogen of *N*-terminal dibenzylacetyl is 4.3 Å due to *cis*-amide in the second lowest minimum energy conformation (13 kJ/mol higher than the lowest energy conformer).

**Cyclo(D-Pro-L-Pro-D-Pro-L-Pro).** We studied cyclo(D-Pro-L-Pro-D-Pro-L-Pro) where Chalmers and Marshall with the original AMBER\* parameters found a poor correlation with experiment.<sup>67</sup> This cyclic tetrapeptide is well characterized in water solution and in the solid state<sup>92</sup> and was found to exist exclusively in a conformation having alternating *cis*- and *trans*-amide bonds: the *cis-trans-cis-trans* (*ctct*) conformation. McDonald and Still reevaluated the conformational preferences of this compound using new AMBER\* all-atom parameters in GB/SA water.<sup>68</sup> The authors found that all conformations within 3 kcal/mol of the global minimum have the experimentally observed *ctct* structure. To compare this result with the new AMBER\* all-atom parameters, we performed the conformational search of this cyclic tetrapeptide with the MMFF\* all-atom force field in GB/SA water. From this search we found that all conformations within 4 kcal/mol of the global minimum have the experimentally observed *ctct* structure.

## Conclusions

As noted above, Monte Carlo searches on the model blocked tetrapeptides of the type Ac-Ala-Pro-Pro-Ala-NHMe with the new AMBER\* parameters show differences from the results with the original AMBER\* parameters. The new set of AMBER\* parameters specifically for proline residues generally decreases the *cis-trans* energy differences for the amide bond. When Monte Carlo/stochastic dynamics simulations from the GB/SA solvation model were performed, calculated observables such as the reverse-turn forming ratios are found to be generally in good agreement with available experimental data measured in solution.

*N*-Methylation and *N*-hydroxylation of the amide bond between residues  $i + 1$  and  $i + 2$  can be used as effective

reverse-turn constraints with D-Pro-NMe-amino acid being a specific example. Constraints by the introduction of two proline residues (Pro-D-Pro or D-Pro-Pro) destabilize the  $\beta$ -turn propensity compared to *N*-methyl and *N*-hydroxy analogues of Pro-Ala, or the larger ring homolog pipecolic acid, which contains a six-membered ring in the third position ( $i + 2$ ) (D-Pro-Pip). Surprisingly, swapping the chirality of only one residue (Pro-Pro) results in the higher percentages of conformers which can be classified as type VIa  $\beta$ -turns than those of Pro-D-Pro or D-Pro-Pro due to the stabilization of the *cis* conformer of the amide bond between residues  $i + 1$  and  $i + 2$ . Simple inclusion of *N*-methylation and *N*-hydroxylation of the amide bond between residues  $i + 1$  and  $i + 2$  and the larger ring homolog pipecolic acid in the third position ( $i + 2$ ) causes significant nucleation of reverse-turn structures.

Spirotricyclic restricts three of the four torsion angles that make up a type II  $\beta$ -turn. Spirolactam also restricts two of the four torsion angles as effective  $\beta$ -turn constraints. However, no interaction was observed between the carbonyl oxygen of residue  $i$  and the amide hydrogen of residue  $i + 3$  in (*R*)-indolizidinone, (*S*)-indolizidinone, and BTD, while the hydrogen bond between the amide hydrogen of residue  $i + 1$  and the carbonyl oxygen of residue  $i + 3$  was found in the lowest energy conformation of (*S*)-indolizidinone. These unexpected results show that the geometry of a turn induced by indolizidinone and BTD differs significantly from that of an ideal  $\beta$ -turn and (*S*)-indolizidinone is more effective as a reverse turn than as a  $\beta$ -turn mimetic. We believe that these non-peptide systems can serve as a useful conformational constraint that, when incorporated into the structure of selected bioactive peptides, will yield new conformationally constrained peptide analogs for combinatorial libraries and structure–activity relationship studies.

The compounds with inclusion of such constraints, predetermined conformational effects, and accessible synthetic routes to fixed side chain placement provide ideal structural probes for applications in combinatorial libraries. Analysis of activity from screening of such libraries can be used to test for a consistent hypothesis concerning the receptor-bound conformation of the parent peptide. This hypothetical conformation can then be used to select additional classes of modifications (cyclization, new scaffold, etc.) to be included in further optimization of the receptor-bound conformation as well as the pharmacological properties.

**Acknowledgment.** The authors thank the National Institutes of Health for partial support of this work (GM-24883 and GM-48184) as well as Richard Head, David K. Chalmers, David Lewis, and Yang C. Fann of the Center for Molecular Design for technical support. We also gratefully acknowledge discussions with D. Quentin McDonald at Columbia University on the new AMBER\* parameters for proline.

JA970855K

(92) Mastle, W.; Weber, T.; Thewalt, U.; Rothe, M. *Biopolymers* **1989**, *28*, 161–174.

## “Libraries from libraries”: Chemical transformation of combinatorial libraries to extend the range and repertoire of chemical diversity

(transformation/peralkylated combinatorial libraries/permethylated peptides/peptide library/antimicrobial)

JOHN M. OSTRESH\*, GREGORY M. HUSAR\*, SYLVIE E. BLONDELLE\*, BARBARA DÖRNER\*,  
PATRICIA A. WEBER†, AND RICHARD A. HOUGHTEN\*‡

\*Torrey Pines Institute for Molecular Studies, San Diego, CA 92121; and †Houghten Pharmaceuticals, San Diego, CA 92121

Communicated by Bruce Merrifield, April 21, 1994 (received for review November 15, 1993)

**ABSTRACT** The generation of diverse chemical libraries using a “libraries from libraries” concept is described. The central features of the approaches presented are the use of well-established solid-phase synthesis methods for the generation of combinatorial libraries, combined with the chemical transformation of such libraries while they remain attached to the solid support. The chemical libraries that are generated by this process have very different physical, chemical, and biological properties compared to the libraries from which they were derived. A wide range of chemical transformations are possible for peptide-based or other libraries, and an almost unlimited range of useful chemical diversities can be envisioned. In the example presented, the amide functionalities in an existing combinatorial library made up of peptides were permethylated while the library remained attached to the solid-phase support used in its synthesis. After removal of the permethylated mixtures from their solid support, this library, now lacking the typical -CONH- amide bonds of peptides, can be tested in solution with virtually all existing assay systems to identify individual compounds having specific biological activities of interest. An illustration of the use of such libraries is presented, in which the described permethylated library was used to identify individual permethylated compounds having potent antimicrobial activity against Gram-positive bacteria.

Recent innovations in peptide chemistry and molecular biology have enabled libraries consisting of tens to hundreds of millions of peptide sequences to be prepared and used to identify highly active, individual sequences. Such libraries can be divided into three broad categories. (i) One category of libraries involves the chemical synthesis of soluble non-support-bound peptide and peptoid libraries (1–3). (ii) A second category involves the chemical synthesis of support-bound peptide libraries composed of L- or D-amino acid sequences presented on solid supports such as plastic pins (4), resin beads (5), or cotton (6). (iii) A third category uses molecular biology approaches to prepare peptides or proteins on the surface of filamentous phage particles or plasmids (7). More recently, the production of small collections of non-peptidic compounds has been described (8–10).

As first presented by this laboratory, soluble, nonsupport-bound peptide libraries [termed synthetic peptide combinatorial libraries (SPCLs)] appear to be usable in virtually all *in vitro* and even *in vivo* assays. Combinatorial libraries of peptides composed of entirely L-amino acids, entirely D-amino acids, or mixtures of L-, D-, and unnatural amino acids have been developed by using this approach. The successful use of these libraries has been reported for the study of antibody/antigen interactions (1, 2) and for the

development of receptor-active opioid peptides (11, 12), enzyme inhibitors (6), and antimicrobial agents (1). The recent development of the soluble positional scanning (PS) approach for the production and screening of SPCLs (2, 12) enables individual, biologically active peptides to be identified in a single screening assay.

In a continuing effort to expand the available repertoire of chemical diversities, we present here an example of a soluble chemical library obtained by the chemical transformation of an existing peptide library. This library, prepared in a positional scanning format, is composed of fully permethylated compounds derived from the direct chemical modification of resin-bound peptide libraries. To our knowledge, a study of individual peptides being permethylated while attached to solid-phase synthesis resins has not yet been reported. The use of chemically transformed libraries is illustrated here by the use of this permethylated PS-SPCL for the identification of potent individual compounds selectively active against the Gram-positive bacteria *Staphylococcus aureus* and *Streptococcus sanguis*.

### MATERIALS AND METHODS

The benzyl protecting group was used for the side-chain protection of asparagine, glutamate, serine, and threonine; methoxybenzyl for cysteine; dinitrophenyl for histidine; chlorobenzylloxycarbonyl for lysine; sulfoxide for methionine; tosyl for arginine; formyl for tryptophan; and bromobenzylloxycarbonyl for tyrosine. Other reagents and materials used have been described (13).

**Permethylated of Protected Peptides.** Twenty model peptide resins (110 mg, 0.1 milliequivalent each) with defined sequences (represented as OGGFL-resin, “O” individually representing each of the 20 naturally occurring amino acids) were prepared on methylbenzhydrylamine resin (MBHA) (0.90 milliequivalent per g) using *t*-butoxycarbonyl (Boc) chemistry combined with simultaneous multiple peptide-synthesis techniques as described (13). After removal of the final *N*- $\alpha$ -Boc protecting group, each of the side-chain-protected resins were then permethylated as described below. The resin-bound PS-SPCL was prepared as described (2, 12).

In a typical example, AGGFL-mBHA resin (90 mg, 0.1 milliequivalent), contained within an individual polypropylene mesh packet (13), was shaken on a reciprocating shaker (Eberbach, Ann Arbor, MI) at 25°C for 16 hr in a 0.25 M

Abbreviations: PS, positional scanning; RP-HPLC, reversed-phase high-performance liquid chromatography; SPCL, synthetic peptide combinatorial library; MRSA, methicillin-resistant *Staphylococcus aureus*. All amino acids used were of the L configuration unless otherwise noted.

‡To whom reprint requests should be addressed.

The publication costs of this article were defrayed in part by page charge payment. This article must therefore be hereby marked “advertisement” in accordance with 18 U.S.C. §1734 solely to indicate this fact.

solution of NaH/dimethyl sulfoxide (32 ml, 8 milliequivalents). Neat methyl iodide (1.5 ml, 24 milliequivalents) was then added to the reaction mixture, and the methylation reaction allowed to proceed for 15 min at 25°C. After successive washes with dimethylformamide (three times, 5 ml), isopropanol (two times, 5 ml), dichloromethane (three times, 5 ml), and methanol (once, 5 ml), the resin was dried under high vacuum. The resin-bound permethylated peptide was cleaved by using 7.5% (vol/vol) anisole/HF (5 ml) for 1 hr at 0°C, dried under high vacuum, extracted with 10 ml of water, and lyophilized. The permethylated peptide was assayed for purity by reversed-phase high-performance liquid chromatography (RP-HPLC) and identified by laser desorption-mass spectral analysis (Kratos). Individual compounds were purified using preparative RP-HPLC. The PS-SPCL was permethylated, cleaved, and analyzed similarly.

**Biological Assays.** Individual permethylated compounds and their nonpermethylated counterparts were assayed for their resistance to proteolytic breakdown by trypsin and chymotrypsin. The assays were done in 1 ml of 0.1 M  $\text{NH}_4\text{HCO}_3$ , pH 7.8, at room temperature for 16 hr at a peptide concentration of 1.0 mg/ml. Enzyme-to-peptide concentration was 1:50. The degradation reaction was monitored by RP-HPLC.

The strains *S. aureus* ATCC 29213, methicillin-resistant *S. aureus* (MRSA) ATCC 33591, *S. sanguis* ATCC 10566, *Escherichia coli* ATCC 25922, and *Candida albicans* ATCC 10231 were used in the bioassays. The assays were done in 96-well tissue culture plates (Costar) as described (14).

Hemolytic activity of the individual compounds identified was determined by using a 0.25% suspension of human red blood cells as described (15).

## RESULTS

**Optimization of Permethylation Conditions.** Various methods for permethylation have been described (16, 17). In such permethylations, strongly basic conditions are reported to favor N-methylation over O-methylation. Although unreported in these earlier studies, the synthetic conditions used also permit permethylation of peptides while they remain attached to the solid-phase resins used in their synthesis. The strength of the solid-phase approach (18) is that all excess reagents can be removed by simple wash procedures.

Satisfactory permethylation conditions for resin-bound peptides were studied using AGGFL-NH<sub>2</sub> due to its ease of synthesis, nonreactive side chains, and its availability from other ongoing studies (12). Temperature, reaction time, reagent ratios, and solvents were studied to determine the most effective and mildest conditions for the formation of the amide anions and their subsequent methylation. Temperatures studied ranged from 25°C to 60°C. Reaction times tested for the generation of the amide anions ranged from 20 min to 16 hr. It was found that while complete amide anion formation occurred within 16 hr at 25°C, higher temperatures led to degraded products, as evidenced by mass spectral analysis and RP-HPLC. Methylation reaction times examined ranged from 1 to 30 min. Because permethylation of a free  $\alpha$ -amino peptide leads to both methylation of the amide backbone and quaternary salt formation, it was necessary to study the relative rates of these two reactions. It was found that while methylation of the backbone amides was complete within the first minute, longer reaction times were required for the quaternary salt formation. Complete methylation of the backbone amide anions within the first minute was demonstrated with the use of Ac-AGGFL-NH<sub>2</sub>. Of the conditions tested, a 16-hr room-temperature treatment of the resin-bound protected peptides, using a 10-fold excess of NaH in dimethyl sulfoxide over the reactive sites of the resin-bound peptide, followed by a 15-min treatment of the resulting amide anions

with a 30-fold excess of methyl iodide over the reactive sites, yielded the best results (Fig. 1). Under these conditions AGGFL-NH<sub>2</sub> was obtained in permethylated form in >90% yield and purity.

**Permethylated Model Peptides.** Once the permethylation conditions had been selected, 20 model peptide resins (represented as OGGFL-NH<sub>2</sub>, where "O" is one of the 20 naturally occurring L-amino acids) were synthesized. Resin compartmentalization (13) permits the simultaneous permethylation of multiple peptide resins. Mass spectral and RP-HPLC analysis of an HF-cleaved aliquot of the nonpermethylated starting resins indicated that the average crude purity of the nonpermethylated peptides was >95%. The peptide resins were permethylated to determine the stability and susceptibility to modification of the 20 naturally occurring L-amino acids. Mass spectral analyses showed that the nitrogen of each amide bond was methylated, including the C-terminal amide resin linkage. In addition to the quaternization of the  $\alpha$ -amino group, small amounts of the mono- and dimethylated  $\alpha$ -amino products were also formed, generally to an extent of <15%. While a preliminary exhaustive N- $\alpha$ -methylation of the model peptides before the sodium hydride/methyl iodide treatment eliminated the mono- and dimethylated products, the strongly basic conditions used in the sodium hydride treatment gave partial Hoffman elimination of the quaternary salts formed. In contrast, while exhaustive N- $\alpha$ -methylation after the initial permethylation did not yield the byproducts associated with Hoffman elimination, the quaternization reaction was not driven to completion under the conditions used.

The subsequent cleavage of the permethylated model peptides from the resin yielded the desired products in ~90% purity for amino acids having nonreactive side chains (Fig. 2). Table 1 summarizes the number of methyl groups incorporated (including side-chain modifications) for each of the other analogs. Similar results were obtained using peptide resins in which the amino acid at the second position was varied, demonstrating the lack of a positional dependence on the modification of the side chains (data not shown).

Although the major product of the permethylation of the model peptide containing cysteine was the methyl thioether,

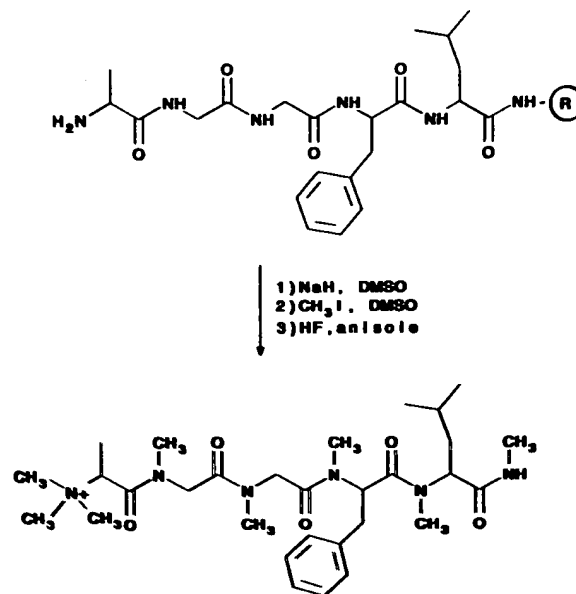


FIG. 1. Illustration of the method used for the permethylation of peptides. DMSO, dimethyl sulfoxide.

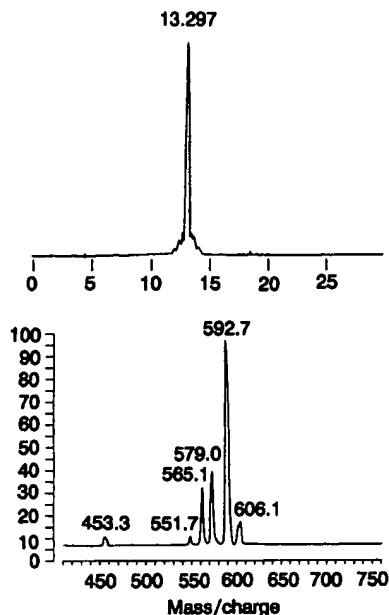


FIG. 2. RP-HPLC and mass spectral analysis of the permethylated form of SGGFL-NH<sub>2</sub>.

the presence of unmodified side chain suggests incomplete removal of the methoxybenzyl protecting group. It was found that the benzyl ester side-chain, protecting groups of aspartate and glutamate were removed during the sodium hydride treatment. The lower purity found suggests that internal cyclization of these compounds occurred (19). The dinitrophenyl protecting group of histidine was found to be removed by the sodium hydride treatment. Methylation of the histidine side chain gave two major products of identical molecular weight, which are assumed to be the  $\tau$ - and  $\pi$ -imidazole side-chain methylation products. The low purity of KGGFL-NH<sub>2</sub>, along with the presence of low-molecular-weight species as evidenced by mass spectral analysis, indicates additional byproducts are due to internal cleavage by nucleophilic attack of the  $\alpha$ -amino group on the peptide backbone.

The sulfoxide of methionine, which is stable to the reaction conditions, also serves to prevent the internal cleavage of the peptides via methyl sulfonium salts of methionine (20). Unexpectedly, some free methionine product was found resulting from reduction of the sulfoxide. The stability of the tosyl

group of arginine to the permethylation reaction resulted in three methyl groups being incorporated onto the guanidinium group of the arginine-containing peptide. The tosyl group was then removed during the standard high HF cleavage procedure (21). Methylation of the rings of aromatic amino acids (22) was not seen.

Treatment of the permethylated peptide resins by using standard low HF conditions (23) was found to result in partial cleavage of permethylated peptides from the resin. The lability of secondary amide bonds relative to primary amide bonds under acidic conditions is well documented (24, 26). In addition, the peptide remaining on the resin after low HF treatment was found to be substantially degraded as determined by RP-HPLC and mass spectral analysis after HF cleavage.

**Racemization Study.** From the literature, it is anticipated that the conditions used here for permethylation would result in minimal racemization or C $\alpha$ -methylation (17). Because the increased acidity of the C $\alpha$ -hydrogen of aromatic amino acids such as phenylalanine (17) makes them more prone to racemization and/or C $\alpha$ -methylation, a test series was devised in which the four possible stereoisomers of GGFL-NH<sub>2</sub> were synthesized and analyzed by RP-HPLC. An aliquot of the GGFL-NH<sub>2</sub> resin was treated with NaH/dimethyl sulfoxide to form the amide anions and then quenched by washing with 1% water/dimethyl sulfoxide. After amino acid cleavage from the resin, the maximum percentage of the D/L, L/D enantiomeric pair, as seen by RP-HPLC, was <0.75%, establishing that the extent of racemization, and therefore potential C $\alpha$ -methylation, was <1% (Fig. 3).

**Enzymatic Susceptibility.** The stability of N-permethylated compounds to proteolysis was examined for two permethylated sequences, AGGFL-NH<sub>2</sub> and RGGFL-NH<sub>2</sub>; their nonpermethylated equivalents were used as controls. Treatment of these four compounds by trypsin and chymotrypsin was monitored by RP-HPLC and mass spectral analysis. Rapid cleavage of AGGFL-NH<sub>2</sub> by chymotrypsin and RGGFL-NH<sub>2</sub> by trypsin was observed (<1 hr), whereas <1% cleavage of the equivalent permethylated peptides was seen after overnight enzyme exposure (3).

**Preparation of the Permethylated Library.** The six separate positional sublibraries of a resin-bound PS-SPCL (2), each consisting of 20 separate peptide mixtures, were permethylated and cleaved as described. The resulting library consisted of 120 hexamer mixtures, in which one position was defined by each of the 20 permethylated amino acids (represented as O), with the remaining five positions made up of mixtures of 18 permethylated amino acids (represented as X;

Table 1. Side-chain modifications of amino acids in permethylated peptides

Parent sequence	Parent $M_r$	Methylated $M_r$ found	Number methyls	Side-chain modification	Nonmethylated purity, <sup>†</sup> %	Methylated <sup>*</sup> purity, <sup>†</sup> %
CGGFL-NH <sub>2</sub>	494.8	620.8	9	Methyl thioether	86	50
DGGFL-NH <sub>2</sub>	506.7	633.6	9	Methyl ester	97	60
EGGFL-NH <sub>2</sub>	520.7	647.8	9	Methyl ester	90	75
HGGFL-NH <sub>2</sub>	528.8	655.8	9	Methyl imidazole	98	40
KGGFL-NH <sub>2</sub>	519.8	673.0	11	Quaternary salt	99	30
LGGFL-NH <sub>2</sub>	504.8	617.2	8	Unmodified	99	81
M(O)GGFL-NH <sub>2</sub>	538.8	651.8	8	Unmodified	98	70
NGGFL-NH <sub>2</sub>	505.7	646.9	10	Dimethyl amide	85	86
QGGFL-NH <sub>2</sub>	519.7	660.0	10	Dimethyl amide	85	80
RGGFL-NH <sub>2</sub>	703.3	547.8	11	Trimethyl guanidine	88	75
WGGFL-NH <sub>2</sub>	577.8	704.8	9	Methyl indole	98	70
YGGFL-NH <sub>2</sub>	554.8	681.5	9	Methyl ether	99	81

<sup>\*</sup>Sum of the mono-, di-, and trimethylated  $\alpha$ -amine products.

<sup>†</sup>Purity of the crude compounds as determined by analytical RP-HPLC. Repetition of these experiments showed a maximum variation of 20% from the values listed. Purities of the unlisted nonpermethylated model peptides were >99%; purities of the unlisted permethylated compounds were >90%. Side chains of the unlisted compounds were unmodified by permethylation treatment.

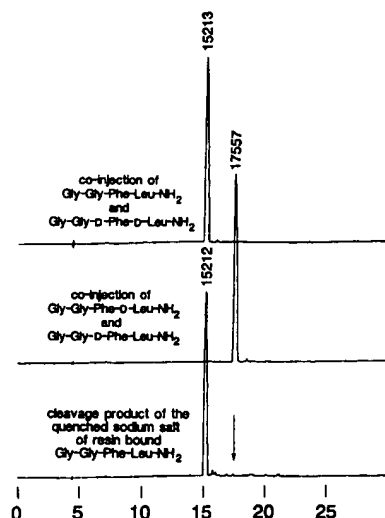


FIG. 3. RP-HPLC analysis of the four stereoisomers of GGFL-NH<sub>2</sub> after the formation and quenching of their amide anions by NaH. Arrow represents the retention time of the D/L and L/D stereoisomers.

cysteine and tryptophan were excluded). Each of the six permethylated sublibraries (represented as pm[OXXXXX], pm[XOXXXX], pm[XXOXXX], pm[XXXOXX], pm[XXXXOX], and pm[XXXXXO]) contained 37,791,360 ( $20 \times 18^5$ ) permethylated compounds in approximately equimolar amounts.

**Antimicrobial Activity.** Each of the 120 permethylated mixtures was assayed at an initial concentration of 2.5 mg/ml for its ability to inhibit the growth of *S. aureus*. A number of permethylated mixtures from each of the six libraries inhibited *S. aureus* growth (Fig. 4). None of the mixtures showed significant hemolytic activity or *in vitro* toxicity as determined by an MTT assay using McCoy cells ATCC 1696-CRL [MTT, 3-(4,5-dimethylthiazol-2-yl)-2,5-diphenyltetrazolium bromide] (25). The amino acids chosen at each of the defined positions from the most active permethylated mixtures were

used to generate a series of individual permethylated compounds. Peptides were thus synthesized and permethylated representing all combinations of the amino acids chosen for the first position (W, F, Y, H, I, L), the second position (F), the third position (W, I, F), the fourth position (W, F), the fifth position (F, H), and the sixth position (F, H). The resultant 144 individual, crude permethylated compounds were screened for their antimicrobial activity. Forty-one compounds had IC<sub>50</sub> values <50  $\mu$ g/ml, whereas 51 compounds had IC<sub>50</sub> values  $\geq$ 250  $\mu$ g/ml against *S. aureus*. Although the permethylated forms of FFIFFF-NH<sub>2</sub>, FFFFFFF-NH<sub>2</sub>, and LFIFFF-NH<sub>2</sub> exhibited the greatest activity of the series (Table 2), the quaternary trimethyl ammonium salt of nonpermethylated FFFFFFF-NH<sub>2</sub> showed no activity (IC<sub>50</sub> >250  $\mu$ g/ml). Similar activities were found against MRSA and *S. sanguis*, whereas none of the permethylated compounds or mixtures exhibited activity against *E. coli* or *C. albicans* (IC<sub>50</sub> values >600  $\mu$ g/ml) or showed significant toxicity as evidenced by lysis of red blood cells (<2% hemolysis at 100  $\mu$ g/ml). These compounds showed activities similar to a range of previously described peptides made up of L-amino acids (1). However, in contrast to the L-amino acid peptides, these compounds appear completely stable to proteolytic enzymes. Mass spectral and RP-HPLC analysis showed that, in some cases, incomplete methylation had occurred. For the permethylated form of FFFFFFF-NH<sub>2</sub>, similar antimicrobial activity was found after purification, suggesting that incompletely methylated byproducts also had antimicrobial activity.

The potent antimicrobial activity of the permethylated hexaphenylalanine prompted a study to determine the length at which a permethylated polyphenylalanine has the greatest antimicrobial activity. The set of compounds prepared varied in length from one to eight residues. The antimicrobial activities of these compounds against the two Gram-positive bacteria, *S. aureus* and *S. sanguis*, are shown in Table 2. Significant activities were found for those permethylated compounds having a length of at least five residues, with an optimal length of seven residues. In addition, the seven- and eight-residue permethylated polyphenylalanine compounds exhibited similar activities against MRSA.

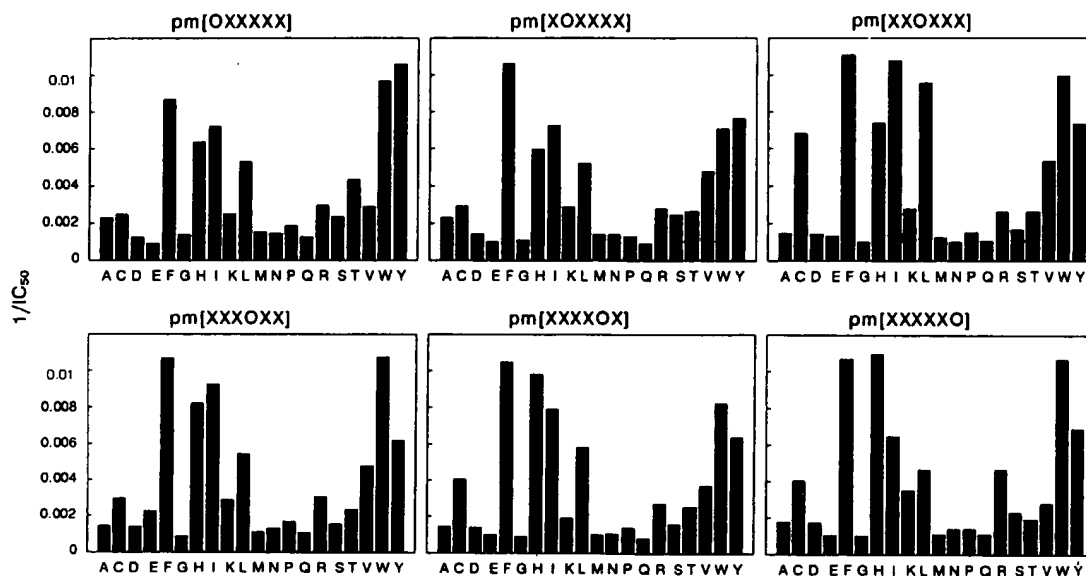


FIG. 4. Antimicrobial activity of the permethylated (pm-) PS-SPCL against *S. aureus*. Each individual bar represents the inverse of the IC<sub>50</sub> of a permethylated peptide mixture defined in the "O" position with one of the 20 naturally occurring amino acids.

Table 2. Antimicrobial and hemolytic activities of permethylated peptides derived from a permethylated SPCL

Parent sequence	<i>S. aureus</i>		<i>S. sanguis</i>	
	IC <sub>50</sub> , μg/ml	MIC, μg/ml	IC <sub>50</sub> , μg/ml	MIC, μg/ml
LFIFFF-NH <sub>2</sub>	6	11–15	1.7	3–5
FFIFFF-NH <sub>2</sub>	6	11–15	14	20–40
FFFFF-NH <sub>2</sub>	7	11–15	9	15–20
LFFFF-NH <sub>2</sub>	10	21–31	14	20–40
F-NH <sub>2</sub>	>500	>500	>500	>500
FF-NH <sub>2</sub>	>500	>500	>500	>500
FFF-NH <sub>2</sub>	288	>500	446	>500
FFFF-NH <sub>2</sub>	116	250–500	85	125–250
FFFFF-NH <sub>2</sub>	19	21–31	20	25–30
FFFFF-NH <sub>2</sub>	7	11–15	5	7–8
FFFFF-NH <sub>2</sub>	2.5	3–4	2.3	3–4
FFFFF-NH <sub>2</sub>	5	6–8	7	8–9

MIC, lowest concentration at which no growth is detected after 21-hr incubation.

## DISCUSSION

Biologically active peptides can now be readily identified through the use of SPCLs and PS-SPCLs (1, 2, 11, 12). Peptides, however, have limitations as potential therapeutics; this is due to their lack of oral activity, rapid breakdown by proteolytic enzymes, rapid clearance from circulation, and typical inability to pass through the blood-brain barrier to effect central nervous system activity. The generation of libraries consisting of nonpeptidic compounds can be expected to circumvent a number of these limitations. We are pursuing a library approach in which existing and/or readily accessible peptide or other chemical diversities are chemically transformed to yield libraries (termed here chemically transformed libraries) having more desirable physical and chemical properties.

For the chemical transformation of peptide libraries to be of practical use, there are two requirements. (i) One must begin with a well-defined peptide library, and (ii) one must have access to chemical reagents that can effectively alter chemical moieties in a known manner, while leaving either all of the compound mixture on the resin or alternatively removing all of the mixture from the resin. The solid-phase synthesis of individual peptides (13, 18) and peptide libraries (1, 2) satisfies the first requirement because the preparation of libraries on solid supports can be done with a high degree of confidence and exactitude by recently described approaches (1, 2, 5, 12). Such libraries can then be chemically altered before their resin cleavage. The integrity of the peptide library used in the present study has been well demonstrated in earlier work (2, 12), and this library can be used for chemical transformation with confidence. The second requirement is satisfied here by the successful generation of chemically transformed peptide libraries. Initial studies with individual peptides indicate that peptides can be fully permethylated while bound to the resin support used in their synthesis. The average yield was >85% and was achieved independently of the sequence being permethylated.

Peptoid libraries (3), which are derived from the step-wise synthesis of amide-functionalized polyglycines, consist of

compounds having a number of physical-chemical properties similar to the permethylated peptides described here (resistance to enzymes, favorable aqueous/lipid partitioning, etc.). We believe the use and transformation of existing resin-bound peptide libraries offer significant advantages, due to their general availability and to the familiarity of the procedures for the synthesis of peptides (13, 18) and peptide libraries (1, 2, 5, 12).

Thus, the transformation described here is an example of a more general approach to produce large diversities from readily accessible existing peptide libraries. We believe that the chemical transformation of a wide range of existing and future combinatorial libraries, as exemplified by the permethylated library presented here, offers a straightforward and rapid means to increase the available chemical diversity for use in basic research and drug discovery.

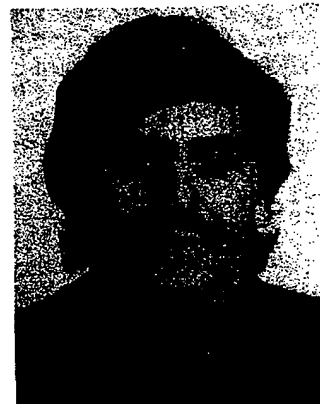
We thank Ema Takahashi for her expert technical assistance, Eileen Silva for help in document preparation. This work was funded by Houghten Pharmaceuticals, Inc., San Diego.

- Houghten, R. A., Pinilla, C., Blondelle, S. E., Appel, J. R., Dooley, C. T. & Cuervo, J. H. (1991) *Nature (London)* **354**, 84–86.
- Pinilla, C., Appel, J. R., Blanc, P. & Houghten, R. A. (1992) *Biotechniques* **13**, 901–905.
- Simon, R. J., Kania, R. S., Zuckermann, R. N., Huebner, V. D., Jewell, D. A., Banville, S., Ng, S., Wang, L., Rosenberg, S., Marlowe, C. K., Spellmeyer, D. C., Tan, R., Frankel, A. D., Santi, D. V., Cohen, F. E. & Bartlett, P. A. (1992) *Proc. Natl. Acad. Sci. USA* **89**, 9367–9371.
- Geysen, H. M., Rodda, S. J. & Mason, T. J. (1986) *Mol. Immunol.* **23**, 709–715.
- Lam, K. S., Salmon, S. E., Hersh, E. M., Hruby, V. J., Kazmierski, W. M. & Knapp, R. J. (1991) *Nature (London)* **354**, 82–84.
- Eichler, J. & Houghten, R. A. (1993) *Biochemistry* **32**, 11035–11041.
- Scott, J. K. & Craig, L. (1994) *Curr. Opin. Biotechnol.* **5**, 40–48.
- DeWitt, S. H., Kiely, J. S., Stankovic, C. J., Schroeder, M. C., Cody, D. M. R. & Pavia, M. R. (1993) *Proc. Natl. Acad. Sci. USA* **90**, 6909–6913.
- Chen, C., Ahlberg-Randall, L. A., Miller, R. B., Jones, A. D. & Kurth, M. J. (1994) *J. Am. Chem. Soc.* **116**, 2661–2662.
- Bunin, B. A., Plunkett, M. J. & Ellman, J. A. (1994) *Proc. Natl. Acad. Sci. USA* **91**, 4708–4712.
- Dooley, C. T., Chung, N. N., Schiller, P. W. & Houghten, R. A. (1993) *Proc. Natl. Acad. Sci. USA* **90**, 10811–10815.
- Dooley, C. T. & Houghten, R. A. (1993) *Life Sci.* **52**, 1509–1517.
- Houghten, R. A. (1985) *Proc. Natl. Acad. Sci. USA* **82**, 5131–5135.
- Blondelle, S. E. & Houghten, R. A. (1992) *Biochemistry* **31**, 12688–12694.
- Blondelle, S. E., Simpkins, L. R., Pérez-Payá, E. & Houghten, R. A. (1993) *Biochim. Biophys. Acta* **1282**, 331–336.
- Hakomori, S. I. (1964) *J. Biochem. (Tokyo)* **55**, 205.
- Challis, B. C. & Challis, J. A. (1970) in *The Chemistry of Amides*, ed. Zabicky, J. (Wiley, New York), pp. 731–857.
- Merrifield, R. B. (1963) *J. Am. Chem. Soc.* **85**, 2149–2154.
- Ibrahim, H. H. & Lubell, W. D. (1993) *J. Org. Chem.* **58**, 6438–6441.
- Lawson, W. B., Gross, E., Foltz, C. M. & Witkz, B. (1962) *J. Am. Chem. Soc.* **84**, 1715–1718.
- Houghten, R. A., Bray, M. K., De Graw, S. T. & Kirby, C. J. (1986) *Int. J. Pept. Protein Res.* **27**, 673–678.
- Russell, G. A. & Weiner, S. A. (1966) *J. Am. Chem. Soc.* **31**, 248–251.
- Tam, J. P., Heath, W. F. & Merrifield, R. B. (1983) *J. Am. Chem. Soc.* **105**, 6442–6455.
- Piskiewicz, D., Landon, M. & Smith, E. L. (1970) *Biochem. Biophys. Res. Commun.* **40**, 1173–1177.
- Mosmann, T. (1983) *J. Immunol. Methods* **65**, 55–63.
- Kornreich, W., Anderson, H., Porter, J., Vale, W. & Rivier, J. (1985) *Int. J. Pept. Protein Res.* **25**, 414–420.

## Macrocyclic Peptidomimetics - Forcing Peptides into Bioactive Conformations

David P. Fairlie\*, Giovanni Abbenante and Darren R. March

Centre for Drug Design and Development, University of Queensland, Brisbane, Qld 4072, Australia.



**Abstract:** Cyclic peptides that are potent regulators of biological processes are rapidly emerging as important mechanistic probes and drug leads. Nature clearly uses macrocycles to constrain peptides into conformations that can selectively bind proteins or small molecules. Therapeutic effects of such macrocycles, often containing additional conformational constraints that fine-tune structure (e.g. D-amino acids, N-methyl substituents, aromatic rings, to name a few), have so far been mainly discovered by accident. However it is now becoming possible to rationally design synthetic macrocycles to selectively recognize and inhibit a specific protein. A receptor-binding structure is more easily adopted by macrocyclic peptidomimetics than more flexible acyclic peptides because the former have less conformational entropy. Macrocycles are often stable to hydrolysis by peptidases that degrade acyclic peptides and hydrophobic side chains can protect peptide bonds in macrocycles from hydrolysis, as well as enhance lipophilicity, cell permeability and bioavailability. Synthetic efforts to obtain bioactive conformations of short peptides have so far been *substrate-based*, guided by molecular modelling predictions and structure-activity data for modified amino acid sequences of substrates. However, dramatic advances in molecular biology, X-ray crystallography, NMR spectroscopy and computing are rapidly producing three dimensional structures of proteins, promising direct observation of protein-bound conformations of small molecules and *receptor-based* design of peptidomimetics with surface complementarity for proteins. This perspective review highlights examples of both natural and synthetic bioactive macrocyclic peptides containing constraints that fix conformation, and briefly illustrates the promise that receptor-based design holds for structural and functional mimicry of peptides by macrocycles.

### Introduction

Peptides display a diverse range of biological, and potentially therapeutic, properties but their use as drugs is severely limited by their conformational flexibility, instability to peptidases, poor oral bioavailability and poor pharmacodynamics [1-3]. Whereas bioactive peptides tend to exist in a myriad of conformations in water, a single specific conformation is usually involved in binding to a receptor. Accessible peptide conformations can be limited through cyclization and further by the incorporation of conformational constraints into the cycle. There are many examples of natural and synthetic cyclic bioactive peptides (*vide infra*). As a consequence of their structural diversity and unique properties, cyclic

bonds from degradative peptidases and facilitates penetration of cell membranes. This increased resistance to proteolytic degradation often leads to longer lifetimes in biological media. The cycle also imposes limitations to conformational flexibility, macrocycles being more discriminating than acyclic peptides in their interactions with bioreceptors and therefore often less toxic. Also by adopting a single conformation, akin to that which binds to a receptor, cyclic peptides are 'preorganized' for receptor-binding and have a lower entropy cost, relative to acyclic peptides, associated with binding to a particular receptor.

With the goal of limiting conformational freedom, numerous constraints have been identified and incorporated into synthetic peptides. However there

aid the design and development of synthetic macrocycles with desired biological properties. This review will highlight the presence of conformational constraints in macrocyclic peptides (a) found in nature, (b) synthesized on the basis of structure-activity investigations and modelling predictions, and (c) synthesized based upon receptor structures. Such peptidomimetic macrocycles promise important applications as therapeutics and mechanistic tools.

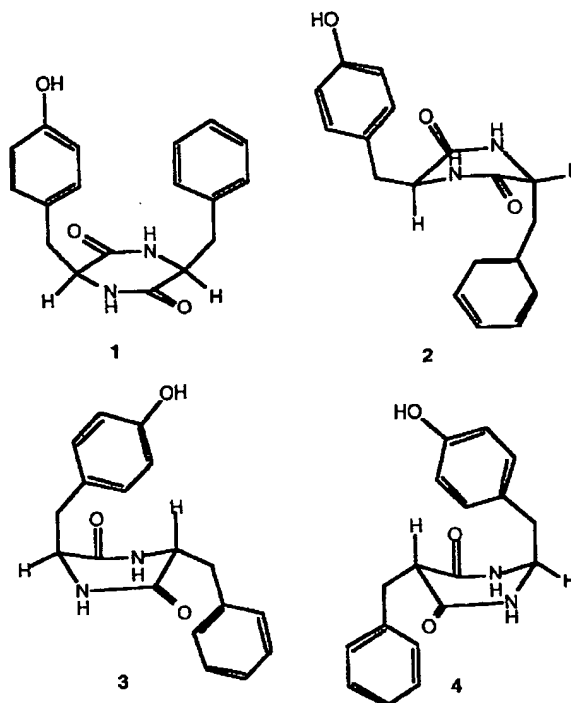
## Constraints In Natural Cyclic Peptides

In recent years increasing numbers of novel cyclic peptides containing unusual amino acids, such as aminoalkyl(oxazoline/thiazole)carboxylic acids, N-methyl- and D-amino acids to name a few (e.g. 1-28), have been isolated from bacteria, fungi, plants, insects, mammals & marine organisms [11-15]. Many such peptides are potent and selective regulators of cellular functions [16-21]. These macrocycles are generally not synthesised like proteins from ribosomes via RNA & DNA, instead their amino acid components are activated as thiol esters by multienzyme complexes. Why has Nature evolved such alternative syntheses, what properties do the unusual components confer on macrocycles, and can these features be designed into synthetic macrocycles to obtain desired bioactivities?

### Common Amino Acids as Constraints

Cyclisation of a linear peptide rarely imposes severe constraints on available conformational space, except when the cycles are small. For example cyclic dipeptides (diketopiperazines) by virtue of the small ring size are very constrained molecules that generally adopt only one or two conformations in solution [22,23]. Conformational preferences in these compounds change depending on stereochemistry of the amino acids used. For example the major solution conformation of *c*-[L-Tyr-L-Phe] (1) was shown to have both aromatic rings sharing the same space over a planar diketopiperazine ring, while *c*-[L-Tyr-D-Phe] exhibits two different boat structures (2) & (3) with side chains in pseudoaxial and pseudoequatorial positions

[24], in equal proportions. The two boat conformations of *c*-[L-Tyr-D-Phe] can be further constrained in this series by making the retro-inverse diketopiperazine. In this case only one conformation (4) dominates. Of the large number of diketopiperazines isolated from fermentation broths and cultures only five (*c*-[L-His-L-Pro], *c*-[L-Leu-L-Gly], *c*-[L-Tyr-L-Arg], *c*-[L-Asp-L-Pro], *c*-[L-Pro-L-Phe]) are known to exhibit any biological activity in mammals [25].



Larger cyclic peptides are more flexible and usually require additional constraints in order to stabilise or favour a particular conformation. Common amino acids typically impose some conformational limitations on the location of amino acid side chains in cyclic peptides. In particular L-proline, D-amino acids and their combinations frequently occur in cyclic peptides as conformational constraints that stabilise turns in the peptide backbone. For example (Fig. 1), X-ray and NMR studies

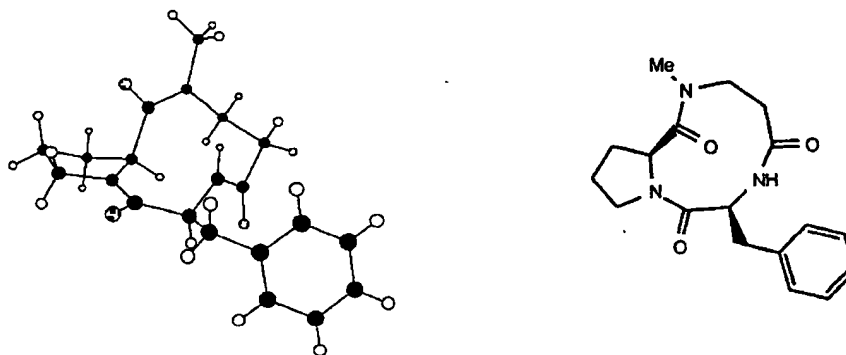


Fig. (1). X-ray crystal structure of cyclo (-MeβAla-Phe-Pro-) [26] showing the conformational preference of this strained 10-membered ring system. Two of the amide bonds are in the cis conformation and all of the amide bonds deviate from planarity.

## Forcing Peptides into Bioactive Conformations

Current Medicinal Chemistry, 1995, Vol. 2, No. 2 656

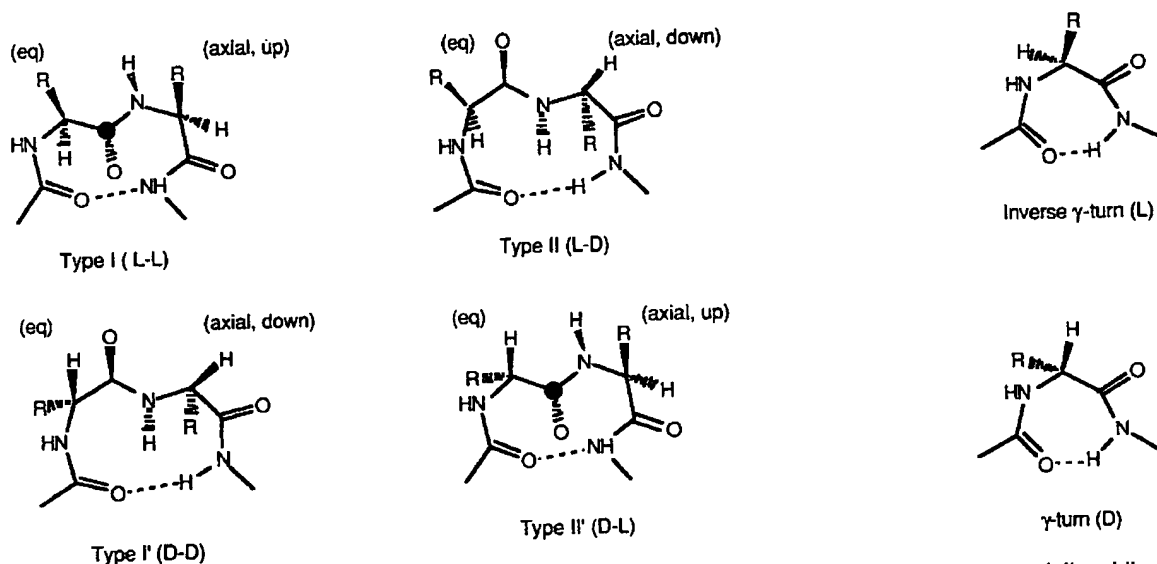


Fig. (2). Some common H-bonded turn types. The side chains of the  $i+1$  residues are oriented equatorially while the next residues along ( $i+2$ ) are in an axial position, either up or down.

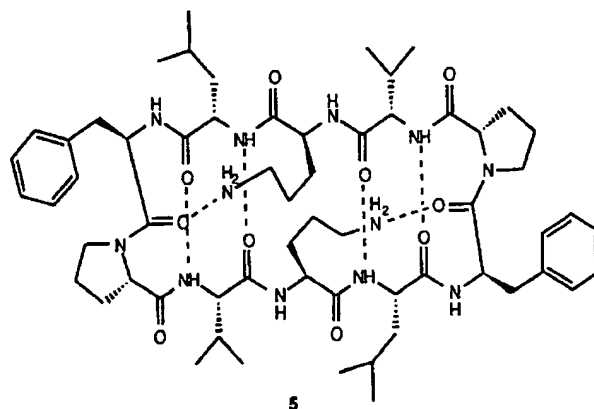
have shown that the 10-membered cyclic tripeptide c-(Me $\beta$ Ala-Phe-Pro-) [26] is very rigid and adopts the same conformation in solution as it does in the solid state. The two tertiary amide bonds adopt a cis conformation while the Phe-Ala amide bond is trans, and all the amide bonds deviate from planarity by 7° to 18°. In cyclic pentapeptides turns can be positioned through introduction of a D-amino acid in an all L-amino acid sequence [27]. If a proline residue is also present, the cycle becomes further constrained to adopt specific types of  $\beta$ -turns which are found widely in nature.

Four of the major types of  $\beta$ -turns are shown in Fig. (2) [28]. A  $\beta$ -turn is, generally speaking, any tetrapeptide sequence where the  $\alpha$ -carbons of the first and fourth residues are  $\leq 7\text{\AA}$  apart and which does not occur in a helical portion of a protein. Structures in Fig. (2) are classified according to different sets of torsion angles of the peptide backbone and are the best defined of a set of about 10 different types of  $\beta$ -turns [28]. A less cumbersome way of classifying  $\beta$ -turns has been proposed [29]. Substituting alkyl groups, particularly bulky ones, for hydrogens in the peptide backbone results in loss of conformational flexibility, not only in the backbone and side chain of the N- or C-alkylated residue but also of the residue preceding it in the sequence [30].

Alternating D and L amino acids in pentapeptides introduces a combination of a type-II  $\beta$  turn and an inverse  $\gamma$ -turn [31] in the peptide backbone. This is the major conformation adopted by the recently discovered selective endothelin-A receptor antagonist c-(D-Glu-L-AlaD-allo-Ile-L-Leu-D-Trp) ( $\text{IC}_{50}$  1.4  $\mu\text{M}$ ), isolated from bacteria [32-35]. Structure activity relationship studies of this cycle have led to even more potent cyclic hexapeptide endothelin-1 antagonists, e.g. c-(D-Asp-

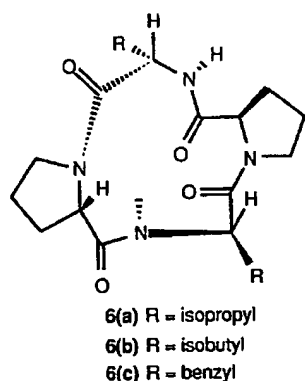
L-Pro-D-Val-L-Leu-D-Trp) ( $\text{IC}_{50}$  22nM). Here the incorporation of a proline residue has further constrained the pentapeptide to a bioactive conformation [35].

The antibiotic Gramicidin S (5) is an example where these simple constraints are combined to restrict, to some degree, the conformation of a cyclic decapeptide. In this case two D-amino acids (Phe, Orn) and two proline residues are incorporated into the macrocycle. The X-ray crystal structure of gramicidin S shows a two stranded anti-parallel  $\beta$ -sheet connected by type II'  $\beta$ -turns formed by D-Phe-Pro sequences at either end [36]. Four hydrogen bonding interactions occur along the  $\beta$ -sheet and two further hydrogen bonds are formed between the side chain of ornithine and the D-Phe carbonyl. There is evidence to suggest that this is the biologically active conformation [37].



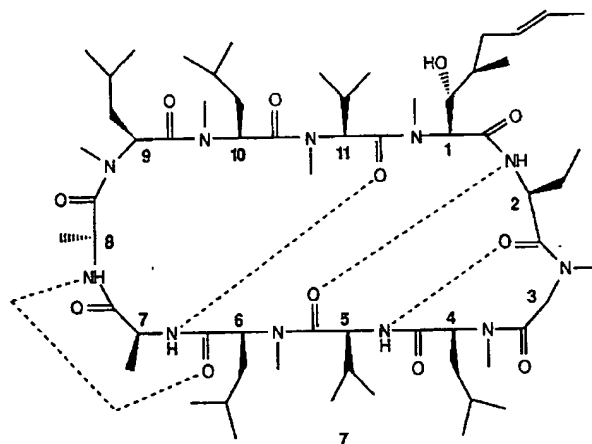
Examples of proline-constrained cyclic peptides from the marine environment include three

tetrapeptides (**6a**, **6b**, **6c**) isolated from a species of ascidian [38]. In these cases two proline residues, separated by either two L-Val, L-Leu or L-Phe residues, create conformations with potent antitumor activity ( $LD_{50}$  1.5  $\mu$ g/ml, L1210 cells). Extensive NMR spectroscopy revealed that these peptides are locked into one dominant solution conformation with a cis-amide bond at one proline residue and trans at the other. The cyclic peptide c-(Pro-Gly)<sub>3</sub> is an example of a model for the ion selectivity of calcium-binding proteins and demonstrates the role of Pro in dictating conformational mobility [39].



A spectacularly successful example [40,41] of a cyclic peptide that illustrates the therapeutic viability of macrocyclic peptides is the immunosuppressant drug cyclosporin A (**7**). A decade or so ago this 11 residue cyclic peptide fungal metabolite made possible organ transplantation without tissue rejection and now has sales of ~\$800 million per annum. Cyclosporin A has no less than seven N-methylated amide bonds, several D-amino acids and some unusual C-alkylated substituents which all combine, together with 3 endocyclic and one exocyclic hydrogen bonds, to limit conformation

freedom. In deuterated chloroform, benzene, THF or in the solid state (Fig. 3a) the hydrophobic peptide forms a twisted  $\beta$ -sheet ( $\beta$ II' turn [42]) with one of the N-Me amide bonds (MeLeu<sup>9</sup>-MeLeu<sup>10</sup>) fixed in the cis-conformation [42, 43]. Nevertheless **7** still adopts half a dozen different solution conformations in polar solvents like methanol, dimethylsulfoxide or water with isomerism occurring about that amide bond. It dramatically changes conformation upon binding to cyclophilins (Fig. 3b) [44] or lithium ions [45], turning



itself inside out with all amide bonds becoming trans and the internal hydrogen bonds being broken. It rearranges again when the cyclosporin-cyclophilin complex binds to another protein calcineurin, regenerating a conformation more like free cyclosporin. This demonstrates that regulating conformational freedom is very important in determining the outcome of receptor-drug interactions. The success of **7** as a drug stimulated the development of other macrocyclic

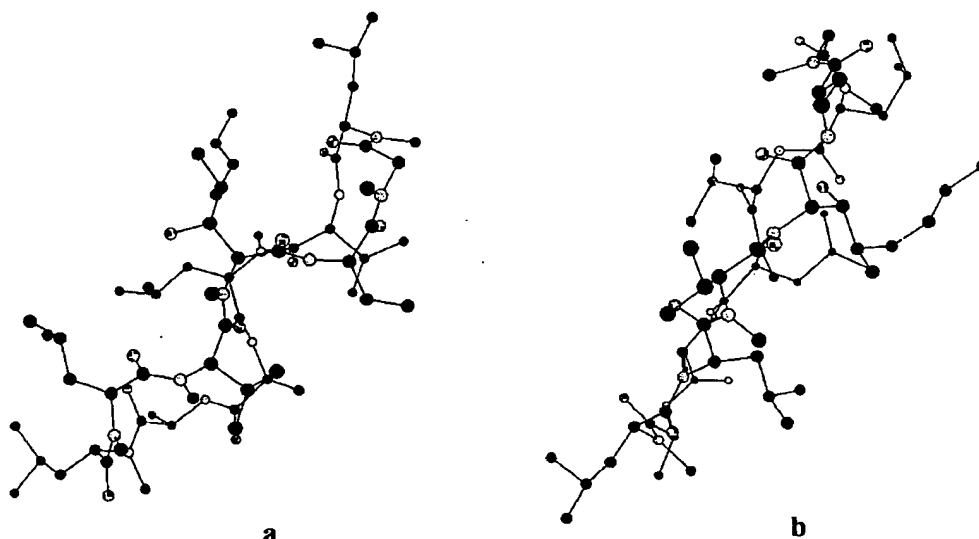
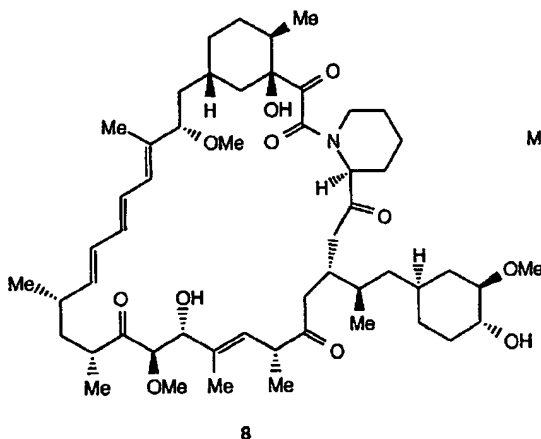


Fig. (3). Two crystal structures of Cyclosporin A orientated along the plane of the peptide backbone, showing the conformation adopted by free cyclosporin A monohydrate (a) [42] versus its cyclophilin-bound conformation (b) [44].

### Forcing Peptides into Bioactive Conformations

non-peptidic drugs, such as the fungal metabolites **8**, **9** which may be structural mimics of unknown Leu-Pro containing acyclic peptidic substrates [46].



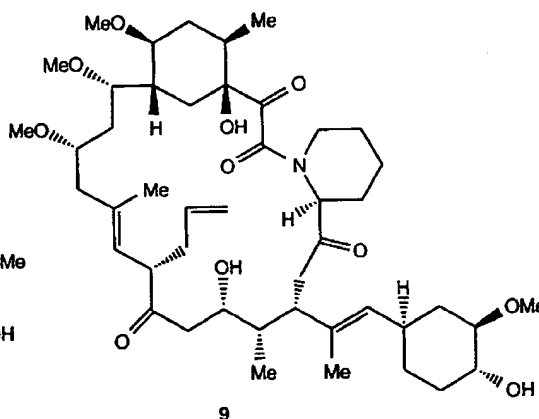
As the size of a cycle increases so does its conformational flexibility, resulting in numerous rapidly interconverting structures. To further restrict conformation it would appear that Nature specifically incorporates unusual amino acids and other constraints into cyclic peptides to fine tune structure, usually fixing a bioactive structure that mimics a protein-binding conformation of an acyclic peptide. A few classes of these constraints are now described.

### Disulfide Bonds

Examples of peptides cyclized through disulfide bonds are described ahead (e.g. somatostatin, oxytocin, vasopressin). There are of course countless examples of disulfide bonds in proteins and peptides where the macrocycle imposes conformational restrictions over acyclic polypeptides. However the macrocycles are usually very large, and it is the combination of disulfide bonds and the elements of secondary structure in the peptide (e.g. helices, turns, sheets) that determine the conformation of polypeptides. On the otherhand, in short disulfide-containing peptides the disulfide bonds provide the

*Current Medicinal Chemistry*, 1995, Vol. 2, No. 2 658

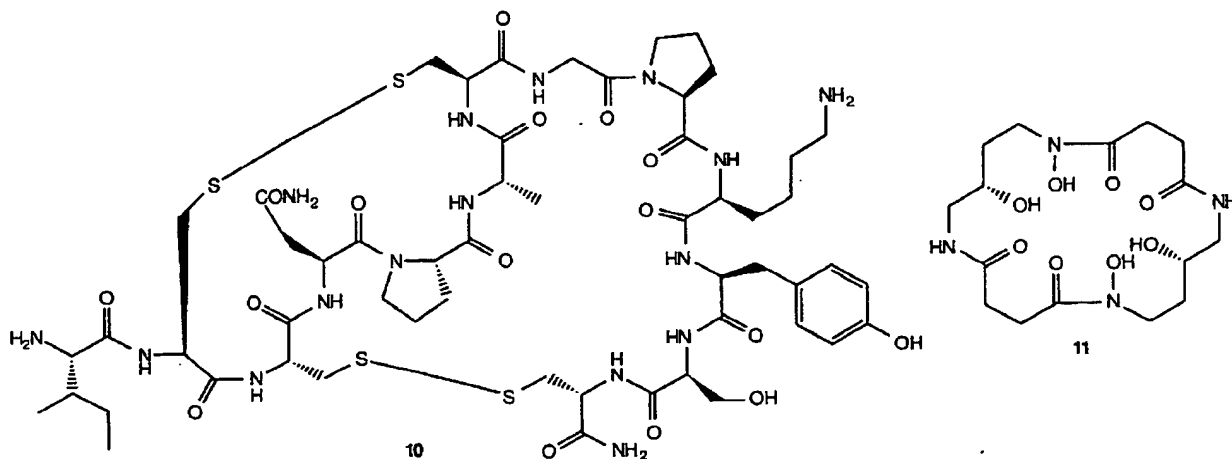
main conformational constraint. For example conotoxins (e.g. **10**) are peptidic toxins from marine cone snails that contain multiple disulfide bonds [47].



Many conotoxins are highly potent and selective blockers of acetylcholine, calcium-channel and sodium-channel receptors. The selectivity is a direct result of each uniquely folded peptide conformation possessing a surface that is complementary for a specific receptor.

### Metal Ions

Metal ions similarly act like disulfide bonds in 'clipping' together discontinuous polypeptide surfaces, via cysteine and/or histidine residues, into macrocycles which facilitate peptide folding. Secondary structural elements like  $\alpha$ -helices,  $\beta$ -turns and  $\beta$ -sheets have all been induced in short peptides through bonding to metal ion templates [48-51]. Other examples include the structural roles of  $Zn^{2+}$ , in zinc finger peptides and metalloproteins [52-54], and  $Ca^{2+}$  in proteins and small peptides [55-57], especially those containing  $\gamma$ -carboxyglutamic acid as a residue.  $Fe^{3+}$  and  $Cu^{2+}$  are also known to link linear peptides together into macrocyclic structures, such as in their metalloproteins. Metal ions can also restrict the conformational freedom of cyclic peptides as in alcaligin (**11**) a naturally



659 *Current Medicinal Chemistry*, 1995, Vol. 2, No. 2

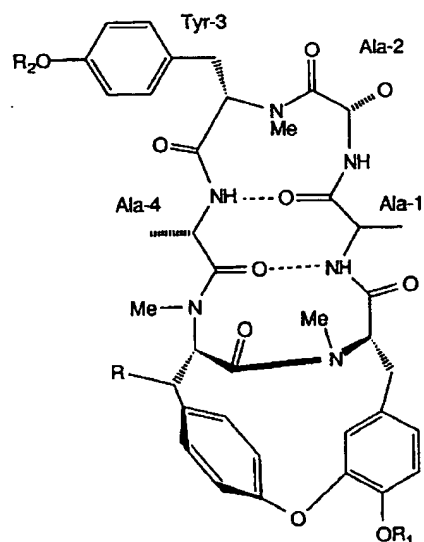
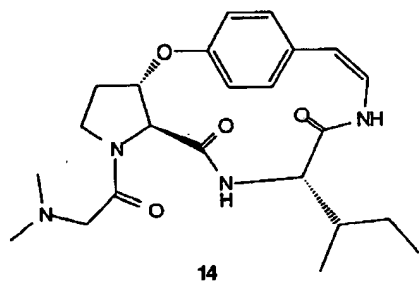
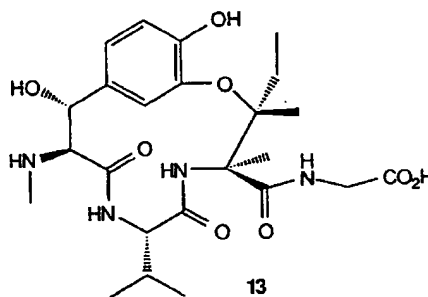
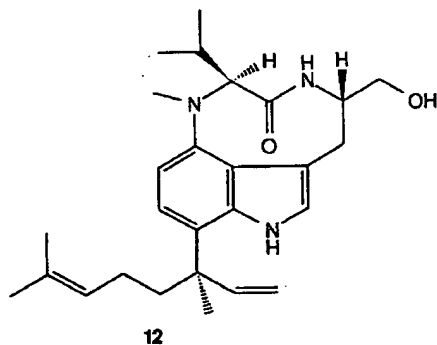
occurring siderophore isolated from bacteria. The cyclic hydroxamate [58] forms a 3:2 complex with ferric ion with a stability constant of  $10^{37} \text{ M}^{-1}$ .

### Aromatic Rings

By virtue of their planarity, aromatic rings can impose severe conformational constraints on the structure of cyclic peptides. The 9-membered ring in the teleocidin (12) family of dipeptide alkaloids (tumor promoters and activators of Protein Kinase C) incorporates the indole ring of Trp as the constraining linker [59]. Ustiloxin D (13) is a recently discovered member of the phomopsin-ustiloxin class of antibiotics [60]. This 13-membered cycle, formed via an ether linkage between the side chains of tyrosine and threonine residues, imparts antitubulin activity ( $\text{IC}_{50} 6.6 \mu\text{M}$ ). Nummularine F (14), isolated from *Ziziphus* plants, is representative of a series of sedative alkaloids which contain two amino

acids cyclised into a 14 membered ring by a 4-hydroxystyrylamino linker [61], also present in 26.

A class of bicyclic hexapeptides isolated from the *Bouvardia ternifolia*, *Rubia akane* or *R. cordifolia* species of plant that display potent cytotoxic and antitumour properties is represented by RA-VII (15) [62]. This compound is a cytotoxic antitumour agent ( $\text{IC}_{50} 1.3 \text{ ng/ml}$ , P388 leukaemia cells) which is currently being evaluated for clinical use [63]. The peptide backbone is conformationally constrained by the 14-membered dityrosine ring (forcing the amide bond between the two residues into the normally, less favourable cis configuration), three methylated amide bonds, a D-alanine residue and two hydrogen bonds between  $\text{Ala}^1$  and  $\text{Ala}^4$ . Due to these combined restraints the molecule is restricted to two conformations arising from cis-trans isomerism (1 : 9 ratio respectively) about the N-methylated  $\text{Tyr}^3\text{-Ala}^2$  amide bond [64]. There is substantial conformational



**Forcing Peptides into Bioactive Conformations**

Current Medicinal Chemistry, 1995, Vol. 2, No. 2 660

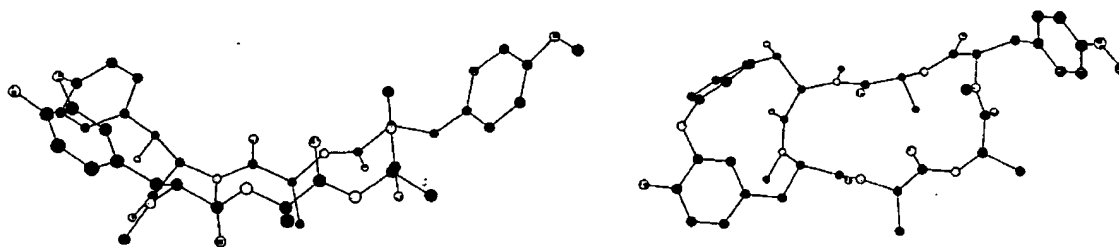


Fig. (4). Two alternative views of the X-ray crystal structure of bouvardin [65], which is representative of this class compounds. In this case the Ala-Tyr amide bond is not methylated, adopting the trans configuration and stabilising a type II  $\beta$ -turn.

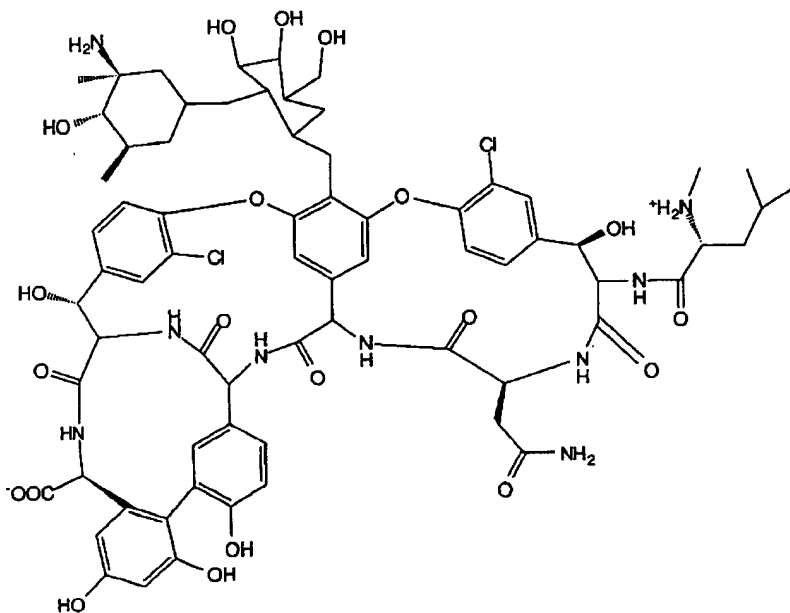
difference in the cyclic backbone of the two conformers [65], the major trans conformation adopts a type II  $\beta$ -turn in this region (Fig. 4), while the cis isomer adopts a type VI  $\beta$ -turn. This difference seems to be reflected in their biological activity. Demethylation of this amide bond results in stabilisation of the trans conformation (100% in  $\text{CDCl}_3$ ,  $d_6$ -DMSO,  $\text{CD}_3\text{OD}$ ) which is cytotoxic ( $\text{IC}_{50}$  90  $\mu\text{g/ml}$ ) but has no antitumor activity [66]. This suggests that antitumor activity resides in the less favoured cis isomer and the N-Me substituent acts as a constraint to fix the conformation. Interestingly the biological activity of this series of compounds is attributed to the dityrosine ring system [67] which is constrained by the peptide backbone into a bioactive conformation.

There are numerous other examples in nature of the use of aromatic ring constraints, particularly peptides containing oxidatively coupled tyrosine derivatives. Many are potent antibiotics of bacterial origin (e.g.

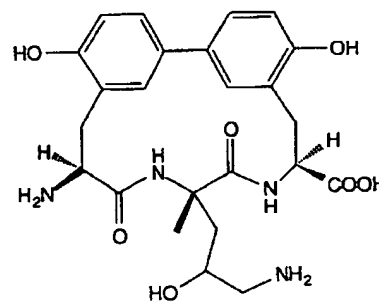
vancomycin 16 [68, 69], biphenomycin 17 [70]). There are also numerous amino acid derived alkaloids of medicinal importance including bisbenzylisoquinolines [71], such as tetrandrine 18, derived from Tyr.  $^{14}\text{C}$ -Tyr feeding experiments have revealed that 4 tyrosines are incorporated into these molecules resulting in highly conformationally constrained cycles that approximate tetrapeptides [72]. These diphenyl ether linked compounds have potent antiinflammatory, immunosuppressant and cytokine-regulating properties both *in vitro* and *in vivo* [73-75].

**Unsaturated Backbone Constraints**

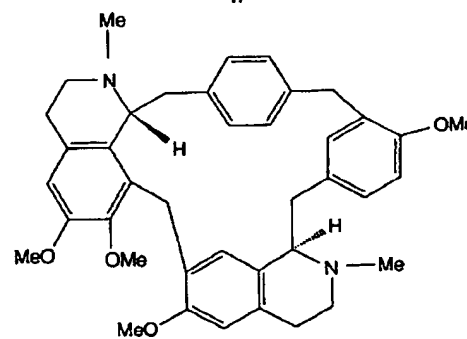
Many naturally occurring bioactive cyclic peptides contain dehydro amino acid residues. Studies on model systems generally show that incorporation of a dehydro amino acid in a peptide induces a  $\beta$ -turn in the backbone [76], as in the case of the model peptide Boc-Leu-dehydro(Z)Phe-Ala-Leu-OMe [77]. An X-ray



16



17



18

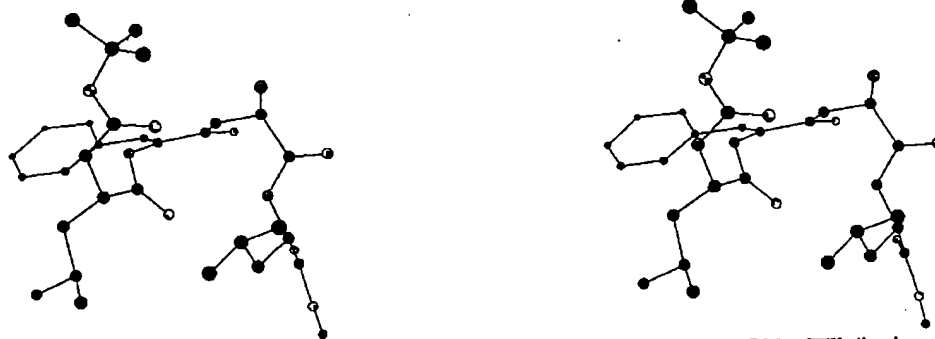
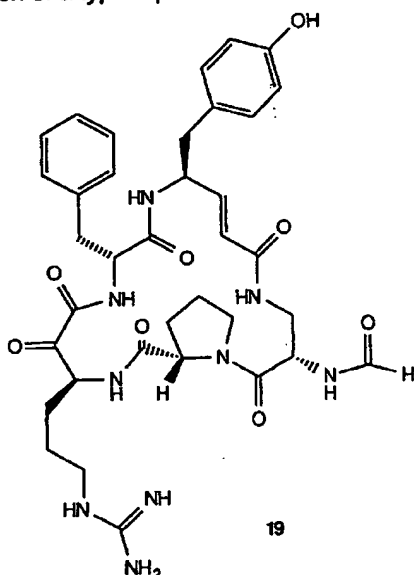


Fig. (5). Stereoview of the X-ray crystal structure of Boc-Leu-dehydro(Z)Phe-Ala-Leu-OMe [77] (hydrogens not included) showing two  $\beta$ -turns which are induced in the peptide backbone by the dehydrophenylalanine residue.

crystal structure (Fig. 5) of this peptide reveals two  $\beta$ -turns. The dehydrophenylalanine is common to both turns being in the  $i+1$  position of a type III  $\beta$ -turn and the  $i+2$  position of a type II  $\beta$ -turn.



Notable exceptions to this generalisation are peptides which contain dehydro alanine residues in the backbone. These residues tend to give extended conformations [78]. Vinyllogous amino acids are extended amino acids with a (E)-ethenyl unit inserted between the  $\alpha$ -carbon and the carbonyl carbon. The ethenyl moiety is conjugated with the amide bond in an *s-cis* conformation leading to a region of planarity in the residue. Dimers of vinyllogous alanine were found to form parallel and anti-parallel sheet secondary structures, both in the solid state and solution [79].

The naturally occurring thrombin inhibitor [80] cyclotheonamide A (19), isolated from the marine sponge genus *Theonella*, is an example where a vinyllogous tyrosine residue has been incorporated into a cyclic tetrapeptide packed with other constraints such as Pro, two D-amino acids, and a 'retro inverse' or  $\alpha$ -keto-amide that is also found in 2 & 3 above. X-ray crystal structures of cyclotheonamide A bound to bovine Trypsin [81] and  $\alpha$ -Thrombin [82] (Fig. 6) show that the keto-amide functions as a transition state isostere for the scissile amide bond of Arg-Phe and that cyclotheonamide A exhibits conventional Pro-Arg molecular recognition typical of other inhibitors of serine proteases. The double bond of the vinyllogous

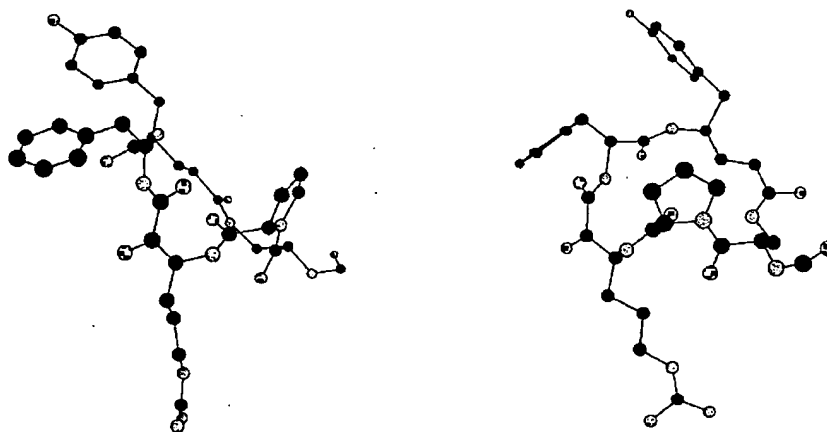


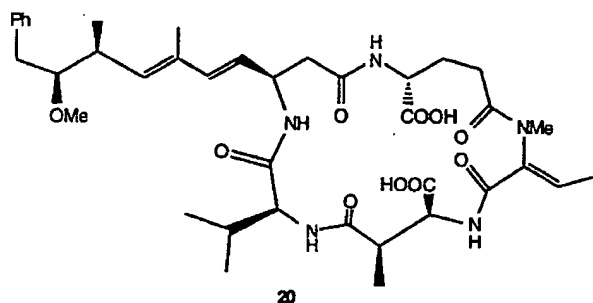
Fig. (6). Two orthogonal views of the X-ray crystal structure of cyclotheonamide A bound to  $\alpha$ -thrombin [82]. The vinyllogous tyrosine is directed away from the active site and into empty space. It may function as a restraint, helping to hold the molecule in the relatively open conformation required for binding.

### Forcing Peptides into Bioactive Conformations

Current Medicinal Chemistry, 1995, Vol. 2, No. 2 662

tyrosine moiety does not appear to interact with the enzymes but rather serves to lock the 19-membered cycle into the relatively open conformation required for binding.

In contrast to the endocyclic double bond of vinylogous amino acids (eg. 14), there is an exocyclic double bond from the dehydrothreonine moiety of the cyclic pentapeptide mutropin 20, also isolated from *Theonella* [83]. Since this is conjugated to each flanking amide bond, a region of planarity is produced in this potent phosphatase inhibitor.

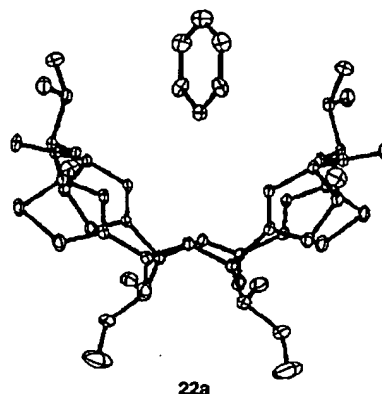
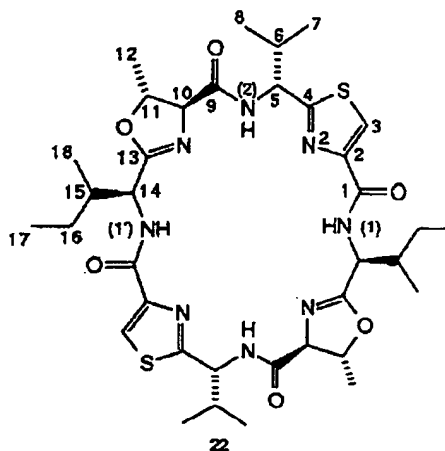
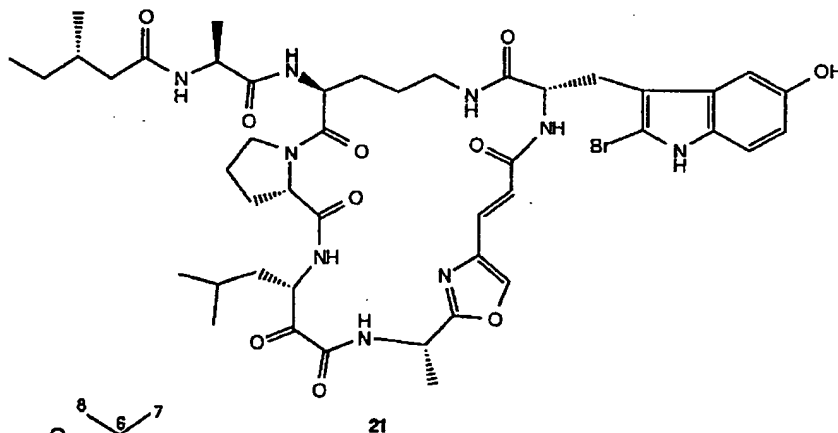


### Unusual Amino Acids

From the same marine sponge, there are many other bioactive peptides that contain these same

constraints as well as the uncommon amino acid (theonalanine) containing an oxazole ring. A representative is orbiculamide A 21 [84], which is cytotoxic against L388 murine leukemia cells ( $IC_{50}$  4.7  $\mu$ g/ml), where the oxazole is conjugated to an endocyclic double bond resulting in localised planarity. This molecule also contains four common amino acids (L-Pro, L-Ala, L-Orn, L-Aba (2-aminobutyric acid)), an unusual amino acid (theonleucine) containing an  $\alpha$ -keto- $\beta$ -amino acid, an unusual tryptophan derivative, and 3-methylvaleric acid.

Two adjacent amino acids are sometimes found fused together to form an unusual amino acid that is often a very effective constraint. For example the octapeptide c-[Thr-D-Val-Cys-Ile-Thr-D-Val-Cys-Ile-] can adopt a multitude of conformations but, after intramolecular condensation of the threonine and cysteine side chains with adjacent amide bonds to form oxazoline and thiazole rings respectively as in 22, a single saddle shaped conformation 22a is detected by X-ray crystallography and NMR spectroscopy [85-87]. 22 is ascidiacyclamide of the patellamide class found in ascidians from the Great Barrier Reef, and some members of this class with oxazoline rings in the cycle have antitumour activity [8,9]. The unusual conformation in 22 stems from the 4 pseudo-planar rings conjugated to 4 planar amide bonds, the only flexibility in the macrocycle arising from the 4  $sp^3$



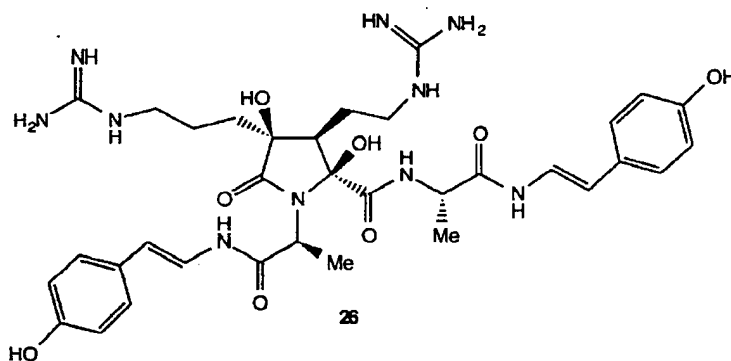
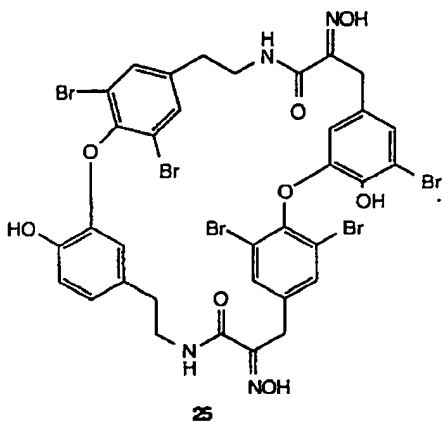
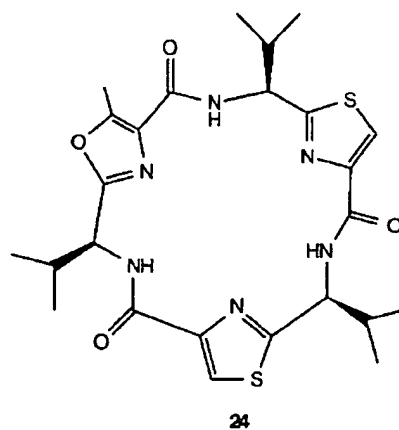
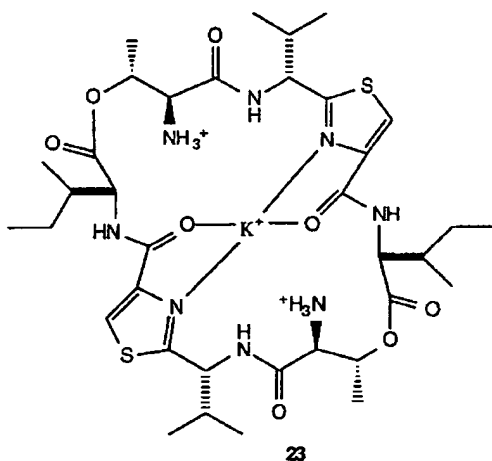
hybridized C $\alpha$  carbons that support D-Val or L-Ile side chains. The D-valines extend the depth of the macrocyclic saddle creating a hydrophobic pocket that can capture small organic molecules (e.g. benzene) [87] or metal ions (e.g. Cu $^{2+}$ ) [88, 89].

Interestingly the saddle can accommodate 2 copper ions, found concentrated 10 $^5$  fold in the organism over surrounding sea water [90], which are able to capture CO $_2$  or CO $_3^{2-}$  to form a carbonate-bridged dimer [Cu $_2$ (ascidH $^2$ )(CO $_3$ )]. This first [91] example of a structurally defined metal complex of a marine cyclic peptide may be involved in uptake and transport of CO $_2$ /CO $_3^{2-}$  in ascidians, which concentrate CO $_3^{2-}$  in their spicules. Acid hydrolysis of **22** selectively opens the oxazoline ring constraints to give **23** which has significantly more conformational flexibility resulting in very different metal-binding properties. X-ray structural data [92] indicates that the two flexible acyclic sides of **23** contort into an unusual potassium-binding cleft.

Another example of the constraint that oxazole and thiazole ring formation can impose on a cyclic peptide is

illustrated by a cyclic hexapeptide of marine origin, Bistratamide C **24** [93]. Apart from the presence of two thiazole rings, this compound also incorporates an uncommon oxazole ring in the peptide backbone. The three aromatic constraints impose a high degree of planarity to the peptide backbone, the solution structure of the compound showed it to be almost flat with the sidechains of the L-Val and L-Ala residues perpendicular to the plane of the backbone and extending on the same side of the plane.

Macrocyclic compounds containing highly modified amino acids are also found in nature. The bastadins are a class of sponge metabolites which are biogenetically derived from four tyrosine amino acid residues. Bastadin 16, **25**, is representative of the class [94]. Another class of compounds, the anchinopeptolides (**26**) are probably derived from two arginines and two L-alanine residues constrained by cyclisation into a pyrrolidone ring. In addition the C-terminal of both alanines are coupled to a *trans*-4-hydroxystyrylamino moiety. An interesting variant, isolated from the same sample of sponge was the tricyclic Anchinopeptolide C



al.

**Forcing Peptides into Bioactive Conformations**

Current Medicinal Chemistry, 1995, Vol. 2, No. 2 664

(26a) which is formed from a [2+2] cyclisation of the two side chains. These compounds bind with reasonable affinity to receptors for somatostatin, human B2 bradykinin and neuropeptide Y receptors [95].

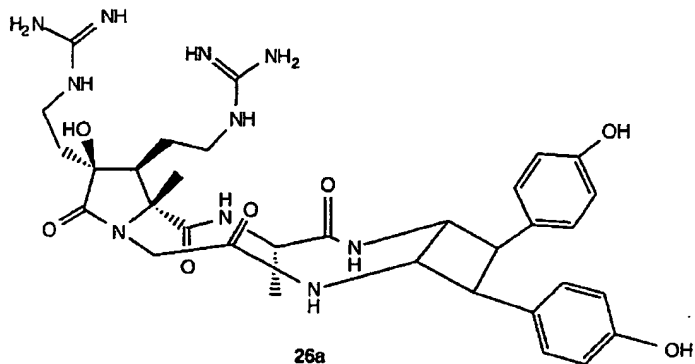
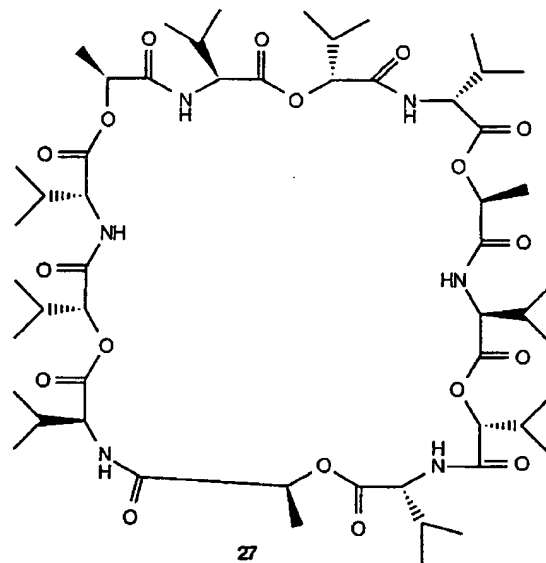


(Fig. 7a) [96] and the molecule complexed with  $K^+$  (Fig. 7b) [97,98] have shown that the molecule changes from an ovoidal shape to the bracelet shape of the bound form with substantial reorganisation of the hydrogen bonded framework. In the complexed form,



Valinomycin 27 is a cyclododecadepsipeptide antibiotic of bacterial origin with alternating L-valine, D- $\alpha$ -hydroxyisovaleric acid, D-valine and L-lactic acid residues. As a consequence of the incorporation of lactic and isovaleric acids in the cycle, the backbone consists of alternating amide and ester bonds. Valinomycin has been shown to affect the energy-linked accumulation of alkali metal ions by mitochondria. X-ray crystal structures of uncomplexed valinomycin

methyl and isopropyl groups project out of the complex forming a hydrophobic exterior ideal for transporting the bound alkali metal across a lipid membrane. Interestingly, valinomycin displays remarkable selectivity for potassium over sodium (the  $K^+$  complex is  $10^4$  times more stable than the  $Na^+$  complex), which is unusual considering its high degree of conformational flexibility [97].

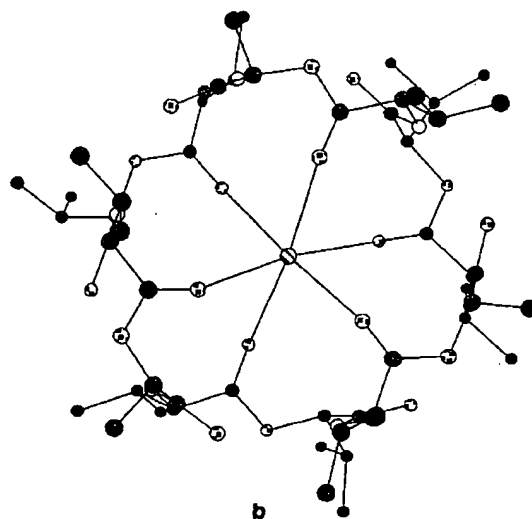
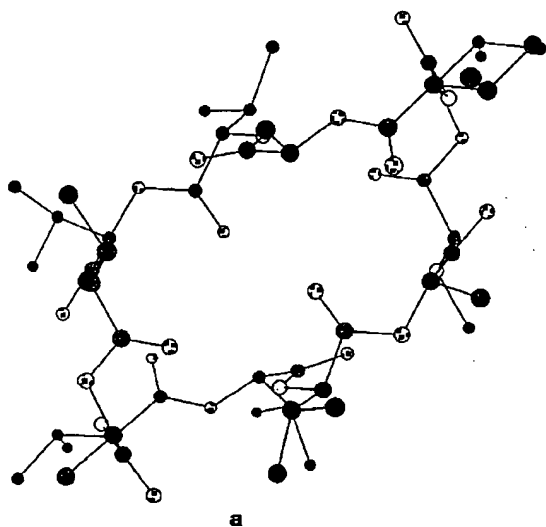
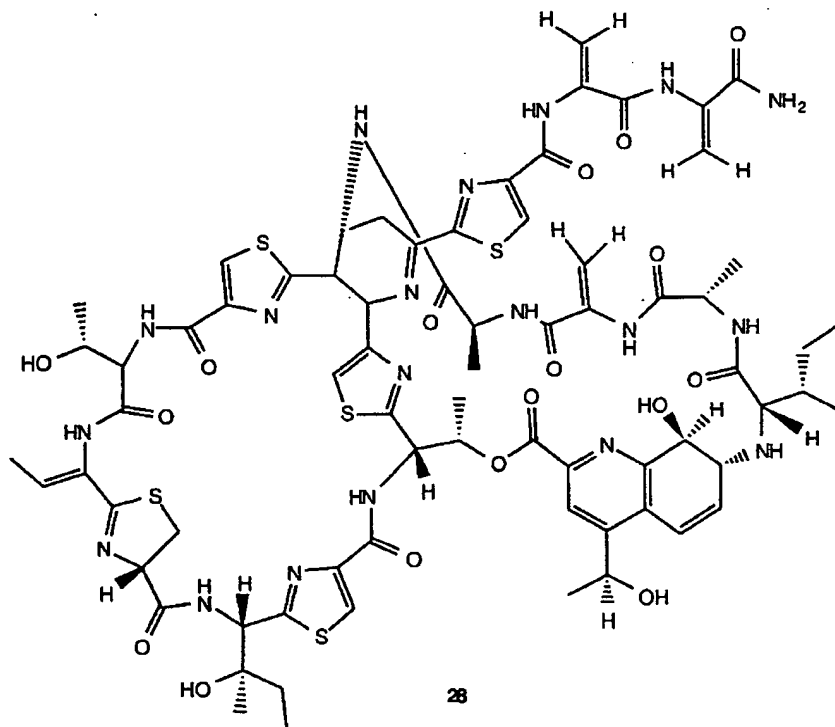


Fig. (7). The crystal structures of valinomycin (a) [96] and valinomycin bound to potassium (b) [98] showing the conformational change that occurs on complexation. The potassium complex is doughnut shaped and six hydrogen bonds are formed with the six ester carbonyls of valinomycin.



Thiostrepton **28** belongs to a class of macrocyclic thiopeptide antibiotics [4]. Like other members of this class **28** consists of one macrocycle, containing three thiazoles and a dihydrothiazole, fused via a reduced pyridine ring and a threonine side chain to a second macrocycle containing alanine, dehydroalanine, thiazole and a quinaldic acid moiety. The three dimensional structure is unknown, but the molecules in this class appear to share a common mechanism of action involving inhibition of protein synthesis through binding to the complex of 23S ribosomal RNA - ribosomal protein L11.

Non-covalent bonds are also very important devices used in all proteins for constraining peptides. These include hydrogen bonds, ionic or salt bridges, aromatic-aromatic interactions, and the often unconsidered hydrophobic packing forces. Intramolecular hydrogen and ionic bonds stabilise secondary structures like turns, sheets and helices all of which can be viewed as macrocyclic peptides with H-bond or ionic linkers.

### Constraints in Synthetic Cyclic Peptides

Attempts to design bioactive macrocycles, by analogy to the structures of flexible bioactive peptides (unbound to proteins), have generally proven frustrating. Synthetic macrocycles have emerged through either simply joining together two atoms of a bioactive linear peptide or, more rationally, by systematically replacing amide bonds or side chains in peptide substrates with constraints designed to

increase rigidity, fix conformation, and reduce susceptibility to proteolytic enzymes [99-103]. At the very least cyclic peptides and their derivatives are proving to be valuable tools for investigating the influence of conformational restrictions on biological activity.

The objective of all synthetic efforts has been to direct side chain residues into appropriate three dimensional space to maximise interaction with receptors. However three dimensional structural data for inhibitors bound to protein receptors has not been available until very recently, so there has been comparatively little done on rational design of macrocyclic peptidomimetics based upon precise surface complementarity for a protein receptor (fitting designed cycles to their receptor structures). Instead synthetic efforts have had to rely on predictive modelling studies, the outcome of structure-activity relationships, and the use of conformational constraints to limit flexibility in the hope of obtaining or imitating unknown receptor-binding conformations of bioactive linear peptides. Although many studies have been undertaken to discover the preferred conformation of synthetic macrocycles in various solvents, the deduced conformations are frequently different from those which bind to a receptor. Examples of designed substrate-based and (the more promising) receptor-based bioactive macrocycles are given below, but in most cases the relationships between conformational constraints, the protein-bound macrocycle conformation, and bioactivity remain uncertain or unoptimised.

## General Constraints

Cyclic peptides can be viewed broadly as being composed of turn conformations and linkers. Turns found in Nature are predominantly  $\beta$ -turns which direct peptide side chains into particular regions of three dimensional space. There has been enormous effort (reviewed elsewhere) put into the synthetic development of libraries of  $\beta$ -turns, each turn being designed to direct side chains into different regions of space. Prior to this, synthetic chemists followed Nature's lead by using simple devices like D-amino acids, disulfide bonds or constrained amino acids such as proline to lock in a  $\beta$ -turn and several examples of this are shown below for macrocyclic peptide analogues of hormones.

cyclisations can be effected (Fig. 8) over a short range (29) by condensations between consecutive amino acids ( $i$  to  $i+1$ ) [104], over a longer range between alternating residues ( $i$  to  $i+2$ ) (29), or over longer ranges that invariably lead to >20 membered macrocycles. The method of cyclisation can be from side chain to side chain (30); from side chain to mainchain N, O or C (31); or by connecting main chain atoms (32). All of these types have been constructed and are exemplified below.

## Substrate-Based Macrocycles

### Somatostatin

One of the earliest successful uses of cyclisation resulted in bioactive synthetic mimics of somatostatin

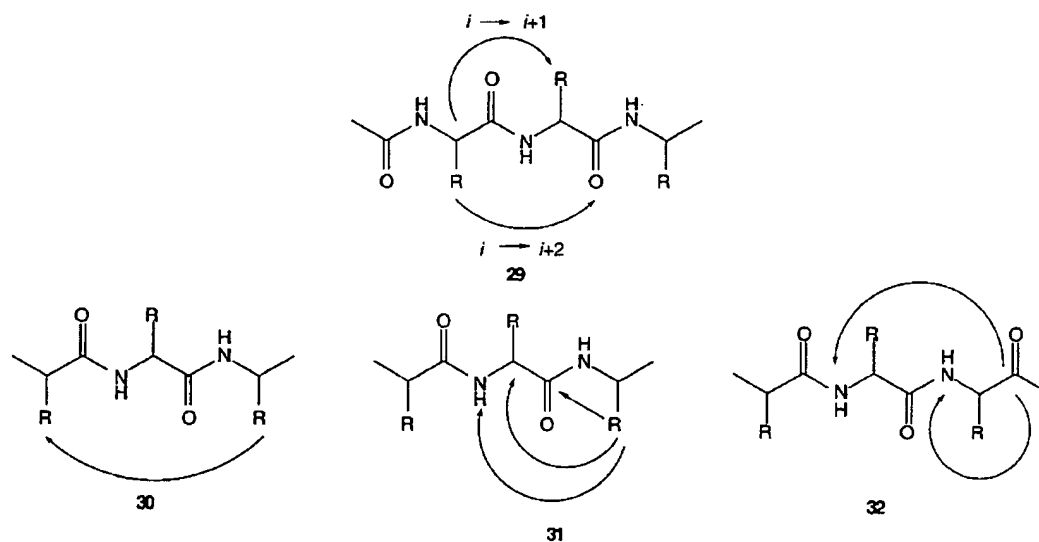
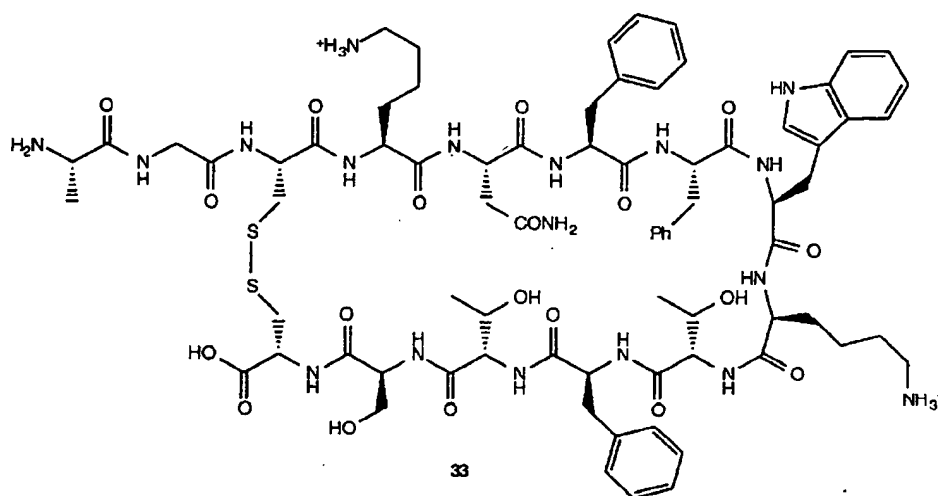


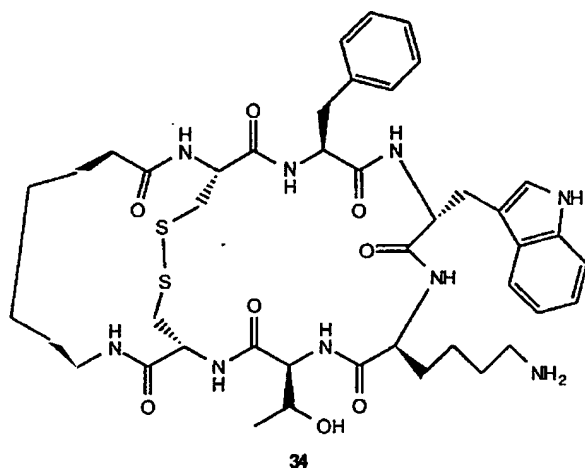
Fig. (8). Connections for cyclising peptides.

Turns can be envisaged to be combined in a macrocycle with almost any molecular spacers. Linkers like those reported above for natural macrocycles have also been used in synthetic macrocycles. Alternatively,

which possessed restricted conformational freedom, high receptor affinity and specificity, and improved bioavailability [105-111]. Somatostatin (33) is a naturally occurring cyclic peptide containing 14 amino



acids, 12 in a macrocycle linked by a disulfide bond. It affects physiological functions in the brain and endocrine glands by inhibiting release of peptide hormones such as insulin, glucagon, growth hormone, gastrin, and secretin. Only the 38 membered cycle was associated with activity, and only its  $\beta$ -turn component (Phe<sup>7</sup>-Trp<sup>8</sup>-Lys<sup>9</sup>-Thr<sup>10</sup>) was critical for receptor-binding and activity. Mimetics of the active tetrapeptide sequence had much lower affinity for the receptor than somatostatin [112], but high affinity compounds were obtained by incorporating this tetrapeptide turn into cyclic hexapeptides. Extensive structure-activity investigations using a turn conformation stabilised by substituting D-Trp<sup>8</sup> for L-Trp<sup>8</sup>, and incorporating disulfide bond constraints and  $\alpha$ - and  $\beta$ -methylated residues, have produced numerous cyclic hexapeptides and derivatives with high inhibitory potency [28, 108-113]. Examples include D-Phe<sup>5</sup>-c-[Cys<sup>6</sup>-Tyr<sup>7</sup>-D-Trp<sup>8</sup>-Lys<sup>9</sup>-Thr<sup>10</sup>-Cys<sup>11</sup>]-Thr<sup>12</sup>-NH<sub>2</sub>; c-[Aha<sup>5</sup>-c-[Cys<sup>6</sup>-Phe<sup>7</sup>-D-Trp<sup>8</sup>-Lys<sup>9</sup>-Thr<sup>10</sup>-Cys<sup>11</sup>]-] (34), Aha=7-aminoheptanoic acid; and the smaller but potent inhibitors c-[Pro<sup>6</sup>-Phe<sup>7</sup>-D-Trp<sup>8</sup>-Lys<sup>9</sup>-Thr<sup>10</sup>-Phe<sup>11</sup>]-, IC<sub>50</sub> 1nM; and c[Pro<sup>6</sup>-Phe<sup>7</sup>-(2R,3S)- $\beta$ -MeTrp<sup>8</sup>-Lys<sup>9</sup>-Thr<sup>10</sup>-Phe<sup>11</sup>]-, IC<sub>50</sub> <1nM.

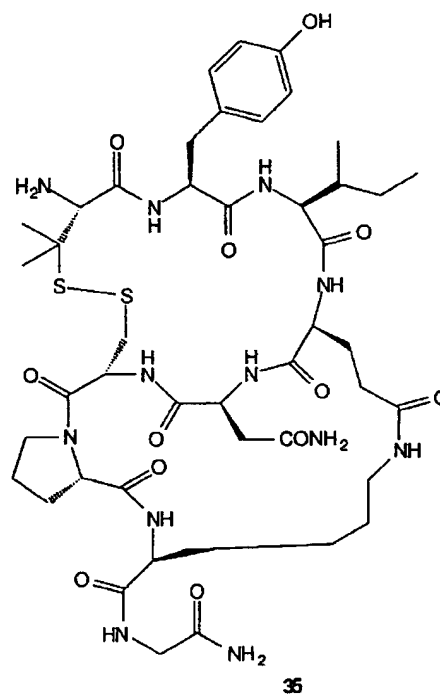


The Trp residue at position 8 plays an important role in fixing the bioactive conformation of somatostatin and its hexapeptide mimetics. A type I  $\beta$ -turn is favoured for L-Trp, although somatostatin shows a host of solution conformations at ambient temperature in its NMR spectra. On the otherhand a type II'  $\beta$ -turn is preferred for D-Trp, and there is NMR evidence that this conformation is present for somatostatin as well at low temperature. The high potency of inhibitors containing the D-Trp residue argues strongly for a conformational preference by the receptor for a type II'  $\beta$ -turn where the side chains are orientated differently but correctly for inhibitor-receptor binding. NMR studies for c-[Pro<sup>6</sup>-Phe<sup>7</sup>-D-Trp<sup>8</sup>-Lys<sup>9</sup>-Thr<sup>10</sup>-Phe<sup>11</sup>]- suggested a type II'  $\beta$ -turn around D-Trp<sup>8</sup>-Lys<sup>9</sup> and a type VI  $\beta$ -turn around Phe<sup>11</sup>-Pro<sup>6</sup> with a cis amide bond [106]. While a  $\beta$ -turn/ $\beta$ -sheet backbone conformation is required in somatostatin analogues to inhibit growth hormone

release, it is not yet clear whether the same conformation is required for other activities of somatostatin [111].

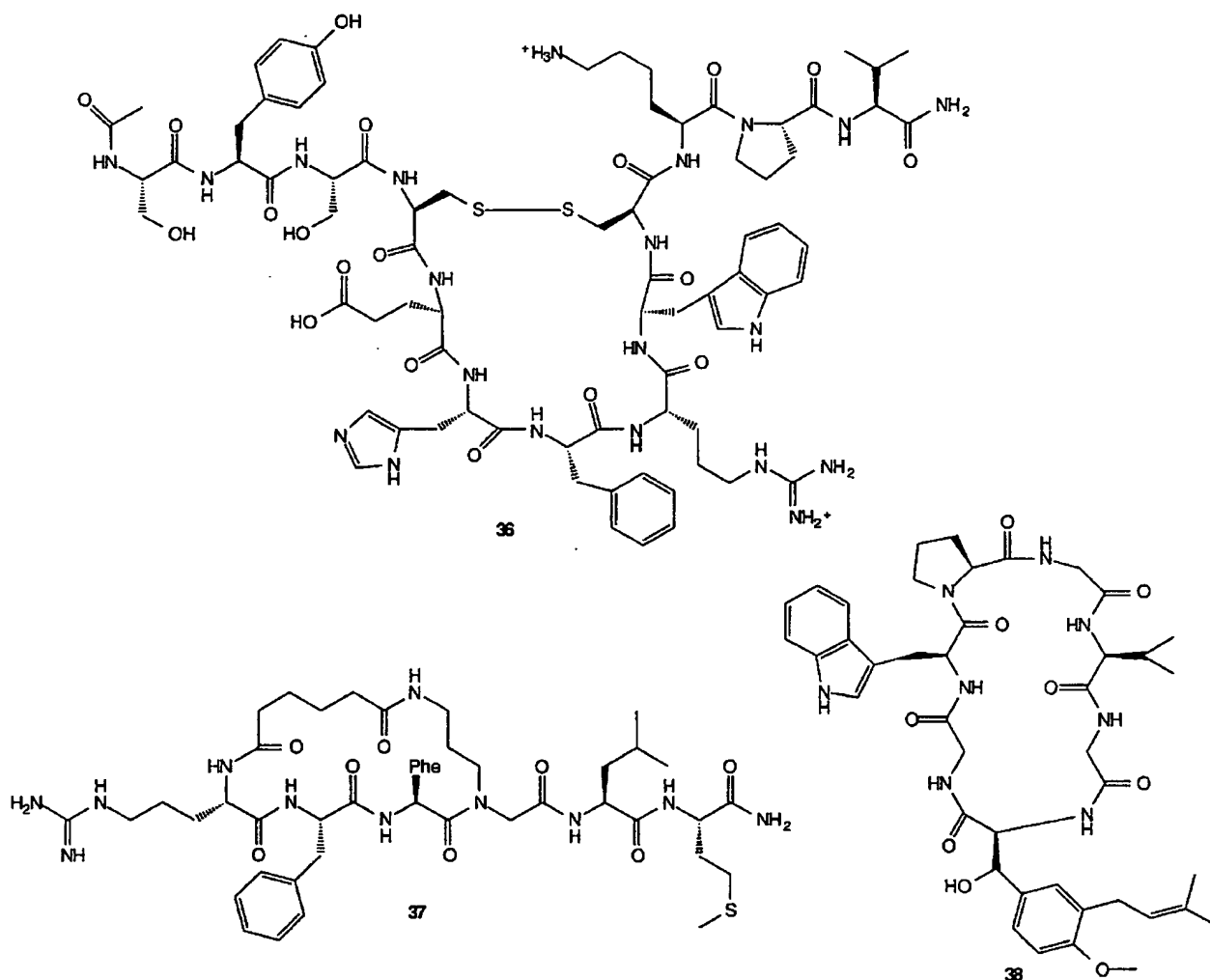
#### Melanocyte-Stimulating Hormone

$\alpha$ -Melanocyte stimulating hormone (melanotropin) is a 13 residue peptide (Ser-Tyr-Ser-Met-Glu-His-Phe-Arg-Trp-Gly-Lys-Pro-Val) that activates adenylate cyclase, tyrosinase and melanin release. The Glu-His-Phe-Arg-Trp component is thought to contain a turn that is important for melanin release in a frog skin bioassay. Since substituting D-Phe for L-Phe improved activity, a covalent link was sought to form a cycle that would lock in the turn conformation. Thus the cyclic heptapeptide derivative, Ser<sup>1</sup>-Tyr<sup>2</sup>-Ser<sup>3</sup>-c-[Cys<sup>4</sup>-Glu<sup>5</sup>-His<sup>6</sup>-Phe<sup>7</sup>-Arg<sup>8</sup>-Trp<sup>9</sup>-Cys<sup>10</sup>]-Lys<sup>11</sup>-Pro<sup>12</sup>-Val<sup>13</sup> (35), was found to be a superagonist, 104 times more potent than the native hormone [113, 114]. The cycle may not only fix a receptor-binding conformation but may also increase hydrolytic stability over the linear form. Other macrocyclic analogues have been made, some with lactam bridges between Gly<sup>5</sup> and Lys<sup>10</sup>, and are reviewed elsewhere [115].



#### Oxytocin and Vasopressin

Oxytocin, c-[Cys-Tyr-Ile-Gln-Asn-Cys]-Pro-Leu-Gly-NH<sub>2</sub>, enhances lactation and promotes uterus contraction during labor while Vasopressin, c-[Cys-Tyr-Phe-Gln-Asn-Cys]-Pro-Arg-Gly-NH<sub>2</sub>, increases blood pressure and causes antidiuresis. These naturally occurring nonapeptides contain a cyclic hexapeptide, formed through a disulfide bond, to which a tripeptide side chain is attached through a Cys<sup>6</sup>-Pro<sup>7</sup> peptide bond [99, 116]. Since they are highly homologous,



they tend to bind to each others receptors and this has inspired enormous effort to derive cyclic peptides that are receptor-selective. Attempts have been made to vary both the size of these 20 membered macrocyclic hexapeptides and the nature of the cycle linkage (S-S to C-S, S-C or C-C) without improvement in activities [99].

Numerous cyclic peptides have been constructed generally through systematic amino acid replacements, constraints being incorporated into oxytocin antagonists to increase affinity for receptors [117-120]. For example [117] the peptide backbone of oxytocin has been successfully constrained by cyclising the side chains of the fourth and eighth residues via an amide bond, resulting in potent bioactivity. The bicyclic compound, [D-Pen<sup>1</sup>, cyclo(Glu<sup>4</sup>,Lys<sup>8</sup>)]-oxytocin (**36**), was a more potent antagonist at the uterine receptor than the monocyclic analogue (pA<sub>2</sub> 8.74 as compared to [D-Pen<sup>1</sup>]-oxytocin pA<sub>2</sub> 6.86). This was attributed to the cyclic restraint locking the peptide into the binding conformation required for the uterotonic receptor, as

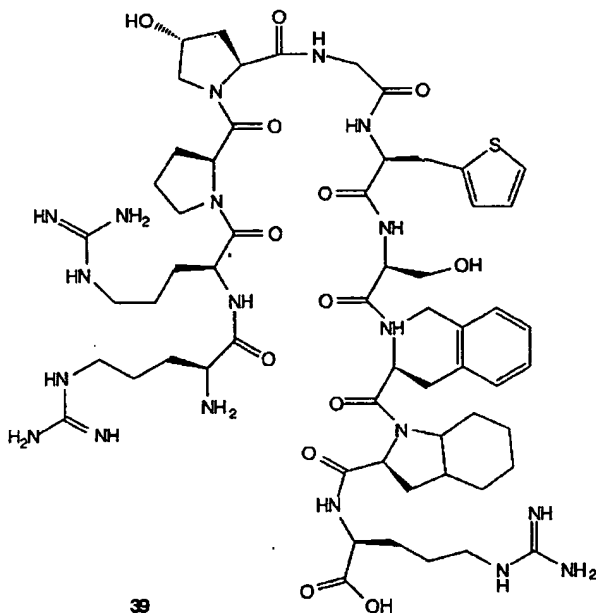
the compound was 400 times less potent at the pressor receptor.

#### Substance P Antagonists

The mammalian tachykinin, Substance P, is an 11 residue neurotransmitter peptide (Arg-Pro-Lys-Pro-Gln-Gln-Phe-Phe-Gly-Leu-Met-NH<sub>2</sub>) which selectively binds to the neurokinin-1 receptor (NK-1). It regulates smooth muscle contraction, lowers blood pressure, stimulates salivary secretion [121, 122], and is important in pain and inflammation [123, 124]. Cyclic analogues containing disulfide bonds have been examined by NMR spectroscopy [125] and have high affinity for NK-1 but not NK-2 receptors [126]. Other active and selective tachykinin cyclic analogues (e.g. **37**) were made by backbone cyclisation [127-129], the degree of activity and selectivity has been attributed to the extent of conformational restraint. A naturally occurring cyclic heptapeptide antagonist of substance P (Ki 8nM), containing a critical 3-prenyl- $\beta$ -hydroxytyrosine group, was modified to the more active (Ki 120nM) derivative (**38**) by simple methylation [130].

Conformationally restricted phenylalanines have been extensively employed in structure-activity studies to optimise for NK-1 receptor-binding [131]. Hexapeptides based on the C-terminus of substance P have been cyclised and, despite conformational flexibility, were found to be NK-2 antagonists (IC<sub>50</sub> 10-100nM) with 10<sup>2</sup>-10<sup>3</sup> fold binding selectivity over the NK-1 receptor [132, 133].

#### Bradykinin Antagonists



Antagonists of bradykinin (Arg<sup>1</sup>-Pro<sup>2</sup>-Pro<sup>3</sup>-Gly<sup>4</sup>-Phe<sup>5</sup>-Ser<sup>6</sup>-Pro<sup>7</sup>-Phe<sup>8</sup>-Arg<sup>9</sup>), a depressor and myotropic agent released from kininogens, have potential therapeutic applications in the treatment of conditions like asthma, rhinitis, bronchitis or septic shock. Based on studies of Ramachandran maps, Phe<sup>5</sup> or Phe<sup>8</sup> were replaced with  $\alpha$ -methyl substituted analogues to limit conformational freedom but with little success. Cyclic analogues such as c-(eLys-Pro-Pro-Gly-Phe-Gly-Pro-Phe-Arg) have similar potency to bradykinin as a depressor in rats but with more selectivity and extended lifetimes (hours instead of minutes) [134]. NMR studies revealed  $\beta$ -turn reversals at Pro<sup>3</sup>-Gly<sup>4</sup> and Pro<sup>7</sup>-Phe<sup>8</sup> residues [135] suggesting

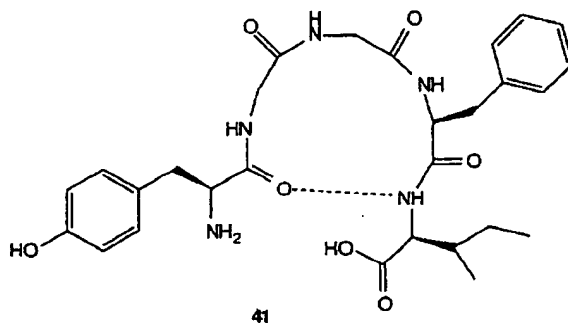
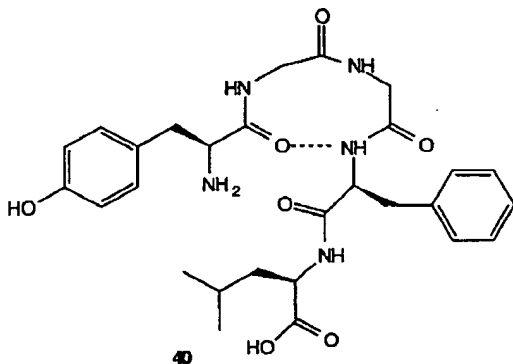
that the cycle mimics a receptor-binding conformation of bradykinin. Other cyclic derivatives with various D-configured, C- or N-alkylated amino acids to constrain conformation have had mixed success [98]. Substituting D-Phe for L-Pro at position 7 in linear peptides gave potent antagonists [136-138] for bradykinin B<sub>2</sub> receptors, while multiple substitutions with constrained hydrophobic amino acids D-Tic and Oic gave the even better inhibitors (e.g. D-Arg<sup>0</sup>-[Hyp<sup>3</sup>,Thi<sup>5</sup>, D-Tic<sup>7</sup>, Oic<sup>8</sup>]-bradykinin (39); K<sub>i</sub> 0.1nM) [139, 140]. Combinations with dehydro-Phe<sup>5</sup> and L-NMePhe<sup>2</sup> also gave potent inhibitors [141]. Conformational analysis of the linear 39 revealed a type II'  $\beta$ -turn [140] and strongly suggests that cyclic derivatives may be effective antagonists.

#### Opioid Peptides

Endogenous ligands for  $\delta$ -,  $\mu$ - and  $\kappa$ - opioid receptors include enkephalins, dynorphins and endorphins, which are short peptides that characteristically have aromatic groups at i and (i+3) positions (usually Tyr and Phe respectively) as well as an  $\alpha$ -amino group.

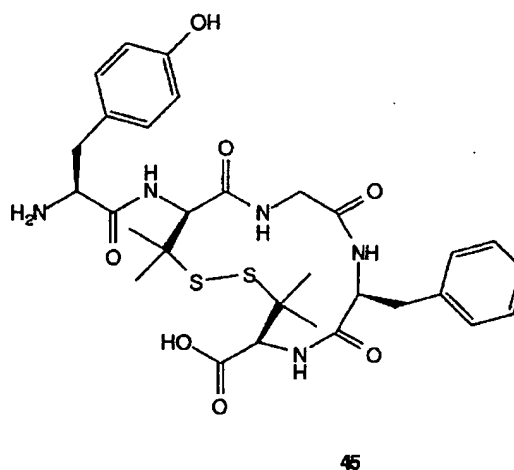
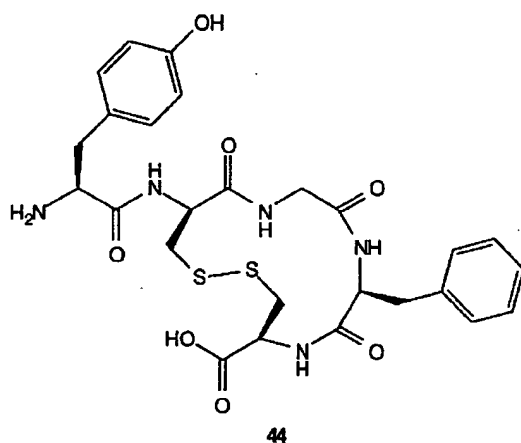
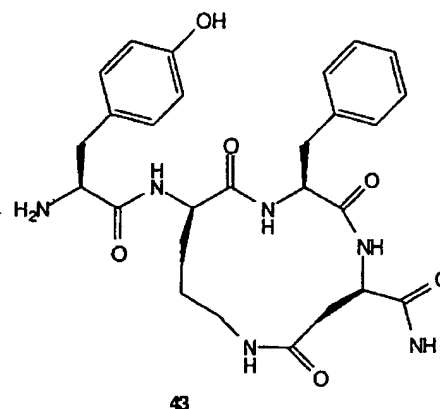
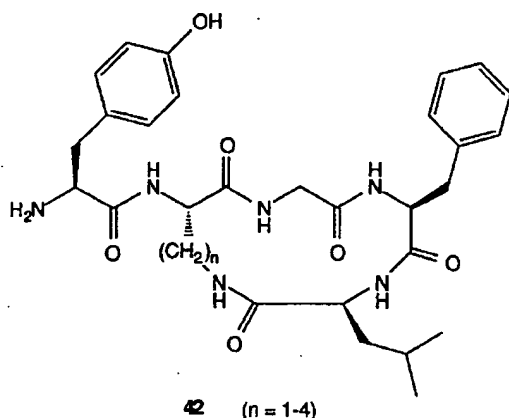
Enkephalins are linear pentapeptides (e.g. Tyr-Gly-Gly-Phe-Met/Leu) with potent analgesic properties that are thought to arise through receptor-binding of a folded form containing a turn. Enkephalins act on multiple receptors but most synthetic work has focused on developing antagonists with activity against the  $\delta$ -receptors [3, 99, 100, 108, 142-144], which also bind to the (constrained cyclic) opioid alkaloids. Examples below show macrocycles formed using hydrogen bonds (40, 41), side chain to backbone bonds (42), side chain to side chain amide bond formation (43) and disulfide bonds (44-46).

An X-ray structure for crystals of Tyr-Gly-Gly-Phe-Leu grown from water/DMF showed a macrocycle formed by a hydrogen bond between Tyr and Phe residues (40), with the Gly-Gly residues forming a type I'  $\beta$ -turn [145]. On the other hand NMR studies [28] in water or DMSO indicated a conformational preference for a macrocycle formed through hydrogen bonding between Tyr-Leu residues, and with Gly-Phe residues constituting the turn (41). These and other conformational studies suggest that different



## Forcing Peptides into Bioactive Conformations

Current Medicinal Chemistry, 1995, Vol. 2, No. 2 670



backbone arrangements still direct their side chains into approximately the same three dimensional space, and this has frustrated attempts to characterise the preferred receptor-bound conformation of macrocyclic enkephalin mimics in the absence of the receptor-mimic structure.

Nevertheless numerous constrained cyclic enkephalin analogues have been synthesized and found to have higher activity than the native enkephalin. Among these are H-Tyr-[D-NHCH<sup>+</sup>-CO-Gly-Phe-NH-CH<sup>+</sup>-CO]NH<sub>2</sub> (\*atoms connected by CH<sub>2</sub>-S-CH<sub>2</sub>), which was 100 times more potent than morphine against guinea pig ileum and mouse vas deferens *in vitro* assays but had little selectivity [146]; the conformationally rigid 13-16 membered rings (e.g. **42**) formed through side chain to C-terminus cyclisation [147]; and the morphiceptin analogue Tyr-c-[D-Orn-Phe-Asp]-CONH<sub>2</sub> (**43**) formed through an amide bond between side chains [148]. Interestingly, when D-Orn

and L-Asp are respectively replaced by D-Lys and D-Glu in **43**, the resulting 15- (instead of 13-) membered ring reduces selectivity by two orders of magnitude for  $\mu$ -receptors. The macrocycle has also been constructed using disulfide bridges with D-Cys **44** [148] or the less flexible D-Pen at positions 2 or 5 [149]. While the latter can all adopt the proposed  $\beta$ -turns, the former does not appear to mimic any of the turns. Further analogues with D-Pen at positions 2 and 5, for example [D-Pen<sup>2</sup>, D-Pen<sup>5</sup>]enkephalin **45** [150, 151], dramatically improved both potency and selectivity for  $\delta$  over  $\mu$  receptors. Compound **45** was found to adopt three different conformations in the solid state differing in the location of the exocyclic tyrosine residue. Similar but not identical conformations were found in solution indicating that **45** still possesses some residual flexibility. Another restricted analogue of enkephalin [152], where the cycle has been made smaller by deletion of the glycine residue, also exhibits some conformational flexibility. In this

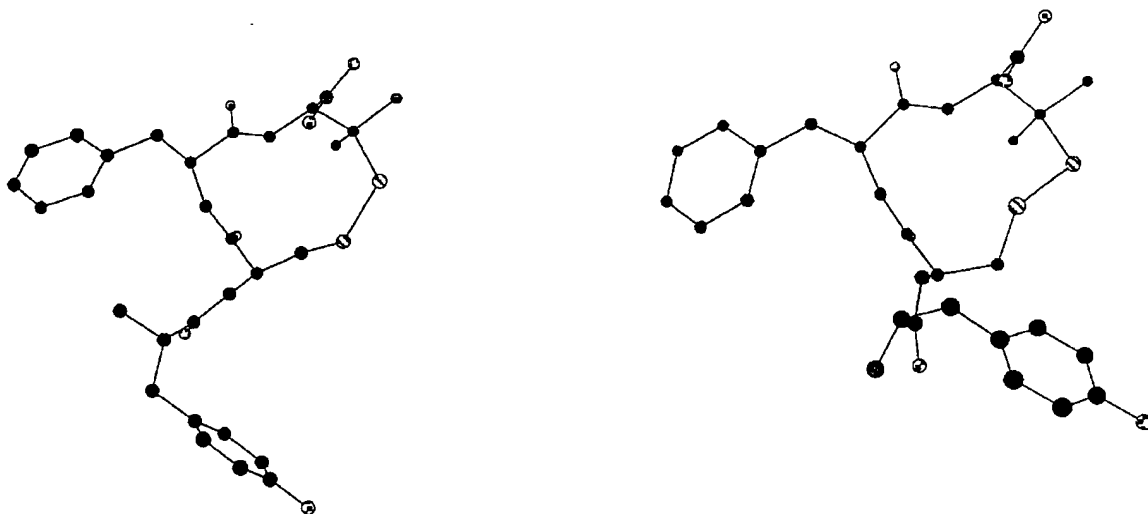
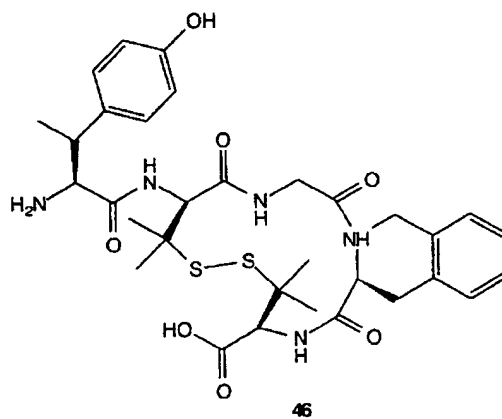


Fig. (9). X-ray crystal structures [152] of the co-crystallised conformers of Tyr-cyclo[D-Cys-Phe-D-Pen]-OH showing differences in the positions of the side chains of Tyr, Phe and the disulfide bond.

system two conformations are observed both in the solid state (Fig. 9) and in solution. The main differences were again found in the exocyclic tyrosine residue but also in the location of the disulfide bond. Compounds 45 and Tyr-cyclo[D-Cys-Phe-D-Pen]-OH display similar binding selectivity and affinity at  $\delta$  opioid receptors.

In general a combination of molecular modelling, molecular mechanics calculations and dynamic simulations, have been used to create tentative models for the bioactive conformations of all these macrocycles. For  $\delta$ -opioid receptor binding, the hydrophobic side chains of Tyr<sup>1</sup>, D-Pen<sup>2</sup> and Phe<sup>5</sup>, are believed to cluster on one face with the cycle contorting into a type-4  $\beta$ -turn. Topographical requirements for  $\delta$ -opioid ligands have subsequently been further explored. For enkephalins, side chains of residues in positions 1 and 4 in particular have been further constrained with N-Me and  $\beta$ -Me substituents at position 1 and with tetrahydroisoquinoline at position 4 (46) [153]. The related Deltorphin I (Tyr-D-Ala-Phe-Asp-Val-Val-Gly-NH<sub>2</sub>), isolated from skin extracts of frogs, has also been mimicked with cyclic analogues [154], including Tyr<sup>1</sup>-c-[D-Cys<sup>2</sup>-Phe<sup>3</sup>-Asp<sup>4</sup>-Cys<sup>5</sup>]-Val<sup>6</sup>-Gly<sup>7</sup>-NH<sub>2</sub>, Tyr<sup>1</sup>-c-[D-Pen<sup>2</sup>-Gly<sup>3</sup>-Phe<sup>4</sup>-D-Pen<sup>5</sup>]. The disulfide bonds did not interfere with activity against the  $\delta$ -opioid receptor, but the C-terminal tripeptide was essential for activity. Dynorphin A (H-Tyr-Gly-Gly-Phe-Leu-Arg-Arg-Ile-Arg-Pro-Lys-Leu-Lys-Trp-Asp-Asn-Gln-OH) is thought to be an endogenous ligand for the  $\kappa$ -opioid receptor. It contains a Tyr-Gly-Gly-Phe message sequence and up to 6 residues have been deleted from the C-terminus without loss of activity. Cyclic disulfide bonded analogues (e.g. [Cys<sup>5</sup>, Cys<sup>11</sup>]-Dyn<sup>1-11</sup>-NH<sub>2</sub> and [Cys<sup>5</sup>, D-Ala<sup>8</sup>-Cys<sup>11</sup>]-Dyn<sup>1-11</sup>-NH<sub>2</sub>) were found to be highly potent and  $\kappa$ -selective peptides [155]. Putative binding conformations have been proposed based upon modelling studies, one

conformation was  $\alpha$ -helical [156]. Structureactivity studies produced compounds with up to 1000 fold selectivity for  $\kappa$  and  $\delta$  opioid receptors and led to a proposal that residue 1-5 contain the message, residues 6 & 7 are important for receptor selection (basic for the  $\kappa$ -receptor) and residues 9-11 potentiate binding to both  $\kappa$ - and  $\delta$ - receptors [157].

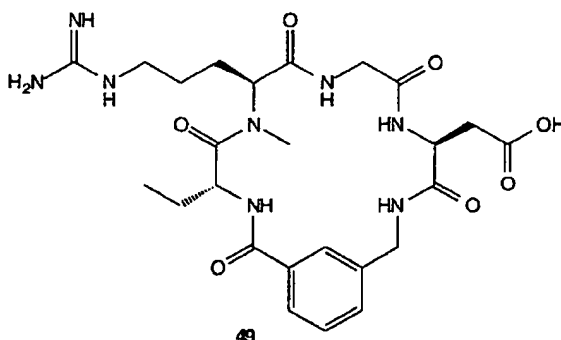
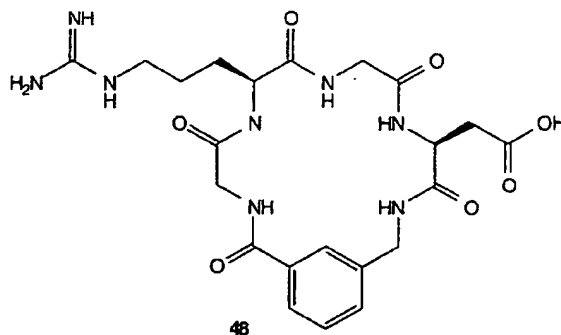
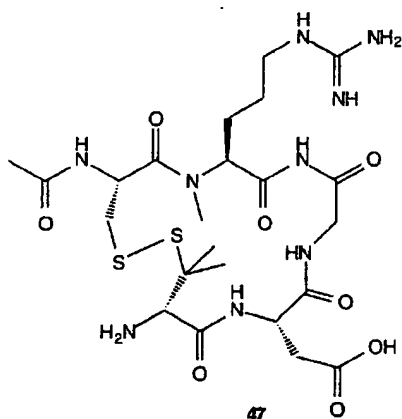


#### RGD Macrocycles

The consensus tripeptide Arg-Gly-Asp (RGD) of the adhesive proteins fibrinogen, fibronectin and thrombospondin, binds to a membrane glycoprotein (GPIIb/IIIa) of the heterodimeric integrin receptor IIb/IIIa involved in platelet aggregation [158-160]. The sequence has been widely studied because of its role in cell-adhesion and cell-migratory processes such as those involved in thrombosis, tumour cell invasion, osteoporosis and wound healing. Its possible incorporation into a range of potential therapeutic agents [161] has inspired the development of many RGD-containing cyclic peptides with high affinity for GPIIb/IIIa [161170].

## Forcing Peptides into Bioactive Conformations

Current Medicinal Chemistry, 1995, Vol. 2, No. 2 672



Numerous cyclic pentapeptides (e.g. c-(-Arg-Gly-Asp-D-Phe-Val-)) have been designed to vary the  $\beta$ - and  $\gamma$ -turn backbone conformations, particularly with D-amino acids in the sequence. The cyclic peptide SKF 106760 c-[Ac-Cys-N $\alpha$ -methyl-Arg-Gly-Asp-Pen-NH<sub>2</sub>] (47)[162], containing an N-methyl substituent, a penicillamine (C $\beta$ ,C $\beta'$ -dimethylCys) and a disulfide bond linker, binds GPIIb/IIIa with a K<sub>i</sub> 58nM, and has an IC<sub>50</sub> 0.4 $\mu$ M in platelet aggregation assays[158] compared with IC<sub>50</sub> 90  $\mu$ M for Ac-RGDS-NH<sub>2</sub>[162].

NMR and X-ray analysis [163-169] of SKF 106760 and similar peptides indicated that the RGD backbone conformation was extended, and led to the

replacement of the disulfide-forming residues with the more rigid *m*-aminomethylbenzoic acid linker (Mamb) giving c-[GlyArg-Gly-Asp-Mamb] (48). This was about five fold worse in inhibiting platelet aggregation. Further replacement of Gly-Arg with D-Pro-NMeArg gave constrained cyclic pentapeptide inhibitors of platelet aggregation with IC<sub>50</sub> 20nM, compared with IC<sub>50</sub> 9nM for the uncyclised identical sequence. Systematic changes to N $\alpha$ - and C $\alpha$ -alkyl substituents resulted in macrocycles with K<sub>d</sub> in the pM range, some of which are orally active [169]. Solution and solid state structures have been determined for this family of compounds [170] all having a structure c-[X-NMeArg-Gly-Asp-Mamb], eg. 49 (Fig.10), where X was a small

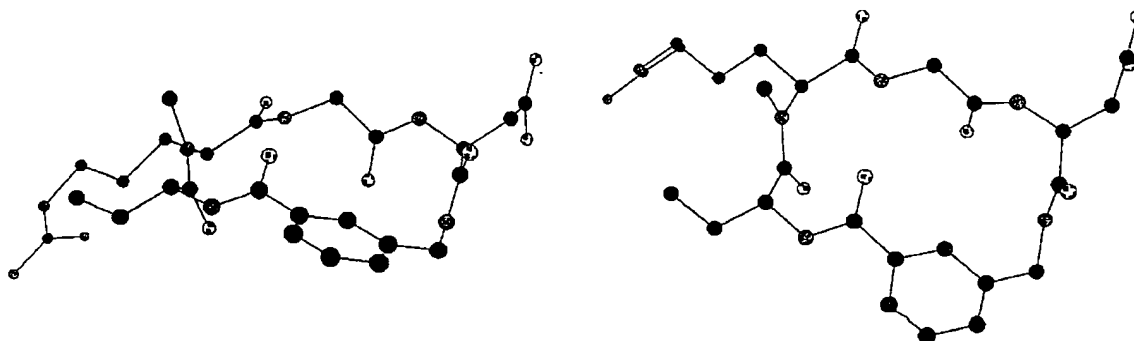
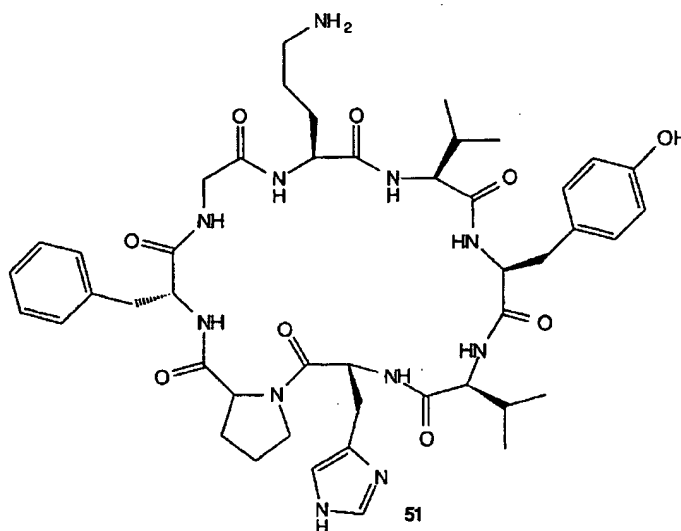
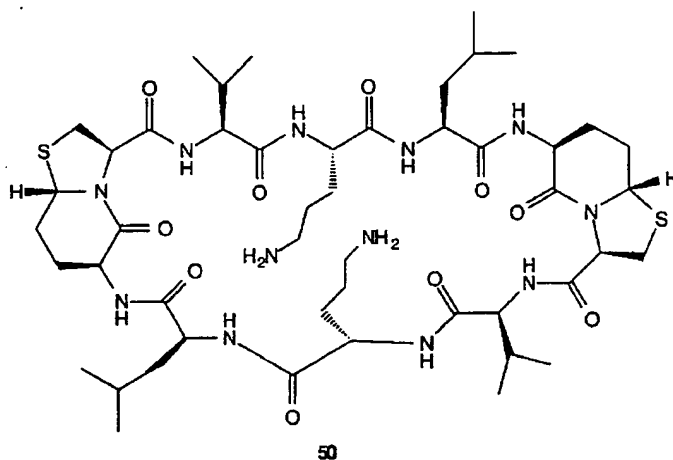


Fig. (10). Alternative views of the X-ray crystal structure of cyclo[D-Abu-NMeArg-Gly-Asp-Mamb] 49 [179] showing the relative orientation of the RGD peptide backbone. A type II'  $\beta$ -turn is centred around the D-Abu-NMeArg amide bond.



aliphatic D-amino acid, and a common backbone conformation with a Type II'  $\beta$ -turn centred at the X-Arg bond. The side chain of the D-amino acid, the methyl group of NMeArg, and the phenyl group of Mamb form a continuous hydrophobic surface which may interact with the receptor.

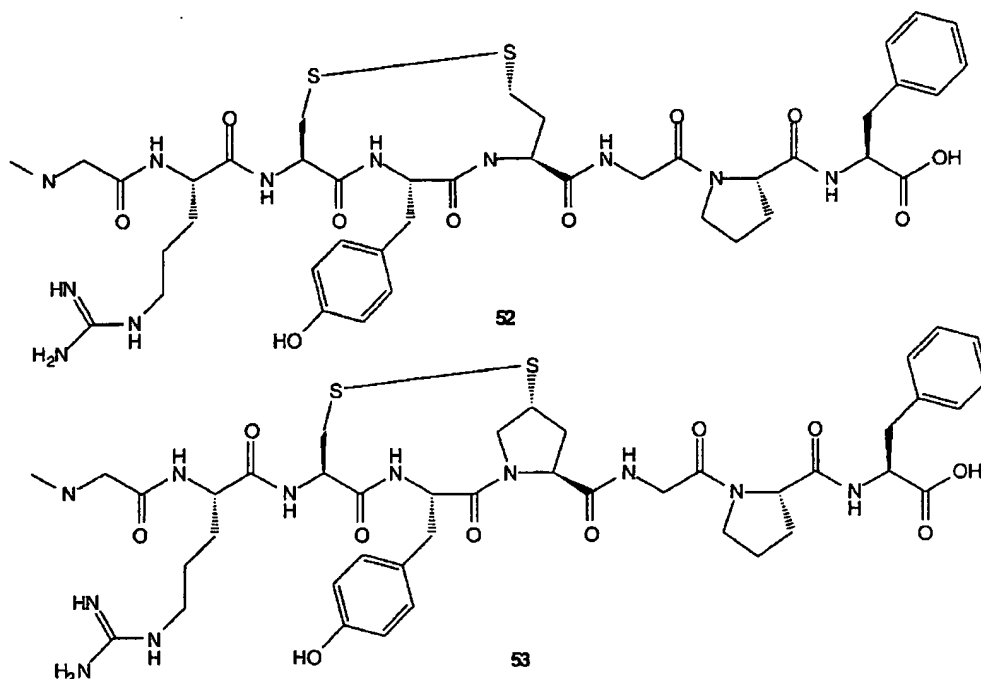
#### Miscellaneous

*Gramicidin S* (**50**), which has biological activity known to be related to its conformation, has been used as a model cyclic peptide to test the ability of different molecules, particularly benzodiazepines [171] and the bicyclic thiazolidine (**50**) [35] to function as  $\beta$ -turn mimetics.

*Cholecystokinin* (CCK) is a 33 residue peptide hormone from the central nervous system and gastrointestinal tract. The C-terminal octapeptide

fragment CCK<sub>26-33</sub> (or CCK-8), Asp<sup>26</sup>-Tyr(SO<sub>3</sub>H)<sup>27</sup>-Met<sup>28</sup>-Gly<sup>29</sup>-Trp<sup>30</sup>-Met<sup>31</sup>-Asp<sup>32</sup>-Phe<sup>33</sup>-NH<sub>2</sub>, has high (nM) affinity for both known receptor sub-types. CCK antagonists may have therapeutic potential in the treatment of pancreatitis, biliary diseases, irritable bowel syndrome and psychiatric complaints. Numerous peptidic inhibitors have been described with selective action for A or B type receptors and conformational studies have also been undertaken [103, 172-176]. However few cyclic inhibitors have been reported to date, these include c-[Gly-Trp-N-MeNle-Asp-Phe] [175] and Boc-c-[D-Asp-Tyr(SO<sub>3</sub>)Nle-D-Lys]-Trp-NLe-Asp-Phe-NH<sub>2</sub> [176] which are selective for the CCK-B receptor.

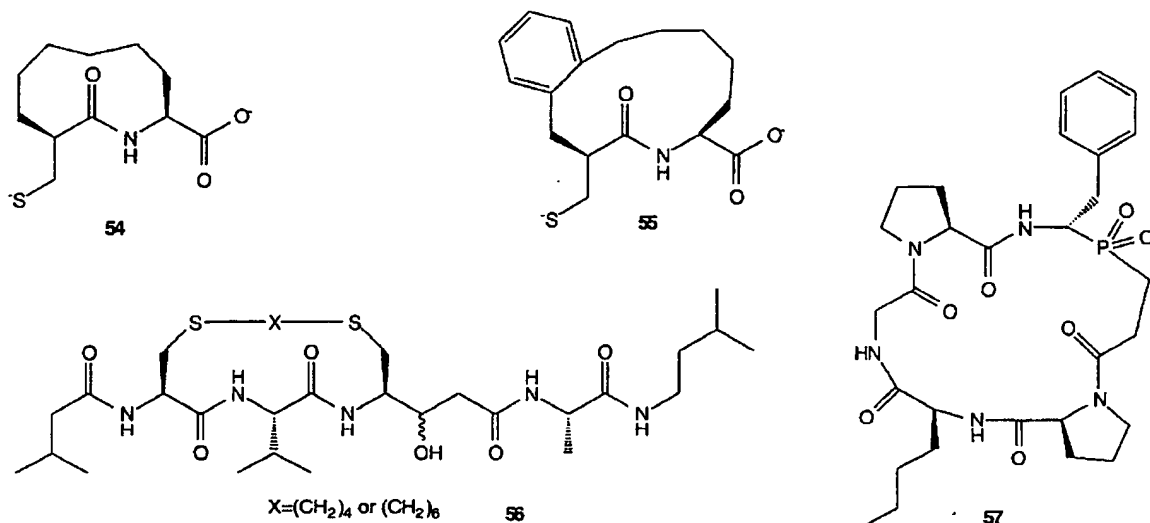
Cyclic analogues of Angiotensin II (Asp<sup>1</sup>-Arg<sup>2</sup>-Val<sup>3</sup>-Tyr<sup>4</sup>-Val<sup>5</sup>-Ile<sup>6</sup>-His<sup>7</sup>-Pro<sup>8</sup>-Phe<sup>9</sup>) have been constructed. For example [101, 177], **51** was only slightly active *in vivo* but is missing the C-terminal carboxylate that is



necessary for activity, **52** displayed similar activity to angiotensin II, while **53** was a potent agonist. Cyclic analogues have also been made for *human parathyroid hormone* fragments [178], involving a lactam connection and an amphipathic  $\alpha$ -helix which is thought to be important for receptor-binding; *tuftsin* [179], a tetrapeptide component of leukokinin that stimulates phagocytosis and *luteinizing hormone release hormone* (LHRH) [101].

Inhibitors of *proteolytic enzymes* have also been the subject of cyclisation strategies. Cyclic inhibitors again have the advantage of being more conformationally constrained than acyclic peptide inhibitors. Also they

are less susceptible to cleavage by other proteolytic enzymes. In addition to those detailed below for renin and *HIV-1 protease*, macrocyclic peptide inhibitors have been synthesized for *thermolysin* (e.g. **54**,  $K_i$  3.8  $\mu$ M; **55**,  $K_i$  19 nM), using amide and aromatic ring constraints [180]; *porcine pepsin* (**56**,  $K_i$  2.7 nM) and *penicillopepsin* (**56**,  $K_i$  4.6 nM) using disulfide bond constraints [181]; bacterial collagenase (**57**,  $IC_{50}$  nM) containing a phosphinic bond and the unusual type VIII  $\beta$ -turn [182]; porcine pancreatic  $\alpha$ -amylase involving small mimetics of the proteinaceous inhibitor tendamistat ( $K_i$  0.2 nM) [183], trypsin and chymotrypsins [10].



## Renin Inhibitors

Renin, a highly specific aspartic protease that is implicated in hypertension, cleaves angiotensinogen to the decapeptide angiotensin I. This is subsequently cleaved by angiotensin converting enzyme (ACE) to the octapeptide angiotensin II, a potent vasoconstrictor that stimulates secretion of catecholamine and aldosterone, and controls fluid volume and sodium excretion. Inhibitors of both renin and ACE are effective modulators of blood pressure and we note that **58** is a naturally occurring 16-membered macrocyclic peptide of microbial origin that inhibits ACE (Ki 349nM) [184]. In the absence of X-ray crystallographic data for human renin [185], several groups [186-193] used molecular modelling techniques to design conformationally constrained cyclic peptide inhibitors of human renin. The compounds were analogues of the linear substrate angiotensinogen, modified with transition state isosteres replacing the scissile amide bond, and typically contained 10-20 membered rings (e.g. **59-62**) formed by linking various side chains in the linear inhibitor.

**59** contains a bridge between the side chain at position P1 and the main chain NH of position P2. Different size macrocycles, namely 10- ( $n = 3$ ), 12- ( $n = 4$ ) and 14- ( $n = 5$ ) membered rings, had different inhibitor potencies against human renin ( $IC_{50} > 100$ , 69, 3  $\mu$ M respectively) [186]. The difference was traced by NMR spectroscopy to a cis-trans isomerization of the Phe(P3)-Ala(P2) amide bond, the 10-membered ring being all cis, the 12-membered ring being 80% cis, and the 14-membered ring being 50% cis [186]. The cis conformation was stabilized, like proline, when the main chain NH was substituted and in this form is unable to fit

into the enzyme active site. The designed molecule **60** was similarly only a modest ( $IC_{50} \mu$ M) inhibitor of renin and the NMR solution structure suggested that an endocyclic hydrogen bond produces an unexpected conformation of the macrocycle [192]. **61** contains a 14-membered cycle produced by linking the N-terminal Pro at P4 to the imidazole ring of His at P2 with a carboxymethylene group. This N-terminal cyclic peptide contains four conformational constraints (proline, imadazole and two amide bonds) which conferred inhibitor potency ( $IC_{50}$  0.28nM ( $R = H$ ) versus 0.5nM for the linear inhibitor) [193]. **62** contains a 13-membered macrocycle, based on linking P2 and P1' side chains of angiotensinogen, and is particularly potent ( $IC_{50}$  56nM) [188]. It is notable for incorporating the scissile bond replacement within the cycle and for containing two amide and one ester bond constraints.

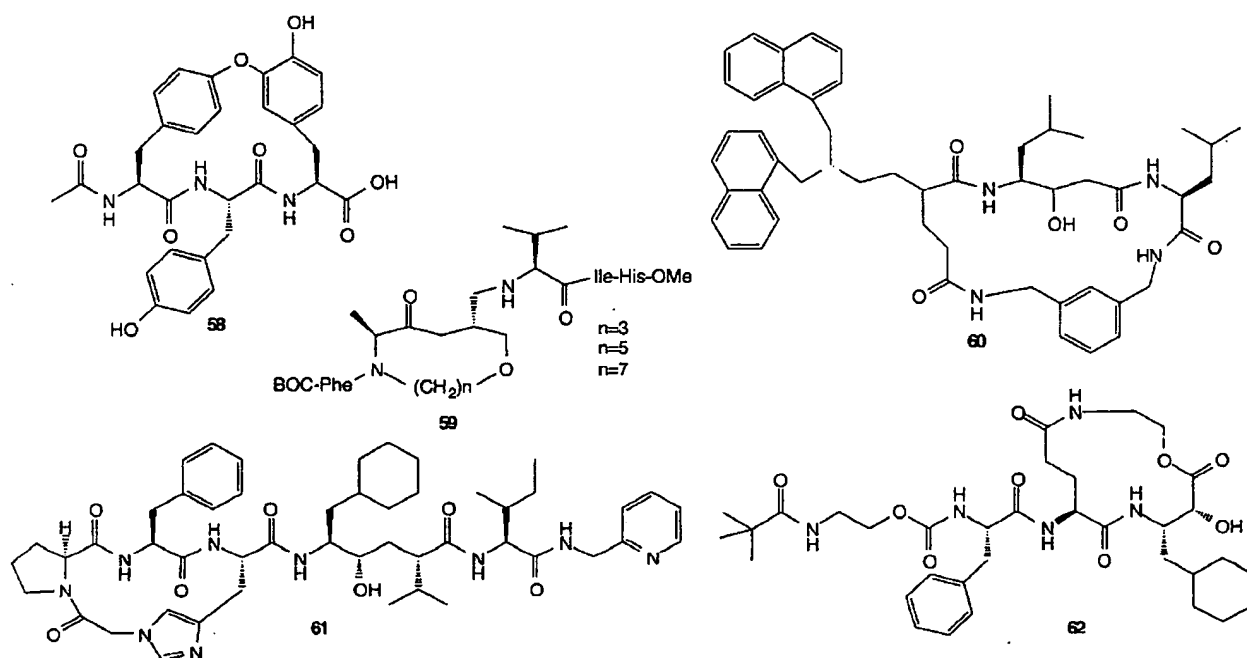
The cyclic feature of these compounds made them much more resistant than their acyclic parent compounds to cleavage by other proteolytic enzymes (e.g. chymotrypsin).

## Receptor-Based Macrocycles

This section focuses on only two proteins to briefly outline the potential for macrocyclic peptidomimetics, designed from a knowledge of the three dimensional structure of the protein.

### HIV-1 Protease

Macrocyclic peptides have also been developed as constrained mimics of components of peptidic inhibitors of another aspartic protease, HIV-1 protease, which is essential for replication of the Human Immunodeficiency Virus (Type 1) [194-196]. For



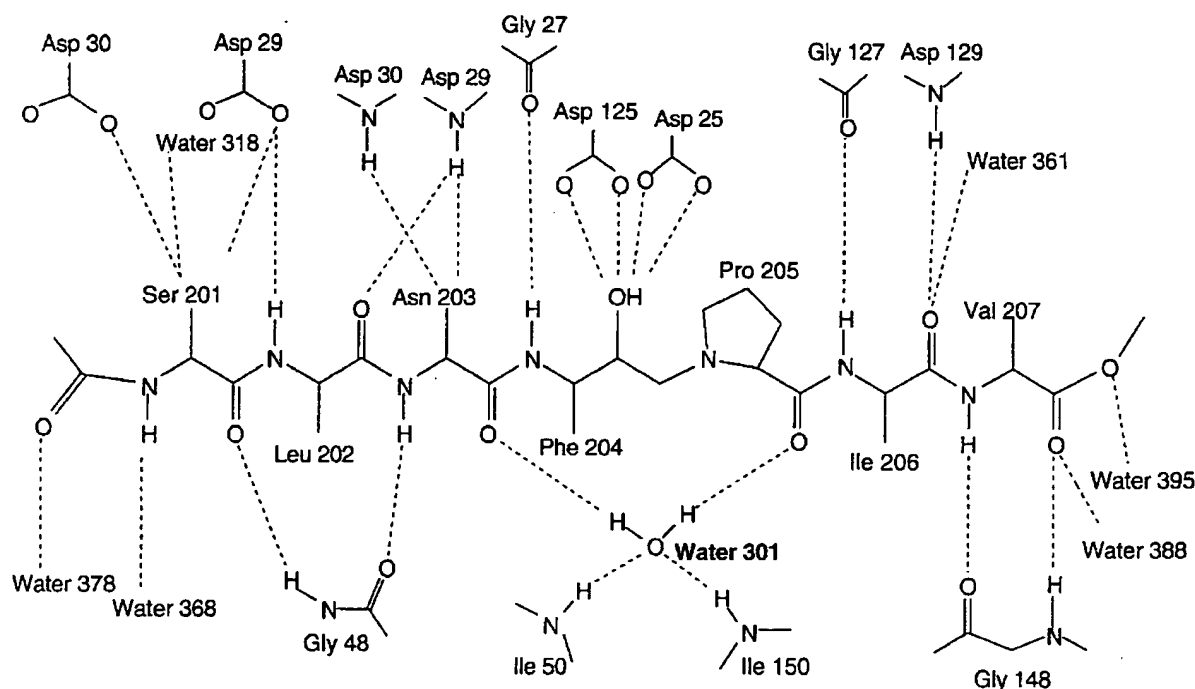


Fig. (11). Hydrogen-bonding between JG-365 and HIV-1 protease [197].

example, one of the eight natural substrates for HIV-1 protease fills the substrate-binding groove with the sequence Ser-Leu-Asn-Phe-Pro-Ile-Val containing a Phe-Pro cleavage site. Replacing the cleavable amide bond by a hydroxyethylamine 'transition state isostere' gave the potent heptapeptide inhibitor JG-365 (Ac-Ser-Leu-Asn-Phe- $\psi$ [CH(OH)CH<sub>2</sub>N] Pro-Ile-Val-OMe, IC<sub>50</sub> 1nM) which has been co-crystallised with the enzyme and the X-ray structure determined [197]. Fig. 11 shows the hydrogen bonds made between JG-365 and HIV-1 protease. Fig. 12 shows the receptor-

bound, extended conformation of the inhibitor fitted into the substrate-binding groove of the enzyme, the S-diastereomeric alcohol (pictured) being 10 fold more potent than the R-diastereomer.

Unlike the earlier work with renin inhibitors, designed in the absence of experimentally determined structural data for renin, researchers have been able to take advantage of X-ray data on inhibitor-complexed HIV-1 protease to rationally design potent inhibitors. Based upon connecting the closely approaching Leu and Phe side chains, two research groups [198-200]

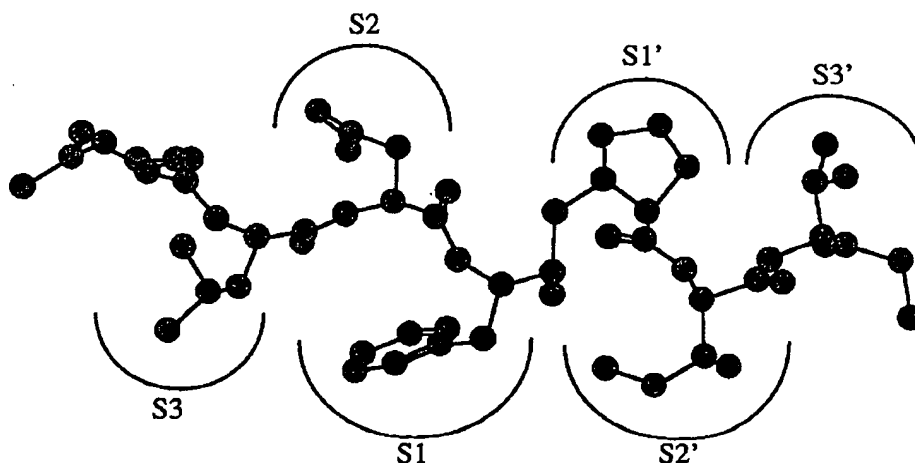
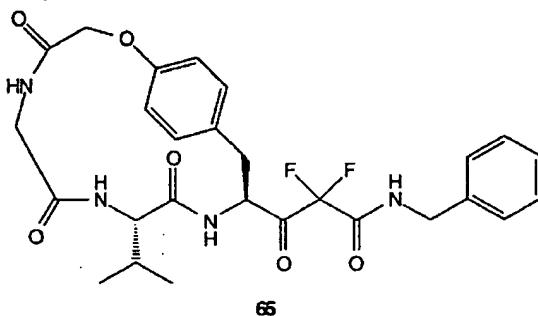
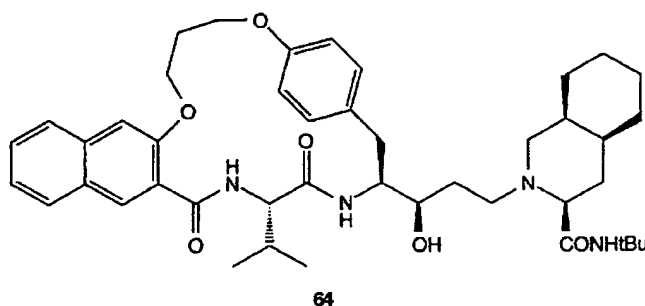
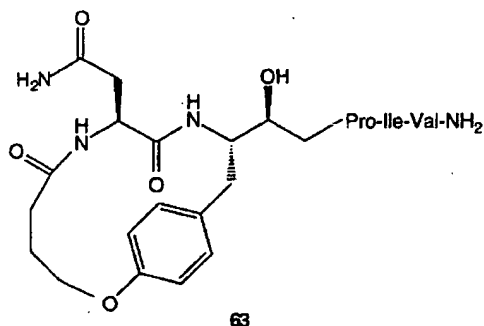


Fig. (12). Receptor bound conformation of JG365 (X-ray structure) [197].

677 *Current Medicinal Chemistry*, 1995, Vol. 2, No. 2

Fairlie et al.



have independently incorporated macrocycles (**63**, **64**) into the truncated inhibitor Ac-Leu-Asn-Phe- $\psi$ (CH(OH)CH<sub>2</sub>N)Pro-Ile-Val-NH<sub>2</sub> IC<sub>50</sub> 30nM. A third group [201] used the X-ray structure of the related inhibitor MVT-101 bound to HIV-1 protease to develop a similar macrocyclic inhibitor (**65**). Compound **64** also replaces Pro-Ile-Val with the bulky but shorter DicNHtBu terminus [202], while **65** replaces  $\psi$ (CH(OH)CH<sub>2</sub>N)Pro-Ile-Val with a difluorostatone isostere.

All three of these "N-terminal" cycles, constrained into fairly rigid conformations by the aromatic ring(s) and multiple amide bonds; mimic to some degree the receptor-binding conformation of the Leu-(Asn/Val)-

Phe component of the bioactive hexapeptide upon which they were designed. For example Fig. 13 shows the receptor-bound conformations of **63** overlayed on JG-365 and there is an excellent match of both main chain and side chain atoms of the inhibitors. A consequence of this structural mimicry is that **63** and derivatives are also functional mimics, potently inhibiting HIV-1 protease (IC<sub>50</sub> 1-30nM). Also because their amide bonds are not recognizable by peptidases, they display enhanced stability toward degradative proteolytic enzymes.

The corresponding C-terminal cycle replacement for Phe-Ile-Val-OMe has also been incorporated into an optimised hexapeptide sequence, Ac-Leu-Val-Phe-

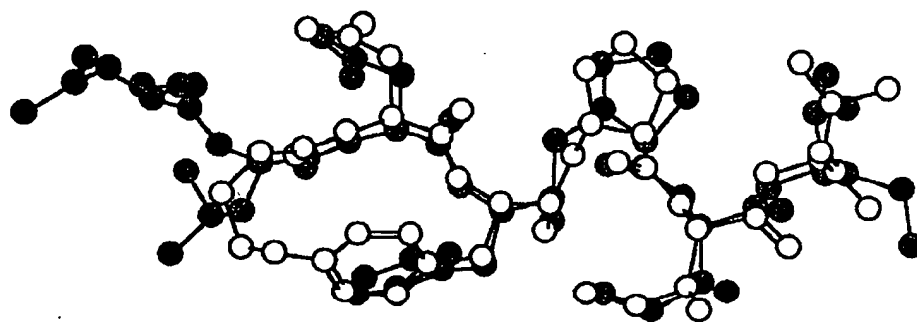
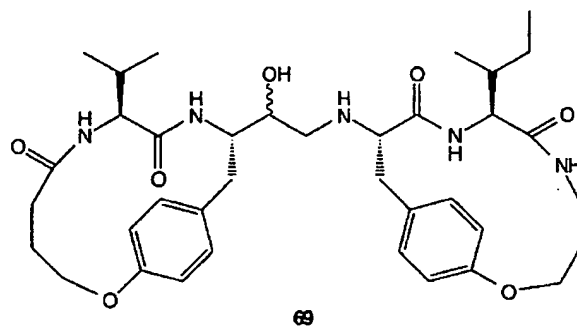
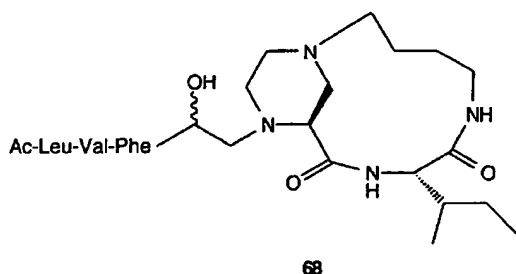
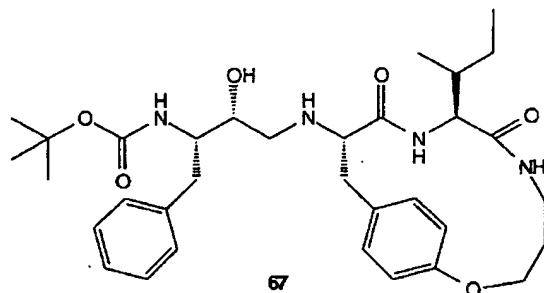
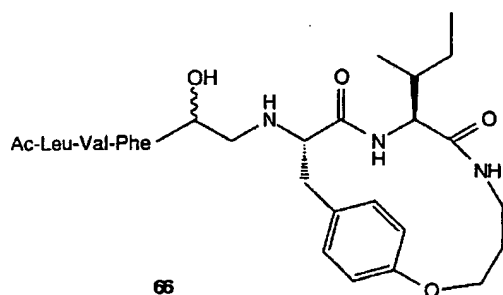


Fig. (13). Overlay of receptor bound conformations of **63** (modelled structure) [199] on JG-365 (X-ray structure) [197].

*Forcing Peptides into Bioactive Conformations**Current Medicinal Chemistry, 1995, Vol. 2, No. 2 678*

$\psi\{\text{CH}(\text{OH})\text{CH}_2\text{N}\}\text{Phe-Ile-Val-OMe}$  ( $\text{IC}_{50}$  5nM), leading to **66** ( $\text{IC}_{50}$  2nM) [203]. Curiously there was no discrimination by the enzyme for R- and S-diastereomeric alcohols of this hexapeptide, unlike JG-365 or **63-65**. The C-terminal cycle is not a precise structural mimic of Pro-Ile-Val (Fig. 14), the endocyclic aromatic ring being translocated out of the S1' pocket and along the groove towards S3'. Data from the X-ray crystal structure of **67** revealed that the

hydroxyethylamine nitrogen is hydrogen bonded to both catalytic aspartic acids (Asp25 & Asp125) of the enzyme active site.

On the other hand the piperazine derivative cycle **68** fills the pocket much better (Fig. 15) and more precisely mimics the receptor-bound conformation of the acyclic peptide [203]. Both N- and C- terminal cycles have also been combined into the bicycle **69**,

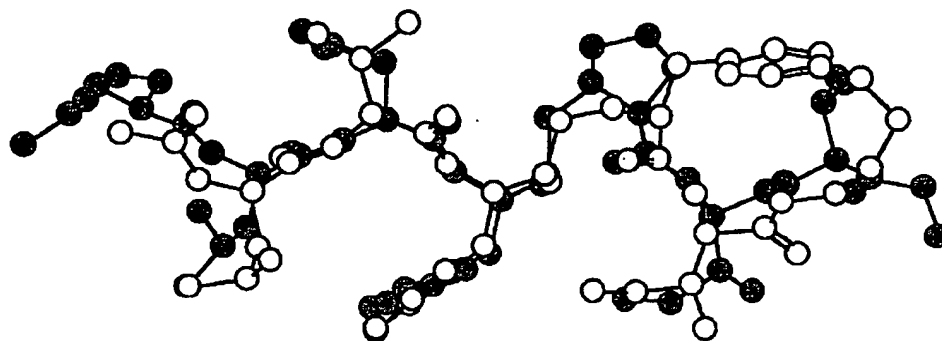


Fig. (14). Overlay of receptor bound conformation of **66** (modelled structure) [203] on JG-365 (X-ray structure) [197].

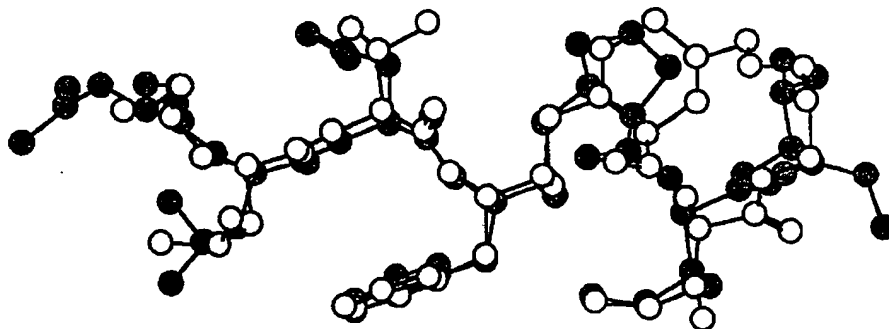


Fig. (15). Overlay of receptor bound conformation of **68** (modelled structure) [203] on JG-365 (X-ray structure) [197].

shown overlayed on JG-365 in Fig. (16). Despite an unoptimised match of the structures, in particular the incomplete occupancy of S1' pocket, compound **69** was still quite potent ( $IC_{50}$  2nM) [203].

A 9 residue peptide fragment (**70**) of a CD4 protein surface analogous to the third complementarity determining region (CDR3) in immunoglobulin, contains two antiparallel  $\beta$ -strands connected by a reverse

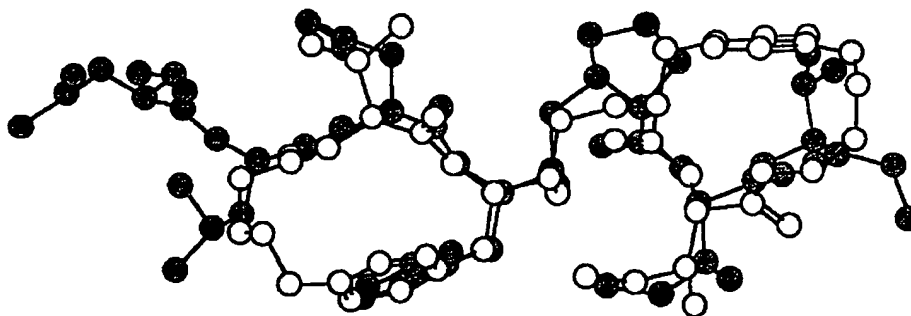
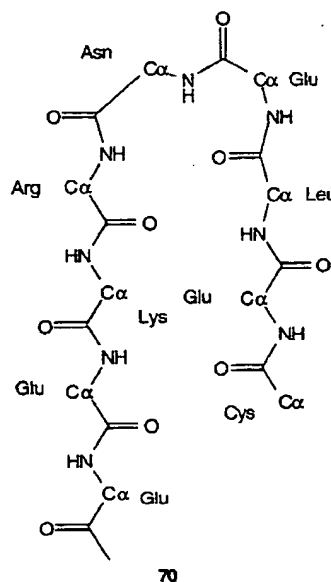


Fig. (16). Overlay of receptor bound conformation of **69** (modelled structure [203] on JG-365 (X-ray structure) [197].

The increasing availability of protein structures promises that the use of receptor-based molecular design approaches, such as those described above, for choosing conformational constraints to be incorporated into enzyme inhibitors will likely become the most rational and cost effective method for future inhibitor and drug development.

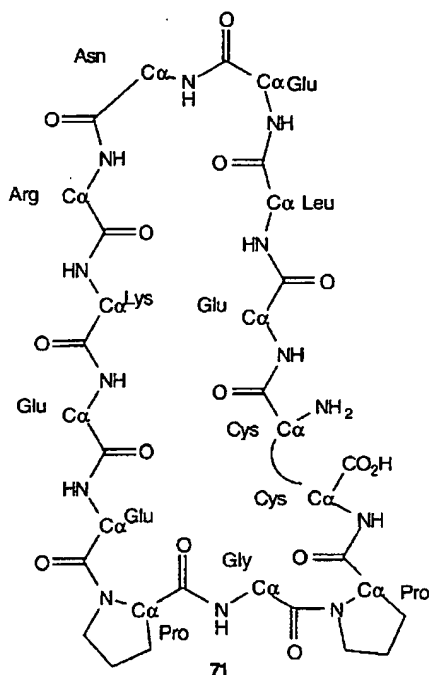
#### CD4 Mimetics

CD4 is a glycoprotein found on the surface of T lymphocytes and other immune cells. It acts cooperatively with class II MHC molecules and the T cell receptor in the recognition of foreign antigens and activation of T cells. It is also recognized by a glycoprotein (gp120) of the human immunodeficiency virus, for which it has a particularly high affinity ( $K_d$   $10^{-9}$  M) and facilitates viral attachment to immune cells. Various cyclic peptides like **71-72** have been rationally designed and prepared as mimics of surface regions of CD4.



### Forcing Peptides into Bioactive Conformations

turn [204]. To fix this conformation, the peptide was cyclised using a forced turn constraint (Pro-Gly-Pro-) and a disulfide bond to yield macrocyclic analogue **71**, which inhibited *in vitro* CD4-dependent T-cell responses [204]. An NMR study [205] revealed that the PGP turn did in fact force the the macrocyclic peptide to adopt a conformation in which the putative binding region (Arg<sup>6</sup> to Glu<sup>9</sup>) was similar in solution to that in native protein. Replacing the L-amino acids with D-amino acids and reversing the sequence gave a cyclic peptide that inhibited *in vivo* experimental rodent allergic encephalomyelitis (EAE), an acute inflammatory autoimmune disease of the central nervous system that is commonly used as a model of multiple sclerosis [204]. Similarly, a well known 10-14 membered ring constraint **72** has also been used [206] to fix a type II  $\beta$ -turn in cyclic peptide mimics of CD4 corresponding to the CDR2 of the immunoglobulins (e.g. 2rhe) and the structures match CD4 from X-ray data.



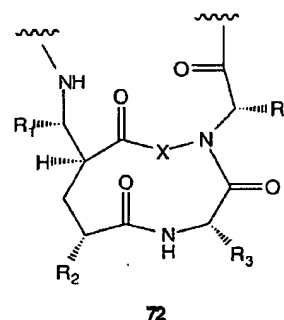
### Summary & Future Directions

The indicated studies of conformationally constrained cyclic analogues of bioactive peptides have provided important information on the relationships between constraints, conformation and bioactivity. In the majority of cases the putative receptor-bound bioactive conformations of acyclic peptides have had to be deduced from painstaking and detailed conformational studies and structure-activity data for acyclic and cyclic peptides. Even then there is uncertainty about the precise receptor-bound structures. The process will however become more efficient in the future due to improved access to protein-inhibitor structures.

*Current Medicinal Chemistry*, 1995, Vol. 2, No. 2 680

Macrocyclic peptides have been constructed using a variety of connections, including disulfide bonds, hydrogen bonds, side chain to side chain, side chain to backbone, and backbone to backbone. The macrocycles have been demonstrated to stabilise a variety of different turns and loops, as well as helices and sheet structures in some cases. Amide bonds have been protected by N- or C- alkylation or replaced altogether. Most of the constraints described above are simple units and although much has been done to design more sophisticated, and more constraining,  $\beta$ -,  $\gamma$ - and other turn mimetic structures for peptides (reviewed elsewhere [28, 29, 207, 208]), unfortunately there have been comparatively few studies to date where designed constraints have been incorporated into macrocyclic peptides. This is likely to be a fertile research area over the next few years.

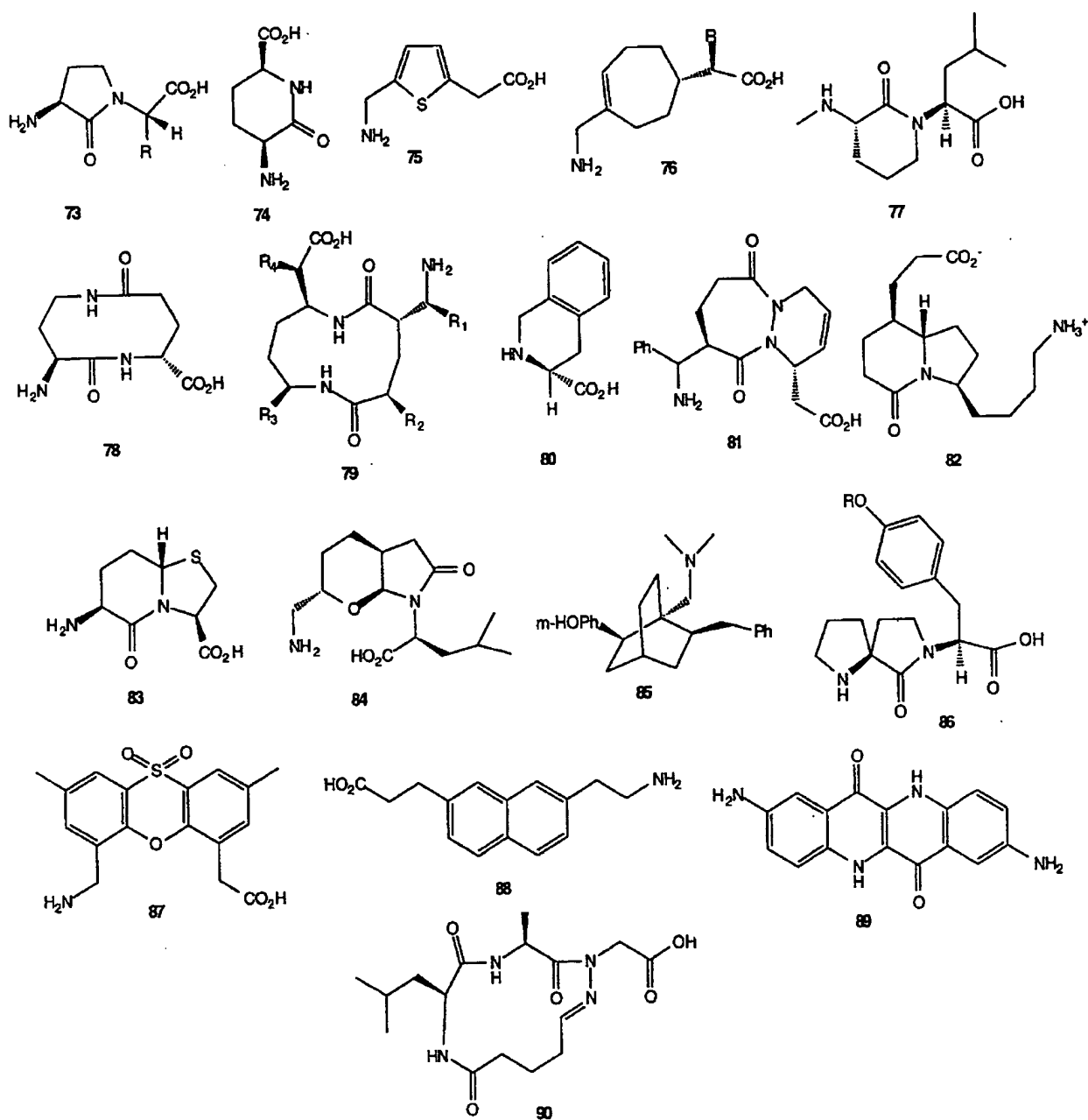
Some examples of designed constraints that are known to enforce specific conformations in macrocyclic



peptides are **73-89** [207, 208, 29 and refs. therein].  $\beta$ -II' turn mimetics that have been successfully incorporated into macrocyclic peptides include **73** (in LHRH [209]); **77** (in cyclosporin [210]); **83** (in gramicidin, enkephalins and LRF [211]). Derivatives of **76** have been used as  $\gamma$ -turn mimetics and incorporated into enkephalins [207]. Two dimensional NMR spectroscopy [212] showed that a macrocyclic peptide containing **88** was a mimic of exposed  $\Omega$  loop (amino acids 41-48) of interleukin-1, a key inflammatory mediator and regulator of the immune response. Anti-parallel  $\beta$ -sheets have been induced by **89** [213], while **90** [214] is among  $\alpha$ -helix nucleators [215-216]. Helix bundles are also being extensively studied, particularly the template assembled synthetic proteins (TASPS) [217-219] although these are presently restricted to

681 *Current Medicinal Chemistry*, 1995, Vol. 2, No. 2

Fairlie et al.



the mounting of identical amphipathic helix-forming peptides upon flexible and semi-rigid templates.

One can envisage continued development of specialised sets of constraints towards the goal of mimicking specific protein surfaces. A great challenge will be the successful mimicry of multiple (discontinuous) protein surfaces, such as multiple loops and complementarity determining regions (CDRs) of immunoglobulins [220]. Three dimensional structural information on proteins and protein-mimetic complexes will increasingly be the key to successful developments in these areas.

## Acknowledgments

Partial support for this work was provided by the National Health and Medical Research Council, University of Queensland and the Australian Research Council.

## References

- [1] Milner-White, E. J. *Trends Pharmacol. Sci.* 1989, 10, 70-74.
- [2] Verber, D. F.; Freidinger, R. M. *Trends Neurosci.* 1985, 8, 392-396.

**Forcing Peptides into Bioactive Conformations***Current Medicinal Chemistry*, 1995, Vol. 2, No. 2 682

- [3] Hruby, V. J. in *Peptides, Proc. Thirteenth American Peptide Symposium*, Hodges, R. S.; Smith, J. A. (eds), ESCOM : Liden, Netherlands, 1994, pp 3-17.
- [4] Mocek, U.; Zeng, Z.; O'Hagan, D.; Zhou, P.; Fan, L.-D. D.; Beale, J. M.; Floss, H. G. *J. Am. Chem. Soc.* 1993, 115, 7992-8001.
- [5] Rinehart, J. B.; Gloer, J. B.; Coock, J. C.; Mizsak, S. A.; Scahill, T. A. *J. Am. Chem. Soc.* 1981, 103, 1857.
- [6] Faulkner, D. J., *Nat. Prod. Rep.* 1986, 3, 1-33.
- [7] Rinehart, K. L.; Kishure, V.; Bible, K. C.; Sakai, R.; Sullins, D. W.; Li, K. M. *J. Nat. Prod.* 1988, 51, 1-21.
- [8] Ireland, C. M.; Durso, A. R.; Newman, R. A.; Hacker, M. P. *J. Org. Chem.* 1982, 47, 1807-11.
- [9] Shiomi, T.; Hamada, Y.; Kato, S.; Shibata, M.; Kondo, Y.; Nakagawa, H.; Kohda, K. *Biochem. Pharmacol.* 1987, 36, 4181-5.
- [10] Ovchinnikov, Y. A.; Ivanov, V. T. *Tetrahedron* 1975, 31, 2177-2209.
- [11] Lewis, J. R., *Natural Products Reports*, 1989, 6, 503.
- [12] Faulkner, D. J. *Natural Products Reports*, 1994, 11, 355-394.
- [13] Krebs, H. C. *Fortschr. Chem. Org. Naturst.* 1986, 49, 151.
- [14] Davies, J. S., *Amino acids, peptides and proteins*, 1993, 25, 247-295.
- [15] Bladon, C. M., *Amino acids, peptides and proteins*, 1993, 25, 154-245.
- [16] Rosen, M. K.; Schreiber, S. L. *Angew. Chem., Int. Ed. Engl.* 1992, 31, 384-400.
- [17] Evans, D. A.; Ellman, J. A. *J. Am. Chem. Soc.* 1989, 111, 1063-72.
- [18] Fusetani, N.; Sugawara, T.; Matsunaga, S. *J. Am. Chem. Soc.* 1991, 113, 7811-2.
- [19] Kobayashi, J.; Itagaki, F.; Shigemori, H.; Ishibashi, M.; Takahashi, K.; Ogura, M.; Nagasawa, S.; Nakamura, T.; Hirota, H.; Ohta, T.; Nozoe, S. *J. Am. Chem. Soc.* 1991, 113, 7812-3.
- [20] Hagihara, M.; Schreiber, S. J. *Am. Chem. Soc.* 1992, 114, 6570-71.
- [21] Dilip de Silva, E.; Williams, D. E.; Anderson, R. J.; Klix, H.; Holmes, C. F. B.; Allen, T. M. *Tet. Lett.* 1992, 33, 1561-4.
- [22] For example : Budesinsky, J.; Symersky, J.; Jecny, J.; Van Hecke, N.; Hosten, M.; Anteuio, M.; Borremans, F. *Int. J. Pept. Protein Res.*, 1992, 39, 123.
- [23] North, M. *Tetrahedron*, 1992, 48, 5509.
- [24] Yamazaki, T.; Nunami, K.-I.; Goodman, M. *Biopolymers*, 1991, 31, 1513-1528.
- [25] Prasad, C. *Peptides*, 1995, 16, 151-164.
- [26] Cerrini, S.; Gavuzzo, E.; Lucente, G.; Luisi, G.; Pinnen, F.; Radics, L. *Int. J. Pept. Protein Res.*, 1991, 38, 289-297.
- [27] Aumailly, M.; Gurrath, M.; Meuller, G.; Calvete, J.; Timpl, R. Kessler, H. *FEBS Lett.*, 1991, 291, 50-54.
- [28] Rose, G. D.; Gierasch, L. M.; Smith J. A., *Adv. Protein Chemistry*, 1985, 37, 1-109.
- [29] Ball, J. B.; Hughes, R. A.; Alewood, P. F.; Andrews, P. R.; *Tetrahedron*, 1993, 49, 3467-3478.
- [30] Manavalan, P.; Momany, F.A. *Macromolecules*, 1980, 19, 1943.
- [31] Stradley, S.; Rizo, J.; Bruch, M.; Stroup, A.; Gierasch, L. *Biopolymers*, 1990, 29, 263-287.
- [32] Ihara, M.; Fukuroda, T.; Saeki, T.; Nishikibe, M.; Kojiri, K.; Suda, H.; Yano, M. *Biochem. Biophys. Res. Comm.* 1991, 178, 132-137.
- [33] Coles, M.; Sowemimo, V.; Scanlon, D.; Munro, S. L. A.; Craik, D. *J. J. Med. Chem.* 1993, 36, 2658.
- [34] Ihara, M.; Noguchi, K.; Saeki, T.; Fukuroda, T.; Tsuchida, S.; Kimura, S.; Fukami, T.; Ishikawa, K.; Nishikibe, M.; Yano, M. *Life Sciences* 1992, 50, 247.
- [35] Bean, J.W.; Peishoff, C. E.; Kopple, K.D. *Int. J. Protein Res.* 1994, 44, 1994, 223.
- [36] Hull, S. E.; Karlsson, R.; Main, P.; Woolfson, M. M.; Dodson, E. *J. Nature (London)*, 1978, 275, 206-207.
- [37] Sato, K.; Nagai, U. *J. Chem. Soc., Perkins Trans. I*, 1986, 1231.
- [38] Aracil, J. M.; Badre, A.; Fadli, M.; Jeanty, G.; Banaigs, B.; Francisco, C.; Larfargue, F.; Heltz, A.; Aumelas, A. *Tet. Lett.*, 1991, 32, 2609-2612.
- [39] Sussman, F.; Weinstein, H. *Proc. Nat. Acad. Sci. USA* 1989, 86, 7880.
- [40] Schreiber, S. L.; Crabtree, G. R. *Immunol. Today* 1992, 13, 136-142.
- [41] Liu, J.; Albers, M. W.; Wandless, T. J.; Luan, S.; Alberg, D. G.; Belshaw, P. J.; Cohen, P.; MacKintosh, C.; Klee, C. B.; Schreiber, S. L. *Biochem.* 1992, 31, 3896-3901.
- [42] Kessler, H.; Kock, M.; Wein, T.; Gehrke, M. *Helv. Chim. Acta* 1990, 73, 1818.
- [43] Loosli, H.-R.; Kessler, H.; Ochkinat, H.; Weber, H.-P.; Petcher, T. J.; Widmer, A. *Helv. Chim. Acta* 1985, 68, 682.
- [44] Wuthrich, K.; von Freyberg, B.; Weber, C.; Wider, G.; Traber, R.; Widmer, H.; Braun, W. *Science*, 1991, 254, 953.
- [45] Kock, M.; Kessler, H.; Seebach, D.; Thaler, A. *J. Am. Chem. Soc.* 1992, 114, 2676.
- [46] Schreiber, S. L. *Science* 1991, 251, 283.
- [47] Myers, R. A.; Cruz, L. J.; Rivier, J. E.; Olivera, B. M. *Chem. Rev.* 1993, 93, 1923-1936.
- [48] Ruan, F.; Chen, Y.; Hopkins, P. B. *J. Am. Chem. Soc.* 1990, 112, 9403.
- [49] Ghadiri, M. R.; Fernholz, A. K. *J. Am. Chem. Soc.* 1990, 112, 9633.
- [50] Imperiali, B.; Kapoor, T. M. *Tetrahedron*, 1993, 49, 3501-3510.
- [51] Schneider, J. P.; Kelly, J. W. *J. Am. Chem. Soc.* 1995, 117, 2533-2546.
- [52] Vallee, B. L.; Auld, D. S. *Acc. Chem. Res.* 1993, 26, 543.
- [53] Otsuka, S.; Yamanaka, T. (eds) *Metalloproteins in Bioactive Molecules*, Elsevier, Tokyo, 1988, 8, pp 1-568.
- [54] Hooper, N. M. *FEBS Lett.* 1994, 354, 1-6.
- [55] Gerday, Ch.; Bolis, L.; Gilles, R. (eds) *Calcium and Calcium Binding Proteins*, Springer-Verlag, Berlin, 1988, pp 1-259.
- [56] Strydom, N. C. J.; James, M. N. E. *Ann. Rev. Biochem.* 1989, 58, 951-998.
- [57] Colplitts, T. L.; Castellino, F. J. *Biochemistry* 1994, 33, 3501-3508.

Fairlie et al.

683 *Current Medicinal Chemistry*, 1995, Vol. 2, No. 2

- [58] Takayuki, N.; Tanaka, N.; Hiratake, J.; Katsube, Y.; Ishida, Y.; Oda, J. *J. Am. Chem. Soc.*, **1988**, *110*, 8733-8734.
- [59] Fujiki, H.; Sugimura, T. *Adv. Cancer Res.* **1987**, *49*, 223.
- [60] Mutoh, R.; Shirai, R.; Koiso, Y.; Iwasaki, S. *Heterocycles*, **1995**, *41*, 9.
- [61] Heffner, R. J.; Jiang, J.; Joutlie, M. M. *J. Am. Chem. Soc.*, **1992**, *114*, 10181; and references therein.
- [62] Itokawa, H.; Takeya, K.; Mihara, N.; Mori, N.; Hamanaka, T.; Sonobe, T.; Itaka, Y. *Chem. Pharm. Bull.*, **1983**, *31*, 1224.
- [63] Majima, H.; Tsukagoshi, S.; Furue, H.; Suminaga, M.; Sakamoto, K.; Wakabayashi, R.; Kishino, S.; Niitani, H.; Murata, A.; Genma, A.; Nukariya, N.; Uematsu, K.; Furuta, T.; Kurihara, M.; Yoshida, F.; Isomura, S.; Takemoto, T.; Hirashima, M.; Izumi, T.; Nakao, I.; Ohashi, Y.; Ito, K.; Asai, R. *Jpn. J. Cancer Chemother.*, **1993**, *31*, 1424.
- [64] Morita, H.; Kondo, K.; Hitotsuyanagi, K.; Takeya, K.; Tomoika, N.; Itai, A.; Itaka, Y. *Tetrahedron*, **1991**, *47*, 2757.
- [65] Jolad, S. D.; Hoffmann, J. J.; Torrance, S. J.; Wiedhopf, R. M.; Cole, J. R.; Arora, S. K.; Bates, R. B.; Gargiulo, R. L.; Kriek, G. R. *J. Am. Chem. Soc.* **1977**, *99*, 8040-8044.
- [66] Itokawa, H.; Saitou, K.; Morita, H.; Takeya, K.; Yamada, K. *Chem. Pharm. Bull.*, **1992**, *40*, 2984-2989.
- [67] Boger, D. L.; Myers, J. B. *J. Org. Chem.*, **1991**, *56*, 5385-5390.
- [68] For a review, see: Williams, D. H. *Acc. Chem. Res.* **1984**, *17*, 364-369.
- [69] X-ray crystal structure: Sheldrick, G. M.; Jones, P. G.; Kennard, O.; Williams, D. H.; Smith, G. A. *Nature (London)*, **1978**, *271*, 223.
- [70] Schmidt, U.; Meyer, R.; Leitenberger, V.; Lieberknecht, A.; Griesser, G. *J. Chem. Soc., Chem. Commun.*, **1991**, 275.
- [71] Buck, K. T., *The Benzylisoquinoline Alkaloids in The Alkaloids*, Academic Press, New York, **1987**, *30*, pp. 1-222.
- [72] Sugimoto, Y.; Sugimura, Y.; Yamada, Y. *FEBS Lett.* **1990**, *273*, 82-86.
- [73] Whitehouse, M. W.; Fairlie, D. P.; Thong, Y. H. *Agents and Actions* **1994**, *42*, 123.
- [74] Seow, W. K.; Nakamura, K.; Sugimura, Y.; Sugimoto, Y.; Yamada, Y.; Fairlie, D. P.; Thong, Y. H. *Mediators Inflammation* **1993**, *2*, 199.
- [75] Li, S. Y.; Ling, L. H.; Teh, B. S.; Seow, W. K.; Thong, Y. H. *Int. J. Immunopharm.* **1989**, *11*, 395.
- [76] Pietrzynski, G.; Rzeszotarska, B.; Kubica, Z. *Int. J. Pept. Protein Res.* **1992**, *40*, 524.
- [77] Chauhan, V. S.; Bhandary, K. K. *Int. J. Pept. Protein Res.* **1992**, *39*, 223-228.
- [78] Padmanabhan, B.; Dey, S.; Khandelwal, B.; Rao, G. S.; Singh, T. P. *Biopolymers*, **1992**, *32*, 1271.
- [79] Hagihara, M.; Anthony, N. J.; Stout, T. J.; Clardy, J.; Schrieber, S. L. *J. Am. Chem. Soc.*, **1992**, *114*, 6568.
- [80] Fusetani, N.; Matsunaga, S.; Matsumoto, H.; Takebayashi, Y. *J. Am. Chem. Soc.*, **1990**, *112*, 7053-7054.
- [81] Lee, A. Y.; Hagihara, M.; Karmacharya, M.; Albers, M. W.; Schrieber, S. L.; Clardy, J. *J. Am. Chem. Soc.*, **1993**, *115*, 12612-12620.
- [82] Maryanoff, B. E.; Qiu, X.; Padmanabhan, K. P.; Tulinsky, A.; Almond, H. R.; Andrade-Gordon, P.; Greco, M. N.; Kauffman, J. A.; Nicolaou, K. C.; Liu, A.; Brungs, P. H.; Fusetani, N. *Proc. Natl. Acad. Sci. USA*, **1993**, *90*, 8048-8052.
- [83] Dilip de Silva, E.; Williams, D. E.; Andersen, R. J. *Tett. Lett.*, **1992**, *33*, 1561-1564.
- [84] Fusetani, N.; Sugawara, T.; Matsunaga, S. *J. Am. Chem. Soc.*, **1991**, *113*, 7811-7812.
- [85] Ishida, T.; Inoue, M.; Hamada, Y.; Kato, S.; Shioiri, T., *J. Chem. Soc., Chem. Commun.* **1987**, 370-371.
- [86] Ishida, T.; Tanaka, M.; Nabaie, M.; Inoue, M.; Kato, S.; Hamada, Y.; Shioiri, T. *J. Org. Chem.* **1988**, *53*, 107-112.
- [87] Ishida, T.; In, Y.; Doi, M.; Inoue, M.; Hamada, Y.; Shioiri, T. *Biopolymers*, **1992**, *32*, 131.
- [88] van den Brenk, A.; Byriel, K. A.; Fairlie, D. P.; Gahan, L. R.; Hanson, G. R.; Hawkins, C. J.; Jones, A.; Kennard, C. H. L.; Murray, K. S. *Inorg. Chem.* **1994**, *33*, 3549.
- [89] van den Brenk, A.; Fairlie, D. P.; Gahan, L. R.; Hanson, G. R.; Hawkins, C. J.; Jones, A. *Inorg. Chem.* **1994**, *33*, 2280.
- [90] Kustin, K.; Weaver, R. *Adv. Inorg. Chem.* **1990**, *35*, 81.
- [91] Michael, J. P.; Pattenden, G. *Angew. Chem. Int. Ed. Engl.* **1993**, *32*, 1.
- [92] van den Brenk, A. *PhD dissertation*, University of Queensland, **1994**.
- [93] Foster, M. P.; Concepcion, G. P.; Caraan, G. B.; Ireland, C. M. *J. Org. Chem.*, **1992**, *57*, 6671.
- [94] Park, S. K.; Jurek, J.; Carney, J. R.; Scheuer, P. J. *J. Nat. Products*, **1994**, *57*, 407.
- [95] Casapullo, A.; Minale, L.; Zollo, F. *J. Nat. Products*, **1994**, *57*, 1227.
- [96] Smith, G. D.; Daux, W. L.; Langs, D. A.; DeTitta, G. T.; Edmonds, J. W.; Rohrer, D. C.; Weeks, C. M. *J. Am. Chem. Soc.* **1975**, *97*, 7242-7247.
- [97] Marrone, T. J.; Merz, K. M. Jr. *J. Am. Chem. Soc.* **1995**, *117*, 779-791.
- [98] Neupert-Laues, K.; Dobler, M. *Helv. Chim. Acta* **1975**, *58*, 432-442.
- [99] Hruby, V. J.; Al-Obeidi, F.; Kazmierski, W. *Biochem. J.* **1990**, *268*, 249-262.
- [100] Hruby, V. J.; Sharma, S. D. *Curr. Opinion Biotech.* **1991**, *2*, 599.
- [101] Nikiforovich, G. V. *Int. J. Peptide Protein Res.* **1994**, *44*, 513.
- [102] Marshall, G. R. *Tetrahedron* **1993**, *49*, 3547-3558.
- [103] Olsen, G. L.; Bolin, D. R.; Pat Bonner, M.; Bos, M.; Cook, C. M.; Fry, D. G.; Graves, B. J.; Hatada, M.; Hill, D. E.; Khan, M.; Madison, V. S.; Rsiecki, V. K.; Sarabu, R.; Sepinwall, J.; Vincent, G. P.; Voss, M. E. *J. Med. Chem.* **1993**, *36*, 3039-3049.
- [104] Toniolo, C. *Int. J. Peptide Protein Res.* **1990**, *35*, 287-300.
- [105] Verber, D. F.; Freidinger, R. M.; Perlrow, D. S.; Palveda, W. F. Jr.; Holly, F. W.; Strachan, R. G.; Nutt, R. F.; Arison, B. H.; Homrick, C.; Randall, W. C.; Glitzer, M. S.; Saperstein, R.; Hirschman, R. *Nature*, **1981**, *292*, 55-58.
- [106] Verber, D. F. in *Peptides, Synthesis, Structure and Function*, Rich, D. H.; Gross, V. J. (eds) Pierce Chem. Co.: Rockford, IL, Proc. Seventh Am. Peptide Symp. **1981**, pp 685-694.
- [107] Freidinger, R. M.; Verber, D. F. in *Conformationally Directed Drug Design*, ed. Vida, J. A.; Gordon, M.; ACS Symp. Ser. 251; *Am. Chem. Soc.: Washington, DC*, **1984**, 169-187.
- [108] Schiller, P. W. in *The Peptides*, Udenfriend, S.; Meienhofer, J. (eds); Academic Press, New York, **1984**, Vol. 6, pp. 219.
- [109] Murphy, W. A.; Heiman, M. L.; Lance, V. A.; Mezo, I.; Coy, D. H. *Biochem. Biophys. Res. Comm.* **1985**, *132*, 922-928.

## Forcing Peptides into Bioactive Conformations

Current Medicinal Chemistry, 1995, Vol. 2, No. 2 684

- [110] He, Y.-B.; Huang, Z.; Raynor, K.; Reisine, T.; Goodman, M. J. *Am. Chem. Soc.* **1993**, *115*, 8066-8072.
- [111] Jaspers, H.; Horvath, A.; Mezo, I.; Keri, G.; van Binst, G. *Int. J. Peptide Protein Res.* **1994**, *271-276*.
- [112] Hirschmann, R.; Nicolau, K. C.; Pietranico, S.; Salvino, J.; Leahey, E. M.; Sprengeler, P. A.; Furst, G.; Smith, A. B. III; Strader, C. D.; Cascieri, M. A.; Candelore, M. R.; Donaldson, C.; Vale, W.; Maechler, L. *J. Am. Chem. Soc.* **1992**, *114*, 9217-8.
- [113] Sawyer, T. K.; Hruby, V. J.; Darman, P. S.; Hadley, M. E. *Proc. Natl. Acad. Sci. USA* **1982**, *79*, 1751.
- [114] Lebl, M.; Cody, W. L.; Wilkes, B. C.; Hruby, V. J.; De L. Castrucci, A. M.; Hadley, M. E. *Int. J. Peptide Protein Res.* **1984**, *24*, 472.
- [115] Hruby, V. J.; Sharma, S. D.; Toth, K.; Jaw, J. Y.; Al-Obeidi, F.; Sawyer, T. K.; Hadley, M. E. *Ann. N. Y. Acad. Sci.* **1993**, *680*, 51.
- [116] Manning, M.; Chan, W. Y.; Sawyer, W. H. *Regulatory Peptides*, **1993**, *45*, 279-283.
- [117] Smith, D. D.; Slaninova, J.; Hruby, V. J. *J. Med. Chem.* **1992**, *35*, 1558-1563.
- [118] Manning, M.; Stoev, S.; Chan, W. Y.; Sawyer, W. H. *Ann. N. Y. Acad. Sci.* **1993**, *689*, 219-232.
- [119] Hill, P. S.; Smith, D. D.; Slaninova, J.; Hruby, V. J. *J. Am. Chem. Soc.* **1990**, *112*, 3110-3113.
- [120] Williams, P. D.; Ball, R. G.; Clineschmidt, B. V.; Bradley, V.; Culberson, J. C.; Erb, J. M.; Freidinger, R. M.; Pawluczyk, J. M.; Perlow, D. S.; Pettibone, D. J.; Verber, D. F. *Bioorg. Med. Chem.* **1994**, *2*, 971-985.
- [121] Pemow, B. *Pharmacol. Rev.* **1983**, *35*, 85-141.
- [122] Regoli, D.; Drapeau, G.; Dion, S.; Couture, R. *Trends Pharmacol. Sci.* **1988**, *9*, 290-295.
- [123] Lotz, M.; Carson, D. A.; Vaughan, J. H. *Science*, **1987**, *235*, 893-895.
- [124] Barnes, P. J.; Belvisi, M. G.; Rogers, D. F. *Trends Pharmacol. Sci.*, **1990**, *11*, 185-189.
- [125] Convert, O.; Ploux, O.; Lavielle, S.; Cotrait, M.; Chassaing, G. *Biochim. Biophys. Acta* **1988**, *954*, 287.
- [126] Ploux, O.; Lavielle, S.; Chassaing, G.; Julien, S.; Marquet, A.; d'Orleans-Juste, P.; Dion, S.; Regoli, D.; Beaujouan, J.-C.; Bergstrom, L.; Torrens, Y.; Glowinski, J. *Proc. Natl. Acad. Sci. USA*, **1987**, *84*, 8095.
- [127] Gilon, C.; Halle, D.; Chorev, M.; Selinger, Z.; Byk, G. *Biopolymers*, **1991**, *31*, 745.
- [128] Saulitis, J.; Mierke, D. F.; Byk, G.; Gilon, C.; Kessler, H. *J. Am. Chem. Soc.* **1992**, *114*, 4818.
- [129] Grdadolnik, S. G.; Mierke, D. F.; Byk, G.; Zeltser, I.; Gilon, C.; Kessler, H. *J. Med. Chem.* **1994**, *37*, 2145-2152.
- [130] Barrow, C. J.; Dolman, M. S.; Bobko, M. A.; Cooper, R. *J. Med. Chem.* **1994**, *37*, 356-363.
- [131] Josien, H.; Lavielle, S.; Brunissen, A.; Saffroy, M.; Torrens, Y.; Beaujouan, J.-C.; Glowinski, J.; Chassaing, G. *J. Med. Chem.* **1994**, *37*, 1586-1601 and refs. therein.
- [132] Holzemann, G.; Low, A.; Harting, J.; Greiner, H. E. *Int. J. Peptide Protein Res.* **1994**, *44*, 105-111.
- [133] Williams, B. J.; Curtis, N. R.; McNight, A. T.; Maguire, J. J.; Young, S. C.; Verber, D. F.; Baker, R. *J. Med. Chem.* **1993**, *36*, 2-10.
- [134] Chipens, G. I.; Mutulis, F.; Katayev, B. S.; Klusha, V. E.; Misina, I. P.; Myshlyakova, N. V. *Int. J. Peptide Protein Res.* **1981**, *18*, 302.
- [135] Shenderovich, M. D.; Nikiforovich, G. V.; Saulitis, J. B.; Chipins, G. I. *Biophys. Chem.* **1988**, *31*, 163-173.
- [136] Varek, R. J.; Stewart, J. M. *Peptides* **1985**, *6*, 161-164.
- [137] Burch, R. M. (ed); *Bradykinin Antagonists Basic and Clinical Research*, Marcel Dekker, Inc., New York, **1991**.
- [138] Bathon, J. M.; Proud, D. *Ann. Rev. Pharmacol. Toxicol.* **1991**, *31*, 129-162.
- [139] Lembeck, F.; Griesbacher, T.; Eckardt, M.; Henke, St.; Breipohl, G.; Knolle, J. *Br. J. Pharmacol.* **1991**, *102*, 297.
- [140] Sawutz, D. G.; Salvino, J. M.; Seoane, P. R.; Douty, B. D.; Houck, W. T.; Bobko, M. A.; Dolaman, M. S.; Dolle, R.; Wolfe, H. R. *Biochem.* **1994**, *33*, 2373-2379.
- [141] Reissmann, S.; Pineda, L. F.; Seyfarth, L.; Greiner, G.; Scholkens, B.; Vietinghoff, G.; Paegelow, I. *Proc. Eur. Pept. Symp.*; Maia, H. L. S. (ed.), ESCOM, Leiden, Netherlands **1994**, pp 619-620.
- [142] Schiller, P. W. in *Progress in Med. Chem.*, Ellis, G. P.; West, G. B. (eds.), Amsterdam : Elsevier, **1991**, *28*, 301.
- [143] De Grado, W. F. *Adv. Prot. Chem.* **1988**, *39*, 51.
- [144] Hruby, V. J. *Epilepsia* **1989**, Suppl. 1, S42-S50.
- [145] Smith, G. D.; Griffin, J. F. *Science* **1978**, *199*, 1214.
- [146] Polinsky, A.; Cooney, M. G.; Toy-Palmer, A.; Osapay, G.; Goodman, M. *J. Med. Chem.* **1992**, *35*, 4185-4194.
- [147] DiMaio, J.; Nguyen, T. M.-D.; Lemieux, C.; Schiller, P. W. *J. Med. Chem.* **1982**, *25*, 1432.
- [148] Schiller, P. W.; Nguyen, T. M.-D.; Lemieux, C.; Maziak, L. A. *J. Med. Chem.* **1985**, *28*, 1766-1771.
- [149] Mosberg, H. I.; Hurst, R.; Hruby, V. J.; Galligan, J. J.; Burks, T. F.; Gee, K.; Yamamura, H. I. *Biochem. Biophys. Res. Comm.* **1982**, *106*, 506.
- [150] Mosberg, H. I.; Hurst, R.; Hruby, V. J.; Gee, K.; Yamamura, H. I.; Galligan, J. J.; Burks, T. F. *Proc. Nat. Acad. Sci. USA* **1983**, *80*, 5871.
- [151] Flippen-Anderson, J. L.; Hruby, V. J.; Collins, N.; George, C.; Cudney, B. *J. Am. Chem. Soc.* **1994**, *116*, 7523.
- [152] Lomize, A. L.; Flippen-Anderson, J. L.; George, C.; Mosberg, H. I. *J. Am. Chem. Soc.* **1994**, *116*, 429-436.
- [153] Hruby, V. J. in *Peptides, Proc. Thirteenth American Peptide Symposium*, Hodges, R. S.; Smith, J. A. (eds), ESCOM : Lieden, Netherlands, **1994**, see pp 7-11.
- [154] Misicka, A.; Nikiforovich, G.; Lipkowski, A. W.; Horvarth, R.; David, P.; Kramer, T. H.; Yamamura, H. I.; Hruby, V. J. *Bioorg. Med. Chem. Lett.* **1992**, *2*, 547-552.
- [155] Meyer, J.-P.; Collins, N.; Lung, F.-D.; Davis, P.; Zalewska, T.; Porreca, F.; Yamamura, H. I.; Hruby, V. J. *J. Med. Chem.* **1994**, *37*, 3910-3917.
- [156] Collins, N.; Hruby, V. J. *Biopolymers* **1994**, *34*, 1231-1241.
- [157] Hruby, V. J.; Collins, N.; Lung, F.-D.; Meyer, J.-P.; Davis, T. P.; Yamamura, H. I.; Porreca, F. *Regul. Pept.* **1994**, *54*, 123-124.
- [158] Pierschbacher, M. D.; Ruoslahti, E. *Nature (London)* **1984**, *309*, 30.
- [159] Ruoslahti, E.; Pierschbacher, M. D. *Cell* **1986**, *44*, 517.

Fairlie et al.

685 *Current Medicinal Chemistry*, 1995, Vol. 2, No. 2

- [160] Gartner, T. K.; Bennett, J. S. *J. Biol. Chem.* **1985**, *260*, 11891-11894.
- [161] Craig, W. S.; Cheng, S.; Mullen, D. G.; Blevitt, J.; Pierschbacher, M. D. *Biopolymers*, **1995**, *37*, 157-175.
- [162] Samanen, J.; Ali, F.; Romoff, T.; Calvo, R.; Sorenson, E.; Vasko, J.; Storer, B.; Berry, D.; Bennett, D.; Strohsacker, M.; Powers, D.; Stadel, J.; Nichols, A. *J. Med. Chem.* **1991**, *34*, 3114-3125.
- [163] McDowell, R. S.; Gadek, T. R. *J. Am. Chem. Soc.* **1992**, *114*, 9245-9253.
- [164] Barker, P. L.; Bullens, S.; Bunting, S.; Burdick, D. J.; Chan, K. S.; Deisher, T.; Eigenbrot, C.; Gadek, T. R.; Gantzios, R.; Lipari, M. T.; Muir, C. D.; Napier, M. A.; Pitti, R. M.; Padua, A.; Quan, C.; Stanley, M.; Struble, M.; Tom, J. Y.; Burnier, J. P. *J. Med. Chem.* **1992**, *35*, 2040-2048.
- [165] McDowell, R. S.; Gadek, T. R.; Barker, P. L.; Burdick, D. J.; Chan, K. S.; Quan, C.; Skelton, N.; Struble, M.; Thorsett, E. D.; Tischler, M.; Tom, J. Y. K.; Webb, T. R.; Burnier, J. P. *J. Am. Chem. Soc.* **1994**, *116*, 5069-5076.
- [166] Bogusky, M. J.; Naylor, A. M.; Pitzenberger, S. M.; Nutt, R. F.; Brady, S. F.; Colton, C. D.; Sisko, J. T.; Anderson, P. S.; Verber, D. F. *Int. J. Peptide Protein Res.* **1992**, *39*, 63-76.
- [167] Gurrath, M.; Muller, G.; Kessler, H.; Aumailley, M.; Timpl, R. *Eur. J. Biochem.* **1992**, *210*, 911-921.
- [168] Scarborough, R. M.; Naughton, M. A.; Teng, W.; Rose, J. W.; Phillips, D. R.; Nannizzi, L.; Arsten, A.; Campbell, A. M.; Charo, I. F. *J. Biol. Chem.* **1993**, *268*, 1066.
- [169] Jackson, S.; De Grado, W. F.; Dwivedi, A.; Parthasarathy, A.; Higley, A.; Krywko, J.; Rockwell, A.; Markwalder, J.; Wells, G.; Wexler, R.; Mousa, S.; Harlow, R. *J. Am. Chem. Soc.* **1994**, *116*, 3220-3230.
- [170] Bach, H. A. C.; Eyermann, C. J.; Gross, J. D.; Bower, M. J.; Harlow, R. L.; Weber, P. C.; De Grado, W. F. *J. Am. Chem. Soc.* **1994**, *116*, 3207-3219.
- [171] Ripka, W. C.; De Lucca, G. V.; Bach, H. A. C.; Pottorf, R. S.; Blaney, J. M. *Tetrahedron* **1993**, *49*, 3609-3628.
- [172] Horwell, D. C.; Hughes, J.; Hunter, J. C.; Pritchard, M. C.; Richardson, R. S.; Roberts, E.; Woodruff, G. N. *J. Med. Chem.* **1991**, *34*, 404-414.
- [173] Tokarski, J. S.; Hopfinger, A. J. *J. Med. Chem.* **1994**, *37*, 3639-3654.
- [174] Kolodziej, S. A.; Nikiforovich, G. V.; Skeeane, R.; Lignon, M.-F.; Martinez, J.; Marshall, G. R. *J. Med. Chem.* **1995**, *38*, 137-149.
- [175] Hruby, V. J.; Wilke, S.; Al-Obeidi, F.; Jiao, D.; Lin, Y. *Reactive Polymers* **1994**, *22*, 231-241.
- [176] Charpentier, B.; Peleprat, D.; Durieux, C.; Dor, A.; Reibaud, M.; Blanchard, J.-C.; Roques, B. P. *Proc. Natl. Acad. Sci. USA* **1988**, *85*, 1968-1972.
- [177] Pluncinska, K.; Kataoka, T.; Yodo, M.; Cody, W. L.; He, J. X.; Humblet, C.; Lu, G. H.; Lunney, E.; Major, T. C.; Panek, R. L.; Schelkun, P.; Skeeane, R.; Marshall, G. R. *J. Med. Chem.* **1993**, *36*, 1902-1913.
- [178] Neugebauer, W.; Gagnon, L.; Whitfield, J.; Willick, G. E. *Int. J. Peptide Protein Res.* **1994**, *43*, 555-562.
- [179] O'Connor, S. D.; Smith, P. E.; Al-Obeidi, F.; Pettitt, B. M. *J. Med. Chem.* **1992**, *35*, 2870-2881.
- [180] Bohacek, R. S.; McMartin, C. *J. Am. Chem. Soc.* **1994**, *116*, 5560-5571.
- [181] Szewczuk, Z.; Rebholz, K.; Rich, D. H. *Int. J. Peptide Protein Res.* **1992**, *40*, 233-242.
- [182] Curiasso, P.; Paynal, I.; Lecoq, A.; Yiotakis, A.; Dive, V. *J. Med. Chem.* **1995**, *38*, 553-564.
- [183] Etzkorn, F. A.; Guo, T.; Lipton, M. A.; Goldverg, S. D.; Bartlett, P. A. *J. Am. Chem. Soc.* **1994**, *116*, 10412-10425.
- [184] Kase, H.; Kaneko, M.; Yamada, K. *J. Antibiot.* **1987**, *40*, 450.
- [185] Dhanaraj, V.; Dealwis, C. G.; Frazao, C.; Badasso, M.; Sibanda, B. L.; Tickle, I. J.; Cooper, J. B.; Driessen, H. P. C.; Newman, M.; Aguilar, C.; Wood, S. P.; Blundell, T. L.; Hobart, P. M.; Geoghegan, K. F.; Ammirati, M. J.; Danley, D. E.; O'Connor, B. A.; Hoover, D. J. *Nature*, **1992**, *357*, 466-472.
- [186] Sham, H. L.; Bolis, G.; Stein, H. H.; Fesik, S. W.; Marcotte, P. A.; Plattner, J. J.; Rempel, C. A.; Greer, J. *J. Med. Chem.* **1988**, *31*, 284-295.
- [187] Sham, H. L.; Rempel, C. A.; Stein, H. H.; Cohen, J. *J. Chem. Soc. Chem. Comm.* **1990**, 666-7.
- [188] Weber, A. E.; Halgren, T. A.; Doyle, J. J.; Lynch, R. J.; Siegl, P. K. S.; Parsons, W. H.; Greenlee, W. J.; Patchett, A. *J. Med. Chem.* **1991**, *34*, 2692-2701.
- [189] Rivero, R. A.; Greenlee, W. J. *Tet. Lett.* **1991**, *32*, 2453-6.
- [190] Dhanoa, D. S.; Parsons, W. H.; Greenlee, W. J.; Patchett, A. A. *Tet. Lett.* **1992**, *33*, 1725-8.
- [191] Wittenberger, S. J.; Baker, W. R.; Donner, B. G.; Hutchins, C. W. *Tet. Lett.* **1991**, *32*, 7655-8.
- [192] Rely, M. D.; Thanabal, V.; Lunney, E. A.; Repine, J. T.; Humblet, C. C.; Wagner, G. *FEBS Lett.* **1992**, *302*, 97-103.
- [193] Thaisrivongs, S.; Blinn, J. R.; Pals, D. T.; Turner, S. R. *J. Med. Chem.* **1991**, *34*, 1276-82.
- [194] Wlodawer, A.; Erickson, J. W. *Ann. Rev. Biochem.* **1993**, *62*, 543-585.
- [195] Darke, P. L.; Huff, J. R. *Adv. Pharm.* **1994**, *25*, 399-454.
- [196] West, M. L.; Fairlie, D. P. *Trends Pharmacol. Sci.* **1995**, *16*, 67-75.
- [197] Swain, A. L.; Miller, M. M.; Green, J.; Rich, D. H.; Schneider, J.; Kent, S. B. H.; Wlodawer, A. *Proc. Natl. Acad. Sci. USA* **1990**, *87*, 8805-8809.
- [198] Abbenante, J.; Bergman, D. A.; Brinkworth, R. I.; Dancer, R. J.; Fairlie, D. P.; Garnham, B.; Hunt, P. A.; March, D. R.; Martin, J. L. *Aust. Patent* **1994**, PM9825.
- [199] Abbenante, G.; March, D. R.; Bergman, D. A.; Hunt, P. A.; Garnham, B.; Dancer, R. J.; Martin, J. L.; Fairlie, D. P. *J. Am. Chem. Soc.* manuscript accepted for publication.
- [200] Smith, R. A.; Coles, P. J.; Chen, J. J.; Robinson, V. J.; Macdonald, I. D.; Carriere, J.; Krantz, A. *Bioorg. Med. Chem. Lett.* **1994**, *4*, 2217-2222.
- [201] Podlogar, B. L.; Farr, R. A.; Friedrich, D.; Tamus, C.; Huber, E. W.; Cregge, R. J.; Schirlin, D. *J. Med. Chem.* **1994**, *37*, 3684-3692.
- [202] Roberts, N. A.; Martin, J. A.; Kinchington, D.; Broadhurst, A. V.; Craig, J. C.; Duncan, I. B.; Galpin, S. A.; Handa, B. K.; Kay, J.; Krohn, A.; Lambert, R. W.; Merrett, J. M.; Mills, J. S.; Parkes, J. E. B.; Redshaw, S.; Ritchie, A. J.; Taylor, D. L.; Thomas, G. J.; Machin, P. J. *Science* **1990**, *248*, 358-361.
- [203] March, D. *PhD studies*, 1995, University of Queensland.
- [204] Jameson, B. A.; McDonnell, J. M.; Marini, J. C.; Komgold, R. *Nature*, **1994**, *368*, 744.
- [205] McDonnell, J. M.; Vamum, J. M.; Mayo, K. H.; Jameson, B. A. *Immunomethods* **1992**, *1*, 33-39.
- [206] Chen, S.; Chrusciel, R. A.; Nakanishi, H.; Raktabutr, A.; Johnson, M. E.; Sato, A.; Weiner, D.; Hoxie, J.; Saragovi, H. U.; Greene, M. I.; Kahn, M. *Proc. Natl. Acad. Sci. USA* **1992**, *89*, 5872-5876.

**Forcing Peptides into Bioactive Conformations***Current Medicinal Chemistry*, 1995, Vol. 2, No. 2 686

- [207] Holzemann, G. *Kontakte* (Darmstadt) 1991, 1, 3-12; 2, 55-63.
- [208] Giannis, A.; Kolter, T. *Angew Chem. Int. Ed. Engl.* 1993, 32, 1244.
- [209] Freidinger, R. M.; Perlow, D. S.; Verber, D. F. *J. Org. Chem.* 1982, 47, 104-109.
- [210] Aebi, J. D.; Guillaume, D.; Dunlap, B. E.; Rich, D. H. *J. Med. Chem.* 1988, 31, 1805-1815.
- [211] Nagai, U.; Sato, K.; Nakamura, R.; Kato, R. *Tetrahedron* 1993, 49, 3577-3592.
- [212] Sarabu, R.; Lovey, K.; Madison, V. S.; Fry, D. C.; Greeley, D. N.; Cook, C. M.; Olson, G. L. *Tetrahedron* 1993, 49, 3629-3640.
- [213] Kemp, D. S.; Curran, T. P. *Tet. Lett.* 1988, 29, 4931-4938.
- [214] Kemp, D. S.; Bowen, B. R. *Tet. Lett.* 1988, 29, 5077-5080.
- [215] Muller, K.; Obrecht, D.; Knierzinger, A.; Stankovic, Ch.; Spiegler, W.; Bannwarth, W.; Trzeciak, A.; Englert, G.; Labhardt, A. M.; Schonholzer, P. in *Perspectives in Medicinal Chemistry*, Testa, B.; Kyburz, E.; Fuhrer, W.; Giger, R. (eds), Verlag Helv. Chim. Acta Basel, 1993, 513-531.
- [216] Obrecht, D.; Bohdal, U.; Ruffieux, R.; Muller, K. *Helv. Chim. Acta* 1994, 77, 1423-1429.
- [217] Grove, A.; Mutter, M.; Rivier, J. E.; Montal, M. *J. Am. Chem. Soc.* 1993, 115, 5919.
- [218] Akerfeldt, K. S.; Kim, R. M.; Camac, D.; Groves, J. T.; Lear, J. D.; De Grado, W. F. *J. Am. Chem. Soc.* 1992, 114, 9656.
- [219] Dawson, P. E.; Kent, S. B. H. *J. Am. Chem. Soc.* 1993, 115, 7263.
- [220] Smythe, M. L.; von Itzstein, M. *J. Am. Chem. Soc.* 1994, 116, 2725-2733.

## Research Article

## Comparison of the Proteolytic Susceptibilities of Homologous L-Amino Acid, D-Amino Acid, and N-Substituted Glycine Peptide and Peptoid Oligomers

Susan M. Miller, Reyna J. Simon, Simon Ng, Ronald N. Zuckermann, Janice M. Kerr, and Walter H. Moos

University of California, San Francisco, Department of Pharmaceutical Chemistry, San Francisco (S.M.M.) and Chiron Corporation, Emeryville (R.J.S., S.N., R.N.Z., J.M.K., W.H.M.), California

Strategy, Management and Health Policy				
	Preclinical Research	Preclinical Development Toxicology, Formulation Drug Delivery, Pharmacokinetics	Clinical Development Phases I-III Regulatory, Quality, Manufacturing	Postmarketing Phase IV

**ABSTRACT** A series of homologous L-amino acid, D-amino acid, and both parallel and anti-parallel (retro) sequence N-substituted glycine peptide and peptoid oligomers were prepared and incubated with a series of enzymes representative of the major classes of proteases. Each respective L-amino acid containing peptide sequence was readily cleaved by the appropriate enzyme, namely Ac-L-ala-L-leu-L-phe-L-ala-L-leu-L-arg-NH<sub>2</sub> by chymotrypsin, Ac-L-ala-L-ala-L-ala-L-leu-L-phe-L-arg-NH<sub>2</sub> by elastase, Ac-L-ala-L-phe-L-glu-L-leu-L-ala-L-ala-NH<sub>2</sub> by papain, Z-L-ala-L-his-L-phe-L-phe-L-arg-L-leu-NH<sub>2</sub> by pepsin, Ac-L-phe-L-ala-L-arg-L-ala-L-arg-L-asp-NH<sub>2</sub> by trypsin, and Ac-L-ala-L-tyr-L-ala-L-phe-OH for carboxypeptidase A. In contrast, equivalent D-amino acid containing and N-substituted glycine containing oligomers were cleaved minimally or not at all by the respective enzymes. The N-substituted glycine peptoids represent a new class of combinatorial diversity for lead discovery with improved pharmaceutical characteristics relative to L-amino acid containing peptides. © 1995 Wiley-Liss, Inc.

**Key Words:** combinatorial chemistry, molecular diversity, peptide, peptoid, protease

### INTRODUCTION

The use of molecular diversity approaches to drug discovery has mushroomed in the last several years [Maeji et al., 1991; Houghten et al., 1991; Lam et al., 1991; Furka et al., 1991; Gallop et al., 1994; Gordon et al., 1994; Desai et al., 1994]. With automated techniques and the combinatorial use of various types of building blocks, e.g., both genetically encoded standard L-amino acids, as well as non-natural building blocks like N-substituted glycines (NSGs), libraries of unprecedented numbers of compounds can be generated and screened over very short time periods. However, the discovery aspects of molecular diversity represent only one segment of pharmaceutical research and development. Many leads ultimately fail because

of deficiencies in one or more important pharmaceutical property, such as absorption, distribution, metabolism, and excretion (ADME), not to mention safety and efficacy. While small (i.e., non-protein) peptide and modified peptide therapeutics are well known (e.g., calcitonin, captopril, cyclosporin, oxytocin), peptides often exhibit several of these deficiencies. Consequently, peptide libraries per se may hold less immediate promise than non-peptide or peptoid li-

Received December 16, 1994; final version accepted January 26, 1995.

Address reprint requests to Susan M. Miller, Department of Pharmaceutical Chemistry, University of California, 513 Parnassus Ave, Box 0446, San Francisco, CA 94143-0446.

## PROTEASE STABILITY OF NSG PEPTOIDS

21

TABLE 1. Properties of Enzymes Used in This Study

Enzyme	Specificity <sup>a</sup>	Class	Substrate example
Carboxypeptidase A 3.4.17.1	P <sub>1</sub> , aromatic free carboxyl preferred, extended site to P <sub>3</sub> or P <sub>4</sub>	Metallo	Z-gly-gly-L-phe-OH, $k_{cat}/K_m$ $5.3 \times 10^4 \text{ M}^{-1} \text{ s}^{-1}$ , pH 7.6, 27°C <sup>b</sup>
Papain 3.4.22.2	P <sub>2</sub> aromatic or hydrophobic, P <sub>1</sub> , large hydrophobic, extended site P <sub>4</sub> -P <sub>3</sub>	Cysteine	Z-gly-L-val-L-glu-L-leu-gly-OH, $k_{cat}/K_m$ $3.2 \times 10^3 \text{ M}^{-1} \text{ s}^{-1}$ , pH 6.5, 40°C <sup>c</sup>
Pepsin 3.4.23.1	P <sub>1</sub> and P <sub>1</sub> ', aromatic, extended site P <sub>4</sub> -P <sub>3</sub>	Aspartyl	L-phe-gly-L-his-L-(4NO <sub>2</sub> )phe-L-phe-L-val-L-leu-OMe, $k_{cat}/K_m$ $1.5 \times 10^6 \text{ M}^{-1} \text{ s}^{-1}$ , pH 3.5-4.0, 37°C <sup>d</sup>
Trypsin 3.4.21.4	P <sub>1</sub> L-lys or L-arg, some extension to P <sub>3</sub>	Serine	Bz-L-phe-L-val-L-arg-pNA, $k_{cat}/K_m$ $1.1 \times 10^6 \text{ M}^{-1} \text{ s}^{-1}$ , pH 8.1, 37°C <sup>e</sup>
Elastase 3.4.21.36	P <sub>1</sub> hydrophobic preferred, but extended site P <sub>4</sub> -P <sub>2</sub>	Serine	Boc-L-ala-L-ala-L-leu-SBzl, $k_{cat}/K_m$ $4.3 \times 10^6 \text{ M}^{-1} \text{ s}^{-1}$ , pH 7.5, 25°C <sup>f</sup>
Chymotrypsin 3.4.21.1	P <sub>1</sub> aromatic, extended site P <sub>3</sub> -P <sub>3</sub>	Serine	Glt-L-ala-L-ala-L-leu-L-phe-pNA, $k_{cat}/K_m$ $1.4 \times 10^6 \text{ M}^{-1} \text{ s}^{-1}$ , pH 7.8, 25°C <sup>g</sup>

<sup>a</sup>Polgár [1989].<sup>b</sup>Z: carbobenzyloxy. Abramowitz et al. [1967].<sup>c</sup>Lowbridge and Fruton [1974].<sup>d</sup>Fruton [1976].<sup>e</sup>Bz: benzoyl; pNA: p-nitroanilide. Pozsgay et al. [1981].<sup>f</sup>SBzl: SCH<sub>2</sub>C<sub>6</sub>H<sub>5</sub>; Boc: t-butyloxycarbonyl. Harper et al. [1984].<sup>g</sup>Glt: glutaric acid. Fischer et al. [1984].

braries, especially for orally available therapeutics (at least until drug delivery methods achieve greater success).

A significant effort in our molecular diversity research focuses on the seemingly peptide-like oligo (NSGs). We have developed a "sub-monomer" process for synthesizing NSG peptoids that allows the use of simple acetates and amines to prepare highly diverse libraries quickly and inexpensively [Zuckermann et al., 1992a]. The NSG peptoids, which can mimic both peptides and non-peptides, demonstrate potent and specific biological activity [Simon et al., 1992; Zuckermann et al., 1994]. From an ADME perspective, work by Conradi et al. [1992] would predict improved absorption characteristics for NSG peptoids because of N-substitution. But the gut and the bloodstream, to mention only two biological milieus, provide unfavorable environments for peptides owing to the various classes of proteases present in these physiological compartments. As a further step in characterizing the pharmaceutical potential of new diversities, we report herein a qualitative assessment of the stability of a set of NSG peptoids against a series of common proteases.

For this study, we selected enzymes representative of the four known classes of relevant proteases (Table 1): carboxypeptidase A, papain, pepsin, elastase, trypsin, and chymotrypsin. Based on known sequence specificities, we have designed L-amino acid peptide (all-L) substrates to directly compare with homologous D-amino acid containing (all-D) and N-substituted glycine containing oligomers. For most of the enzymes, both parallel (all-N) and anti-parallel (retro all-N) NSGs were prepared to cover both possible reading

frames (Fig. 1). A preliminary report of these data has been presented elsewhere [Miller et al., 1994].

## MATERIALS AND METHODS

## Enzymes and Reagents

Bovine pancreatic chymotrypsin A<sub>4</sub>, trypsin, and carboxypeptidase A, porcine pancreatic elastase, and papain were from Boehringer Mannheim (Indianapolis, IN). Porcine stomach mucosa pepsin was from Calbiochem (La Jolla, CA). 4-Fluoro-7-nitro-benzofurazan was from Aldrich (Milwaukee, WI). Z-L-glu-L-phe-OH, Suc-L-phe-pNA, Boc-L-ala-ONp, Bz-D,L-arg-pNA-HCl, and Z-L-his-L-4-nitro-phe-L-phe-OMe were from Bachem Bioscience (Philadelphia, PA). The carboxypeptidase A all-L and all-D peptides were obtained from Chiron Mimotopes (Clayton, Victoria, Australia). All reagents were of analytical grade.

## Peptides and NSG Peptoids

## Design

Figure 2 summarizes the peptide and NSG peptoid sequences designed and synthesized for these proteolysis studies. Hexapeptides were chosen for all of the enzymes except carboxypeptidase A, since previous studies indicate extended recognition sites for most proteases of at least 6 or 7 residues [Polgár, 1989]. In each case, the sequences are based on literature studies defining good peptide substrates and/or inhibitors. For carboxypeptidase A, a tetramer was designed based on the structure of the potato peptide inhibitor bound to the enzyme, which shows interactions of only 4 amino acids of the inhibitor with the

22

MILLER ET AL.

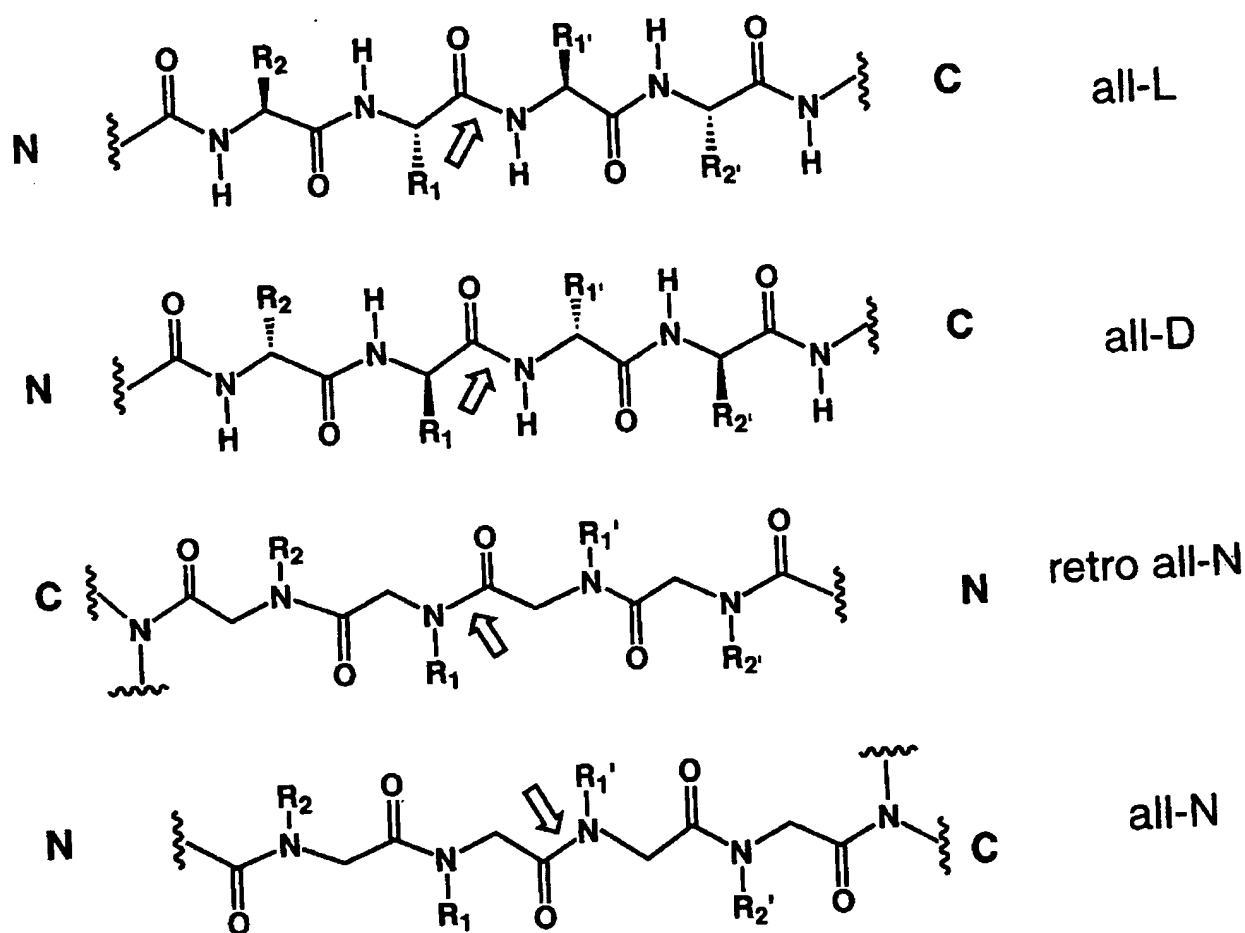


Figure 1. Comparison of general structures of all-X peptides and peptoids. The side chain labels illustrate the standard nomenclature for all-L peptide cleavage by proteases (arrows), which occurs at the carboxyl end of the  $P_1$  residue and the amino end of the  $P_1'$  residue [Schechter and Berger, 1967].

active site [Rees and Lipscomb, 1982]. Because of the requirement for a free carboxylate group in the carboxypeptidase A substrate, a fully homologous retro NSG peptoid could not be synthesized. For papain, Schechter and Berger [1967] demonstrated that extended binding from  $P_4$ - $P_3'$  improves activity, and later demonstrated [1968] that the primary specificity is for aromatic residues at  $P_2$ . Inclusion of L-glu-L-leu at the  $P_1$ - $P_1'$  sites is based on the studies of Lowbridge and Fruton [1974], which demonstrate the further specificity of the  $P_1$  site of papain for large hydrophobic residues in substrates. For pepsin, the  $P_3$ - $P_1'$  sequence and the inclusion of a carbobenzyloxy capping group is based on the extensive studies from the lab of Fruton [see Fruton, 1976], which explore site specificities and demonstrate an extended substrate binding site from  $P_4$ - $P_3'$ . The L-arg-L-leu sequence in the

$P_2$ - $P_3'$  position is based on an analysis by Powers et al. [1977] of cleavage sites reported for a wide variety of protein substrates for pepsin. The retro NSG peptoid sequence as a benzamide derivative was designed as a homolog for the pepsin peptide, but was not synthesized for this study. For trypsin, the  $P_3$ - $P_1$  sequence is based on substrate studies by Pozsgay et al. [1981], while the  $P_1$ - $P_3'$  fragment is based on the sequence of the pancreatic trypsin inhibitor complexed with trypsin [Huber and Bode, 1978]. For elastase, extension of the peptide out to  $P_4$  or  $P_5$  appears to be more important for activity than extension on the  $P'$  side [Thompson and Blout, 1973]. Thus, the sequence of  $P_4$ - $P_1$  is based on the studies by Thompson and Blout [1973], as well as those by Harper et al. [1984], which show that substitution of L-leu for L-ala at  $P_1$  gives a better  $k_{cat}/K_m$  value. L-phe at the  $P_1'$  site of the

## PROTEASE STABILITY OF NSG PEPTOIDS

23

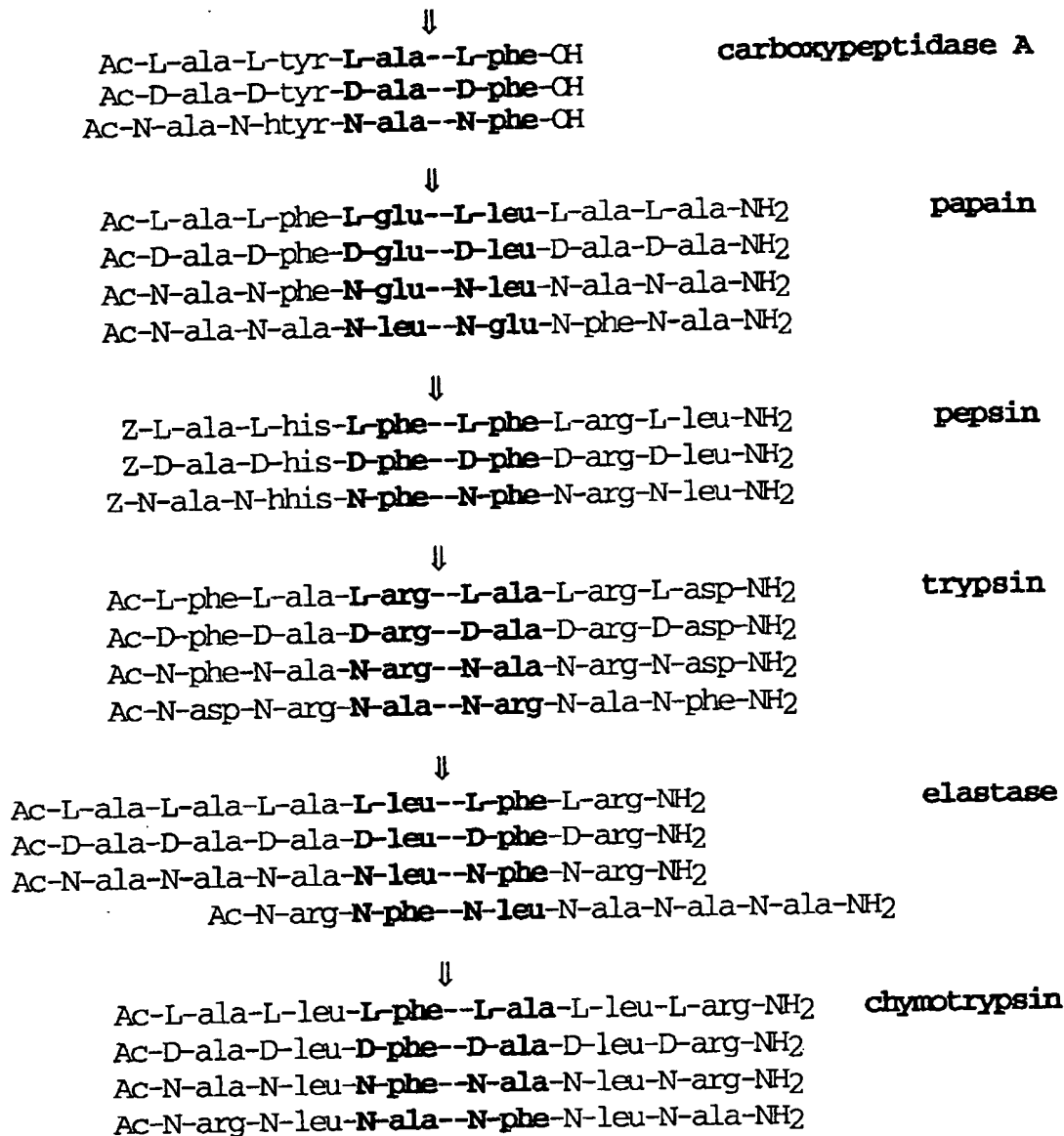


Figure 2. Sequences of peptides and NSG peptoids designed for the indicated proteases. Expected cleavage sites are indicated by boldface residues and arrows. In the NSG oligomers, the R-groups attached to nitrogen are identical to the R-groups of the L- and D-amino acids except for the N-hhis and N-htyr residues, which are extended by an additional methylene group.

elastase peptide is based on studies by Bauer et al. [1976]; and L-arg at P<sub>2</sub> was included to improve solubility of the peptide. For chymotrypsin, P<sub>3</sub>-P<sub>1</sub> residues are based on the analysis by Fischer et al. [1984] of extended peptides as substrates, while P<sub>1</sub>-P<sub>3</sub> residues are based on tight binding inhibitors described by Imperiali and Abeles [1987].

#### Synthesis

L- and D-amino acid containing peptides were synthesized by solid-phase 9-fluorenylmethoxycarbonyl (Fmoc) chemistry on an automated synthesizer as described [Zuckermann et al., 1992b]. NSG peptoids, except for the pepsin and carboxypeptidase

all-N oligomers, were prepared using the method of Zuckermann et al. [1992a]. The pepsin all-N hexamer and the carboxypeptidase A all-N tetramer were synthesized from the Fmoc-protected N-substituted glycine monomers [Simon et al., 1992] using solid-phase chemistry on an ABI synthesizer (Foster City, CA).

### Purification

All peptides and peptoids were purified by gradient elution from Vydac (Hesperia, CA) C<sub>18</sub> semiprep or prep HPLC columns using Rainin HPLC chromatographs (Woburn, MA) controlled by software operating on Apple Macintosh (Cupertino, CA) computers. Samples were loaded with the column equilibrated at 0 or 5% acetonitrile in water, with 0.1% trifluoroacetic acid in both phases, and were eluted with a gradient up to 65% acetonitrile, increased at 2%/min. Purified samples were lyophilized and stored at 4°C. L- and D-amino acid containing peptides were characterized by amino acid analysis by the ninhydrin method using a Beckman amino acid analyzer (Fullerton, CA). Samples of the purified NSG-peptoids were characterized by mass spectral analysis performed at Mass Search, Inc., 1560 Cummins Dr., Suite C, Modesto, CA 95351.

### Proteolysis Controls, Conditions, and Analysis

#### Solvent controls

Dissolution of the peptides and peptoids required 10–20% organic solvent, thus the effect of potential solvents (Tween-80 or DMSO) on the activity of the various enzymes was evaluated using colorimetric substrates for each enzyme. Using Suc-L-phe-pNA for chymotrypsin, Bz-D,L-arg-pNA·HCl for trypsin and papain, and Boc-L-ala-ONp for elastase, activity was measured by the increase in absorbance at 405 nm for release of p-nitroaniline or p-nitrophenol. Using Z-L-glu-L-phe-OH for carboxypeptidase A and Z-L-his-L-(4NO<sub>2</sub>)phe-L-phe-OMe for pepsin, activity was measured by the decrease in the peptide absorbance band between 220 and 230 nm. Concentrations of 0, 1, 2.5, 5, and 10% of either Tween-80 or DMSO in the buffers indicated below were evaluated for inhibition of activity. Absorbance measurements were made using a Shimadzu UV160U spectrophotometer (Columbia, MD).

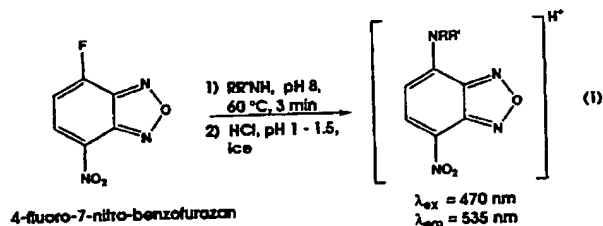
#### Proteolysis conditions

Reaction conditions for each enzyme were set to approximate physiological conditions as shown in Table 2. Preliminary experiments with the all-L peptides were conducted to establish useful concentrations and

times of reaction. Stock solutions of enzymes (100 μM) in their respective buffers were made fresh the day of each experiment. Chymotrypsin and trypsin were made as 1.0 mM stocks in 1.0 mM HCl and then diluted to 100 μM final concentration with bicarbonate buffer just before use. Papain was activated by incubation of the 100 μM stock with 2 mM dithiothreitol at 37°C for 5 min before dilution into the reaction mixtures. Concentrations of the peptides and peptoids in the stock solutions were determined by amino acid analysis as described above. For the analysis of the NSG peptoids, the N-phe derivative was found to elute with the same retention time as the L-phe derivative but gives a lower response. By comparing the analysis of several hexapeptides containing five L-amino acids and a single N-phe, the response factor for the N-phe derivative (area under HPLC peak/pmol) was found to be  $62.5 \pm 1.9\%$  of the L-phe response. Using this percentage and an L-phe standard, the concentration of N-phe, and of each NSG peptoid was quantitated, since each of the compounds of interest contained at least one N-phe residue.

### Quantitation of Cleavage

For each reaction, separate enzyme and peptide/peptoid controls at the same dilutions as the complete reaction mixture were incubated simultaneously at 37°C. Reaction mixtures were preequilibrated at 37°C for approximately 3 min before initiation of reaction by addition of enzyme. The extent of peptide cleavage was quantitated in a discontinuous assay by the fluorescence developed upon reaction of the 1° or 2° amine product with 4-fluoro-7-nitro-benzofurazan (NBD-F; see structure below) [Imai and Watanabe, 1981; Miyano et al. 1985].



At appropriate time points, 40 μL aliquots of reaction or control were quenched by dilution into a mixture of 0.2 mL acetonitrile plus 0.2 mL × 0.1 M sodium borate buffer, pH 8.05, in 10 × 75 mm test tubes on ice. NBD-F (2.0 μL × 50 mM in acetonitrile) was added and the samples were immediately incubated for 3.25 min at 60°C in a heating block, after which they were placed on ice, and 20 μL × 3

## PROTEASE STABILITY OF NSG PEPTOIDS

25

TABLE 2. Proteolysis Conditions\*

Enzyme (MW) <sup>a</sup>	Concentration in assay ( $\mu$ M)	Reaction buffer	Substrate concentration in assay (mM) <sup>b</sup>
Carboxypeptidase A (34,500)	1.0	25 mM sodium bicarbonate, pH 7.8	L: 1.79 D: 1.73 N: 1.03
Papain (23,400)	2.0	50 mM potassium phosphate, pH 6.95	L: 0.92 D: 1.06 N: 2.63 RN: 3.73
Pepsin (34,000)	2.0	8.4 mM HCl/34 mM NaCl, pH 2.05	L: 1.02 D: 1.73 N: 1.62
Trypsin (24,000)	2.0	25 mM sodium bicarbonate, pH 7.8	L: 0.78 D: 0.72 N: 0.83 RN: 0.85
Elastase (22,000)	1.0	25 mM sodium bicarbonate, pH 7.8	L: 0.38 D: 0.48 N: 2.22 RN: 0.73
Chymotrypsin (22,500)	2.0	25 mM sodium bicarbonate, pH 7.8	L: 0.88 D: 0.59 N: 0.85 RN: 1.36

\*All reactions were run at 37°C.

<sup>a</sup>Schomburg and Salzmann [1990].<sup>b</sup>All substrates were dissolved in 20% DMSO/80% respective reaction buffer and were diluted 10-fold into the reactions, except the chymotrypsin all-L peptide, which was dissolved in 13% DMSO/87% buffer and was diluted 5-fold into the assay. Concentrations of the stock solutions were determined by amino acid analysis as described in the text and are accurate to  $\pm 4\%$ . Separate reactions were run simultaneously for each compound, where L is the all-L peptide; D is the all-D peptide; N is the all-N peptide; RN is the retro all-N peptide.

N HCl was added to each to stabilize the 4-amino-7-nitro-benzofurazan product. The fluorescence was read using a Hitachi fluorimeter (Hitachi Instruments, Danbury, CT) with  $\lambda_{\text{ex}} = 470$  nm and  $\lambda_{\text{em}} = 535$  nm. As standards for approximate quantitation of the peptide/peptoid products, duplicate or triplicate fluorescence curves were generated for 0 to 110  $\mu$ M concentrations of L-phe, N-benzyl-gly-OEt (N-phe), L-leu, N-leu-N-htyr-NH<sub>2</sub>, L-ala, and sar-OEt (N-ala) using the same protocol and measuring a 40  $\mu$ L aliquot of water for the baseline hydrolysis background. (Because of only limited availability of deprotected N-glu and N-arg monomers and their minimal occurrence as expected amino products, these two standards were not evaluated.) The data were fit to a second-order polynomial equation using the curvefit capability in the graphing program KaleidaGraph (version 3.0.1) (Synergy Software, Reading, PA) for the Macintosh.

## RESULTS

## Synthesis and Purification

After synthesis, the purity of the peptides and NSG peptoids was evaluated by analytical reverse phase HPLC as described in Materials and Methods. The all-L and all-D peptides showed only very minor impurities by HPLC; however, when tested for background fluorescence, they all showed sufficient signal to warrant purification. Thus, all were purified by preparative HPLC. HPLC analysis of the NSG peptoids showed more than one product for all of the sequences. However, for each forward (all-N) and related retro all-N sequence, a major peak was identified with nearly the same retention time as the corresponding all-L and all-D peptides (which are enantiomeric and have identical retention times). Figure 3 shows a comparison of the all-L, all-N, and retro

all-N papain peptides/peptoids before purification. Upon purification and mass spectral analysis, those peaks with the similar retention times were found to have the predicted masses for the desired sequences in all cases.

## Solvent Controls

Except for the trypsin and carboxypeptidase A peptides, the designed substrates are fairly hydrophobic and require some organic solvent/buffer mix for dissolution. In an effort to maximize the concentration of peptides in the assays and minimize solvent inhibition of the enzymes, we evaluated the effect of both Tween-80, which is sometimes employed in formulating drugs for animal experiments, and DMSO, which is often a good solvent for peptides but not typically desirable in pharmacological assays. Tween-80, even at only 1%, severely inhibited chymotrypsin, elastase, papain, and trypsin. (Pepsin and carboxypeptidase A were not tested because Tween-80 absorbs in the region used to monitor their activity.) By contrast, up to 2.5% DMSO had very little effect on the activity of any of the enzymes (data not shown). Thus, peptide and NSG peptoid stock solutions were made using 20% DMSO, which upon 10-fold dilution into the assays gave an essentially noninhibitory concentration of 2% DMSO.

## Fluorescence Conditions

The conditions for the fluorescence assays are based on the extensive characterization reported by Imai and Watanabe [1981] and Miyano et al. [1985]. From those studies it is clear that: (1) borate buffer at pH 8.0 gives maximal development and stability of fluorescence; (2) the presence of 50% organic solvent increases the yield of amine product and decreases the yield of hydrolysis product; (3) quenching the reaction by addition of hydrochloric acid to give a final

26

MILLER ET AL.

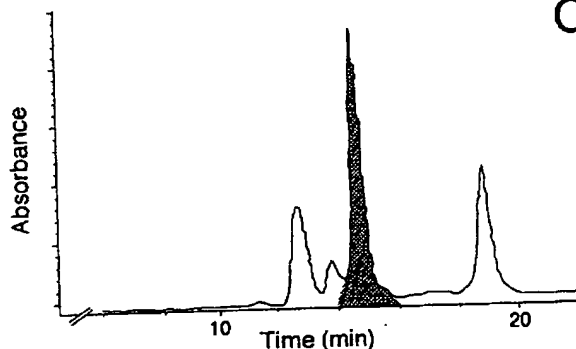
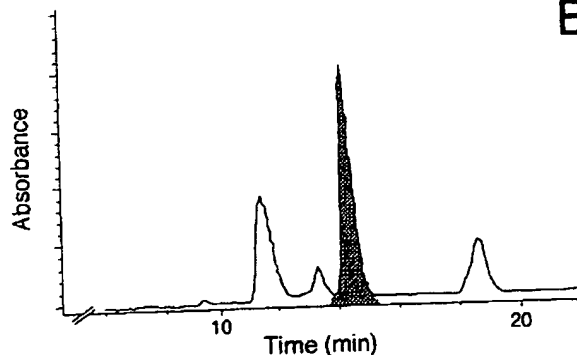
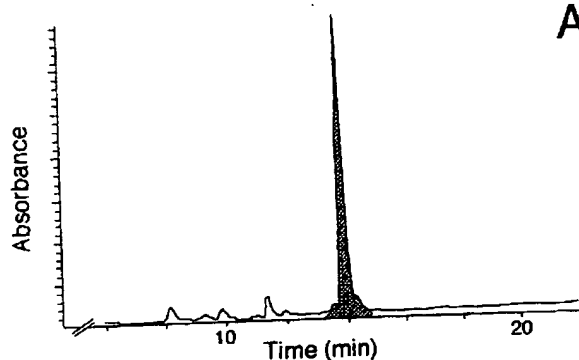


Figure 3. Comparison of analytical reverse phase HPLC elution pattern for papain peptides/peptoids before purification. The peptide gradient was 0 to 60% acetonitrile, 0 to 30 min, while the peptoid gradient was 1 to 61% acetonitrile, 0 to 30 min. Desired compounds are marked. A: All-L peptide elutes at 27.5% acetonitrile. B: All-N peptide and C: retro all-N peptoid elute at 29.8% acetonitrile.

pH between 1 and 3 further increased and stabilized the net fluorescence of the product. To further optimize the assay for our compounds, we evaluated two

A

TABLE 3. Optimization of Fluorescence Assay Variables\*

Variable	Signal/noise		Net relative fluorescence	
	L-phe	N-phe	L-phe	N-phe
Solvent <sup>a</sup>				
EtOH	8	9	33	31
CH <sub>3</sub> CN	19	13	124	78
Temperature and time (min) <sup>b</sup>				
60°C				
1.5	nd	28	nd	57
3.0	nd	20	nd	90
5.0	nd	15	nd	87
10.0	nd	11	nd	83
70°C				
1.0	nd	25	nd	40
2.0	nd	19	nd	69
5.0	nd	10	nd	70
10.0	nd	9	nd	72
Concentration NBD-F (μM) <sup>c</sup>				
215	23	18	99	73
431	19	10	151	80
855	4	2	147	38

\*nd = not determined.

<sup>a</sup>Conditions: 50% solvent, 50% 0.1 M sodium borate buffer, pH 8.0, 246 μM 4-fluoro-7-nitro-benzofurazan (NBD-F), 9.9 μM amino acid, heated at 70°C for 4 min and quenched on ice with addition of 20 μL × 3 N HCl.

<sup>b</sup>Conditions as in Solvent with solvent = acetonitrile, but with temperature and time varied as indicated.

<sup>c</sup>Conditions as in Temperature and time with temperature = 60°C and time = 3.0 min, but with varied NBD-F as indicated.

C

organic solvents, ethanol and acetonitrile, the time and temperature of heating, and the concentration of NBD-F in the assay, focusing primarily on the reaction of N-phe, since the more sterically hindered secondary amines are expected to react more slowly with the reagent and therefore yield lower overall fluorescence. As summarized in Table 3, maximal net fluorescence coupled with nearly optimal signal to noise was obtained for both L-phe and N-phe using acetonitrile as solvent with incubation at 60°C for approximately 3 min in the presence of 215 μM NBD-F. Under these conditions, as little as 0.5 μM L-phe or N-phe could be detected. Higher temperatures, longer incubation times, and higher concentrations of NBD-F led to increased hydrolysis of the reagent and a significant reduction in signal to noise. The final conditions adopted for all of the assays included acetonitrile as solvent, 215 μM NBD-F, and incubation at 60°C for 3.25 min.

#### Fluorescence Standards

Figure 4 shows average fluorescence standard curves measured for the L- and N-amino acids expected to occur at the amino termini of the peptide or peptoid cleavage products in this study. Standards

## PROTEASE STABILITY OF NSG PEPTOIDS

27

were run in each case up to the maximal concentration expected for complete cleavage of the all-L peptides at the expected primary site of cleavage. All of the amino acids evaluated show decreasing fluorescence at high concentrations indicative of self-quenching. As indicated by the dashed lines in Figure 4, the observed fluorescence can be described by the following parabolic dependences on concentration, which result from the inner-filter effect at high concentrations of fluorophore [Schenk, 1973]. Thus,

L-ala-OH:	Fluorescence = $1.63 + 4.49x - 0.014x^2$	$R^2 = 0.981$ (2)
N-ala-OEt:	Fluorescence = $24.38 + 13.53x - 0.116x^2$	$R^2 = 0.927$ (3)
L-leu-OH:	Fluorescence = $5.79 + 9.25x - 0.048x^2$	$R^2 = 0.975$ (4)
N-leu-N- htyr-NH <sub>2</sub> :	Fluorescence = $0.26 + 5.49x - 0.031x^2$	$R^2 = 0.999$ (5)
L-phe-OH:	Fluorescence = $2.94 + 11.20x - 0.062x^2$	$R^2 = 0.979$ (6)
N-phe-OEt:	Fluorescence = $-1.28 + 7.17x - 0.033x^2$	$R^2 = 0.999$ (7)

where  $x$  equals the concentration of the standard. Concentrations of unknown amine solutions are then quantitated from fluorescence values by solving for the negative root of the appropriately rearranged equation. Standards for N-glu and N-arg, which would only be expected for cleavage of the reverse NSG peptoids for papain and trypsin, respectively, were unavailable for comparison in these studies and were assumed to give at least the minimal fluorescence observed with the N-leu standard in the calculation of fractional conversions below. Since no fluorescence above the background water samples was observed for any time point in the assays with either the trypsin or papain retro all-N compounds, this analysis seems reasonable.

## Proteolysis

Data for the proteolysis of the respective peptides and peptoids are displayed as fractional conversions, by enzyme, in Figure 5. As indicated by the open circles for each plot, the all-L peptides are indeed substrates for their respective enzymes. The peptide designed for elastase (Fig. 5E) clearly undergoes cleavage at more than one site over the course of the experiment. The concentration of amine product for elastase cleavage was calculated using the equation for fluorescence of an L-phe amino derivative, which is the expected initial cleavage site, as indicated in Figure 2. Further cleavage would likely occur after any of the alanine residues, yielding L-leu and/or L-ala amino termini. Since the fluorescence standard curves for both of these are shallower than for L-phe, the fractional conversions indicated for the elastase peptide represent minimal values.

With the other enzymes, a fairly rapid but variable extent of cleavage of the all-L peptides occurs in

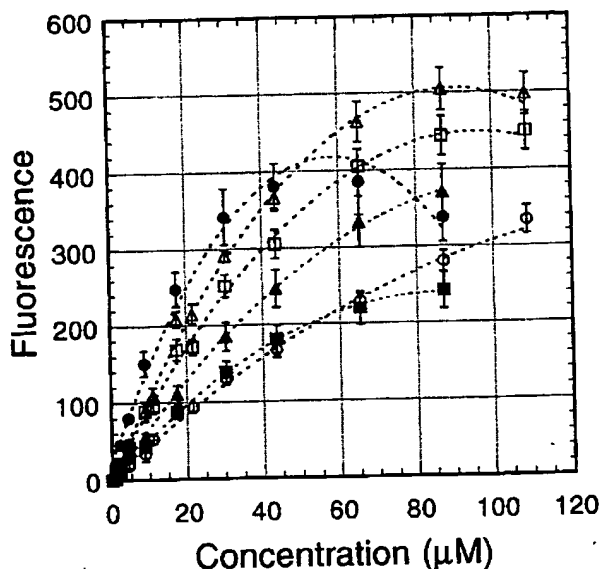


Figure 4. Fluorescence standard curves. Conditions are as indicated in Materials and Methods. Data are for (○) L-ala-OH, (●) N-ala-OEt, (□) L-leu-OH, (■) N-leu-N-htyr-NH<sub>2</sub>, (△) L-phe-OH, (▲) N-phe-OEt. Points are presented as the mean  $\pm$  s.e.m. of duplicate (N-substituted) or quadruplicate (L) measurements run on separate days. Dashed lines are parabolic fits to all of the data points for a given compound as described in the text.

the first 6 to 12 min of the assay followed by a much slower, further cleavage (except for pepsin, where cleavage does not appear to proceed any further after 6 min). This behavior could result from instability of enzyme activity upon extended incubation (perhaps due to self-proteolysis) or may be due to inhibition of the enzymes by the cleavage products from the reaction, since several of the peptides were designed for good binding based on sequences and structural information for naturally occurring protein protease inhibitors. Another alternative explanation is that the initial cleavage is nearly complete in the burst, but inaccurately measured by the standards, and the slow phase is due to further cleavage of the primary fragments. Since the issue is not critical to the conclusions of the study, we have not pursued this point further at this time.

In sharp contrast to the significant cleavage seen for the all-L peptides with each enzyme, there is only minimal cleavage of three all-D peptides, and no convincing cleavage of any of the all-N or retro all-N peptoids. With chymotrypsin, there may be 1–2% cleavage of the all-D peptide, but the points are scattered over the course of the incubation. With trypsin and carboxypeptidase A, the all-D peptides show increasing trends in percent cleavage, with approxi-

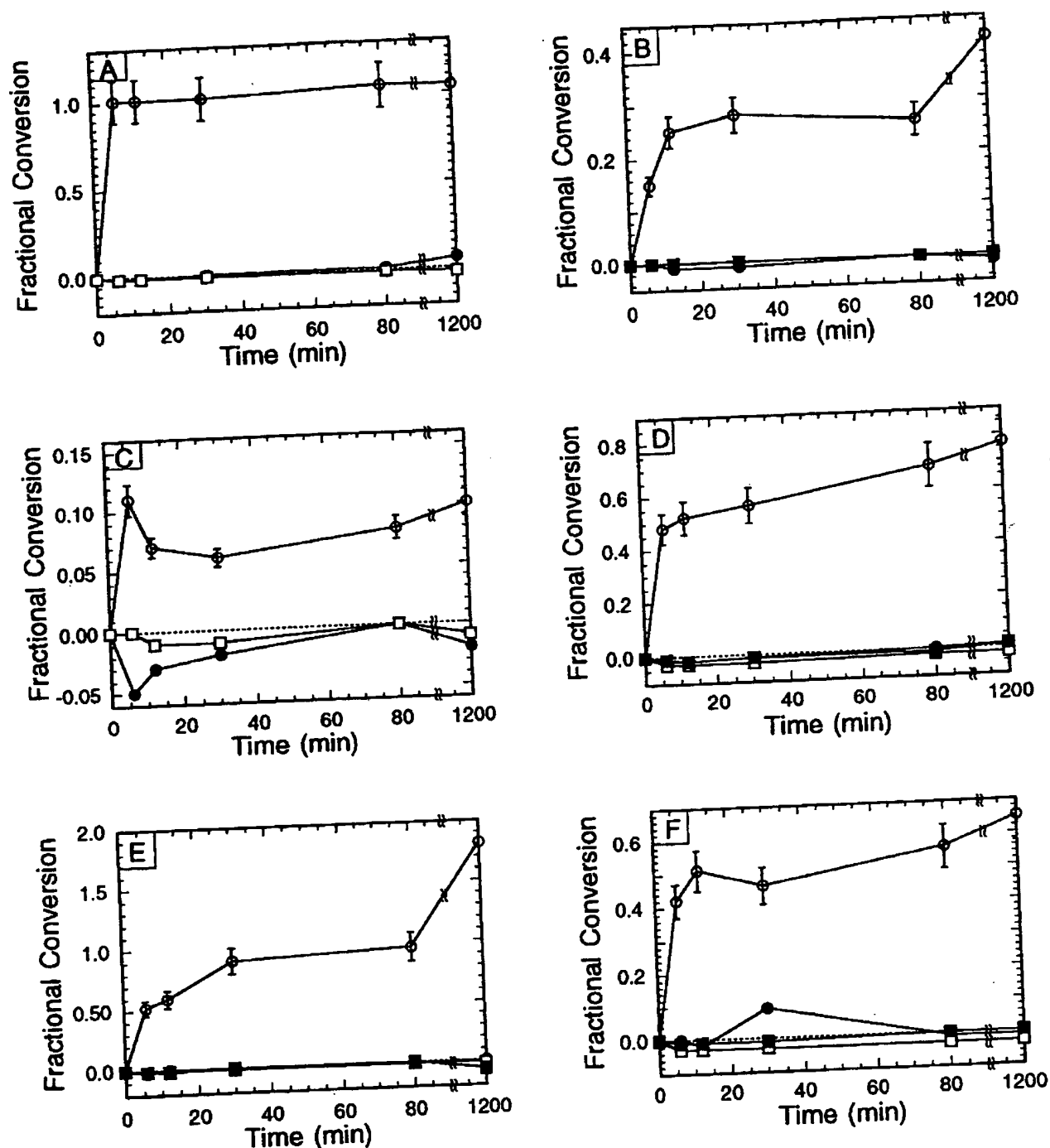


Figure 5. Fractional conversions of peptides and peptoids in simultaneous reactions. Reaction conditions are described in Table 2. Fluorescence values for each time point were corrected for respective enzyme and substrate background fluorescence. Concentrations of amino product were calculated from the fluorescence using the appropriate standard for the resultant amino terminal residue at the expected cleavage site, as indicated in Figure 2, and are divided by the initial substrate concentration to obtain fractional conversion. Error bars indicate the uncertainty of the values propagated from the uncertainties in the fluorescence values and in the peptide and peptoid concentrations. Reactions

with all-L substrates run on different days gave fractional conversions within the errors indicated. (No error bars are given for the D or N compounds since the fluorescence values were within experimental error of 0 in all cases.) Concentrations of amino products from the reverse peptoids of trypsin and papain, where the expected amino products are Narg and Nglu, respectively, were estimated using the standard curve for Nleu-Nhtyr-NH<sub>2</sub>, the least fluorescent peptoid standard evaluated. For each panel (○) all-L peptide, (●) all-D peptide, (□) all-N peptoid, (■) retro all-N peptoid. Enzymes are (A) carboxypeptidase A, (B) papain, (C) pepsin, (D) trypsin, (E) elastase, (F) chymotrypsin.

## PROTEASE STABILITY OF NSG PEPTOIDS

29

mately 1% cleavage for the trypsin all-D and approximately 6% cleavage for the carboxypeptidase A all-D peptides after 20 h. The only NSG peptoid giving any hint of cleavage is the all-N peptoid for papain, which may be cleaved to 0.2%; however, again, the data are scattered over the course of the incubation. No production of detectable amine products was found for any of the other NSG peptoids.

### Inhibitory Effects of NSG Peptoids on All-L Cleavage

As described further in the discussion, the absence of cleavage of any of the NSG peptoids is likely to result from a misalignment of the bound peptoids with the catalytic residues at the active sites of the enzymes. However, weak or tight binding properties of the compounds could also contribute to the result. On the one hand, peptoid cleavage may occur at a low rate, but if the  $K_m$  values for the peptoids are substantially higher than those for the all-L peptides, reflecting weak binding, the concentrations examined may be too low to observe significant cleavage over the time of the reaction. By contrast, if cleavage occurs, but one or both product fragments bind very tightly with a slow rate of dissociation, the peptoid could act as an inhibitor. As a qualitative test to distinguish between these two possibilities, we evaluated the extent of cleavage of the all-L peptides in the absence and presence of their respective NSG peptoids for four of the enzymes. As shown in Figure 6, the NSG peptoids designed for this study are not potent inhibitors against cleavage of the homologous all-L peptides by these proteases, eliminating the hypothesis that tight binding prohibits extensive cleavage of the NSG peptoids by the proteases. At the single concentrations evaluated, three of the NSG peptoids showed inhibition of cleavage of their homologous all-L peptides: the papain all-N peptoid, present at 2.8-fold greater concentration than the all-L peptide; the elastase all-N peptoid, at 5.8-fold greater concentration than the all-L peptide; and the elastase retro all-N peptoid, at 2-fold greater concentration than the all-L peptide. The inhibition is weak, even with the elevated concentrations, indicating that the NSG peptoids bind rather weakly to the proteases. The papain retro all-N peptoid showed no inhibition at a 4-fold greater concentration over the all-L substrate, suggesting that it binds only very weakly, if at all. The other three NSG peptoids that showed no inhibition were present at only equimolar or lower concentrations than their respective all-L peptides (carboxypeptidase A, N/L = 0.6; trypsin, N/L and RN/L approximately 1). Clearly these three compounds are not tight binders, but weak binding

may simply not be detectable at the concentrations evaluated.

### DISCUSSION

While molecular diversity approaches to lead discovery and lead optimization are receiving increasing attention, few groups have addressed potential development hurdles, such as the ADME characteristics of the novel classes of oligomeric compounds being generated. Our interest in NSG peptoids both as homologs of peptides [Simon et al., 1992] and as de novo leads [Zuckermann et al., 1994], has led us to begin investigation of the ADME characteristics of these compounds. Notable among the many obstacles encountered in developing orally available peptides and peptidomimetics are the proteases found in the gut, the bloodstream, and other physiological compartments. Since the NSG peptoids are homologous in their backbone structure to peptides, we have begun our investigations with a comparison of the relative stabilities of homologous sequences of all-L, all-D, all-N, and retro all-N peptides/peptoids toward representative classes of proteases that compounds would be expected to encounter *in vivo*. Additional studies of de novo leads are being pursued and will be reported in detail elsewhere; however, stability studies of one de novo lead (CHIR 2279 [Zuckermann et al. 1994]) do indicate that the compound is proteolytically stable upon extended storage in plasma (Gibbons and Spear, unpublished results).

For the present study, we selected enzymes representative of the major classes of relevant proteases as delineated in Table 1: carboxypeptidase A, papain, pepsin, trypsin, elastase, chymotrypsin. From the extensive data in the literature on sequence specificities for these proteases, we designed L-amino acid peptide substrates, for which we could synthesize fairly homologous D-amino acid containing and N-substituted glycine containing oligomers. Parallel and anti-parallel (retro) NSG peptoids were prepared to cover both the N to C and C to N reading frames along the peptoid. As illustrated by the generic structures in Figure 1, the all-D peptides, being enantiomers of the normal all-L substrates, are not expected to bind properly to the protease active sites, and, hence, should not be subject to cleavage. Likewise, the parallel all-N sequence results in a misalignment of the side chains and the carbonyl groups, causing the susceptible peptide bond to be out of range of the normal nucleophilic catalysts at the active sites, and hence, not cleavable. The retro all-N sequence is more likely to mimic the parent peptide for binding, since the orientation of the side chains and the car-

30

MILLER ET AL.

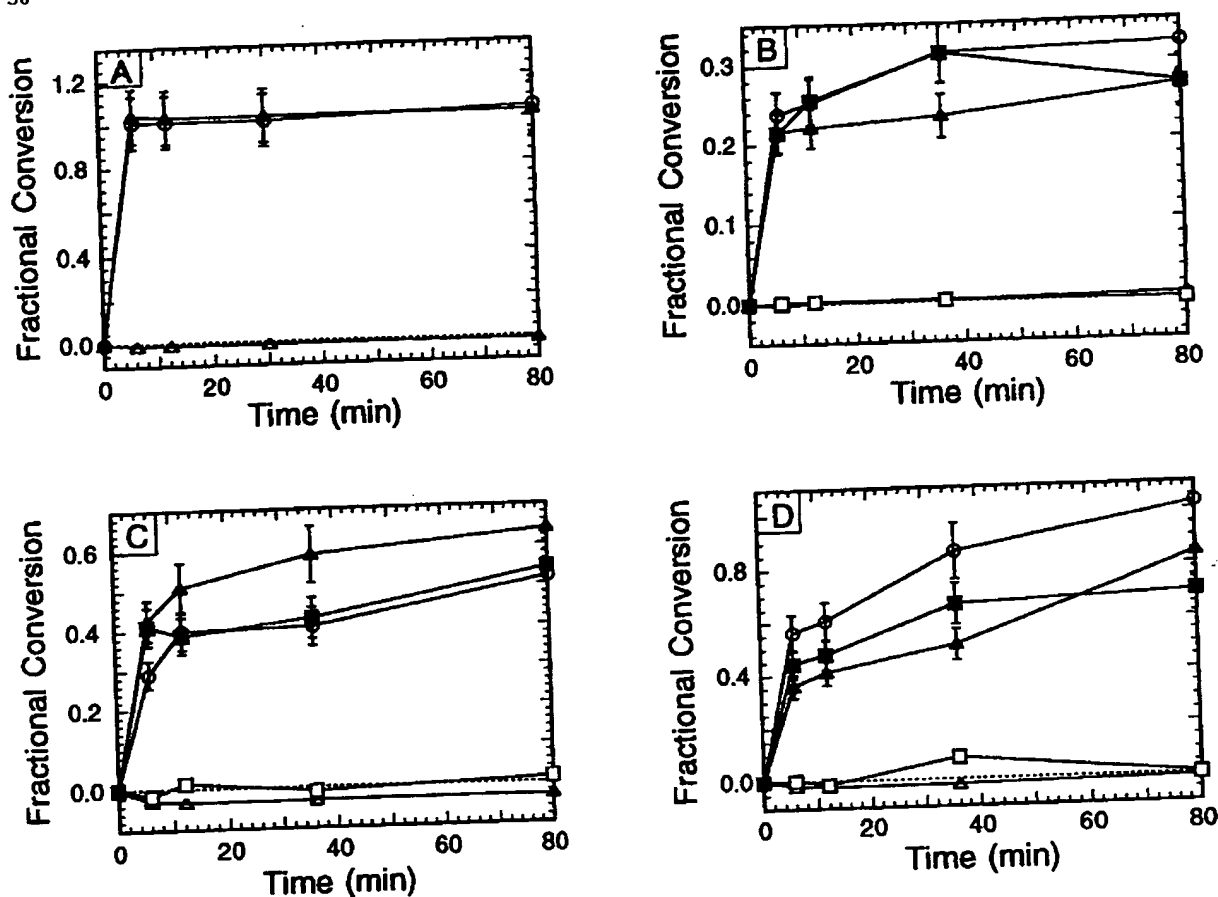


Figure 6. Effect of all-N and retro all-N peptoids on all-L peptide cleavage. Reaction conditions and concentrations of peptides and peptoids for each enzyme are as indicated in Table 2. For the mixtures, equal volumes of the stock peptide and peptoid solutions were diluted to give the same concentrations as in the individual incubations. Fractional conversions and errors are deter-

mined as in Figure 5. For each enzyme, reactions are: (○) all-L peptide alone, (△) all-N peptoid alone, (▲) all-L + all-N mixture, (□) retro all-N peptoid alone, (■) all-L + retro all-N mixture. Enzymes shown are: (A) carboxypeptidase A, (B) papain, (C) trypsin, (D) elastase.

bonyl groups are the same for the two (Fig. 1). Note, however, that the polarity of the cleavable C-N bond would be reversed at the active site for the retro peptoid, such that the nitrogen would be out of reach of the normal enzymic groups involved in protonation of the leaving amino group. Thus, binding may be optimized for the retro all-N sequences, but they too might be expected to be stable to proteolysis.

After synthesis and purification of the requisite compounds, we compared their stabilities against the proteases, as measured by fluorescence resulting from conjugation of the cleaved amines with 4-fluoro-7-nitro-benzofurazan, a compound that shows good reactivity with both 1° and 2° amines. The L-amino acid containing peptides designed for this study were readily proteolyzed by all of the enzymes studied. In

contrast, but as expected from the above analysis, the D-amino acid containing peptides, N-substituted glycine containing peptoids and their anti-parallel or "retro" sequences, were essentially untouched by the enzymes studied. While this study was designed to compare the proteolytic susceptibility of homologous NSG-peptoid and amino acid peptide sequences to specific proteases, it does not address the more general question of proteolytic stability of random NSG-peptoids to a variety of proteases. However, we have previously examined the susceptibility of several random NSG-peptoid sequences to proteolysis by a panel of different proteases and have not found any evidence for hydrolysis of the peptide bonds [Simon et al., 1992] (Miller et al., unpublished results). Results of the inhibition experiments indicate that some of the

## PROTEASE STABILITY OF NSG PEPTOIDS

31

NSG peptoids designed for the study do appear to bind as they weakly inhibit proteolysis of the all-L peptides. It is interesting to note that both forward and reverse peptoids designed for elastase inhibited proteolysis of the homologous all-L peptide, while neither of the peptoids designed for trypsin showed any inhibition. This may reflect the greater importance of extended binding interactions of ligands with elastase as compared with a greater importance of the P<sub>1</sub> residue in binding of ligands to trypsin.

For the quantitation of the extent of hydrolysis of the compounds, we have assumed that cleavage occurs at the sites indicated in Figure 2. With the exception of elastase, the proteases studied have fairly well defined specificities; thus, the assumption is likely to be valid. In the case of elastase, the results clearly indicate multiple cleavage of the all-L peptide, as expected from the low specificity of the enzyme even though the quantitation is not perfect. Another factor that could affect the quantitation is that the relative fluorescence for the expected di- or tripeptide products may differ from that obtained for the simple amino acids used as standards. However, data from the literature indicate only small variations in fluorescence yield (no more than 10%) when reactions of equimolar free amino acid and the same amino acid at the N-termini of several different peptides are compared [Codini et al., 1991]. At this point, the quantitation may not be perfect, but a more complete quantitation seems unnecessary since the reactions with the NSG-peptoids showed no significant fluorescence above the background control reactions, i.e., none of the NSG-peptoids showed any proteolytic cleavage.

In conclusion, under conditions wherein L-amino acid containing peptides are rapidly hydrolyzed, homologous D-amino acid, N-substituted glycine, and retro-sequence N-substituted glycine containing oligomers were essentially untouched by a series of proteases. NSG peptoid diversities thus join the medicinal chemist's repertoire of traditional peptidomimetic and other approaches designed to enhance the absorption, distribution, metabolism, and excretion characteristics of peptides.

## ACKNOWLEDGMENTS

The authors thank Cathy Chu for performing the amino acid analyses and Prof. Jack Kirsch for a critical reading of the manuscript.

## REFERENCES

- Abramowitz N, Schechter I, Berger A (1967): On the size of the active site in proteases. II. Carboxypeptidase-A. *Biochem Biophys Res Commun* 29:862-867.
- Bauer CA, Thompson RC, Blout ER (1976): The active centers of *Streptomyces griseus* protease 3,  $\alpha$ -chymotrypsin, and elastase: Enzyme-substrate interactions close to the scissile bond. *Biochemistry* 15:1296-1299.
- Codini M, Palmerini CA, Fini C, Lucarelli C, Floridi A (1991): High-performance liquid chromatographic method for the determination of prolyl peptides in urine. *J Chromatogr* 536:337-341.
- Conradi RA, Hilgers AR, Ho NFH, Burton PS (1992): The influence of peptide structure on transport across Caco-2 cells. II. Peptide bond modification which results in improved permeability. *Pharm Res* 9:435-438.
- Desai MC, Zuckermann RN, Moos WH (1994): Recent advances in the generation of chemical diversity libraries. *Drug Dev Res* 33:174-188.
- Fischer G, Bang H, Berger E, Schellenberger A (1984): Conformational specificity of chymotrypsin toward proline-containing substrates. *Biochim Biophys Acta* 791:87-97.
- Fruton JS (1976): The mechanism of the catalytic action of pepsin and related acid proteinases. *Adv Enzymol* 44:1-36.
- Furka Á, Sebestyén M, Asgedom M, Dibó G (1991): General method for rapid synthesis of multicomponent peptide mixtures. *Int J Pept Protein Res* 37:487-493.
- Gallop MA, Barrett RW, Dower WJ, Fodor SP, Gordon EM (1994): Applications of combinatorial technologies to drug discovery. 1. Background and peptide combinatorial libraries. *J Med Chem* 37:1233-1251.
- Gordon EM, Barrett RW, Dower WJ, Fodor SP, Gallop MA (1994): Applications of combinatorial technologies to drug discovery. 2. Combinatorial organic synthesis, library screening strategies, and future directions. *J Med Chem* 37:1385-1401.
- Harper JW, Cook RR, Roberts CJ, McLaughlin BJ, Powers JC (1984): Active site mapping of the serine proteases human leukocyte elastase, cathepsin G, porcine pancreatic elastase, rat mast cell proteases I and II, bovine chymotrypsin A<sub>0</sub>, and *Staphylococcus aureus* protease V-8 using tripeptide thiobenzyl ester substrates. *Biochemistry* 23:2995-3002.
- Houghten R, Pinilla C, Blondelle S, Appel J, Dooley C, Cuervo J (1991): Generation and use of synthetic peptide combinatorial libraries for basic research and drug discovery. *Nature* 354:84-86.
- Huber R, Bode W (1978): Structural basis of the activation and action of trypsin. *Accounts Chem Res* 11:114-122.
- Imai K, Watanabe Y (1981): Fluorimetric determination of secondary amino acids by 7-fluoro-4-nitrobenzo-2-oxa-1,3-diazole. *Anal Chim Acta* 130:377-383.
- Imperiali B, Abeles RH (1987): Extended binding inhibitors of chymotrypsin that interact with leaving group subsites S<sub>1</sub>-S<sub>3</sub>. *Biochemistry* 26:4474-4477.
- Lam K, Salmon S, Hersh E, Hruby V, Kazmiersky W, Knapp R (1991): A new type of synthetic peptide library for identifying ligand-binding activity. *Nature* 354:82-84.
- Lowbridge J, Fruton JS (1974): Studies on the extended active site of papain. *J Biol Chem* 249:6754-6761.
- Maciej NJ, Bray AM, Valerio RM, Seldon MA, Wang JX, Geysen HM (1991): Systematic screening of bioactive peptides. *Pept Res* 4:142-146.
- Miller SM, Simon RJ, Ng S, Zuckermann RN, Kerr JM, Moos WH (1994): Proteolytic studies of homologous peptide and N-substi-

## MILLER ET AL.

32

- tuted glycine peptoid oligomers. *Bioorg Med Chem Lett* 4:2657-2662.
- Miyano H, Toyooka T, Imai K (1985): Further studies on the reaction of amines and proteins with 4-fluoro-7-nitrobenzo-2-oxa-1,3-diazole. *Anal Chim Acta* 170:81-87.
- Polgár L (1989): *Mechanisms of Protease Action*. Boca Raton, FL: CRC Press, Inc.
- Powers JC, Harley AD, Myers DV (1977): Subsite specificity of porcine pepsin. In Tang J (ed): *Acid Proteases, Structure, Function, and Biology*. New York: Plenum Press, pp 141-157.
- Pozsgay M, CS. Szabó G, Bajusz S, Simonsson R, Gáspár R, Elodi P (1981): Investigation of the substrate-binding site of trypsin by the aid of tripeptidyl-p-nitroanilide substrates. *Eur J Biochem* 115:497-502.
- Rees DC, Lipscomb WN (1982): Refined crystal structure of the potato inhibitor complex of carboxypeptidase A at 2.5 Å resolution. *J Mol Biol* 160:475-498.
- Schechter I, Berger A (1967): On the size of the active site in proteases. I. Papain. *Biochem Biophys Res Commun* 27:157-162.
- Schechter I, Berger A (1968): On the active site of proteases. III. Mapping the active site of papain; specific peptide inhibitors of papain. *Biochem Biophys Res Commun* 32:898-902.
- Schenk, GH (1973): *Absorption of Light and Ultraviolet Radiation: Fluorescence and Phosphorescence Emission*. Boston: Allyn and Bacon, Inc.
- Schomburg D, Salzmann M (eds) (1990): *Enzyme Handbook*. Berlin: Springer-Verlag.
- Simon RJ, Kania RS, Zuckermann RN, Huebner VD, Jewell DA, Banville S, Ng S, Wang L, Rosenberg S, Marlowe CK, Spellmeyer DC, Tan R, Frankel AD, Santi DV, Cohen FE, Bartlett PA (1992): Peptoids: A modular approach to drug discovery. *Proc Natl Acad Sci USA* 89:9367-9371.
- Thompson RC, Blout ER (1973): Dependence of the kinetic parameters for elastase-catalyzed amide hydrolysis on the length of peptide substrates. *Biochemistry* 12:57-65.
- Zuckermann RN, Kerr JM, Kent SBH, Moos WH (1992a): Efficient method for the preparation of peptoids [oligo (N-substituted glycines)] by sub-monomer solid-phase synthesis. *J Am Chem Soc* 114:10646-10647.
- Zuckermann RN, Kerr JM, Siani MA, Banville SC (1992b): Design, construction and application of a fully automated equimolar peptide mixture synthesizer. *Int J Pept Protein Res* 40:498-507.
- Zuckermann RN, Martin EJ, Spellmeyer DC, Stauber GB, Shoemaker KR, Kerr JM, Figliozzi GM, Coff DA, Siani MA, Simon RJ, Banville SC, Brown EG, Wang L, Richter LS, Moos WH (1994): Discovery of nanomolar ligands for 7-transmembrane G-protein coupled receptors from a diverse (N-substituted) glycine peptoid library. *J Med Chem* 37:2678-2685.

## Design of a Potent Combined Pseudopeptide Endothelin-A/Endothelin-B Receptor Antagonist, Ac-dBhg<sup>16</sup>-Leu-Asp-Ile-[NMe]Ile-Trp<sup>21</sup> (PD 156252): Examination of Its Pharmacokinetic and Spectral Properties

Wayne L. Cody,\* John X. He, Michael D. Reilly, Stephen J. Haleen,<sup>†</sup> Donnelle M. Walker,<sup>†</sup> Eric L. Reyner,<sup>§</sup> Barbra H. Stewart,<sup>§</sup> and Annette M. Doherty

Departments of Chemistry, Vascular and Cardiac Diseases, and Pharmacokinetics & Drug Metabolism, Parke-Davis Pharmaceutical Research, Division of Warner-Lambert Company, Ann Arbor, Michigan 48105

Received March 12, 1997<sup>¶</sup>

The endothelins (ETs) are a family of bicyclic 21-amino acid peptides that are potent and prolonged vasoconstrictors. It has been shown that highly potent combined ET<sub>A</sub>/ET<sub>B</sub> receptor antagonists can be developed from the C-terminal hexapeptide of ET (His<sup>16</sup>-Leu<sup>17</sup>-Asp<sup>18</sup>-Ile<sup>19</sup>-Ile<sup>20</sup>-Trp<sup>21</sup>), such as Ac-dDip<sup>16</sup>-Leu-Asp-Ile-Ile-Trp<sup>21</sup> (PD 142893) and Ac-dBhg<sup>16</sup>-Leu-Asp-Ile-Ile-Trp<sup>21</sup> (PD 145065). However, these compounds are relatively unstable to enzymatic proteolysis as determined in an *in vitro* rat intestinal perfusate assay. This instability is thought to be due to carboxypeptidase activity. In fact, incubation of PD 145065 with carboxypeptidase inhibitors greatly increased its half-life in rat intestinal perfusate. By performing a reduced amide bond and *N*-methyl amino acid scan, it was discovered that *N*-methylation of Ile<sup>20</sup> resulted in a compound (Ac-dBhg<sup>16</sup>-Leu-Asp-Ile-[NMe]Ile-Trp<sup>21</sup>, PD 156252) that retained full receptor affinity at both endothelin receptor subtypes along with enhanced proteolytic stability and cellular permeability. Interestingly, *N*-methylation of this bond allows the *cis* configuration to be readily accessible which greatly alters the preferred structure of the entire molecule and may be responsible for the observed enhanced metabolic stability.

### Introduction

Endothelin-1 (ET-1; Figure 1) is a potent peptidic constrictor of vascular smooth muscle that was first isolated and characterized from the supernatant of porcine endothelial cells.<sup>1-3</sup> ET-1 is one member of a family of isopeptides that includes ET-2 and ET-3<sup>4</sup> along with the structurally and functionally related mouse vasoactive intestinal contractor (VIC),<sup>5</sup> the cardiotoxic sarafotoxins (SRTXs),<sup>6,7</sup> and bibrotoxin.<sup>8</sup> All members of this family possess disulfide bridges between positions 1-15 and 3-11, along with a highly conserved C-terminal hydrophobic hexapeptide, His<sup>16</sup>-Xxx-Asp-Yyy-Ile-Trp<sup>21</sup> (Xxx = Leu or Gln, Yyy = Ile or Val).<sup>9-12</sup>

Initially, two endothelin receptors were cloned, sequenced, and characterized from the bovine and rat lung, respectively.<sup>13,14</sup> The ET<sub>A</sub> receptor is selective for ET-1 and ET-2 over ET-3, while the ET<sub>B</sub> receptor possesses equal affinity for all of the ET isopeptides. Subsequently, the corresponding human receptors have been cloned.<sup>15,16</sup> The endothelin receptor subtype populations (ET<sub>A</sub>/ET<sub>B</sub>) are widely distributed in several tissues and possess different functions dependent upon the species and location. For example, a highly selective ET<sub>B</sub> receptor ligand, sarafotoxin-6c (SRTX-6c),<sup>17</sup> has linked the ET<sub>B</sub> receptor to vasodilation in the rat aortic ring,<sup>18</sup> while it is functionally linked to vasoconstriction in several other tissues.<sup>19</sup> The existence of additional ET<sub>B</sub> receptor subtypes and/or species differences has also been reported.<sup>20-23</sup>

The identification of these receptors has facilitated the development of peptidic and nonpeptidic endothelin

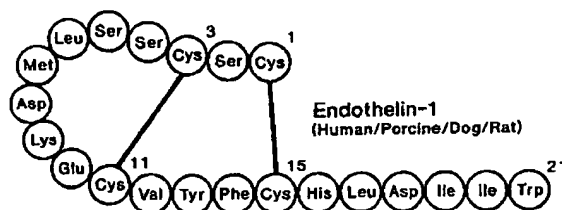


Figure 1. Structure of endothelin-1 (ET-1).

antagonists for the ET<sub>A</sub> and ET<sub>B</sub> receptors or combined antagonists for both the ET<sub>A</sub> and ET<sub>B</sub> receptors (for recent reviews, see refs 9-12). This research has focused on a series of combined ET<sub>A</sub>/ET<sub>B</sub> peptidic antagonists based upon the C-terminal hexapeptide (His<sup>16</sup>-Leu-Asp-Ile-Ile-Trp<sup>21</sup>) of the endothelins. In designing these antagonists the importance of the following structural features were considered: (i) the neutralization of the amine terminus by acetylation enhanced activity ~10-fold, (ii) the preference for D-aromatic amino acids in the 16 position, (iii) the requirement for a tryptophan of the L-stereochemistry in the C-terminal 21 position, and (iv) the necessity of a C-terminal carboxylate.<sup>24-26</sup> These observations resulted in the design and preparation of Ac-dDip<sup>16</sup>-Leu-Asp-Ile-Ile-Trp<sup>21</sup> [compound 2, PD 142893 (Dip = 3,3-diphenylalanine)]<sup>25,27-29</sup> and Ac-dBhg<sup>16</sup>-Leu-Asp-Ile-Ile-Trp<sup>21</sup> [PD 145065, compound 3 (Bhg = 10,11-dihydro-5H-dibenzo[a,d]cycloheptene-glycine)].<sup>30-32</sup> Both of these compounds exhibited low-nanomolar affinity for the ET<sub>A</sub> (58 and 4.0 nM, respectively) and ET<sub>B</sub> (130 and 30 nM, respectively) receptors. Likewise, compounds 2 and 3 were able to antagonize ET-1-stimulated vasoconstriction *in vitro* in the rabbit femoral artery (ET<sub>A</sub>, pA<sub>2</sub> = 6.6 and 6.8, respectively) and SRTX-6c-stimulated vaso-

\* Author to whom correspondence should be addressed. Phone: (313) 996-7729. Fax: (313) 996-3107. E-mail: codyw@aa.wl.com.

<sup>†</sup> Department of Vascular and Cardiac Diseases.

<sup>§</sup> Department of Pharmacokinetics & Drug Metabolism.

<sup>¶</sup> Abstract published in *Advance ACS Abstracts*, June 15, 1997.

*Design of a Combined ET<sub>A</sub>/ET<sub>B</sub> Receptor Antagonist*

constriction in the rabbit pulmonary artery (ET<sub>B</sub>, pA<sub>2</sub> = 6.3 and 7.0, respectively).<sup>25,27-32</sup> Unfortunately, both of these compounds have relatively short half-lives (18.1 ± 3.4 and 10.6 ± 2.2 min, respectively) in rat intestinal perfusate, suggesting limited utility of these compounds for further *in vivo* evaluation.<sup>33,34</sup>

In an attempt to further stabilize these compounds against proteolytic degradation while maintaining receptor affinity, a reduced amide bond and N-methylated amino acid scan of compound 2 was performed. These modifications, in particular the incorporation of N-methylated amino acids, should have significant effects on the conformational preferences of the peptide backbone. In the case of the N-methylated analogues, the energy barrier between the *cis* and *trans* amide bond conformers is greatly reduced.

In all cases, these modifications, save one, resulted in significant losses of affinity at one or both of the endothelin receptor subtypes. In particular, the incorporation of [NMe]Ile in the 20 position of compound 2 resulted in an analogue, Ac-Dip<sup>16</sup>-Leu-Asp-Ile-[NMe]-Ile-Trp<sup>21</sup> (compound 13, PD 149764), that maintained good affinity at both receptor subtypes. This modification was incorporated into the more potent compound 3 template which resulted in an analogue, Ac-DBhg<sup>16</sup>-Leu-Asp-Ile-[NMe]Ile-Trp<sup>21</sup> (compound 15, PD 156252), that had high affinity for both receptor subtypes and greatly enhanced pharmacokinetic properties (stability in rat intestinal perfusate and cellular permeability).

In an effort to help understand the reasons for the improved pharmacokinetic properties of compound 15 and, in particular, its conformational preferences with respect to compound 3, an examination of these analogues by <sup>1</sup>H-NMR spectroscopy in solution was performed. One powerful <sup>1</sup>H-NMR technique for the conformational/structural analysis of macromolecules is isotope-edited NMR spectroscopy. This strategy is limited to cases where the soluble macromolecule (in this case, the receptor) is readily available and either it or the ligand can be isotopically enriched with <sup>13</sup>C and/or <sup>15</sup>N. Unfortunately, in the present scenario this was not the case, since the ET<sub>A</sub> and ET<sub>B</sub> receptor subtypes were not readily available. A second, more generally applicable, although less powerful, approach is to determine structural parameters of the receptor ligand under a variety of conditions (e.g., solvent, temperature, pH, and the like). If the conformational preferences of the ligand are preserved under several different conditions, there is a reasonable expectation that such conformations are the energetically preferred ones.<sup>35</sup> If a compound's three-dimensional structure can survive severe environmental changes, it is even more reasonable to propose that the solution conformation is likely to represent a biologically relevant conformation.

There are several examples of solvent-dependent conformational changes in peptides/pseudopeptides. For example, it is well known from circular dichroism (CD) and NMR studies that fluorinated alcohols, such as trifluoroethanol (TFE) and hexafluoro-2-propanol (HFIP), can induce increased helical structure in linear peptides. There is also abundant literature available describing large conformational changes observed for certain cyclic peptides such as cyclosporin A (CsA) in polar and apolar solvents.<sup>36</sup> In fact, it has been shown that the predicted conformation of CsA in lipophilic solvents and the

*Journal of Medicinal Chemistry*, 1997, Vol. 40, No. 14 2229

similar X-ray structure that was suggested to be the bioactive conformation were incorrect using isotope-edited NMR techniques. The opposite was shown in the case of rampamycin, in which the solution structure,<sup>37</sup> crystal structure<sup>38</sup> and receptor-bound conformations are identical.<sup>35</sup> In addition, it has been shown for the cases of the  $\delta$  receptor selective opioid antagonist [DPe<sup>n</sup>, DPe<sup>n</sup>]enkephalin and the cyclic octapeptide known as sandostatin that it is not possible to rely on only the X-ray crystal or solution NMR structure to determine the bioactive structure.<sup>39,40</sup> In fact, depending upon the particular situation, either method could be argued to be more predictive.

The ability to measure a large number of NMR observables, particularly nuclear Overhauser effects (NOEs), and coupling constants in biomolecules has made possible the determination of several protein structures in solution.<sup>41</sup> It is generally accepted that these data are more abundant and easier to quantitate when internal motion is limited as in the case of medium-sized proteins with extensive secondary and tertiary structure. A much more difficult problem exists, however, when NMR is used to measure the conformational preferences of small peptides in solution. As is often the case in aqueous solution, linear peptides exhibit random coil chemical shifts and yield few structurally relevant NOEs. The lack of NOEs is due to several factors, including multiple conformations and dilution of the intramolecular dipolar interactions by dipolar interactions with solvent. One of the more useful and informative techniques available is analysis of the carbon and proton chemical shifts. Since chemical shifts are sensitive to the peptide backbone angles and the time scale is much faster than for cross-relaxation (10<sup>-9</sup> versus 10<sup>-6</sup> s), chemical shifts can yield information on peptides that are undergoing fast exchange between multiple conformations.<sup>42</sup>

Analysis of the proton NMR characteristics of compound 15 suggested pronounced conformational preferences that were dependent upon the solvent, ionization state, and concentration. For example, in DMSO-*d*<sub>6</sub>, the sodium salt of the peptide adopted a *cis* peptide bond between Ile<sup>19</sup> and [NMe]Ile<sup>20</sup>, whereas in aqueous solution, this peptide bond was *trans*. In DMSO-*d*<sub>6</sub> solution the structure was characterized by a wide dispersion in the amide protons with little dispersion in the methyl protons of Ile and Leu. Similar effects were observed by modifying the ionization state or concentration of compound 15 in solution (see below). By comparison, there were not similar spectral changes in compound 3 which lacks the [NMe]Ile<sup>20</sup> residue.

Herein, this paper will describe the synthesis of a series of endothelin hexapeptide antagonists based upon compound 3 that contain reduced and N-methylated amide bonds along with structure-activity relationships (SAR) and pharmacokinetic properties. In addition, this manuscript suggests a potential explanation for the increased stability observed in rat intestinal perfusate of compound 15 along with implications to the bioactive conformation of C-terminal endothelin hexapeptide antagonists based upon the measurable NMR parameters.

### Chemistry

**Peptide Synthesis, Purification, and Characterization.** All of the peptide analogues were prepared

Table 1. Binding Affinities (IC<sub>50</sub>,  $\mu$ M) for Synthetic Analogues of Compounds 2 and 3 at the ET<sub>A</sub> and ET<sub>B</sub> Receptor Subtypes

no.	compound	ET <sub>A</sub> ( $\pm$ SEM) <sup>a</sup>	ET <sub>B</sub> ( $\pm$ SEM) <sup>b</sup>
2 <sup>c</sup>	Ac-Dip <sup>16</sup> -Leu-Asp-Ile-Ile-Trp <sup>21</sup>	0.058 $\pm$ 0.01 <sup>e</sup>	0.130 $\pm$ 0.03 <sup>e</sup>
3 <sup>d</sup>	Ac-DBhg <sup>16</sup> -Leu-Asp-Ile-Ile-Trp <sup>21</sup>	0.0040 $\pm$ 0.0004 <sup>f</sup>	0.015 $\pm$ 0.003 <sup>f</sup>
4	Ac-Dip <sup>16</sup> -[CH <sub>2</sub> NH]-Leu-Asp-Ile-Ile-Trp <sup>21</sup>	2.7	1.3
5	Ac-Dip <sup>16</sup> -Leu-[CH <sub>2</sub> NH]-Asp-Ile-Ile-Trp <sup>21</sup>	0.26	> 0.25
6	Ac-Dip <sup>16</sup> -Leu-Asp-[CH <sub>2</sub> NH]-Ile-Ile-Trp <sup>21</sup>	0.25	0.020
7	Ac-Dip <sup>16</sup> -Leu-Asp-Ile-[CH <sub>2</sub> NH]-Ile-Trp <sup>21</sup>	0.26	> 0.25
8	Ac-Dip <sup>16</sup> -Leu-Asp-Ile-Ile-[CH <sub>2</sub> NH]-Trp <sup>21</sup>	0.88	> 0.25
9	Ac-[NMe]Dip <sup>16</sup> -Leu-Asp-Ile-Ile-Trp <sup>21</sup>	4.5	8.0
10	Ac-Dip <sup>16</sup> -[NMe]Leu-Asp-Ile-Ile-Trp <sup>21</sup>	0.20	0.60
11	Ac-Dip <sup>16</sup> -Leu-[NMe]Asp-Ile-Ile-Trp <sup>21</sup>	3.2	1.5
12	Ac-Dip <sup>16</sup> -Leu-Asp-[NMe]Ile-Ile-Trp <sup>21</sup>	0.70	> 1.0
13 <sup>h</sup>	Ac-Dip <sup>16</sup> -Leu-Asp-Ile-[NMe]Ile-Trp <sup>21</sup>	0.030	0.080
14	Ac-Dip <sup>16</sup> -Leu-Asp-Ile-Ile-[NMe]Trp <sup>21</sup>	3.0	11.0
15 <sup>i</sup>	Ac-DBhg <sup>16</sup> -Leu-Asp-Ile-[NMe]Ile-Trp <sup>21</sup>	0.0010 $\pm$ 0.0003 <sup>g</sup>	0.040

<sup>a</sup> Binding data in rabbit renal vascular smooth muscle cells  $\pm$  standard error of the mean where more than one IC<sub>50</sub> was determined. <sup>b</sup> Binding data in rat cerebellar membranes  $\pm$  standard error of the mean where more than one IC<sub>50</sub> was determined. <sup>c</sup> PD 142893. <sup>d</sup> PD 145065. <sup>e</sup>  $n$  = 15 IC<sub>50</sub> determinations. <sup>f</sup>  $n$  = 19 IC<sub>50</sub> determinations. <sup>g</sup>  $n$  = 4 IC<sub>50</sub> determinations. All other values represent one IC<sub>50</sub> determination. IC<sub>50</sub> values were derived from single competition experiments in which data points were measured in duplicate. Binding data were computer-analyzed by nonlinear least squares analysis giving the best fit for a one-site model. <sup>h</sup> PD 149764. <sup>i</sup> PD 156252.

by solid-phase peptide synthetic (SPPS) methodologies.<sup>43,44</sup> The peptide analogues were prepared utilizing a *tert*-butyloxycarbonyl (*N*<sup>t</sup>-*t*-Boc) protecting group strategy on a PAM<sup>45</sup> (phenylacetamidomethyl) resin. *N*<sup>t</sup>-*t*-Boc-protected unusual and *N*-methyl amino acids were purchased from commercial sources or prepared utilizing literature methods.<sup>46–48</sup> The reduced amide bonds were prepared by reductive amination of the corresponding amino aldehyde.<sup>49,50</sup> The *N*<sup>t</sup>-*t*-Boc-protected amino aldehydes were prepared by reduction of the corresponding *N,O*-dimethylamide ("Weinreb" amides) of the amino acid with lithium aluminum hydride or for aspartic acid by oxidation of the protected amino alcohol.<sup>51</sup> In some cases, *N*-methyl amino acids were prepared on the solid support utilizing a temporary protecting group followed by reductive amination with formaldehyde or for aspartic acid which was prepared in solution by reduction of the corresponding oxazolidinone (see the Experimental Section).<sup>52,53</sup>

Each *N*<sup>t</sup>-*t*-Boc group was removed with 50% trifluoroacetic acid (TFA) in dichloromethane (DCM) and neutralized with 10% diisopropylethylamine (DIEA) in DCM prior to incorporation of the next protected amino acid. All amino acids were single coupled as either their symmetrical anhydrides or *N*-hydroxybenzotriazole (HOBt)-activated esters unless incomplete coupling was indicated, by the Kaiser test.<sup>54</sup> If incomplete incorporation of the acylating agent was indicated the amino acid was recoupled until a negative Kaiser test was obtained. After coupling of the last amino acid and *N*<sup>t</sup>-amine deprotection, the peptide was acetylated with an excess of 1-acetylimidazole in DCM or 10% acetic anhydride in DCM with a catalytic amount of 4-(dimethylamino)-pyridine (DMAP). The peptides were simultaneously deprotected and cleaved from the resin by treatment with anhydrous liquid hydrogen fluoride (HF) and anisole (9:1, v/v) at 0 °C for 1 h. The resin was filtered and washed with diethyl ether, and the crude peptide was extracted into aqueous solution, concentrated under reduced pressure, resuspended in water, and lyophilized.

All crude peptides were purified to homogeneity by preparative reversed-phase high-performance liquid chromatography (HPLC) eluting with a linear gradient of 0.1% aqueous TFA with increasing concentrations of 0.1% TFA in acetonitrile (AcCN). Peptide fractions that

were determined to be homogenous by analytical reversed-phase HPLC were combined and lyophilized. For secondary *in vitro* functional evaluation, the purified peptides were converted to the corresponding disodium salt, by treating the fully protonated analogue with 5% aqueous sodium bicarbonate, followed by solid-phase extraction on a C18 cartridge, elution with methanol, concentration under reduced pressure, resuspension in water, and lyophilization. All final compounds were analyzed for homogeneity by analytical reversed-phase HPLC and/or capillary electrophoresis (CE) and characterized for structural integrity by elemental analysis, electrospray mass spectrometry (FAB/MS) and proton nuclear magnetic resonance (<sup>1</sup>H-NMR) spectroscopy.

## Results and Discussion

It has been well documented that potent ET<sub>A</sub> and ET<sub>B</sub> receptor antagonists can be developed from the C-terminal hexapeptide of endothelin, such as Ac-Dip<sup>16</sup>-Leu-Asp-Ile-Ile-Trp<sup>21</sup> (compound 2, PD 142893)<sup>25,27–29</sup> and Ac-DBhg<sup>16</sup>-Leu-Asp-Ile-Ile-Trp<sup>21</sup> (compound 3, PD 145065)<sup>30–32</sup> (Table 1). Both compounds showed similar binding affinities to the ET<sub>A</sub> (rabbit renal vascular smooth muscle cells; IC<sub>50</sub> = 58 and 4.0 nM, respectively) and ET<sub>B</sub> (rat cerebellar membranes; IC<sub>50</sub> = 130 and 15 nM, respectively) receptors. In addition, *in vitro* compound 2 was able to block ET-1-stimulated vasoconstriction in the rabbit femoral artery (ET<sub>A</sub>) and sarafotoxin-6c (SRTX-6c)-stimulated vasoconstriction in the rabbit pulmonary artery (ET<sub>B</sub>) with pA<sub>2</sub> values of 6.6 and 6.3, respectively.<sup>25,27–29</sup> Likewise, compound 3 possessed pA<sub>2</sub> values of 6.6 and 6.8 for the ET<sub>A</sub> and ET<sub>B</sub> receptors, respectively.<sup>30–32</sup>

Both of these compounds had relatively short half-lives (18.1  $\pm$  3.4 and 10.6  $\pm$  2.2 min, respectively) in rat intestinal perfusate, thus limiting the utility of these compounds for further *in vivo* evaluations.<sup>33,34</sup> Each compound was degraded to a primary metabolite plus several other fragments under initial rate conditions. Incubation of compound 3 with a carboxypeptidase inhibitor from potato tuber reduced the rate of hydrolysis by 75%. Given that an aromatic amino acid is at the C-terminus of the peptide, this provided evidence of the involvement of carboxypeptidase A which prefers this substrate configuration.<sup>55</sup> In addition, it was shown by reversed-phase high-performance liquid chromatog-

### Design of a Combined ET<sub>A</sub>/ET<sub>B</sub> Receptor Antagonist

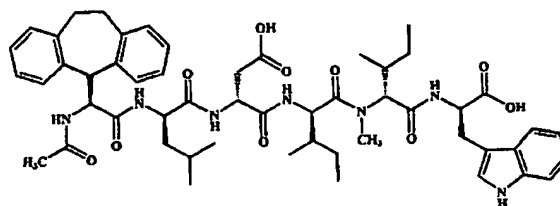
raphy, as well as mass spectrometry, that Ac-Dip<sup>16</sup>-Leu-Asp-Ile-Ile and Ac-DBhg<sup>16</sup>-Leu-Asp-Ile-Ile were the primary metabolites of compounds 2 and 3, respectively.<sup>33,34</sup>

It has been previously shown that N-terminal acetylation of these molecules was required for high receptor affinity; however, modifications of the C-terminus to protect against exopeptidases, such as carboxypeptidases, have not been tolerated.<sup>29–31</sup> In addition, multiple D-amino acid substitutions all led to significant losses of receptor affinity.<sup>56,57</sup> Thus, we have undertaken a reduced amide and N-methyl amino acid scan of the C-terminal hexapeptide to explore the structural features that will maintain receptor affinity while enhancing stability to enzymatic proteolysis.

**Reduced Amide Bond Scan of Compound 2.** The reduced amide (aminomethylene) analogues (compounds 4–8) were prepared by reductive amination with the appropriate N<sup>α</sup>-t-Boc-protected amino aldehyde to the growing peptide on the solid phase or in solution.<sup>49,50</sup> The protected amino aldehydes were prepared by reduction of the corresponding N,O-dimethylamides ("Weinreb" amides) with lithium aluminum hydride or for aspartic acid by oxidation of the protected amino alcohol.<sup>51</sup> Alternatively, the aminomethylene-containing dipeptide was prepared, suitably protected, and coupled directly to the growing peptide (see the Experimental Section). In general, it was observed that the reduced amide analogues (compounds 4–8; Table 1) had 7–70-fold less affinity for the ET<sub>A</sub> receptor than the parent peptide (compound 2). Likewise, 4-fold or more loss in binding affinity was observed for the ET<sub>B</sub> receptor with respect to compound 2. However, compound 6 with the reduced amide bond between Asp<sup>18</sup> and Ile<sup>19</sup> actually showed 3-fold enhancement of binding affinity to ET<sub>B</sub> with respect to compound 2. In spite of the interesting profile of compound 6, the reduced amide bond series was not pursued further, since the goal of this study was to discover a stabilized ET<sub>A</sub>/ET<sub>B</sub> receptor antagonist with high affinity for both receptor subtypes, thus a profile similar to that of compounds 2 and 3.

**N-Methyl Amino Acid Scan of Compound 2.** The mono-N-methylated analogues (compounds 9–14) were prepared by incorporation of the N<sup>α</sup>-t-Boc- or N<sup>α</sup>-Fmoc-protected N-methyl amino acid to the growing peptide on the resin (purchased from commercial sources or prepared by the method of Freidinger et al.<sup>53</sup>) or by reductive amination on the resin with formaldehyde using a temporary monoprotecting group [4,4'-dimethoxyphenylmethyl (Dod)] on the N<sup>α</sup>-terminal amine (see the Experimental Section).<sup>52</sup> Similar to the reduced amide bond analogues, most of the N-methylated analogues of compound 2 (compounds 9–12 and 14; Table 1) showed losses in receptor affinity of 7–160-fold. However, Ac-Dip<sup>16</sup>-Leu-Asp-Ile-[NMe]Ile-Trp<sup>21</sup> (compound 13) maintained high affinity for both the ET<sub>A</sub> and ET<sub>B</sub> receptor subtypes (30 and 80 nM, respectively).<sup>33</sup> [Several conditions were explored [N,N-diisopropylcarbodiimide (DIC), DIC/HOBt, (benzotriazol-1-yloxy)tris(dimethylamino)phosphonium hexafluorophosphate (Bop reagent), O-(benzotriazol-1-yl)-1,1,3,3-tetramethyluronium hexafluorophosphate (HBTU), and O-(7-azabenzotriazol-1-yl)-1,1,3,3-tetramethyluronium hexafluorophosphate (HATU)] for the coupling of Ile<sup>19</sup> to [NMe]Ile<sup>20</sup> with little success (<20% incorporation). The use of the

Journal of Medicinal Chemistry, 1997, Vol. 40, No. 14 2231



PD 156252

Figure 2. Structure of compound 15 (PD 156252).

acid chloride of N<sup>α</sup>-Fmoc-Ile proved to be highly effective for this coupling (see the Experimental Section for preparation of compounds 13 and 15).] Also, *in vitro* compound 13 was able to block ET-1-stimulated vasoconstriction in the rabbit femoral artery (ET<sub>A</sub>) and SRTX-6c-stimulated vasoconstriction in the rabbit pulmonary artery (ET<sub>B</sub>) with pA<sub>2</sub> values of 6.6 and 6.3, respectively.

Due to the profile of compound 13, the [NMe]Ile<sup>20</sup> substitution was incorporated in the more potent Ac-DBhg<sup>16</sup>-Leu-Asp-Ile-Ile-Trp<sup>21</sup> (compound 3) template to produce compound 15. Compound 15 showed enhanced binding affinity to both the rabbit ET<sub>A</sub> and the rat ET<sub>B</sub> receptor subtypes with IC<sub>50</sub>'s of 1.0 and 40 nM, respectively. Likewise, compound 15 was able to antagonize ET-1-stimulated vasoconstriction *in vitro* in the rabbit femoral artery (ET<sub>A</sub>, pA<sub>2</sub> = 7.3) and SRTX-6c-stimulated vasoconstriction in the rabbit pulmonary artery (ET<sub>B</sub>, pA<sub>2</sub> = 6.6). Thus, compound 15 represents a highly potent combined ET<sub>A</sub> and ET<sub>B</sub> receptor antagonist (Figure 2).<sup>33</sup>

It has been previously reported that a significant species difference between the binding affinity of ligands for endothelin receptors can exist, especially in the case of the ET<sub>B</sub> receptor. In general, compounds have been shown to possess significantly lower affinity (150-fold and greater) for the human cloned ET<sub>B</sub> receptor than for the corresponding rat receptor.<sup>22,23,29</sup> Compound 15 maintained good binding affinity for both the human cloned ET<sub>A</sub> and ET<sub>B</sub> receptor subtypes (3.0 and 25 nM, respectively).

As shown previously, the parent compounds 2 and 3 were unstable in rat intestinal perfusate with half-lives of 18.1 ± 3.4 and 10.6 ± 2.2 min, respectively.<sup>33,34</sup> Large increases in the half-lives of the [NMe]Ile<sup>20</sup> analogues (PD 149764 and PD 156252) were observed. In fact, compounds 13 and 15 were approximately 50-fold more stable than their parent analogues with half-lives in rat intestinal perfusate of 875 ± 145 and 538 ± 52 min, respectively (Table 2).

Caco-2 cells are a continuously cultured cell line derived from human colon adenocarcinoma that spontaneously differentiate to resemble the epithelial cells that line the small intestine and have been widely used as an *in vitro* model of intestinal absorption.<sup>56–58</sup> Several of the hexapeptide antagonists were examined in this model: compounds 2, 3, 13, and 15. All of these compounds are of similar molecular weight and charge (−2 at physiological pH). The Caco-2 permeabilities of the hexapeptide ET antagonists ranged from approximately 2.0 × 10<sup>−4</sup> to 6.3 × 10<sup>−4</sup> cm/min which, when compared to standard compounds, suggests a potential for moderate, but measurable, intestinal absorption *in vivo* in the range of 5–10% (Table 2). Compound 2 was the least permeable, and compound 15 was clearly the

Table 2. Stability in Rat Intestinal Perfusate and Permeability in Caco-2 Cell Monolayers for Compounds 2, 3, 13, and 15

no.	compound	permeability <sup>a</sup> (10 <sup>4</sup> , cm/min)	stability <sup>b</sup> (t <sub>1/2</sub> , min)
2 <sup>c</sup>	Ac-D[Dip <sup>16</sup> -Leu-Asp-Ile-Ile-Trp <sup>21</sup>	2.0 ± 0.5	18.1 ± 3.4
3 <sup>d</sup>	Ac-D[Bhg <sup>16</sup> -Leu-Asp-Ile-Ile-Trp <sup>21</sup>	4.7 ± 0.9	10.6 ± 2.2
13 <sup>e</sup>	Ac-D[Dip <sup>16</sup> -Leu-Asp-Ile-[NMe]Ile-Trp <sup>21</sup>	2.0 ± 0.8	875 ± 145
15 <sup>f</sup>	Ac-D[Bhg <sup>16</sup> -Leu-Asp-Ile-[NMe]Ile-Trp <sup>21</sup>	6.3 ± 2.5	538 ± 52

<sup>a</sup> Each value represents the mean of three to five cell monolayers. Standard errors are tabulated with the mean values. <sup>b</sup> Values are the mean of at least three determinations ± standard error of the mean from two perfusate preparations. Leucine aminopeptidase activity ranged from 0.05 to 0.32 nkat/mL in the perfusate preparations. <sup>c</sup> PD 142893. <sup>d</sup> PD 145065. <sup>e</sup> PD 149764. <sup>f</sup> PD 156252.

most permeable. This increase in permeability is likely due to the enhanced lipophilicity of compound 3. However, the differences between analogues were small and the permeabilities were low, as could be anticipated from the physicochemical properties described above.

In addition, compound 15 was shown to possess *in vivo* activity by inhibition of the pressor response to an ET-1 challenge in a conscious rat model. In particular, a dose of 10 mg/kg of compound 15 was administered iv bolus to conscious rats 5 and 30 min prior to an ET-1 challenge (0.30 nM/kg, iv bolus). Compound 15 was shown to reduce the pressor response to ET-1 by 81% and 58%, respectively. Thus, compound 15 was effective as an antagonist in an *in vivo* model in a time dependent manner.

**NMR Studies of Compounds 3 and 15.** The following discussion involves a description of (1) the <sup>1</sup>H-NMR spectral properties of compounds 3 and 15 under various conditions including solvent content and ionization state and (2) the structural properties of two different conformations of the sodium salt of compound 15. Under each different set of conditions employed, rigorous proton NMR assignments were made using well-established 2D procedures.<sup>41</sup> The <sup>1</sup>H-NMR spectral parameters of compound 3 have been previously reported in dodecylphosphocholine micelles.<sup>61</sup> In micelles, compound 3 was shown to adopt a standard turn topology in three closely related families which were significantly different than the structures observed in aqueous or DMSO-*d*<sub>6</sub> solution. In addition, it was shown that compound 3 was in fast chemical exchange between several closely related conformational states.<sup>61</sup> The proton NMR data for the disodium salt and fully protonated forms of compounds 3 and 15 in aqueous and DMSO-*d*<sub>6</sub> solution are provided in the Supporting Information.

#### Effect of Solvent on Spectral Characteristics.

The 1D <sup>1</sup>H-NMR spectra of the disodium salt forms of compounds 3 (3·Na) and 15 (15·Na) in DMSO-*d*<sub>6</sub> (top trace) and aqueous (bottom trace) solution are shown in Figure 3A,B, respectively. In the case of compound 3·Na, the <sup>1</sup>H-NMR spectrum is slightly different in the two solvents, with small changes in chemical shift dispersion in most regions of the spectrum (Figure 3A).

However, the <sup>1</sup>H-NMR spectra of compound 15·Na in DMSO-*d*<sub>6</sub> and aqueous solution are significantly different from each other (Figure 3B). The DMSO-*d*<sub>6</sub> spectrum (top trace) is characterized by significant spectral dispersion of the amide protons, aspartic acid β protons, and a clustering of the methyl protons of the leucine and isoleucine residues. However, the aqueous spectrum (bottom trace) is characterized by a large degree of dispersion in the methyl region, with the γ methyl protons of Ile<sup>19</sup> at exceptionally high field (0.18 ppm). Other regions of the spectrum are more similar to each other. Interestingly, addition of 10% (v/v) water to a

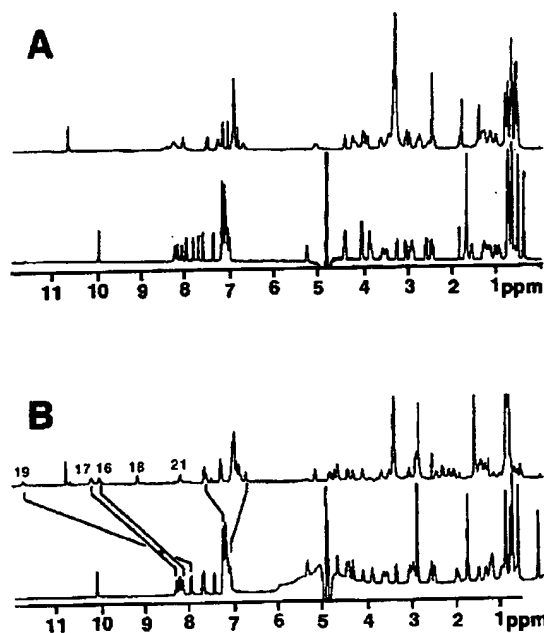


Figure 3. 500 MHz <sup>1</sup>H-NMR spectra of compound 3·Na (A) and compound 15·Na (B). In both cases, the bottom trace is the peptide dissolved in 90% H<sub>2</sub>O/10% D<sub>2</sub>O with the pH adjusted to 6.7 and the top trace is the peptide dissolved in DMSO-*d*<sub>6</sub>.

solution of compound 15·Na in DMSO-*d*<sub>6</sub> caused a collapse of the dispersion in the amide region and an increase in dispersion in the methyl region of the spectrum such that the spectrum becomes similar to the aqueous spectrum (data not shown). In the converse experiment, addition of up to 50% (v/v) DMSO-*d*<sub>6</sub> to an aqueous solution of compound 15·Na resulted in a slight increase in the dispersion in the amide protons and a decrease in the spread of the methyl proton chemical shifts of leucine and isoleucine. These dramatic differences in the <sup>1</sup>H-NMR spectral properties of compound 15·Na that are solvent dependent are most likely due to *cis* = *trans* isomerization around the Ile<sup>19</sup>–[NMe]Ile<sup>20</sup> amide bond.

To further investigate this phenomenon, the <sup>1</sup>H-NMR spectrum was qualitatively analyzed for compound 15·Na in a number of other organic solvents (data not shown). The spectrum of compound 15·Na in methanol-*d*<sub>3</sub> solution was similar to the peptide dissolved in aqueous solution, whereas the spectrum in DMF-*d*<sub>7</sub> was very nearly identical to that observed in DMSO-*d*<sub>6</sub>. The peptide dissolved readily in acetone-*d*<sub>6</sub> and sparingly in AcCN-*d*<sub>3</sub>. The resonances were extremely broad in both solvents, suggesting extensive aggregation.

**Secondary Chemical Shifts.** It has been well established that proton and carbon chemical shifts in

*Design of a Combined ET<sub>A</sub>/ET<sub>B</sub> Receptor Antagonist*

peptides and proteins are sensitive to  $\Phi$  and  $\Psi$  angles.<sup>62</sup> Thus, the secondary  $\alpha$  and  $\text{H}\alpha$  chemical shifts for both forms of compounds **3** and **15** were analyzed. The fully protonated peptides dissolved in DMSO- $d_6$  show only small secondary shifts, indicative of highly flexible conformation properties. For the two analogues in D<sub>2</sub>O, a similar secondary shift pattern is observed for compounds **3**·Na and **15**·Na, with the main difference being a larger negative secondary shift at position 19 in the N-methylated peptide (compound **15**·Na). In DMSO- $d_6$ , both peptides clearly become more ordered, but their secondary shifts now differ significantly in both magnitude and sign. Interestingly, the major difference between the disodium peptides in DMSO- $d_6$  is again at Ile<sup>19</sup>, with a ~5 ppm difference in secondary shift and a change in sign. Also, the magnitudes of the secondary shifts for compound **15**·Na are universally higher than for compound **3**·Na, suggesting a more stable secondary structure for the methylated peptide.

Quantitative analysis of these secondary shifts is complicated by several factors. First, in our analysis of Gly-Gly-[NMe]Ile-Gly-Gly, only the *trans* conformer was observed in aqueous and DMSO- $d_6$  solutions. Therefore, the appropriate random coil chemical shift is not available for the *cis* conformation of [NMe]Ile. Hence, the random coil chemical shift for the *trans* conformation was used for all peptides. This may be a reasonable value, since it is known that Pro  $\alpha$  shifts are not very sensitive to the geometric configuration about the imide bond. Second, the nearest-neighbor corrections for the random coil chemical shift of Ile<sup>19</sup> (when preceding [NMe]Ile) were taken from work with proline-containing peptides.<sup>63</sup> Here again, the assumption that [NMe]Ile is similar to proline with respect to secondary shifts may not be valid.

**Effect of Ionization State.** The <sup>1</sup>H-NMR spectrum of the fully protonated form of compound **15** in DMSO- $d_6$  is characterized by poor dispersion with very little indication of secondary structure. The temperature coefficients and amide to  $\alpha$  proton coupling constants (<sup>3</sup> $J_{\text{NH}\alpha}$ , Table 2) that can be measured are consistent with a conformationally flexible structure. Addition of 20% aqueous sodium hydroxide in approximately equimolar proportional steps initially results in a broadening of the signals in the amide region, and two sets of signals could be seen for some of the aliphatic protons. This is most likely due to *cis* = *trans* isomerization around the Ile<sup>19</sup>–[NMe]Ile<sup>20</sup> amide bond induced by deprotonation of the peptide, *vide infra*. Addition of a third equivalent of base resulted in a spectrum essentially identical with that of compound **15**·Na. When a similar titration was performed with aqueous potassium hydroxide or cesium hydroxide, the results were indistinguishable from those using NaOH.

The above results are consistent with the following hypotheses/observations: Firstly, a distinct conformation is observed for compound **15**·Na in aprotic anhydrous solvents (DMSO- $d_6$ , etc.) that is "more ordered" than the conformation observed in protic solvents or that of the protonated peptide species in aprotic solvents. Thus, the "ordered" structure is not favored when the C-terminal and aspartic acid side chain carboxyl anions are fully or partially neutralized by protons or efficient solvation. Secondly, this "ordered" structure is not readily accessible to an analogue of

*Journal of Medicinal Chemistry*, 1997, Vol. 40, No. 14 2233

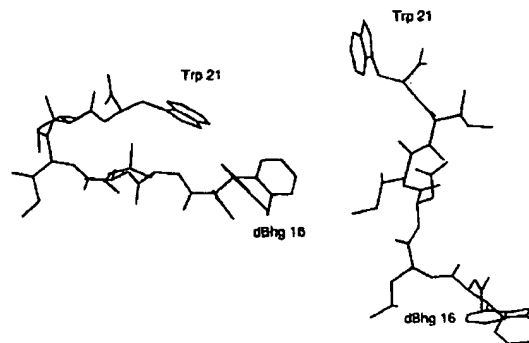


**Figure 4.** Structures of *cis* (left) and *trans* (right) conformers of compound **15**.

compound **15**·Na that does not contain an [NMe]Ile<sup>20</sup>, (i.e., compound **3**·Na).

**Conformational Preferences for Compound 15·Na.** Because of the unique spectral features observed for compound **15** (but not compound **3**), the hypothesis that the structure characterized by the unusually large dispersion of amide proton chemical shifts was due to the formation of a *cis* peptide bond between Ile<sup>19</sup> and [NMe]Ile<sup>20</sup> was investigated. Methylation of the amide of Ile<sup>20</sup> decreases the energy difference between the *trans* and *cis* configurations, making both energetically accessible. NOEs between the  $\alpha$  protons of Ile<sup>19</sup> and Ile<sup>20</sup> or [NMe]Ile<sup>20</sup> established that, indeed, the sodium form of the peptide was 100% *cis* (about the Ile<sup>19</sup>–[NMe]Ile<sup>20</sup> peptide bond) in DMSO- $d_6$ , while the lack of NOEs in aqueous solution established that the peptide bond was 100% *trans*.

In one 15 mM sample of compound **15**·Na in DMSO- $d_6$ , numerous medium and long range NOEs in a NOESY spectrum recorded with a mixing time of 400 ms were observed. The sign of the NOEs was consistent with a correlation time of greater than 1 ns, which was somewhat surprising for a linear hexapeptide. To investigate this further, NOESY spectra were obtained at 80, 120, and 200 ms, respectively. Analysis of the NOE buildup curves provided clear evidence that many of the cross-peaks observed in the 400 ms NOESY were due to spin diffusion. Analysis of the shapes of the buildup curves suggested that all of the NOE information in the 80 ms NOESY was due to direct cross-relaxation. Sixty-five cross-peak volumes were converted to upper bound distance constraints and used to generate structures for compound **15**·Na. In addition to distance constraints, the  $\Phi$  angles of residues 16, 17, and 19 were constrained to the range of  $-75^\circ$  to  $-175^\circ$ , based on <sup>3</sup> $J_{\text{NH}\alpha}$ .

Using these constraints, 20 structures were generated by distance geometry/simulated annealing. Nineteen of these had final DGII optimization errors of  $<0.1$ , and none of these had experimental distance violations of more than 0.3 Å. Representative structures from these calculations are shown in Figure 4.

Several structural features that were consistent with the observed spectral properties were apparent. First, the close proximity of Leu<sup>17</sup> and Ile<sup>19</sup> side chains to the DBhg<sup>16</sup> and Trp<sup>21</sup> side chains, respectively, could explain the high-field-shifted methyl protons observed in the *trans* conformer. These were also consistent with the aromatic methyl NOEs observed for compounds **3**·Na

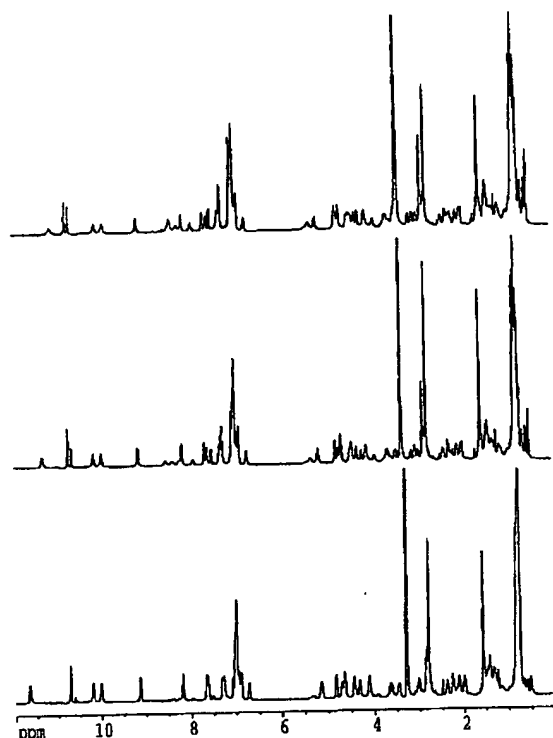


**Figure 5.** Concentration dependence of the  $^1\text{H}$ -NMR spectrum of compound  $15\cdot\text{Na}$  in  $\text{DMSO}-d_6$  at  $35^\circ\text{C}$ . The three concentrations shown are 145 mM (top trace), 72 mM (middle trace), and 36 mM (bottom trace).

and  $15\cdot\text{Na}$  in aqueous solution and for the fully protonated forms of compounds **3** and **15** in  $\text{DMSO}-d_6$ . In the structures calculated for compound  $15\cdot\text{Na}$  in  $\text{DMSO}-d_6$ , the three aliphatic side chains were exposed to solvent and further removed from the aromatic side chains, consistent with the lack of chemical shift dispersion for these species. Second, although the side chain of Trp for compound  $15\cdot\text{Na}$  was not well defined in the ensemble of structures, on average it was closer to the DBhg<sup>16</sup> side chain than in the extended structure. Mutual ring current effects could be invoked to explain the additional dispersion in the aromatic resonances of the DBhg<sup>16</sup> residue and the unusual chemical shifts of the Trp<sup>21</sup> side chains (compared to Trp in a random coil peptide) for the sodium salt in  $\text{DMSO}-d_6$ . Third, the amide protons were internalized in the calculated structures, consistent with their highly disperse chemical shifts and relatively small temperature coefficients. Finally, the C-terminal carboxylate was poised for hydrogen-bonding interactions with the NH of Ile<sup>19</sup> and/or Asp<sup>18</sup> in many of the final structures. The potential for electrostatic interaction between the C-terminal carboxylate and amide protons could be a driving force for *cis*-peptide bond formation in this peptide dissolved in an aprotic solvent. Possible structures for the *cis* and *trans* conformers of compound  $15\cdot\text{Na}$  are shown in Figure 4.

**Concentration Dependence of Compound  $15\cdot\text{Na}$  in  $\text{DMSO}-d_6$  Solution.** In an attempt to measure the three bond  $^{13}\text{C}_\beta\text{-NH}$  coupling constants, a sample was prepared by dissolving 72 mg of compound  $15\cdot\text{Na}$  in 0.5 mL of  $\text{DMSO}-d_6$  ( $\sim 150$  mM). The resulting spectrum was more complex than expected based upon spectra

recorded at lower concentrations. Diluting this sample 4-fold resulted in a return to a more normal spectrum (Figure 5). Some resonances (cf. the Trp indole resonances at 10.6 ppm) suggest a slow exchange between different species, whereas the amide protons simply broaden and/or move to higher field at the higher concentration. A possible explanation for the concentration-dependent behavior of the spectrum is a monomer = multimer equilibrium or an ionic strength/pH effect. The peak positions of the species that forms at higher concentrations are similar to those observed for the fully protonated form of compound **15**, suggesting that this species contains compound **15** in the *trans* configuration.

Addition of substoichiometric amounts of sodium hydroxide to a 60 mM solution of the fully protonated form of compound **15** resulted in a decrease in the amount of this species with a concomitant increase in the species identified as the *cis* configuration of compound  $15\cdot\text{Na}$ . Thus it appears that the second species observed at higher concentrations may be the *trans* configuration of compound **15** and that its relative abundance may be a function of the effective pH and/or ionic strength in the  $\text{DMSO}-d_6$  solution. This is affected by such difficult to control variables as the extent of hydration and the exact protonation state of the peptide, as well as the amount of water present in the solvent.

## Conclusions

Compound **15** represents a constrained analogue of compound **3** that is a highly potent combined  $\text{ET}_\text{A}$  and  $\text{ET}_\text{B}$  receptor antagonist. Compound **15** showed enhanced binding affinity to both the rabbit  $\text{ET}_\text{A}$  and rat  $\text{ET}_\text{B}$  receptor subtypes with  $\text{IC}_{50}$ 's of 1.0 and 40 nM, respectively). Likewise, compound **15** was able to antagonize ET-1-stimulated vasoconstriction *in vitro* in the rabbit femoral artery ( $\text{ET}_\text{A}$ ,  $pA_2 = 7.3$ ) and SRTX-6c-stimulated vasoconstriction in the rabbit pulmonary artery ( $\text{ET}_\text{B}$ ,  $pA_2 = 6.6$ ). In addition, compound **15** was approximately 50-fold more stable than compound **3** in rat intestinal perfusate with a half-life greater than 500 min. Since the only difference between compounds **3** and **15** lies in the N-methylation of the amide bond between Ile<sup>19</sup> and Ile<sup>20</sup>, the enhanced proteolytic stability and cellular permeability must be related physically or conformationally to this modification. In addition, since N-methylation of an amide bond is known to have significant effects on the conformational preferences of the peptide backbone and compound **15** is a highly potent analogue, it must be assumed that this modification has constrained the molecule in a conformation that is favored for interaction with the ET receptor subtypes.

It is intriguing to speculate that the enhanced stability of compound **15** may be a result of the energetically favored accessibility of the *cis* amide bond conformer. From the above  $^1\text{H}$ -NMR studies it had been shown that in aqueous solution compound  $15\cdot\text{Na}$  exists exclusively in the *trans* amide bond form; however, upon the addition of  $\text{DMSO}-d_6$  the *cis* form became accessible. The *cis* form was also shown to depend upon the ionization state of compound **15**. Based upon these results it was obvious that the energy barrier between the *trans* and *cis* conformers is low and readily obtainable; thus it was not possible to predict the preferred structure of compound **15** under physiological conditions. If the *cis* conformer was predominant, it can be

### Design of a Combined ET<sub>A</sub>/ET<sub>B</sub> Receptor Antagonist

seen from Figure 4 that C-terminal carboxylate would be buried and less accessible to carboxypeptidase activity, accounting for the increased stability of compound 15 in rat intestinal perfusate. In the same regard, it is possible that methylation of the p-1 amino acid of a carboxypeptidase substrate may lead to an analogue that does not fit properly into the enzyme, either sterically or simply by disruption of a critical hydrogen-bonding interaction. Resolution of the exact reasons for the increased stability will require additional studies, which are not the focus of this manuscript. Such studies could include replacement of the Ile<sup>19</sup>-[NMe]Ile<sup>20</sup> amide bond with peptidomimetic isosteres (*cis* alkenes and the like) that would lock the molecule into the *cis* configuration.

It is also quite intriguing that the simple modification of N-methylating a single amide bond of a hexapeptide can have such profound effects on the intrinsic stability of the molecule in rat intestinal perfusate without concomitant effects on cellular permeability. In this regard, it should become common practice in the development of second-generation peptidomimetic compounds designed from a peptide lead for extended *in vitro* and *in vivo* evaluations to perform a reduced amide bond and N-methylated amino acid scan. As can be seen from above, this can impart desirable physicochemical properties into the molecule as well as provide insights into the understanding of the bioactive conformation.

### Experimental Section

**Materials and Methods.** Orthogonally protected N<sup>ε</sup>-t-Boc amino acids, N<sup>ε</sup>-Fmoc amino acids, and N<sup>ε</sup>-t-Boc-Trp-PAM resins were purchased from either Advanced Chemtech, Applied Biosystems Inc., Bachem California, Bachem Bioscience, Novabiochem, Peninsula Laboratories, Inc., or Synthetech Inc. All amino acids were of the L-configuration unless otherwise noted.

TFA was purchased from Halocarbon. N,N-Dicyclohexylcarbodiimide (DCC), DIEA, and HOBt were purchased from Applied Biosystems Inc. (ABI). N,N-Dimethylformamide (DMF), DCM, and NMP were purchased from Burdick & Jackson and were of reagent grade or better. HPLC grade solvents (AcCN and water) were obtained from Burdick and Jackson, EM Science, or Mallinckrodt. HF was purchased from Matheson Gas Products. All of the other reagents for chemical synthesis were purchased from Aldrich Chemical Co., Inc. or similar suppliers. Tris(hydroxymethyl)aminomethane (Trizma), ethylenediaminetetraacetate (EDTA), and N-(2-hydroxyethyl)piperazine-N'-(2-ethanesulfonic acid) (HEPES) were purchased from Sigma Chemical Co. Phenylmethanesulfonyl fluoride (PMSF) and bacitracin were purchased from Boehringer Mannheim Biochemicals. Bovine serum albumin (BSA) was purchased from Miles Inc., Diagnostics Division. [<sup>125</sup>I]ET-1 (2000 Ci/mmol) was purchased from New England Nuclear, DuPont and [<sup>3</sup>H]arachidonic acid (218 Ci/mmol) was purchased from Amersham.

The peptides were prepared on an ABI Model 430A or 431A peptide synthesizer using software version 1.40. For N<sup>ε</sup>-t-Boc syntheses, the HF cleavages were performed on an ImmunoDynamics Inc. Model 2A/2B HF Apparatus. High-pressure liquid chromatographs were obtained on a Waters HPLC system from Millipore Corp. equipped with a Model 600E system controller, a Model 600 solvent delivery system, a Model 490 variable wavelength detector operating at 214 and 280 nm, and a Bio-Rad Laboratories Model AS-100 autosampler. Vydac analytical and preparative C18 HPLC columns were purchased from The Nest Group. Preparative reversed-phase HPLC was performed using a C18 preparative scale Vydac column (218TP1022) (2.2 × 25.0 cm, 10–20 mM particle size) eluting with a linear gradient of 0.1% aqueous TFA with increasing concentrations of AcCN at 15 mL/min. Analytical

Journal of Medicinal Chemistry, 1997, Vol. 40, No. 14 2235

reversed-phase HPLC analysis was carried out on a Vydac column (218TP54) (0.46 × 25.0 cm, 5 mM particle size). The analytical HPLC system used was the same as that described in detail above for peptide purification. The mobile phase utilized for the analytical HPLC analysis was 80% A:20% B to 14% A:86% B [0.1% aqueous TFA (A):0.1% TFA in AcCN (B)]; linear gradient was over 22 min at 1.5 mL/min (λ = 214 and 280 nm) on a Vydac 218TP54 column.

Chemical ionization mass spectra (CIMS) were acquired with a Fisons VG Trio-2A quadrupole mass spectrometer using 1% ammonia in methane as the reagent gas. Fast atom bombardment mass spectra (FABMS) were measured with a VG analytical 7070E/HF mass spectrometer in either a thiolglycerol or 3-nitrobenzyl alcohol matrix using xenon as the target gas. Electrospray mass spectra (ESMS) were obtained on either a Finnigan TSQ70 or Fisons VG Trio 2000 quadrupole mass spectrometer using 50:50 water:methanol made 1% in acetic acid as the solvent. Routine <sup>1</sup>H-NMR spectra were measured with a Varian Gemini 2300 or Varian Unity 400 instrument using tetramethylsilane as an external standard in chloroform or dimethyl sulfoxide (CDCl<sub>3</sub> or DMSO-*d*<sub>6</sub>; Cambridge Isotope Laboratories).

[<sup>14</sup>C]PEG-4000 was purchased from New England Nuclear, DuPont (NEN). Reference compounds that were used to establish the correlation between fractions absorbed in humans and transport across CACO-2 cell monolayers were either obtained from Sigma Chemical Co., with the radiolabeled form of the compounds purchased from NEN (D-mannitol, hydrocortisone, phenytoin, and L-phenylalanine), or synthesized at Parke-Davis (gabapentin and cefdinir). Modified MES buffer was prepared from MES [2-(N-morpholino)ethanesulfonic acid], NaCl, and KCl (Sigma Chemical Co.). D-Glucose and human serum albumin were also purchased from Sigma. Anesthetics used included Ketaset (ketamine HCl injection, USP, 100 mg/mL; Aveco Co., Inc.), Rompun (xylazine, 20 mg/mL; Miles Inc.), and sodium pentobarbital (64.8 mg/mL; Anthony Products) for all animal surgery.

**General Strategy: 1. Peptide Synthesis.** All of the peptides were synthesized by solid-phase peptide synthetic techniques on an ABI Model 430A or 431A peptide synthesizer. The peptide analogues were prepared using an N<sup>ε</sup>-t-Boc protection scheme with N<sup>ε</sup>-t-Boc-Trp-PAM resin and the aspartic acid side chain carboxylate protected as the benzyl ester. Individual N<sup>ε</sup>-t-Boc amino acids were coupled via DCC in DMF. Deprotection of the N<sup>ε</sup>-t-Boc group was achieved with 50% TFA in DCM, and removal of the N<sup>ε</sup>-Fmoc group was accomplished with 20% piperidine in DCM. N-Terminal acetylation was carried out on the resin in DCM with an excess of 1-acetylimidazole (20-fold) or 10% acetic anhydride in DCM with a catalytic amount of DMAP. The resin was then washed in turn with DMF, MeOH, and DCM (2 × each) and dried under reduced pressure. The peptides were then deprotected and cleaved from the resin using anhydrous liquid HF:anisole (9:1). The resin was washed with anhydrous ethyl ether, and the crude peptide was extracted from the resin with AcCN: water (1:1) with 0.1% TFA, concentrated under reduced pressure, and lyophilized. (See ref 27 for the detailed solid-phase synthesis of compound 2, which is representative of all solid-phase syntheses in this report.)

**2. Peptide Purification.** Crude peptides were dissolved in a mixture of aqueous 0.1% TFA and AcCN (exact ratio depending on the solubility of the peptide) and then purified by preparative reversed-phase HPLC (see above). Peptide fractions determined to be pure by analytical HPLC were combined, concentrated under reduced pressure, and lyophilized.

**3. Peptide Homogeneity and Characterization.** Peptides were assessed for homogeneity by analytical reversed-phase analytical HPLC. The peptides were characterized by ESMS or FABMS and <sup>1</sup>H-NMR spectroscopy. All final peptidomimetic compounds (4–15) provided an <sup>1</sup>H-NMR spectrum that was consistent with the desired structure; however, due to the complexity of the resulting spectrum individual assignments are not provided.

**Preparation of Ac-Dip-Ψ[CH<sub>2</sub>NH]-Leu-Asp-Ile-Ile-Trp (4).** Preparation of N<sup>ε</sup>-t-Boc-Dip-N(CH<sub>3</sub>)OCH<sub>3</sub>. To

a solution of  $N^{\alpha}$ -*t*-Boc-Dip (3.0 g, 8.8 mmol) in DMF (20 mL) were added HCl·HN(CH<sub>3</sub>)OCH<sub>3</sub> (0.88 g, 8.8 mmol), and DIEA (3.0 mL, 17.2 mmol) followed by BOP reagent (3.9 g, 8.8 mmol). The reaction was allowed to continue for 2 h. The reaction mixture was then concentrated to dryness. The residue was taken up with ethyl acetate (EtOAc; 50 mL), washed with saturated aqueous Na<sub>2</sub>CO<sub>3</sub> (2 × 50 mL), water, and 1 M aqueous KHSO<sub>4</sub> (2 × 50 mL), dried over MgSO<sub>4</sub>, and concentrated under reduced pressure to yield a white foam (3.3 g, 88%); <sup>1</sup>H-NMR (CDCl<sub>3</sub>) δ 1.31 (s, 9H), 2.94 (s, 3H), 3.61 (s, 3H), 4.32 (d, 1H), 4.99 (d, 1H), 5.68 (t, 1H), 7.27 (m, 10H); CIMS ( $m/z$ )<sup>+</sup> calcd 384.2, found 385 (M + H).

**Preparation of  $N^{\alpha}$ -*t*-Boc-Dip-CHO.** To a solution of  $N^{\alpha}$ -*t*-Boc-Dip-N(CH<sub>3</sub>)OCH<sub>3</sub> (3.3 g, 8.5 mmol) in dry THF (50 mL) at 0 °C, was added, in portions, lithium aluminum hydride (0.43 g, 11.1 mmol). The reaction was allowed to continue for 30 min at 0 °C and was quenched by adding 1 M aqueous KHSO<sub>4</sub> (20 mL). The organic phase was separated and the aqueous phase extracted with EtOAc (50 mL). The combined organic layer was washed with brine, dried with MgSO<sub>4</sub>, and concentrated under reduced pressure to give a colorless oil which crystallized on standing at room temperature (2.75 g, 99%); <sup>1</sup>H-NMR (CDCl<sub>3</sub>) δ 1.39 (s, 9H), 4.50 (d, 1H), 4.88 (d, 1H), 5.07 (t, 1H), 7.28 (m, 10H), 9.61 (s, 1H); CIMS ( $m/z$ )<sup>+</sup> calcd 325.4, found 326 (M + H).

**Preparation of Ac-Dip-Ψ[CH<sub>2</sub>NH]-Leu-Asp-Ile-Ile-Trp (4).** The synthesis of  $N^{\alpha}$ -*t*-Boc-Leu-Asp-Ile-Ile-Trp-PAM resin was performed as described in the general procedure on a 1.0 mmol scale.  $N^{\alpha}$ -*t*-Boc-Leu-Asp-Ile-Ile-Trp-PAM resin was treated with 50% TFA in DCM (20 mL) for 30 min at room temperature and washed successively with DCM (3 × 20 mL), 10% DIEA in DCM (20 mL), DMF (3 × 20 mL), and 5% acetic acid in DMF (2 × 20 mL).  $N^{\alpha}$ -*t*-Boc-Dip-CHO (1.2 g, 3.0 mmol) was added followed by 1% acetic acid in DMF (20 mL) and 1 M NaBH<sub>3</sub>CN·THF (3.3 mL, 3.3 mmol). The mixture was shaken at room temperature for 3 h. The resin was then washed in turn with DMF, MeOH, and DCM (2 × 20 mL, each) and dried under reduced pressure. The peptide was deprotected and cleaved from the resin using anhydrous HF as described in the general procedure. The crude peptide was purified by reversed-phase HPLC to afford 230 mg of the title compound: HPLC  $t_R$  = 12.5 min (>99%); ESMS ( $m/z$ )<sup>+</sup> calcd 910.1, found 910.6 (M).

**Preparation of Ac-Dip-Leu-Ψ[CH<sub>2</sub>NH]-Asp-Ile-Ile-Trp (5).** **Preparation of  $N^{\alpha}$ -Benzoyloxycarbonyl(Cbz)-Leu-Ψ[CH<sub>2</sub>NH]-Asp(OBu<sup>t</sup>)-OBzl.**  $N^{\alpha}$ -Cbz-Leu-CHO was prepared in two steps from  $N^{\alpha}$ -Cbz-Leu as described for  $N^{\alpha}$ -*t*-Boc-Dip-CHO (30.8 g, 99%); <sup>1</sup>H-NMR (CDCl<sub>3</sub>) δ 0.95 (m, 6H), 1.74 (m, 3H), 4.38 (m, 1H), 5.12 (s, 2H), 5.38 (m, 1H), 7.34 (s, 5H), 9.60 (s, 1H); CIMS ( $m/z$ )<sup>+</sup> calcd 249.3, found 250 (M + H).

$N^{\alpha}$ -Cbz-Leu-CHO (14.5 g, 58 mmol) was dissolved in dry MeOH (500 mL) and treated with H-Asp(OBu<sup>t</sup>)-OBzl·HCl (16.2 g, 58.0 mmol) followed by NaBH<sub>3</sub>CN (3.77 g, 60.1 mmol) and acetic acid (HOAc; 4.0 mL, 66.5 mmol). The reaction was allowed to continue overnight and concentrated under reduced pressure to dryness. The residue was taken up with EtOAc (200 mL); the organic layer was washed with saturated NaHCO<sub>3</sub> and brine, dried with MgSO<sub>4</sub>, and concentrated under reduced pressure to an oil (15.1 g, 52%); <sup>1</sup>H-NMR (CDCl<sub>3</sub>) δ 0.89 (m, 6H), 1.28 (m, 1H), 1.40 (s, 9H), 1.52–2.51 (m, 4H), 2.75 (m, 4H), 3.75 (m, 2H), 5.08 (s, 2H), 5.17 (s, 2H), 7.32 (m, 10H); CIMS ( $m/z$ )<sup>+</sup> calcd 512.3, found 513 (M + H).

**Preparation of  $N^{\alpha}$ -Fmoc-Leu-Ψ[CH<sub>2</sub>NH]-Asp(OBu<sup>t</sup>).**  $N^{\alpha}$ -Cbz-Leu-Ψ[CH<sub>2</sub>NH]-Asp(OBu<sup>t</sup>)-OBzl was dissolved in MeOH (200 mL), treated with 20% Pd/C (2.0 g), and placed under a hydrogen atmosphere at 50 psi (2 h, room temperature). The reaction mixture was filtered through a Celite pad, and solvent was evaporated under reduced pressure to provide a white solid (6.0 g, 71%) which was suspended in a mixture of *p*-dioxane:water (1:1, 200 mL). The solution was treated with triethylamine (7.35 mL, 52.8 mmol) followed by 9-fluorenylmethoxycarbonyl-*N*-hydroxysuccinimide (Fmoc-OSu, 7.0 g, 20 mmol). The solution was stirred at room temperature overnight and treated with 1 M aqueous KHSO<sub>4</sub> (52.0 mL), and the precipitate was collected by filtration (6.4 g, 55% yield); <sup>1</sup>H-NMR (DMSO-*d*<sub>6</sub>) δ 0.82 (m, 6H), 1.18 (m, 1H), 1.40

(s, 9H), 1.48 (m, 4H), 2.95 (m, 5H), 3.88 (m, 1H), 4.22 (m, 3H), 4.54 (m, 1H), 7.32 (m, 2H), 7.63 (m, 2H), 7.88 (m, 2H); FABMS ( $m/z$ )<sup>+</sup> calcd 510.2, found 511 (M + H).

**Preparation of Ac-Dip-Leu-Ψ[CH<sub>2</sub>NH]-Asp-Ile-Ile-Trp (5).** The peptide synthesis, cleavage from the resin, and deprotection were performed as described in the general procedure. The crude peptide was purified by reversed-phase HPLC to afford 33 mg of the title compound: HPLC  $t_R$  = 14.6 min (>96%); ESMS ( $m/z$ )<sup>+</sup> calcd 910.1, found 910.4 (M).

**Preparation of Ac-Dip-Leu-Asp-Ψ[CH<sub>2</sub>NH]-Ile-Ile-Trp (6).** **Preparation of  $N^{\alpha}$ -*t*-Boc-Asp(OBzl)-CH<sub>2</sub>OH.** To a solution of  $N^{\alpha}$ -*t*-Boc-Asp(OBzl) (6.3 g, 20 mmol) in dry THF (20 mL) at 0 °C under N<sub>2</sub> was added 1 M BH<sub>3</sub>·THF (40 mL, 40 mmol) dropwise over a period of 2 h. The solution was stirred for an additional 2 h at 0 °C, and 20 mL of HOAc was added. The reaction mixture was evaporated under reduced pressure, dissolved in EtOAc (100 mL), washed with 10% aqueous NaHCO<sub>3</sub>, water, 1 N HCl, and brine (2 × 50 mL, each), dried with MgSO<sub>4</sub>, filtered, and concentrated under reduced pressure to an oil (5.5 g, 90%); <sup>1</sup>H-NMR (CDCl<sub>3</sub>) δ 1.45 (s, 9H), 2.15 (d, 2H), 2.20 (br, 1H), 3.65 (d, 2H), 4.01 (m, 1H), 5.12 (s, 2H), 5.33 (d, 1H), 7.45 (m, 5H); CIMS ( $m/z$ )<sup>+</sup> calcd 309.4, found 310 (M), 210 (M – Boc).

**Preparation of  $N^{\alpha}$ -*t*-Boc-Asp(OBzl)-CHO.** To a solution of  $N^{\alpha}$ -*t*-Boc-Asp(OBzl)-CH<sub>2</sub>OH (2.0 g, 9.7 mmol) in DCM was added pyridinium dichromate (5.7 g, 15.0 mmol). The solution was allowed to stir at room temperature overnight. The reaction mixture was filtered through a Celite pad, and the filtrate was evaporated to dryness under reduced pressure to an oil (1.5 g, 75%). This oil was used without further purification.

**Preparation of Ac-Dip-Leu-Asp-Ψ[CH<sub>2</sub>NH]-Ile-Ile-Trp (6).** The peptide synthesis, cleavage from the resin, and deprotection were performed as described in the general procedure. The crude peptide was purified by reversed-phase HPLC to afford 43 mg of the title compound: HPLC  $t_R$  = 15.9 min (>97%); ESMS ( $m/z$ )<sup>+</sup> calcd 910.1, found 910.5 (M).

**Preparation of Ac-Dip-Leu-Asp-Ile-Ψ[CH<sub>2</sub>NH]-Ile-Trp (7).** **Preparation of  $N^{\alpha}$ -Cbz-Ile-Ψ[CH<sub>2</sub>NH]-Ile-OMe.**  $N^{\alpha}$ -Cbz-Ile-CHO was prepared in two steps from  $N^{\alpha}$ -Cbz-Ile as described for  $N^{\alpha}$ -*t*-Boc-Dip-CHO (8.3 g, 64%).  $N^{\alpha}$ -Cbz-Ile-CHO was dissolved in dry MeOH (250 mL) and treated with Ile-OMe·HCl (4.8 g, 33.4 mmol) followed by NaBH<sub>3</sub>CN (2.8 g, 44.3 mmol) and acetic acid (2.0 mL, 33.3 mmol). The reaction mixture was allowed to stir overnight and concentrated under reduced pressure to dryness. The residue was dissolved in EtOAc (100 mL), washed with saturated aqueous NaHCO<sub>3</sub> and brine (2 × 50 mL, each), dried with Na<sub>2</sub>SO<sub>4</sub>, filtered, and concentrated under reduced pressure to an oil which crystallized upon standing (9.35 g, 74%); <sup>1</sup>H-NMR (CDCl<sub>3</sub>) δ 0.88 (m, 12H), 1.45 (m, 7H), 2.42 (m, 1H), 2.78 (m, 1H), 3.02 (d, 1H), 3.59 (m, 1H), 3.69 (s, 3H), 4.88 (m, 1H), 5.10 (s, 2H), 7.35 (s, 5H); CIMS ( $m/z$ )<sup>+</sup> calcd 378.4, found 379 (M + H).

**Preparation of  $N^{\alpha}$ -Cbz-Ile-Ψ[CH<sub>2</sub>NH]-Ile.** To a solution of  $N^{\alpha}$ -Cbz-Ile-Ψ[CH<sub>2</sub>NH]-Ile-OMe (4.35 g, 11.5 mmol) in *p*-dioxane (45 mL) was added 1 M aqueous LiOH (12.5 mL, 12.5 mmol). The reaction mixture was stirred at room temperature for 4 days. The solvent was removed under reduced pressure, and the residue was dissolved in water (10 mL). The resulting solution was treated with 2 N HCl (23 mL). The precipitate which formed was collected and dried (3.1 g, 74%); <sup>1</sup>H-NMR (DMSO-*d*<sub>6</sub>) δ 1.35 (m, 6H), 2.52 (m, 1H), 2.78 (m, 1H), 2.99 (d, 2H), 5.02 (s, 1H), 7.22 (d, 1H), 7.35 (s, 5H); CIMS ( $m/z$ )<sup>+</sup> calcd 364.4, found 365 (M + H).

**Preparation of  $N^{\alpha}$ -Fmoc-Ile-Ψ[CH<sub>2</sub>NH]-Ile.**  $N^{\alpha}$ -Cbz-Ile-Ψ[CH<sub>2</sub>NH]-Ile was dissolved in MeOH (50 mL) and hydrogenated in the presence of 20% Pd/C (0.30 g) for 2 h. The reaction mixture was filtered, and the solvent was concentrated under reduced pressure to a white powder (1.8 g) which was suspended in a mixture of water:*p*-dioxane (1:1, 70 mL). The solution was treated with triethylamine (2.7 mL, 19.5 mmol) followed by Fmoc-OSu (2.6 g, 7.7 mmol). The reaction mixture was stirred at room temperature overnight, and treated with an aqueous solution of KHSO<sub>4</sub> (2.7 g, 19.5 mmol in 100 mL). The precipitate was collected, triturated with

Design of a Combined ET<sub>A</sub>/ET<sub>B</sub> Receptor Antagonist

EtOAc:hexane (1:4), and dried under reduced pressure to a white solid (2.0 g, 51%); CIMS ( $m/z$ )<sup>+</sup> calcd 452.1, found 453 (M + H).

**Preparation of Ac-Dip-Leu-Asp-Ile-Ψ[CH<sub>2</sub>NH]-Ile-Trp (7).** The peptide synthesis, cleavage from the resin, and deprotection were performed as described in the general procedure. The crude peptide was purified by reversed-phase HPLC to afford 190 mg of the title compound: HPLC  $t_R$  = 14.5 min (>98%); FABMS ( $m/z$ )<sup>+</sup> calcd 910.1, found 910.7 (M).

**Preparation of Ac-Dip-Leu-Asp-Ile-Ile-Ψ[CH<sub>2</sub>NH]-Trp (8).** **Preparation of N<sup>ε</sup>-t-Boc-Ile-N(CH<sub>3</sub>)OCH<sub>3</sub>.** To a solution of N<sup>ε</sup>-t-Boc-Ile (10 g, 43.2 mmol) in DMF (20 mL) were added HCl·HN(CH<sub>3</sub>)OCH<sub>3</sub> (4.4 g, 45.1 mmol) and DIEA (15.7 mL, 90.1 mmol) followed by BOP reagent (9.1 g, 43.2 mmol). The reaction mixture was stirred for 2 h. The reaction mixture was then concentrated under reduced pressure to dryness. The residue was taken up with EtOAc (100 mL), washed with saturated aqueous Na<sub>2</sub>CO<sub>3</sub>, water, and 1 M aqueous KHSO<sub>4</sub> (2 × 50 mL, each), dried with MgSO<sub>4</sub>, and concentrated under reduced pressure to give a pale yellow oil (10.1 g, 91%): <sup>1</sup>H-NMR (CDCl<sub>3</sub>) δ 0.95 (m, 6H), 1.38 (s, 9H), 1.50 (m, 2H), 1.74 (m, 1H), 3.21 (s, 3H), 3.80 (s, 3H), 4.80 (m, 1H), 5.33 (d, 1H); CIMS ( $m/z$ )<sup>+</sup> calcd 274.1, found 274 (M).

**Preparation of N<sup>ε</sup>-t-Boc-Ile-CHO.** To a solution of N<sup>ε</sup>-t-Boc-Ile-N(CH<sub>3</sub>)OCH<sub>3</sub> (10.0 g, 38.9 mmol) in dry THF (200 mL) at 0 °C was added, in portions, lithium aluminum hydride (1.7 g, 44.8 mmol). The reaction was stirred for 30 min at 0 °C and quenched by the addition of 1 M aqueous KHSO<sub>4</sub> (100 mL). The organic phase was separated and the aqueous phase extracted with EtOAc (100 mL). The combined organic phases was washed with brine (1 × 50 mL), dried with MgSO<sub>4</sub>, filtered, and concentrated under reduced pressure to a colorless oil (6.6 g 87%): <sup>1</sup>H-NMR (CDCl<sub>3</sub>) δ 0.96 (m, 6H), 1.36 (s, 9H), 1.38–1.84 (m, 3H), 4.38 (m, 1H), 5.38 (d, 1H), 9.60 (s, 1H); CIMS ( $m/z$ )<sup>+</sup> calcd 215.3, found 216 (M + H).

**Preparation of N<sup>ε</sup>-t-Boc-Ile-Ψ[CH<sub>2</sub>NH]-Trp-PAM-Resin.** N<sup>ε</sup>-t-Boc-Trp-PAM resin (1.0 mmol total) was treated with 50% TFA in DCM (20 mL) for 30 min at room temperature; the resin was washed successively with DCM (3 × 20 mL), 10% DIEA in DCM (20 mL), DMF (3 × 20 mL), and 5% HOAc in DMF (2 × 20 mL). N<sup>ε</sup>-t-Boc-Ile-CHO (2.5 mmol) was added followed by 1% acetic acid in DMF (20 mL) and NaBH<sub>3</sub>CN (2.5 mmol). The mixture was shaken at room temperature for 3 h. The resin was washed with DMF, MeOH, and DCM (3 × 20 mL, each) and dried under reduced pressure.

**Preparation of Ac-Dip-Leu-Asp-Ile-Ile-Ψ[CH<sub>2</sub>NH]-Trp (8).** The peptide synthesis, cleavage from the resin, and deprotection were performed as described in the general procedure. The crude peptide was purified by reversed-phase HPLC to afford 30 mg of the title compound: HPLC  $t_R$  = 14.5 min (>98%); FABMS ( $m/z$ )<sup>+</sup> calcd 910.1, found 910.7 (M).

**Preparation of Ac-[NMe]Dip-Leu-Asp-Ile-Ile-Trp (9).** **Preparation of N<sup>ε</sup>-4,4'-Dimethoxyphenylmethyl(Dod)-Dip-Leu-Asp(OBzl)-Ile-Ile-Trp-PAM Resin.** N<sup>ε</sup>-t-Boc-Dip-Leu-Asp(OBzl)-Ile-Ile-Trp-PAM resin (0.5 mmol) was prepared as described in the general procedure. N<sup>ε</sup>-t-Boc-Dip-Leu-Asp(OBzl)-Ile-Ile-Trp-PAM resin (0.5 mmol) was treated with 50% TFA/DCM for 30 min in a manual shaker and washed with DCM (3 × 20 mL), 10% DIEA/DCM (20 mL), and DCM (2 × 20 mL). Dod-Cl (0.20 g, 0.76 mmol) in DCM (20 mL) was added followed by DIEA (0.5 mL). The reaction was allowed to proceed for 1 h. The resin was drained washed with DCM and DMF (3 × 20 mL, each), and dried under reduced pressure.

**Preparation of H-[NMe]Dip-Leu-Asp(OBzl)-Ile-Ile-Trp-PAM Resin.** The formaldehyde in DMF solution was prepared as follows: To a 38% aqueous formaldehyde solution (20 mL) was added to DMF (180 mL) followed by MgSO<sub>4</sub> (50 g). The solution was stirred for 1 h under N<sub>2</sub> and filtered. The filtrate (20 mL) was added to N<sup>ε</sup>-Dod-Dip-Leu-Asp(OBzl)-Ile-Ile-Trp-PAM resin followed by HOAc (0.30 mL) and 1 M NaBH<sub>3</sub>CN in DMF (1.25 mL, 1.25 mmol). The mixture was shaken for 30 min and the procedure repeated. The resin was then treated with 50%TFA/DCM (2 × 20 mL, 20 min each), washed in turn with DCM, 10% DIEA/DCM, and DMF (3 × 20 mL, each), and dried under reduced pressure.

Journal of Medicinal Chemistry, 1997, Vol. 40, No. 14 2237

**Preparation of Ac-[NMe]Dip-Leu-Asp-Ile-Ile-Trp (9).** H-[NMe]Dip-Leu-Asp(OBzl)-Ile-Ile-Trp was cleaved from the resin and deprotected using anhydrous HF:anisole (9:1, 0 °C, 60 min). The crude peptide was purified by reversed-phase HPLC and lyophilized. The purified peptide was dissolved in 90% HOAc (20 mL) and treated with acetic anhydride (2 mL) for 2 h. Evaporation followed by lyophilization afforded 40 mg of the title compound: HPLC  $t_R$  = 18.5 min (97%); ESMS ( $m/z$ )<sup>+</sup> calcd 938.1, found 937.6 (M).

**Preparation of Ac-Dip-[NMe]Leu-Asp-Ile-Ile-Trp (10).** The peptide synthesis, cleavage from the resin, and deprotection were performed as described in the general procedure. N<sup>ε</sup>-t-Boc-[NMe]Leu was obtained from commercial sources. The crude peptide was purified by reversed-phase HPLC to afford 18.0 mg of the title compound: HPLC  $t_R$  = 17.5 min (>98%); ESMS ( $m/z$ )<sup>+</sup> calcd 938.1, found 939.1 (M + H).

**Preparation of Ac-Dip-Leu-[NMe]Asp-Ile-Ile-Trp (11).** **Preparation of N<sup>ε</sup>-Fmoc-[NMe]Asp(OBzl).** To a suspension of N<sup>ε</sup>-Fmoc-Asp(OBzl) (3.0 g, 9.3 mmol) and paraformaldehyde (2.0 g) in toluene (100 mL) was added *p*-toluenesulfonic acid (0.2 g). The mixture was refluxed with azeotropic water removal for 30 min. The reaction mixture was then cooled to room temperature, washed with saturated aqueous NaHCO<sub>3</sub> and brine (2 × 50 mL, each), dried with MgSO<sub>4</sub>, filtered, and concentrated under reduced pressure (oil, 2.8 g) which was then treated with a mixture of CHCl<sub>3</sub> (50 mL), TFA (40 mL), and Et<sub>3</sub>SiH (4.3 mL, 27.0 mmol) at room temperature for 40 h. The reaction mixture was evaporated under reduced pressure to dryness. The residue was dissolved in EtOAc (50 mL), washed with saturated aqueous NaHCO<sub>3</sub>, water, 1 N HCl, and brine (2 × 50 mL, each), filtered, dried with MgSO<sub>4</sub>, and concentrated under reduced pressure to a foam. Crystallization from EtOAc/hexane yielded a white powder (2.5 g, 80%): <sup>1</sup>H-NMR (CDCl<sub>3</sub>) δ 2.85 (m, 1H), 2.90 (s, 3H), 3.11 (m, 2H), 4.25 (m, 2H), 5.12 (m, 2H), 7.25 (m, 7H), 7.55 (m, 3H), 7.78 (m, 3H) [In the <sup>1</sup>H-NMR of this compound a doubling of the resonances was observed, presumably due to rotational isomerization about the urethane bond. In this case the chemical shift of the major isomer is reported (probably the *trans* conformer), but the total integration of both resonances is reported.] FABMS ( $m/z$ )<sup>+</sup> calcd 459.5, found 459.1 (M).

**Preparation of Ac-Dip-Leu-[NMe]Asp-Ile-Ile-Trp (11).** The peptide synthesis, cleavage from the resin, and deprotection were performed as described in the general procedure. The crude peptide was purified by reversed-phase HPLC to afford 25.8 mg of the title compound: HPLC  $t_R$  = 15.0 min (>99%); ESMS ( $m/z$ )<sup>+</sup> calcd 938.1, found 939.4 (M + H), 960.1 (M + Na).

**Preparation of Ac-Dip-Leu-Asp-[NMe]Ile-Ile-Trp (12).** The peptide synthesis, cleavage from the resin, and deprotection were performed as described in the general procedure. N<sup>ε</sup>-t-Boc-[NMe]Ile was obtained from commercial sources. The crude peptide was purified by reversed-phase HPLC to afford 58.5 mg of the title compound: HPLC  $t_R$  = 18.5 min (97%); ESMS ( $m/z$ )<sup>+</sup> calcd 938.1, found 938.1 (M), 960.7 (M + Na).

**Preparation of Ac-Dip-Leu-Asp-Ile-[NMe]Ile-Trp (13).** **Preparation of N<sup>ε</sup>-Fmoc-Ile-COCl.** To a suspension of N<sup>ε</sup>-Fmoc-Ile (10.0 g, 28.3 mmol) in DCM (100 mL) was added oxalyl chloride (2.9 mL, 33.0 mmol) dropwise at 0 °C. The reaction mixture was stirred for 1 h at 0 °C and warmed to room temperature. The reaction mixture was stirred at room temperature for an additional 2 h and evaporated under reduced pressure to an oil (8.5 g, 81%): <sup>1</sup>H-NMR (CDCl<sub>3</sub>) δ 0.85 (t, 3H), 1.05 (d, 3H), 1.18 (m, 1H), 1.45 (m, 1H), 2.12 (m, 2H), 4.25 (t, 1H), 4.50 (m, 2H), 5.25 (d, 1H), 7.25 (t, 2H), 7.38 (t, 2H), 7.55 (m, 2H), 7.74 (d, 2H) [In the <sup>1</sup>H-NMR for this compound a doubling of the resonances was observed, presumably due to rotational isomerization about the urethane bond. In this case the chemical shift of the major isomer is reported (probably the *trans* conformer), but the total integration of both resonances is reported.] CIMS ( $m/z$ )<sup>+</sup> calcd 370.2, found 369 (M + H).

**Preparation of N<sup>ε</sup>-Fmoc-Ile-[NMe]Ile-Trp-PAM Resin.** N<sup>ε</sup>-t-Boc-[NMe]Ile-Trp-PAM resin (0.5 mmol) was prepared as described in the general procedure. N<sup>ε</sup>-t-Boc-[NMe]Ile was obtained from commercial sources. N<sup>ε</sup>-t-Boc-[NMe]Ile-Trp-

PAM resin was treated with 50% TFA/DCM (20 mL) for 30 min and washed with DCM (3 × 20 mL), 10% DIEA/DCM (20 mL), and DCM (3 × 20 mL). *N*<sup>α</sup>-Fmoc-Ile-COCl (0.6 g, 1.6 mmol) in DCM (20 mL) was added followed by DIEA (2.7 mL, 1.55 mmol). The reaction mixture was shaken for 2 h, and the procedure was repeated. The peptide resin was then washed with DCM (3 × 20 mL) and dried under reduced pressure.

**Preparation of Ac-*α*Dip-Leu-Asp-Ile-[NMe]Ile-Trp (13).** The peptide synthesis, cleavage from the resin, and deprotection were performed as described in the general procedure. The crude peptide was purified by reversed-phase HPLC to afford 70.1 mg of the title compound: HPLC  $t_R$  = 17.3 min (98%); ESMS ( $m/z$ )<sup>+</sup> calcd 938.1, found 939.1 (M + H).

**Preparation of Ac-*α*Dip-Leu-Asp-Ile-Ile-[NMe]Trp (14).**  
**Preparation of *N*<sup>α</sup>-Dod-Trp-PAM Resin.** *N*<sup>α</sup>-*t*-Boc-Trp-PAM resin (0.5 mmol) was treated with 50% TFA/DCM for 30 min in a manual shaker and washed with DCM (3 × 20 mL), 10% DIEA/DCM (20 mL), and DCM (2 × 20 mL). Dod-Cl (0.20 g, 0.76 mmol) in DCM (20 mL) was added followed by DIEA (0.5 mL). The reaction was allowed to proceed for 1 h. The resin was drained, washed with DCM and DMF (3 × 20 mL, each), and dried under reduced pressure.

**Preparation of H-[NMe]Trp-PAM Resin.** The formaldehyde in DMF solution was prepared as follows: To a 38% aqueous formaldehyde solution (20 mL) was added DMF (180 mL) followed by MgSO<sub>4</sub> (50 g). The solution was stirred for 1 h and filtered. The filtrate (20 mL) was added to *N*<sup>α</sup>-Dod-Trp-PAM resin followed by HOAc (0.30 mL) and 1 M NaBH<sub>3</sub>CN in DMF (1.25 mL, 1.25 mmol). The mixture was shaken for 30 min and the procedure repeated. The resin was then treated with 50% TFA/DCM (2 × 20 mL, 20 min each), washed in turn with DCM, 10% DIEA/DCM, and DMF (3 × 20 mL, each), and dried under reduced pressure.

**Preparation of Ac-*α*Dip-Leu-Asp-Ile-Ile-[NMe]Trp (14).** The peptide synthesis was performed as described in the general procedure. After the coupling of *N*<sup>α</sup>-*t*-Boc-*α*Dip, the peptide resin was treated with 50% TFA/DCM (30 min), and the peptide was deprotected and cleaved from the resin using anhydrous HF/anisole (9:1, 0 °C, 60 min). The crude peptide was purified by reversed-phase HPLC and lyophilized. The purified peptide was dissolved in 90% acetic acid (20 mL) and treated with acetic anhydride (2 mL) for 2 h. Evaporation followed by lyophilization afforded 40 mg of the title compound: HPLC  $t_R$  = 16.7 min (97%); ESMS ( $m/z$ )<sup>+</sup> calcd 938.1, found 937.6 (M).

**Preparation of Ac-*α*Bhg-Leu-Asp-Ile-[NMe]Ile-Trp (15).** The peptide synthesis, cleavage from the resin, and deprotection were performed as described for Ac-*α*Dip-Leu-Asp-Ile-[NMe]Ile-Trp (compound 13). The crude peptide was purified by reversed-phase HPLC to afford 530 mg of the title compound: HPLC  $t_R$  = 18.0 min (>97%); ESMS ( $m/z$ )<sup>+</sup> calcd 964.1, found 963.4 (M).

**Endothelin Receptor Binding Assay Protocol.** The receptor binding assay protocols using rabbit renal vascular smooth muscle cells (ET<sub>A</sub>), rat cerebellar membranes (ET<sub>B</sub>), or the corresponding cloned human ET<sub>A</sub> and ET<sub>B</sub> receptors have been previously described.<sup>29</sup>

**In Vitro Contractility Studies.** The experimental protocols using vascular rings of rat femoral artery (ET<sub>A</sub>) or rabbit pulmonary artery (ET<sub>B</sub>) have been previously described.<sup>29</sup>

**Caco-2 Cell Transport and Stability in Rat Intestinal Perfusate Experiments.** These studies were performed as previously described.<sup>34</sup>

**Conscious Rat Duration of Action Study with PD 156252.** Nonfasted rats (350–500 g) were anesthetized with methoxyflurane by inhalation and instrumented with a jugular cannula (PE50) for iv administration of test agents and with a carotid artery cannula (PE50) for arterial blood pressure measurements. Rats were attached to a swivel for freedom of movement, and food and water were available ad libitum. Prior to the experiment, the animals were allowed to recover from the anesthesia for 60 min. Following recovery the rats were ganglionically blocked with mecamylamine-HCl (1.25 mg/kg, iv) 20 min prior to the ET-1 challenge (0.30 nM/kg, iv,

bolus). Compound 15 was administered at a dose of 10 mg/kg (iv, bolus) 5 and 30 min prior to the ET-1 challenge.

**Nuclear Magnetic Resonance Studies.** <sup>1</sup>H-NMR spectra were recorded on a Bruker AMX 500 spectrometer using samples typically 5–10 mM dissolved in deuterated solvents obtained from Cambridge Isotope Laboratories. Two-dimensional total correlation spectroscopy (TOCSY),<sup>64</sup> double-quantum-filtered correlation spectroscopy (dqf-COSY),<sup>65</sup> rotating frame nuclear Overhauser spectroscopy (ROESY),<sup>66,67</sup> and nuclear Overhauser spectroscopy (NOESY)<sup>68</sup> were acquired as 1024 × 512 matrices and were processed using UXNMR (Bruker Instruments). Quadrature detection in the  $t_1$  dimension was achieved by the time proportional phase incrementation (TPPI)<sup>69</sup> method in 2D spectra. Prior to zero-filling to 1K in the second dimension and Fourier transformation, cos<sup>2</sup> weighting functions were applied to the time domain data in both dimensions. Finally, the baselines in the 2D time domain matrices were flattened using a polynomial fitting routine. NOE data were converted to distance constraints as previously described.<sup>70</sup> NOESY cross-peaks for which volume buildup curves (80–400 ms) suggested contributions from spin diffusion were excluded from the analysis. Coupling constants were measured directly from resolution-enhanced 1D spectra and were used as converted to dihedral constraints where warranted. Amide temperature coefficients were measured relative to an internal reference [3-(trimethylsilyl)propionic acid-*d*<sub>4</sub> sodium salt (TSP) for aqueous samples, the residual solvent resonance in organic solvents] for at least three different temperatures. Structures were generated using the distance geometry/simulated annealing program DGII (Biosym Technologies) followed by constrained energy minimization using a previously described protocol.<sup>70</sup>

Secondary shifts were calculated by subtracting the random coil chemical shift from the observed chemical shift, and all observed chemical shifts were referenced directly or indirectly to TSP protons at 0.0 ppm.<sup>71</sup> Carbon-13 random coil chemical shifts for natural amino acids were obtained from the appropriate literature references for peptides dissolved in D<sub>2</sub>O<sup>71</sup> and DMSO.<sup>72</sup> To correct the DMSO solution random coil chemical shifts for referencing relative to TSP protons, 3.34 ppm was added to the reported values. For unnatural residues, random coil shifts were measured in the peptides Gly-Gly-Xxx-Gly-Gly, where Xxx = *α*Bhg and [NMe]Ile as previously described.<sup>71</sup> The random coil chemical shifts used to calculate secondary shifts are provided in the Supporting Information. For the disodium salt peptides, 1.5 ppm was added to the random coil chemical shift of the  $\alpha$  carbon of Asp<sup>18</sup> to compensate for differences in ionization state from the literature values. This correction factor was derived from the reported shifts for Asp carbons in the neutral and anionic forms of Asp-containing peptides in D<sub>2</sub>O.<sup>72</sup> For Ile<sup>19</sup> in compound 15, 2.4 ppm was subtracted from the random coil chemical shift of the Ile  $\alpha$  carbon to compensate for its attachment to a tertiary amide group.<sup>63</sup> This correction factor was derived from the reported shifts for Ile in the peptides Gly-Gly-Ile-Ala-Gly-Gly and Gly-Gly-Ile-Pro-Gly-Gly.<sup>72</sup>

**Acknowledgment.** The authors would like to thank Dana DeJohn Joseph Loo, Tracy Stevenson, and Brian Tobias for analytical and spectral data; Michael Flynn and Kathleen Welch for pharmacological data; Vlad Beylin, Huaigu Chen, and Om Goel for the preparation of *α*Dip and *α*Bhg; and James Kaltenbronn and Bill Reisdorph for the preparation of protected intermediates.

**Supporting Information Available:** Tables containing selected <sup>1</sup>H-NMR data for compounds 3 and 15 and the random coil chemical shifts used to calculate secondary shifts and figures illustrating the secondary <sup>13</sup>C/<sup>1</sup>H chemical shifts of compounds 3 and 15 and the titration of compound 15 (7 pages). Ordering information is given on any current masthead page.

Design of a Combined ET<sub>A</sub>/ET<sub>B</sub> Receptor Antagonist

## References

- (1) Hickey, K. A.; Rubanyi, G.; Paul, R. J.; Highsmith, R. F. Characterization of a coronary vasoconstrictor produced by endothelial cells in culture. *Am. J. Physiol.* **1985**, *248*, C550–C556.
- (2) Yanagisawa, M.; Kurihara, H.; Kimura, S.; Tomobe, Y.; Kobayashi, M.; Mitsui, Y.; Goto, K.; Masaki, T. A novel potent vasoconstrictor peptide produced by vascular endothelial cells. *Nature (London)* **1988**, *332*, 411–415.
- (3) Yanagisawa, M.; Inoue, A.; Ishikawa, T.; Kasuya, T.; Kimura, S.; Kumagaye, S.; Nakajima, K.; Watanabe, T. X.; Sakabibara, S.; Goto, K.; Masaki, T. Primary structure, synthesis, and biological activity of rat endothelin, an endothelium-derived vasoconstrictor peptide. *Proc. Natl. Acad. Sci. U.S.A.* **1989**, *86*, 6964–6967.
- (4) Inoue, A.; Yanagisawa, M.; Kimura, S.; Kasuya, Y.; Miyauchi, T.; Goto, K.; Masaki, T. The human endothelin family: Three structurally and pharmacologically distinct isopeptides predicted by three separate genes. *Proc. Natl. Acad. Sci. U.S.A.* **1989**, *86*, 2863–2867.
- (5) Salda, K.; Mitsui, Y.; Ishida, N. A novel peptide, vasoactive intestinal contractor, of a new (endothelin) peptide family. Molecular cloning, expression and biological activity. *J. Biol. Chem.* **1989**, *264*, 14613–14616.
- (6) Kloog, T.; Ambar, I.; Sokolovsky, M.; Kochva, E.; Wolberg, Z.; Bdelah, A. Sarafotoxin, a novel vasoconstrictor peptide: Phosphoinositide hydrolysis in rat heart and brain. *Science* **1988**, *242*, 268–270.
- (7) Bdelah, A.; Wolberg, Z.; Fleminger, G.; Kochva, E. SRTX-d, a new native peptide of the endothelin/sarafotoxin family. *FEBS Lett.* **1989**, *251*, 1–3.
- (8) Becker, A.; Dowdle, E. B.; Hechler, U.; Kauser, K.; Donner, P.; Schleuning, W. D. Bibrotoxin, a novel member of the endothelin/sarafotoxin peptide family, from the venom of the burrowing asp. *Atractaspis bibroni*. *FEBS Lett.* **1993**, *315*, 100–103.
- (9) Doherty, A. M. Endothelin: A new challenge. *J. Med. Chem.* **1992**, *35*, 1493–1508.
- (10) Huggins, J. P.; Pelton, J. T.; Miller, R. C. The structure and specificity of endothelin receptors: Their importance in physiology and medicine. *Pharmacol. Ther.* **1993**, *59*, 55–123.
- (11) Cheng, X. M.; Nikam, S. S.; Doherty, A. M. Development of agents to modulate the effects of endothelin. *Cur. Med. Chem.* **1995**, *1*, 271–312.
- (12) Cody, W. L.; Doherty, A. M. Development of agents to modulate the effects of endothelin. *Biopolymers (Pept. Sci.)* **1995**, *37*, 89–104.
- (13) Arai, H.; Hori, T.; Aramori, I.; Ohkubo, H.; Nakanishi, S. Cloning and expression of a cDNA encoding an endothelin receptor. *Nature (London)* **1990**, *348*, 730–732.
- (14) Sakurai, T.; Yanagisawa, M.; Takawa, Y.; Miyazaki, H.; Kimura, S.; Goto, K.; Masaki, T. Cloning of a cDNA encoding a nonisopeptide-selective subtype of the endothelin receptor. *Nature (London)* **1990**, *348*, 732–735.
- (15) Sakamoto, A.; Yanagisawa, M.; Sakurai, T.; Takawa, Y.; Yanagisawa, H.; Masaki, T. Cloning and functional expression of human cDNA for ET<sub>B</sub> endothelin receptor. *Biochem. Biophys. Res. Commun.* **1991**, *178*, 656–663.
- (16) Hosoda, K.; Nakao, K.; Arai, H.; Suga, S.; Ogawa, Y.; Mukoyama, M.; Shirakami, G.; Saito, T.; Nakanishi, S.; Imura, H. Cloning and expression of human endothelin-1 receptor cDNA. *FEBS Lett.* **1991**, *287*, 23–26.
- (17) Williams, D. L.; Jones, K. L.; Pettibone, D. L.; Lis, E. V.; Clineschmidt, B. V. Sarafotoxin S6c: An agonist which distinguishes between endothelin receptor subtypes. *Biochem. Biophys. Res. Commun.* **1991**, *175*, 556–561.
- (18) Takayanagi, R.; Kitazumi, K.; Takasaki, C.; Ohnaka, K.; Aimoto, S.; Tasaka, K.; Ohashi, M.; Nawata, H. Presence of non-selective type of endothelin receptor on vascular endothelium and its linkage to vasodilation. *FEBS Lett.* **1991**, *282*, 103–106.
- (19) Saeki, T.; Ihara, M.; Fukuroda, T.; Yamagiwa, M.; Yano, M. [Ala<sup>1,3,11,15</sup>]Endothelin-1 analogs with ET<sub>B</sub> agonist activity. *Biochem. Biophys. Res. Commun.* **1991**, *179*, 286–292.
- (20) Panek, R. L.; Major, T. C.; Hingorani, G. P.; Doherty, A. M.; Taylor, D. G.; Rapundalo, S. T. Endothelin and structurally related analogs distinguish between receptor subtypes. *Biochem. Biophys. Res. Commun.* **1992**, *183*, 566–571.
- (21) Sudjarwo, S. A.; Hori, M.; Takai, M.; Urade, Y.; Okada, T.; Karaki, H. A novel type of endothelin B receptor mediating contraction in swine pulmonary vein. *Life Sci.* **1993**, *53*, 431–437.
- (22) Warner, T. D.; Allcock, G. H.; Corder, R.; Vane, J. R. Use of the endothelin antagonists BQ-123 and PD 142893 to reveal three endothelin receptors mediating smooth muscle contraction and the release of EDRF. *Br. J. Pharmacol.* **1993**, *110*, 777–782.
- (23) Reynolds, E. E.; Hwang, O.; Flynn, M. A.; Welch, K. M.; Cody, W. L.; Steinbaugh, B.; He, J. X.; Chung, F. Z.; Doherty, A. M. Pharmacological differences between rat and human endothelin B receptors. *Biochem. Biophys. Res. Commun.* **1995**, *209*, 506–512.
- (24) Doherty, A. M.; Cody, W. L.; Leitz, N. L.; DePue, P. L.; Taylor, M. D.; Rapundalo, S. T.; Hingorani, G. P.; Major, T. C.; Panek, R. L.; Taylor, D. G. Structure-activity studies of the C-terminal region of the endothelins and the sarafotoxins. *J. Cardiovasc. Pharmacol.* **1991**, *17* (Suppl. 7), S59–S61.
- (25) Cody, W. L.; Doherty, A. M.; He, J. X.; DePue, P. L.; Rapundalo, S. T.; Hingorani, G. A.; Major, T. C.; Panek, R. L.; Dudley, D. T.; Haleen, S. J.; LaDouceur, D.; Hill, K. E.; Flynn, M. A.; Reynolds, E. E. Design of a functional hexapeptide antagonist of endothelin. *J. Med. Chem.* **1992**, *35*, 3301–3303.
- (26) Doherty, A. M.; Cody, W. L.; He, J. X.; DePue, P. L.; Leonard, D. M.; Dunbar, J. B.; Hill, K. E.; Flynn, M. A.; Reynolds, E. E. Design of C-terminal peptide antagonists of endothelin: Structure-activity relationships of ET-1[16–21,D-His<sup>19</sup>]. *Bioorg. Med. Chem. Lett.* **1993**, *3*, 497–502.
- (27) Doherty, A. M.; Cody, W. L.; DePue, P. L.; He, J. X.; Waite, L. A.; Leonard, D. M.; Leitz, N. L.; Dudley, D. T.; Rapundalo, S. T.; Hingorani, G. P.; Haleen, S. J.; LaDouceur, D. M.; Hill, K. E.; Flynn, M. A.; Reynolds, E. E. Structure-activity relationships of C-terminal endothelin hexapeptide antagonists. *J. Med. Chem.* **1993**, *36*, 2585–2594.
- (28) Cody, W. L.; Doherty, A. M.; He, J. X.; DePue, P. L.; Waite, L. A.; Haleen, S. J.; LaDouceur, D. M.; Flynn, M. A.; Welch, K. M.; Reynolds, E. E. Endothelin antagonists: The rational design of combined and ET<sub>B</sub> receptor subtype selective antagonists. In *Peptides, Chemistry, Structure and Biology: Proceedings of the Thirteenth American Peptide Symposium*; Hodges, R. S., Smith, J. A., Eds.; ESCOM Science: Leiden, The Netherlands, 1994; pp 598–600.
- (29) Cody, W. L.; He, J. X.; DePue, P. L.; Waite, L. A.; Leonard, D. M.; Seftel, A. M.; Kaltenbronn, J. S.; Haleen, S. J.; Walker, D. M.; Flynn, M. A.; Welch, K. M.; Reynolds, E. E.; Doherty, A. M. Structure-activity relationships of the potent combined endothelin-A/endothelin-B receptor antagonist Ac-Dip<sup>18</sup>-Leu-Asp-Ile-Ile-Trp<sup>21</sup>: Development of endothelin-B receptor selective antagonists. *J. Med. Chem.* **1995**, *38*, 2809–2819.
- (30) Cody, W. L.; Doherty, A. M.; He, J. X.; Topliss, J. G.; Haleen, S. J.; LaDouceur, D.; Flynn, M. A.; Hill, K. E.; Reynolds, E. E. Structure-activity relationships in the C-terminus of endothelin-1 (ET-1): The discovery of potent antagonists. In *Peptides 1992: Proceedings of the Twenty-Second European American Peptide Symposium*; Schneider, C. H., Eberle, A. N., Eds.; ESCOM Science: Leiden, The Netherlands, 1993; pp 687–688.
- (31) Cody, W. L.; Doherty, A. M.; He, J. X.; DePue, P. L.; Waite, L. A.; Topliss, J. G.; Haleen, S. J.; LaDouceur, D.; Flynn, M. A.; Hill, K. E.; Reynolds, E. E. The rational design of a highly potent combined ET<sub>A</sub> and ET<sub>B</sub> receptor antagonist (PD 145065) and related analogues. *Med. Chem. Res.* **1993**, *3*, 154–162.
- (32) Doherty, A. M.; Cody, W. L.; He, J. X.; DePue, P. L.; Cheng, X. M.; Welch, K. M.; Flynn, M. A.; Reynolds, E. E.; LaDouceur, D. M.; Davis, L. S.; Keiser, J. A.; Haleen, S. J. In vitro and in vivo studies with a series of hexapeptide endothelin antagonists. *J. Cardiovasc. Pharmacol.* **1993**, *22* (Suppl. 8), S98–S102.
- (33) Cody, W. L.; He, J. X.; Doherty, A. M.; DePue, P. L.; Kaltenbronn, J. S.; Reisdorff, B. R.; Walker, D. M.; Welch, K. M.; Haleen, S. J.; Reynolds, E. E.; Tse, E.; Reynier, E. L.; Stewart, B. H. The design of potent hexapeptide endothelin antagonists stable to proteolysis. In *Peptides 1994: Proceedings of the Twenty-Third European Peptide Symposium*; Maiz, H. L. S., Ed.; ESCOM Science: Leiden, The Netherlands, 1993; pp 38–39.
- (34) Stewart, B. H.; Reynier, E. L.; Tse, E.; Hayes, R. N.; Werness, S.; He, J. X.; Cody, W. L.; Doherty, A. M. In vitro assessment of oral delivery for hexapeptide endothelin antagonists. *Life Sci.* **1996**, *58*, 971–982.
- (35) Kessler, H.; Knot, R. K.; Schmitt, W. Conformational analysis of peptides: Application to drug design. In *NMR Drug Design*; Craik, D. J., Ed.; CRC Press: Boca Raton, FL, 1996; pp 215–244.
- (36) Kessler, H.; Köck, M.; Wein, T.; Gehrke, M. Reinvestigation of the conformation of cyclosporin A in chloroform. *Helv. Chim. Acta* **1990**, *73*, 1818–1832.
- (37) Kessler, H.; Haessner, R.; Schüller, W. Structure of rapamycin: An NMR and molecular-dynamics investigation. *Helv. Chim. Acta* **1993**, *76*, 117–130.
- (38) Swindells, D. C.; White, P. S.; Findlay, J. A. The X-ray crystal structure of rapamycin, C<sub>15</sub>H<sub>79</sub>NO<sub>13</sub>. *Can. J. Chem.* **1978**, *56*, 2491–2492.
- (39) Flippen-Anderson, J. L.; Hruby, V. J.; Collins, N.; George, C.; Cudney, B. X-ray structure of [DPen<sup>2</sup>,DPen<sup>5</sup>]enkephalin, a highly potent,  $\delta$ -opioid receptor selective compound: Comparisons with proposed solution conformations. *J. Am. Chem. Soc.* **1994**, *116*, 7523–7531.
- (40) Melacini, G.; Zhu, Q.; Goodman, M. Multiconformational NMR analysis of sandostatin (octreotide): Equilibrium between  $\beta$ -sheet and helical structures. *Biochemistry* **1997**, *36*, 1233–1241.
- (41) Wüthrich, K. *NMR of Proteins and Nucleic Acids*; J. Wiley and Sons: New York, 1984.

- (42) Reilly, M. D.; Thanabal, V.; Omecinsky, D. O. Structure-induced carbon-13 chemical shifts: A sensitive measure of transient localized secondary structure in peptides. *J. Am. Chem. Soc.* **1992**, *114*, 6251-6252.
- (43) Stewart, J. M.; Young, J. D. *Solid Phase Synthesis*, 2nd ed.; Pierce Chemical Co.: Rockford, IL, 1984.
- (44) Bodansky, M.; Bodansky, A. *The Practice of Peptide Synthesis*; Springer-Verlag: Berlin, Germany, 1984.
- (45) Mitchell, A. R.; Erickson, B. W.; Ryabtsev, M. N.; Hodges, R. S.; Merrifield, R. B. *Tert*-butoxycarbonylaminoacyl-4-(oxymethyl)-phenylacetamidomethyl-resin, a more acid-resistant support for solid-phase peptide synthesis. *J. Am. Chem. Soc.* **1976**, *98*, 7357-7362.
- (46) Chen, H. G.; Beylin, V. G.; Leja, B.; Goel, O. P. Chiral synthesis of D- and L-3,3-diphenylalanine (DIP), unusual L-amino acids for peptides of biological interest. *Tetrahedron Lett.* **1992**, *33*, 3293-3296.
- (47) Beylin, V. G.; Chen, H. G.; Dunbar, J. B.; Goel, O. P.; Harter, W.; Marlett, M.; Topliss, J. G. Cyclic derivatives of 3,3-diphenylalanine (Dip). II. Novel L-amino acids for peptides of biological interest. *Tetrahedron Lett.* **1992**, *34*, 953-956.
- (48) Knittel, J. J.; He, J. X. Synthesis and resolution of novel 3'-substituted phenylalanine amides. *Pept. Res.* **1990**, *3*, 176-181.
- (49) Sasaki, Y.; Coy, D. H. Solid phase synthesis of peptides containing the CH<sub>2</sub>NH peptide bond isostere. *Peptides* **1987**, *8*, 119-121.
- (50) Sasaki, Y.; Murphy, W. A.; Helman, M. L.; Lance, V. A.; Coy, D. H. Solid-phase synthesis and biological properties of Y[CH<sub>2</sub>NH] pseudopeptide analogs of a highly potent somatostatin octapeptide. *J. Med. Chem.* **1987**, *30*, 1162-1166.
- (51) Fehrentz, J. A.; Castro, B. An efficient synthesis of optically active  $\alpha$ -(*t*-butoxycarbonylamino)-aldehydes from  $\alpha$ -amino acids. *Synthesis* **1983**, 676-678.
- (52) Kaljuste, K.; Uden, A. New method for the synthesis of N-methyl amino acids containing peptides by reductive methylation of amino groups on the solid phase. *Int. J. Pept. Protein Res.* **1993**, *42*, 118-124.
- (53) Freidinger, R. M.; Hinkle, J. S.; Perlow, D. S. Synthesis of 9-fluorenylmethoxycarbonyl-protected N-alkyl amino acids by reduction of oxazolidinones. *J. Org. Chem.* **1983**, *48*, 77-81.
- (54) Kaiser, E.; Colascott, R. L.; Bossinger, C. D.; Cook, P. I. Color test for detection of free terminal amino groups in the solid-phase synthesis of peptides. *Anal. Biochem.* **1970**, *34*, 595-598.
- (55) Woodley, J. F. Enzymic barriers for GI peptide and protein delivery. *Crit. Rev. Ther. Drug Carrier Syst.* **1994**, *11*, 61-95.
- (56) Cody, W. L.; He, J. X.; Flynn, M. A.; Welch, K. M.; Reynolds, E. E.; Doherty, A. M. Parke-Davis Pharmaceutical Research, Division of Warner-Lambert Co., unpublished results.
- (57) Stewart, B. H.; Reynier, E. L.; Tse, E.; Hayes, R. N.; Cody, W. L.; Doherty, A. M. In vitro assessment of oral delivery for hexapeptide endothelin antagonists using stability in intestinal perfusate and Caco-2 permeability. *Pharm. Res.* **1994**, *11*, S-257.
- (58) Artursson, P.; Karlsson, J. Correlation between oral drug absorption in humans and apparent drug permeability coefficients in human intestinal epithelial (Caco-2) cells. *Biochem. Biophys. Res. Commun.* **1991**, *175*, 880-885.
- (59) Hidalgo, I. J.; Raub, R. J.; Borchardt, R. T. Characterization of the human colon carcinoma cell line (Caco-2) as a model system for intestinal epithelial permeability. *Gastroenterology* **1989**, *96*, 736-749.
- (60) Pinto, M.; Robine-Leon, S.; Appay, M. D.; Kedinger, M.; Triadou, N.; Dussaulx, E.; Lacroix, B.; Simon-Assmann, P.; Haffen, K.; Fogh, J.; Zweibaum, A. Enterocyte-like differentiation and polarization of the human colon carcinoma cell line Caco-2 in culture. *Biol. Cell* **1983**, *47*, 232-239.
- (61) Watts, C. R.; Tessmer, M. R.; Cody, W. L.; Doherty, A. M.; Kallick, D. A. High resolution NMR structure and molecular dynamics simulation of a potent ET<sub>A</sub> and ET<sub>B</sub> endothelin receptor antagonist in the presence of dodecylphosphocholine micelles. *Biochemistry* **1997**, in press.
- (62) Szilágyi, L. Chemical shifts in proteins come of age. *Prog. Nucl. Magn. Reson. Spectrosc.* **1995**, *27*, 325-443.
- (63) Wishart, D. S.; Bigam, C. G.; Holm, A.; Hodges, R. S.; Sykes, B. D. <sup>1</sup>H, <sup>13</sup>C and <sup>15</sup>N Random coil NMR chemical shifts of the common amino acids. I. Investigations of nearest neighbor effects. *J. Biomol. NMR* **1995**, *5*, 67-81.
- (64) Braunschweiler, L.; Ernst, R. R. Coherence transfer by isotropic mixing: Application to proton correlation spectroscopy. *J. Magn. Reson.* **1983**, *53*, 521-528.
- (65) Rance, M.; Soerensen, O. W.; Bodenhausen, G.; Wagner, G.; Ernst, R. R.; Wüthrich, K. Improved spectral resolution in COSY proton NMR spectra of proteins via double quantum filtering. *Biochem. Biophys. Res. Commun.* **1983**, *117*, 479-485.
- (66) Bothner-Bj, A. A.; Stephens, R. L.; Lee, J.; Warren, C. D.; Jeanloz, R. W. *J. Am. Chem. Soc.* **1984**, *106*, 811-813.
- (67) Bax, A.; Davis, D. G. Practical aspects of two-dimensional transverse NOE spectroscopy. *J. Magn. Reson.* **1985**, *65*, 355-360.
- (68) Kumar, A.; Ernst, R. R.; Wüthrich, K. A two-dimensional nuclear Overhauser enhancement (2D NOE) experiment for the elucidation of complete proton-proton cross-relaxation networks in biological macromolecules. *Biochem. Biophys. Res. Commun.* **1980**, *95*, 1-6.
- (69) Marion, D.; Wüthrich, K. Application of phase sensitive two-dimensional correlated spectroscopy (COSY) for measurements of proton-proton spin-spin coupling constants in proteins. *Biochem. Biophys. Res. Commun.* **1983**, *113*, 967-974.
- (70) Reilly, M. D.; Thanabal, V.; Adams, M. E. The solution structure of  $\omega$ -Aga-IVB, a P-type calcium channel antagonist from venom of the funnel web spider, *Agelenopsis aperta*. *J. Biomol. NMR* **1995**, *5*, 122-132.
- (71) Thanabal, V.; Omecinsky, D. O.; Reilly, M. D.; Cody, W. L. The <sup>13</sup>C chemical shifts of amino acids in aqueous solution containing organic solvents: Application to the secondary structure characterization of peptides in aqueous trifluoroethanol solution. *J. Biomol. NMR* **1994**, *4*, 47-59.
- (72) Howarth, O. W.; Lilley, D. M. J. Carbon-13 NMR of peptides and proteins. *Prog. Nucl. Magn. Reson. Spectrosc.* **1978**, *12*, 1-40.

JM970161M

## Structure–activity relationships of dermorphin analogues containing *N*-substituted amino acids in the 2-position of the peptide sequence

RALF SCHMIDT<sup>1</sup>\*, ANDRÁS KÁLMÁN<sup>2</sup>, NGA N. CHUNG<sup>1</sup>, CAROLE LEMIEUX<sup>1</sup>, CSABA HORVÁTH<sup>2</sup> and PETER W. SCHILLER<sup>1</sup>

<sup>1</sup> Laboratory of Chemical Biology and Peptide Research, Clinical Research Institute of Montreal<sup>†</sup>, Montreal, Quebec, Canada and <sup>2</sup> Department of Chemical Engineering, Yale University, New Haven, Connecticut, USA

Received 10 November 1994, accepted for publication 8 January 1995

A series of dermorphin analogues containing an *N*-alkylated amino-acid residue Xaa in the 2-position of the peptide sequence was synthesized (Xaa = *N*-methylalanine, proline, pipecolic acid, *N*-methylphenylalanine, 1,2,3,4-tetrahydroisoquinoline-3-carboxylic acid [Tic]). These peptides have the potential of assuming a *cis* Tyr<sup>1</sup>-Xaa<sup>2</sup> peptide bond. Their *in vitro* opioid activity profiles were determined in  $\mu$ - and  $\delta$ -receptor-representative binding assays and bioassays. Aside from [D-Pro<sup>2</sup>]dermorphin, all analogues showed high affinity for  $\mu$ - and/or  $\delta$ -opioid receptors. Whereas most compounds were found to be full  $\mu$ -agonists in the guinea pig ileum (GPI) assay, [Tic<sup>2</sup>]dermorphin (compound 7) was a partial  $\mu$ -agonist. Replacement of Gly<sup>4</sup> in 7 with Phe resulted in an analogue (8) with weak  $\mu$ -antagonist activity. Furthermore, analogues 7 and 8 both were potent  $\delta$ -antagonists ( $K_i$  = 3–40 nM) against the  $\delta$ -agonists Leu-enkephalin, DPDPE and deltorphin I in the mouse vas deferens (MVD) assay. Compound 3, containing L-Pro in the 2-position, turned out to be one of the most  $\mu$ -receptor-selective linear dermorphin analogues reported to date. Low-temperature HPLC experiments using micropellicular octadecyl silica as stationary phase revealed conformational heterogeneity of the dermorphin analogues which was ascribed to *cis*–*trans* isomerization around the Tyr<sup>1</sup>-Xaa<sup>2</sup>- and Tyr<sup>5</sup>-Pro<sup>6</sup> peptide bonds. In the case of analogue 7 four separate peaks corresponding to the four possible isomers were apparent at –5°C. Since opioid peptide analogues with a non-*N*-alkylated L-amino acid residue in the 2-position are nearly inactive and cannot assume a *cis* peptide bond at the 1–2 position, these results support the hypothesis that the bioactive conformation of opioid peptides containing an *N*-alkylated L-amino acid residue in position 2 is characterized by a *cis* Tyr<sup>1</sup>-Xaa<sup>2</sup> peptide bond. © Munksgaard 1995.

**Key words:** *cis*–*trans* peptide bond isomerization; dermorphin analogues, low-temperature HPLC; opioid peptides;  $\delta$ -opioid antagonists

Since the discovery of the enkephalins, other opioid peptides originating from distinct mammalian precur-

sors, from enzymatic digests of mammalian proteins or from non-mammalian sources have been found. Most of these peptides show little selectivity towards the three major opioid receptor classes ( $\mu$ ,  $\delta$ ,  $\kappa$ ), the exception being the  $\mu$ -selective dermorphins (1, 2) and the  $\delta$ -selective deltorphins/dermenkephalins (3, 4). Morphiceptin, the *N*-terminal tetrapeptide fragment of  $\beta$ -casomorphin, also shows high  $\mu$ -selectivity (5).

Morphiceptin (H-Tyr-Pro-Phe-Pro-NH<sub>2</sub>) and dermorphin (H-Tyr-D-Ala-Phe-Gly-Tyr-Pro-Ser-NH<sub>2</sub>) have different configurational requirements at the 2-position residue, as indicated by the observations that [D-Pro<sup>2</sup>]morphiceptin and [Ala<sup>2</sup>]dermorphin are almost completely inactive (5–7). In an attempt to provide a structural explanation for the bioactivity of morphiceptin, several of its analogues containing the proline open-chain analogue *N*-methylalanine (L- and D-con-

**Abbreviations:** Boc, *tert*-butoxycarbonyl; DAMGO, H-Tyr-D-Ala-Gly-MePhe-Gly-ol; [D-Ala<sup>2</sup>]deltorphin I, H-Tyr-D-Ala-Phe-Asp-Val-Val-Gly-NH<sub>2</sub>; DIEA, diisopropylethylamine; DIP, diisopropylcarbodiimide; DMF, *N,N*-dimethylformamide; DPDPE, H-Tyr-D-Pen-Gly-Phe-D-Pen-OH; DSLET, H-Tyr-D-Ser-Gly-Phe-Leu-Thr-OH; GPI, guinea pig ileum; HOBt, 1-hydroxybenzotriazole; MeAla, *N*-methylalanine; MePhe, *N*-methylphenylalanine; MVD, mouse vas deferens; Pip, pipecolic acid; PITC, phenylisothiocyanate; TFA, trifluoroacetic acid; Tic, 1,2,3,4-tetrahydroisoquinoline-3-carboxylic acid; TIP, H-Tyr-Tic-Phe-OH; TIP-NH<sub>2</sub>, H-Tyr-Tic-Phe-NH<sub>2</sub>; TIPP, H-Tyr-Tic-Phe-Phe-OH.

\* Present address: Astra Pain Research Unit, 275bis boul. Armand-Frappier, Laval, Quebec, Canada H7V 4A7.

<sup>†</sup> Affiliated to the University of Montreal.

R. Schmidt *et al.*

figuration) in place of Pro<sup>2</sup> were examined (8–10). The pharmacological evaluation of these compounds in conjunction with conformational analysis by NMR spectroscopy and molecular mechanics studies suggested that a *cis* Tyr<sup>1</sup>-Xaa<sup>2</sup> peptide bond is required for the  $\mu$ -agonist activity of morphiceptin and of its analogues with an L-configured amino acid in the 2-position. In an effort to demonstrate that this hypothesis may also hold true for the dermorphins, we synthesized and tested a series of dermorphin analogues that contain an *N*-alkylated amino acid residue, Xaa, in the 2-position of the peptide sequence (Xaa = *N*-methylalanine, proline, pipecolic acid, *N*-methylphenylalanine, 1,2,3,4-tetrahydroisoquinoline-3-carboxylic acid). *N*-Alkylation of either an L-amino acid or a D-amino acid in a peptide creates the potential for the preceding peptide bond to assume the *cis* conformation.

Furthermore, in the case of proline-containing dipeptides and oligopeptides, it has recently been demonstrated that distinct conformers resulting from *cis-trans* isomerization of the Xaa-Pro peptide bond could be separated by reversed-phase HPLC. Although *cis-trans* isomerization is usually fast at room temperature, it can be slowed down by lowering the temperature, thereby allowing the separation of the different conformers (11–15). On the basis of these results and in an effort to examine the possible coexistence of different conformers of the dermorphin analogues described in this paper, low-temperature reversed-phase HPLC experiments using various stationary phases were also carried out.

## RESULTS AND DISCUSSION

The dermorphin analogues were prepared by solid-phase synthesis using *N*<sup>α</sup>-Boc-protected amino acids with diisopropylcarbodiimide (DIP)/1-hydroxybenzo-

triazole (HOBt) as coupling reagents on a *p*-methylbenzhydrylamine resin (MBHA). Tic was obtained through condensation of phenylalanine with paraformaldehyde, as reported elsewhere (16). Cleavage of the peptides from the resin was performed by HF/anisole treatment in the usual manner. The crude products were purified by low-pressure reversed-phase chromatography (17) and, if necessary, final purification to homogeneity was achieved by semipreparative RP-HPLC. The purified dermorphin analogues were obtained as lyophilisates and were characterized by TLC, RP-HPLC, amino acid analysis, FAB mass spectrometry and <sup>1</sup>H-NMR (Table 1).

The heptapeptide H-Tyr-MeAla-Phe-Gly-Tyr-Pro-Ser-NH<sub>2</sub> (1) was found to be a potent  $\mu$ -agonist which, in comparison with the parent peptide dermorphin, displayed only about five times lower potency in the  $\mu$ -receptor-representative GPI bioassay and a five-fold drop in  $\mu$ -receptor affinity in the receptor binding assay based on displacement of [<sup>3</sup>H]H-Tyr-D-Ala-Gly-MePhe-Gly-ol ([<sup>3</sup>H]DAMGO) from rat brain membrane binding sites (Tables 2 and 3). Thus, *N*-methylation of the L-alanine residue in the nearly inactive L-Ala<sup>2</sup>-dermorphin analogue (6, 7) produced a drastic increase in potency at the  $\mu$ -receptor. The diastereomeric D-MeAla<sup>2</sup>-analogue (2) showed only slightly lower  $\mu$ -affinity than dermorphin, but six times higher potency in the GPI bioassay. In comparison with analogue 1, compound 2 displayed three times higher  $\mu$ -receptor affinity and 30 times higher potency in the GPI assay. This result is in contrast to the previously demonstrated equipotency of the MeAla<sup>2</sup>- and D-MeAla<sup>2</sup>-analogues of morphiceptin (9). Compounds 1 and 2 retained considerable  $\mu$ -receptor selectivity, as indicated by their  $K_i^{\delta}/K_i^{\mu}$  ratios (Table 2), but were about 4–5 times less  $\mu$ -selective than the dermorphin

TABLE 1  
Analytical data of dermorphin analogues<sup>a</sup>

No.	Compound	Amino-acid analysis						TLC <sup>b</sup> ( <i>R<sub>f</sub></i> )			HPLC <sup>c</sup> <i>k'</i>	FAB-MS ( <i>MH</i> <sup>+</sup> )
		Tyr <sup>1</sup>	Xaa <sup>2</sup>	Xaa <sup>3</sup>	Xaa <sup>4</sup>	Pro <sup>6</sup>	Ser <sup>7</sup>	BPAW	BAWE	BFW		
1	H-Tyr-MeAla-Phe-Gly-Tyr-Pro-Ser-NH <sub>2</sub>	1.65	n.d.	1.09	1.00	0.89	0.86	0.70	0.78	0.56	4.01	817
2	H-Tyr-D-MeAla-Phe-Gly-Tyr-Pro-Ser-NH <sub>2</sub>	1.75	n.d.	1.00	1.08	0.95	0.89	0.73	0.82	0.63	5.22	817
3	H-Tyr-Pro-Phe-Gly-Tyr-Pro-Ser-NH <sub>2</sub>	2.00	2.10	1.13	1.14		0.94	0.68	0.77	0.55	4.16	829
4	H-Tyr-D-Pro-Phe-Gly-Tyr-Pro-Ser-NH <sub>2</sub>	2.07	1.99	1.07	1.09		1.00	0.70	0.80	0.59	6.10	829
5	H-Tyr-Pip-Phe-Gly-Tyr-Pro-Ser-NH <sub>2</sub>	1.93	n.d.	1.04	1.08	0.99	1.00	0.72	0.81	0.59	5.84	843
6	H-Tyr-D-Pip-Phe-Gly-Tyr-Pro-Ser-NH <sub>2</sub>	1.96	n.d.	1.00	1.18	0.97	0.86	0.72	0.81	0.59	7.93	843
7	H-Tyr-Tic-Phe-Gly-Tyr-Pro-Ser-NH <sub>2</sub>	1.67	n.d.	1.00	1.15	0.97	1.06	0.72	0.83	0.63	9.16	891
8	H-Tyr-Tic-Phe-Phe-Tyr-Pro-Ser-NH <sub>2</sub>	1.83	n.d.	2.00		0.92	1.04	0.74	0.89	0.73	13.23	981
9	H-Tyr-MePhe-Phe-Gly-Tyr-Pro-Ser-NH <sub>2</sub>	1.82	n.d.	1.16	1.12	1.01	1.00	0.73	0.84	0.63	9.53	893

<sup>a</sup> Structures of peptides were confirmed by one- and two-dimensional <sup>1</sup>H-NMR.

<sup>b</sup> BPAW, 1-butanol-pyridine-acetic acid-water (15/10/3/12); BAWE, 1-butanol-acetic acid-water-ethyl acetate (1/1/1/1); BFW, 2-butanol-formic acid-water (75/15/20).

<sup>c</sup> LiChrospher 100 RP-18e (5  $\mu$ m, 125  $\times$  4 mm), gradient 20–50% B in 25 min [(A) 0.1% TFA (H<sub>2</sub>O), (B) 0.1% TFA (acetonitrile)], detection at 216 and 280 nm.

## Dermorphin analogues

TABLE 2  
Receptor binding assay of dermorphin analogues

No.	Compound	[ <sup>3</sup> H]DAMGO		[ <sup>3</sup> H]DSLET		$K_i^b/K_i^a$
		$K_i^a$ , nM <sup>a</sup>	Rel. potency <sup>b</sup>	$K_i^a$ , nM <sup>a</sup>	Rel. potency <sup>b</sup>	
1	H-Tyr-MeAla-Phe-Gly-Tyr-Pro-Ser-NH <sub>2</sub>	4.69 ± 1.19	2.01 ± 0.51	232 ± 32	0.0109 ± 0.0015	49.5
2	H-Tyr-D-MeAla-Phe-Gly-Tyr-Pro-Ser-NH <sub>2</sub>	1.38 ± 0.20	6.84 ± 0.99	47.5 ± 1.2	0.0533 ± 0.0014	34.4
3	H-Tyr-Pro-Phe-Gly-Tyr-Pro-Ser-NH <sub>2</sub>	1.47 ± 0.021	6.41 ± 0.09	3010 ± 824	0.00084 ± 0.00023	2050
4	H-Tyr-D-Pro-Phe-Gly-Tyr-Pro-Ser-NH <sub>2</sub>	2400 ± 861	0.00391 ± 0.0014	1890 ± 423	0.00134 ± 0.00030	0.787
5	H-Tyr-Pip-Phe-Gly-Tyr-Pro-Ser-NH <sub>2</sub>	5.86 ± 0.98	1.63 ± 0.27	147 ± 32	0.0172 ± 0.0037	25.1
6	H-Tyr-D-Pip-Phe-Gly-Tyr-Pro-Ser-NH <sub>2</sub>	5.78 ± 0.17	1.68 ± 0.05	89.7 ± 6.7	0.0282 ± 0.0021	15.5
7	H-Tyr-Tic-Phe-Gly-Tyr-Pro-Ser-NH <sub>2</sub>	865 ± 246	0.0109 ± 0.0031	1.26 ± 0.16	2.0 ± 0.26	685 <sup>c</sup>
8	H-Tyr-Tic-Phe-Phe-Tyr-Pro-Ser-NH <sub>2</sub>	1250 ± 339	0.00752 ± 0.00204	0.578 ± 0.124	4.38 ± 0.94	2160 <sup>c</sup>
9	H-Tyr-MePhe-Phe-Gly-Tyr-Pro-Ser-NH <sub>2</sub>	26.7 ± 4.1	0.353 ± 0.054	31.5 ± 14.0	0.0803 ± 0.0357	1.18
	H-Tyr-D-Ala-Phe-Gly-Tyr-Pro-Ser-NH <sub>2</sub>	0.839	11.2	160	0.0158	191
	[Leu <sup>5</sup> ]enkephalin	9.43 ± 2.07	1	2.53 ± 0.35	1	3.7

<sup>a</sup> Mean of three determinations ± SEM.

<sup>b</sup> Potencies relative to [Leu<sup>5</sup>]enkephalin.

<sup>c</sup>  $K_i^a/K_i^b$  ratio.

parent peptide. In the  $\delta$ -receptor-representative MVD assay, analogues 1 and 2 both were full agonists. Their agonist effect in this assay system was only slightly diminished by the potent and highly selective  $\delta$ -antagonist H-Tyr-Tic-Phe-Phe-OH (TIPP) (18) but was completely naloxone-reversible. Therefore, these effects seem to be mediated primarily by activation of the  $\mu$ -receptors present in this tissue (19).

Substitution of L-proline for D-Ala<sup>2</sup> in dermorphin led to an analogue (3) with markedly increased  $\mu$ -receptor selectivity due to a drastic drop in  $\delta$ -receptor affinity ( $K_i^b = 3 \mu\text{M}$ ). Compound 3 showed an affinity for the  $\mu$ -receptor comparable to that of the native peptide and of the D-MeAla<sup>2</sup>-containing dermorphin analogue 2, and its  $\mu$ -receptor selectivity was 10 times higher than that of dermorphin. As indicated by its high selectivity ratio ( $K_i^b/K_i^a = 2050$ ), analogue 3 ranks among the most  $\mu$ -selective linear dermorphin analogues reported to date. The opioid agonist effect of 3 in the MVD assay could be completely reversed by naloxone but not by TIPP, indicating an involvement of  $\mu$ -receptors rather than  $\delta$ -receptors. Comparison of the  $\mu$ -receptor affinities of compounds 1, 2 and 3 with their  $\mu$ -agonist potencies determined in the GPI assay reveals that in the case of analogue 3 signal transduction is somewhat hampered, resulting in lower intrinsic efficacy. Compound 4, containing D-Pro in the 2-position, exhibited almost no opioid activity in the GPI and MVD assays as well as very weak opioid receptor affinities, as it had also been observed in the case of D-Pro<sup>2</sup> analogues of morphiceptin and  $\beta$ -casomorphin (5, 20). Therefore, it appears that in general the presence of a D-Pro residue in the 2-position of opioid peptides is incompatible with the structural requirements of both  $\mu$  and  $\delta$  receptors, whereas most other D-amino acids are well tolerated (21).

Replacement of D-Ala<sup>2</sup> in dermorphin with pipecolic acid (Pip), a proline homologue containing a six-membered ring, produced interesting results. Both the L-Pip<sup>2</sup>- and the D-Pip<sup>2</sup>-analogue (compounds 5 and 6) showed similarly high  $\mu$ -receptor affinities and high  $\mu$ -agonist potencies in the GPI assay. Similar observations had previously been made with L- and D-Pip<sup>2</sup>-analogues of  $\beta$ -casomorphins (20). The D-Pip<sup>2</sup>-containing analogue (6) displayed a slightly higher  $\delta$ -affinity than the L-Pip<sup>2</sup>-containing one (5), but again both compounds showed similar potency in the MVD assay. The agonist effect produced by compounds 5 and 6 in the MVD bioassay could be completely reversed by the  $\delta$ -antagonist TIPP, indicating that it was exclusively due to  $\delta$ -receptor activation. Interestingly, the potencies of peptides 5 and 6 are similar to that of analogue 1, which produces its agonist effect in the MVD assay mainly through interaction with  $\mu$ -receptors (see above). These findings suggest that the  $\mu$ -receptors present in the MVD may have structural requirements that are somewhat different from those of the  $\mu$ -receptors in the GPI. The different results obtained for the D-Pro<sup>2</sup>- versus the D-Pip<sup>2</sup>-containing dermorphin- and morphiceptin/casomorphin analogues can be explained on the basis of a recently performed conformational analysis (22). Molecular dynamics simulations showed that the internal backbone torsion angle of proline ( $\phi_2$ ) may vary between  $-40^\circ$  and  $-80^\circ$  in the case of L-Pro and between  $40^\circ$  and  $80^\circ$  in the case of D-Pro. In the case of D-Pip this torsion angle was shown to oscillate between positive and negative values, and therefore the D-Pip<sup>2</sup> analogue is able to assume the "active" conformation of the L-Pro<sup>2</sup> analogue.

Substitution of D-Ala<sup>2</sup> in dermorphin with Tic resulted in a compound (7) which turned out to be a weak partial agonist in the GPI assay ( $\text{IC}_{30} = 5 \mu\text{M}$ ) and to

R. Schmidt *et al.*

have low affinity for  $\mu$ -receptors (Tables 2 and 3). Compound 7 displayed a more than 100 times higher affinity for  $\delta$ -receptors than dermorphin and was  $\delta$ -selective rather than  $\mu$ -selective. In the MVD assay this analogue produced no agonist effect, but was found to be a potent  $\delta$ -antagonist against the  $\delta$ -agonists Leu-enkephalin, DPDPE and [D-Ala<sup>2</sup>]deltorphin I with  $K_e$ -values ranging from 20 to 40 nM (Table 4). The  $\delta$ -opioid antagonist properties of peptide 7 have been reported previously in a preliminary publication (23) and also by Tancredi *et al.* (24). This compound is a C-terminally extended analogue of the recently described tripeptide  $\delta$ -antagonist H-Tyr-Tic-Phe-NH<sub>2</sub> (TIP-NH<sub>2</sub>) (18), and its  $\delta$ -antagonist potency is comparable to that of TIP-NH<sub>2</sub>. Analogue 7 represents another example of a compound with mixed  $\mu$ -agonist/ $\delta$ -antagonist properties (18, 25), albeit its  $\mu$ -agonist activity is rather weak. Replacement of the Gly<sup>4</sup> residue in 7 with phenylalanine resulted in an analogue, H-Tyr-Tic-Phe-Phe-Tyr-Pro-Ser-NH<sub>2</sub> (8), containing the entire sequence of the  $\delta$ -antagonist TIPP (H-Tyr-Tic-Phe-Phe-OH) (18). Dermorphin analogue 8 showed a complete loss of  $\mu$ -agonist activity and lower  $\mu$ -receptor affinity than 7, but was a weak  $\mu$ -antagonist against Leu-enkephalin in the GPI assay ( $K_e$  = 750 nM). Thus compound 8 turned out to be the first Tic<sup>2</sup>-containing opioid peptide analogue with  $\mu$ -antagonist properties. In comparison with 7, analogue 8 displayed increased  $\delta$ -affinity, higher  $\delta$ -selectivity and enhanced  $\delta$ -antagonist potency against the  $\delta$ -agonists Leu-enkephalin, DPDPE and [D-Ala<sup>2</sup>]deltorphin I in the MVD assay ( $K_e$  = 2–5 nM). This result was not unexpected in view of the previously observed higher  $\delta$ -antagonist potency and  $\delta$ -selectivity of TIPP as compared to TIP (H-Tyr-Tic-Phe-OH) (18). These results indicate that substitution of Tic for D-Ala<sup>2</sup>

in dermorphin converted a  $\mu$ -selective opioid agonist into a highly  $\delta$ -selective opioid peptide antagonist. Previous studies had shown that the C-terminal tripeptide segment of dermorphin strengthens binding of this peptide to the  $\mu$ -receptor, but does not significantly affect receptor selection (26). Furthermore, it had been demonstrated that substitution of D-Ala<sup>2</sup> with Tic in the  $\mu$ -selective tetrapeptide agonist Tyr-D-Ala-Phe-Phe-NH<sub>2</sub> (27) also produced a highly selective  $\delta$ -antagonist (18). The opioid activity profiles of the Tic<sup>2</sup>-analogues of dermorphin are in harmony with these earlier results. In particular, our data confirm that the C-terminal tripeptide segment does not play a significant role in receptor selection, and furthermore indicate that the strengthening of  $\mu$ -receptor binding produced by this segment in the case of the native peptide is overwhelmingly suppressed by substitution of Tic in the 2-position of dermorphin. Furthermore, the observation that the Pip<sup>2</sup>-analogue (5) is a  $\mu$ -selective agonist and the Tic<sup>2</sup>-analogue is a  $\delta$ -selective antagonist confirm the previously demonstrated crucial importance of the Tic aromatic ring for the  $\delta$ -antagonist behavior of TIP(P)-related peptides (28).

Opening of the heterocyclic ring of Tic<sup>2</sup> in analogue 8, as achieved by substitution of *N*-methylphenylalanine (compound 9), had a divergent effect on the interaction with  $\mu$ - and  $\delta$ -receptors. Whereas analogue 9 showed 30 times higher  $\mu$ -receptor affinity than 8, its  $\delta$ -affinity was 30-fold reduced, and consequently it was totally non-selective. In both the GPI assay and the MVD assay analogue 9 turned out to be a full agonist, but, as in the case of compounds 1–3, the agonist effect in the MVD assay was only partly reversed by the  $\delta$ -receptor antagonist TIPP, indicating that it was mainly mediated by  $\mu$ -receptor activation. Thus, *N*-methylation of

TABLE 3  
Guinea pig ileum (GPI) and mouse vas deferens (MVD) bioassays of dermorphin analogues

No.	Compound	GPI		MVD		MVD/GPI IC <sub>50</sub> ratio
		IC <sub>50</sub> , nM <sup>a</sup>	Rel. potency <sup>b</sup>	IC <sub>50</sub> , nM <sup>a</sup>	Rel. potency <sup>b</sup>	
1	H-Tyr-MeAla-Phe-Gly-Tyr-Pro-Ser-NH <sub>2</sub>	16.7 ± 5.8	14.7 ± 5.1	50.2 ± 12.2 <sup>c</sup>	0.227 ± 0.055	3.0
2	H-Tyr-D-MeAla-Phe-Gly-Tyr-Pro-Ser-NH <sub>2</sub>	0.515 ± 0.020	478 ± 19	2.35 ± 0.48 <sup>c</sup>	4.84 ± 0.99	4.56
3	H-Tyr-Pro-Phe-Gly-Tyr-Pro-Ser-NH <sub>2</sub>	40.8 ± 4.1	6.02 ± 0.61	430 ± 111 <sup>c</sup>	0.0265 ± 0.0068	10.5
4	H-Tyr-D-Pro-Phe-Gly-Tyr-Pro-Ser-NH <sub>2</sub>	90000 (51%)		50000 (inactive)		–
5	H-Tyr-Pip-Phe-Gly-Tyr-Pro-Ser-NH <sub>2</sub>	5.14 ± 0.50	47.9 ± 4.7	48.1 ± 13.8	0.237 ± 0.068	9.36
6	H-Tyr-D-Pip-Phe-Gly-Tyr-Pro-Ser-NH <sub>2</sub>	7.32 ± 2.44	33.6 ± 11.2	37.6 ± 1.9	0.303 ± 0.0152	5.14
7	H-Tyr-Tic-Phe-Gly-Tyr-Pro-Ser-NH <sub>2</sub>	6000 <sup>d</sup>		antagonist		–
8	H-Tyr-Tic-Phe-Phe-Tyr-Pro-Ser-NH <sub>2</sub>	10000 (inactive)/antagonist		antagonist		–
9	H-Tyr-MePhe-Phe-Gly-Tyr-Pro-Ser-NH <sub>2</sub>	47.7 ± 2.2	5.16 ± 0.24	397 ± 59 <sup>c</sup>	0.0287 ± 0.00428	8.32
	H-Tyr-D-Ala-Phe-Gly-Tyr-Pro-Ser-NH <sub>2</sub>	3.3	74.5	29.0	0.393	8.79
	[Leu <sup>2</sup> ]enkephalin	246 ± 39	1	11.4 ± 1.1	1	0.0463

<sup>a</sup> Mean of three determinations ± SEM.

<sup>b</sup> Potencies relative to [Leu<sup>2</sup>]enkephalin.

<sup>c</sup> Effect not reversible with TIPP.

<sup>d</sup> Value represents the IC<sub>50</sub>.

## Dermorphin analogues

TABLE 4  
*K<sub>i</sub>*-values determined for  $\delta$ -antagonists against various  $\delta$ -agonists in the MVD assay

No.	Compound	<i>K<sub>i</sub></i> , nM <sup>a</sup>		
		[Leu <sup>5</sup> ]enkephalin	[D-Ala <sup>2</sup> ]deltorphan I	DPDPE
7	H-Tyr-Tic-Phe-Gly-Tyr-Pro-Ser-NH <sub>2</sub>	42.6 $\pm$ 3.7	38.9 $\pm$ 1.2	19.9 $\pm$ 5.93
8	H-Tyr-Tic-Phe-Phe-Tyr-Pro-Ser-NH <sub>2</sub>	4.70 $\pm$ 0.80	3.90 $\pm$ 1.48	2.90 $\pm$ 1.00
	H-Tyr-Tic-Phe-NH <sub>2</sub> (TIP-NH <sub>2</sub> ) <sup>b</sup>	43.9 $\pm$ 8.9	58.9 $\pm$ 7.7	98.6 $\pm$ 14.1
	H-Tyr-Tic-Phe-Phe (TIPP) <sup>b</sup>	5.86 $\pm$ 0.33	2.96 $\pm$ 0.02	4.80 $\pm$ 0.20

<sup>a</sup> Mean of 4–10 determinations  $\pm$  SEM.

<sup>b</sup> Ref. 18.

the L-Phe<sup>2</sup> residue of dermorphin produced a compound that bound to both  $\mu$  and  $\delta$ -receptors and was a  $\mu$ -agonist, as it had also been found to be the case when the analogous modification had been performed with the inactive tetrapeptide H-Tyr-Phe-Phe-NH<sub>2</sub> (18). As previously observed in studies on TIPP-related tetrapeptide analogues (18), these results demonstrate that the selectivity profile of opioid peptides can be drastically altered through introduction of local side-chain conformational constraints, such as achieved through replacement of MePhe with Tic.

The *in vivo* opioid activity profiles of the dermorphin analogues described in this paper indicate that the very low activity generally observed with peptides containing an L-amino acid residue in the 2-position of the peptide sequence can be drastically improved by *N*-methylation of that residue. Aside from the Tic<sup>2</sup>-containing analogues, which displayed high  $\delta$ -receptor selectivity, potent  $\delta$ -antagonism and partial  $\mu$ -agonist- (analogue 7) or weak  $\mu$ -antagonist- (analogue 8) activity, all compounds exhibited  $\mu$ -opioid receptor selectivity and  $\mu$ -opioid agonist activity in the GPI assay. Furthermore, the obtained results confirm the observations previously made with morphiceptin that the presence of a D-Pro<sup>2</sup> residue in these peptides is incompatible with the structural requirements of opioid receptors.

#### Evidence for conformational heterogeneity of dermorphin analogues

Dermorphin analogues 1–9 were studied by HPLC using different stationary phases. It has recently been demonstrated that HPLC analysis at low temperature can rapidly provide information about conformational heterogeneity of peptides, in particular with regard to the *cis-trans* isomerization of proline-containing peptides (11–15). The analytical runs performed with the dermorphin analogues at room temperature for purity control showed sharp single peaks in all cases and indicated a high degree of purity (> 98%) (Table 1). Similar results were obtained in chromatographic determinations on unmodified silica gel. Chromatographic runs on porous octadecyl silica with 5  $\mu$ m particle size showed a broadening of the peaks upon lowering of the

temperature and, finally, at  $-5^{\circ}\text{C}$  two major peaks, each containing a shoulder, became apparent (Fig. 1). This result was not too surprising because, owing to the presence of two proline or other *N*-alkylated amino-acid residues in the peptide sequence, the existence of four conformers arising from *cis-trans* isomerization around these amino-acid residues could be expected. The chromatographic pattern is in agreement with similar observations that had been reported for structurally related peptides (14, 15).

Better peak resolution was achieved by using columns packed with micropellicular octadecyl silica of 2  $\mu$ m particle size. This material has been reported to be a highly efficient stationary phase for peptide mapping, allowing high-speed separations (29, 30). Best

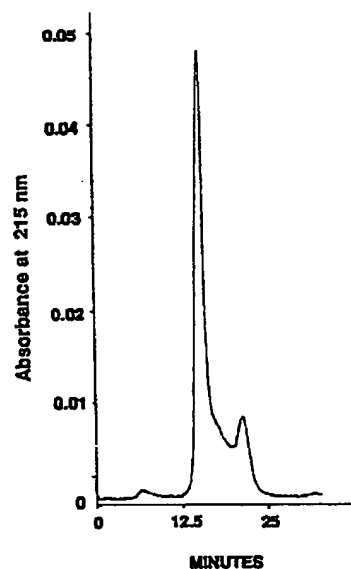


FIGURE 1

HPLC chromatogram of H-Tyr-D-McAla-Phe-Gly-Tyr-Pro-Ser-NH<sub>2</sub> (analogue 2) at  $-5^{\circ}\text{C}$ . Conditions: Ultrasphere ODS column (250  $\times$  4.6 mm, 5  $\mu$ m particle size); mobile phase 0.05 M KH<sub>2</sub>PO<sub>4</sub> pH 2.5/methanol (50:50, v/v), isocratic; flow rate 1.0 mL/min; sample size 10  $\mu$ g.

R. Schmidt *et al.*

peak separation was observed with analogue 7, which showed four separate peaks at  $-5^{\circ}\text{C}$ . These peaks most likely represent the four expected conformers (Fig. 2). Preliminary NMR experiments in  $\text{D}_2\text{O}$  at room temperature demonstrated the existence of four isomers of this compound, indicating that all of them are already present in solution and that their appearance is not induced by the interaction with the stationary phase. NMR studies performed with morphiceptin also had shown the presence of four slowly interconverting conformers (31). The all-*trans* isomer of morphiceptin could be unambiguously identified, and was found to be the most populated one (55%), whereas the second most abundant isomer (25%) was shown to contain a *cis* Tyr<sup>1</sup>-Pro<sup>2</sup> peptide bond. Furthermore, the exchange between these major conformers turned out to be slow on the NMR timescale. An assignment of the other two conformers was not possible. In another NMR study on  $\beta$ -casomorphin-5, all four possible isomers were identified as conformers arising from *cis-trans* isomerization around the two Xaa-Pro amide bonds (32). A low-temperature HPLC run of the *N*-terminal tetrapeptide segment of analogue 7, H-Tyr-Tic-Phe-Gly-OH, gave rise to two well separated peaks representing the two expected isomers. Furthermore, conformers with either a *cis* or a *trans* Tyr-Tic peptide bond were also observed in NMR experiments performed with H-Tyr-Tic-Phe-OH (unpublished results), and the existence of low-energy structures for both the *cis* and the *trans* isomer was also indicated by the results of molecular mechanics studies (33). On the basis of these findings it seems probable that the two major conformers of the

dermorphin analogues detected in the HPLC studies represent the *trans-trans* and the *cis-trans* isomers. A detailed description of the chromatographic separations and of the conformational analysis by NMR spectroscopy will be reported in a subsequent publication.

Whereas all analogues exhibited similar behavior under these chromatographic conditions, best peak separation was achieved with analogue 7. This observation could be explained by the kinetics of the *cis-trans* interconversion of the Tyr-Tic peptide bond, which may be slower than that in dermorphin analogues containing other *N*-alkylated amino acid residues for steric reasons owing to the presence of bulky aromatic side chains in positions 1, 2 and 3 of peptide 7. In all cases the existence of different conformers rather than the presence of impurities was established by peak collection and subsequent rechromatography of the separated peak material.

## CONCLUSIONS

The obtained structure-activity data indicate that *N*-methylation at the 2-position residue of the dermorphin peptide sequence produces potent analogues regardless of whether the 2-position residue has the D- or L-configuration. This result is of interest because dermorphin analogues containing a non-*N*-alkylated L-amino-acid residue at position 2 in general are only weakly active. Substitution of Pro for D-Ala<sup>2</sup> resulted in an analogue which turned out to be one of the most  $\mu$ -selective linear dermorphin analogues reported to date. On the other hand, replacement of D-Ala<sup>2</sup> in dermorphin with Tic turned a  $\mu$ -selective agonist into potent and highly selective  $\delta$ -antagonists (compounds 7 and 8), in analogy with observations that had originally been made with correspondingly modified dermorphin tetrapeptide analogues (18). The results obtained with analogues 7 and 8 support the assumption that the C-terminal peptide segment of dermorphin does not contribute to receptor selection (26) and that the Tic<sup>2</sup> residue plays a dominant role in directing the peptide to the  $\delta$ -receptor (18).

Low-temperature reversed-phase HPLC is a powerful method to demonstrate the existence of slowly interconverting conformers and to determine their relative populations. The chromatographic studies using various stationary phases revealed the presence of multiple conformations of the examined dermorphin analogues, most likely as a result of *cis-trans* isomerization around the two Tyr-L-(or D)-Xaa (Xaa = MeAla, Pro, Pip, MePhe, Tic) peptide bonds present in these molecules. Although all peptide analogues exhibited a similar chromatographic pattern, best peak separation was obtained for H-Tyr-Tic-Phe-Gly-Tyr-Pro-Ser-NH<sub>2</sub>, presumably as a consequence of a slowed-down *cis-trans* interconversion due to stacking interactions of the three aromatic rings present in the *N*-terminal tripeptide segment. Since the dominant conformers are assumed

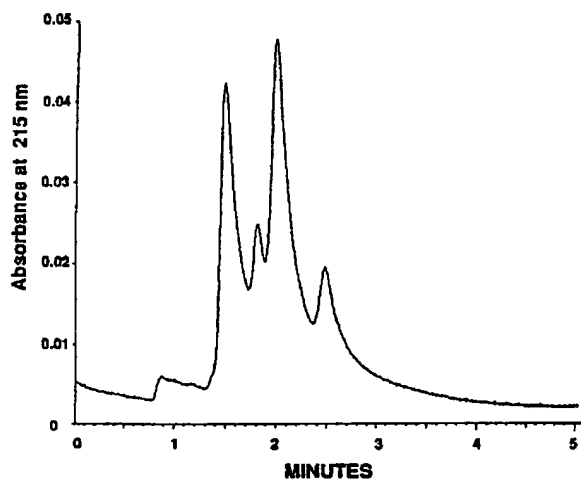


FIGURE 2

Separation of four isomers of H-Tyr-Tic-Phe-Gly-Tyr-Pro-Ser-NH<sub>2</sub> (analogue 7) by HPLC at  $-5^{\circ}\text{C}$ . Conditions: Pellicular ODS column (50  $\times$  4.6 mm, 2  $\mu\text{m}$  particle size); mobile phase 0.05 M  $\text{KH}_2\text{PO}_4$  pH 2.5/methanol (64:36, v/v), isocratic; flow rate 0.25 mL/min; sample size 10  $\mu\text{g}$ .

## Dermorphin analogues

to be the all-*trans* and the *cis-trans* conformers, these findings support the hypothesis previously proposed in the case of morphiceptin and its analogues that the activity displayed by opioid peptide analogues containing an *N*-alkylated L-amino acid residue in the 2-position may be attributed to the presence of a *cis* Tyr<sup>1</sup>-Xaa<sup>2</sup> amide bond in the bioactive conformation (10). Further efforts will be required to isolate and characterize the conformational isomers and to determine their opioid receptor binding profiles separately.

## EXPERIMENTAL PROCEDURES

**General methods.** TLC was performed on precoated silica gel plates 60F-254 (E. Merck, Darmstadt, Germany) in the following solvent systems (all v/v): (A) 1-BuOH/pyridine/AcOH/H<sub>2</sub>O (15/10/3/12), (B) 1-BuOH/AcOH/ethyl acetate/H<sub>2</sub>O (1/1/1/1) and (C) 2-BuOH/formic acid/H<sub>2</sub>O (75/15/20). Peptides were visualized with UV, ninhydrin spray reagent and KI/starch. The HPLC system GOLD (Beckman), consisting of the programmable solvent module 126 and the diode array detector module 168, was used for the purification and the purity control of the peptides. For the recording and quantification of the chromatograms the GOLD software was employed. A LiChrospher 100 RP-18e column (125 × 4 mm, 5 μm particle size) from E. Merck, Darmstadt, Germany, was used for all analytical characterizations. The solvents were of HPLC grade and were filtered and degassed prior to use. HPLC was carried out using a gradient made up from two solvents: (A) 0.1% TFA in water and (B) 0.1% TFA in acetonitrile. The analytical determinations were performed with a linear gradient of 20–50% B over a period of 25 min, absorptions being measured at both 216 and 280 nm (Table 1). Semipreparative reversed-phase HPLC was carried out on a LiChrospher 100 RP-18e column (250 × 25 mm, 10 μm particle size) or a Vydac 218TP1022 column (250 × 22 mm, 10 μm particle size) using the aforementioned solvent system and a linear gradient from 20–50% B over a period of 25 min at a flow rate of 12 mL/min. For amino acid analysis, peptides (0.2 mg) were hydrolyzed in 6 N HCl containing a small amount of phenol for 24 h at 110°C in deaerated tubes. The samples were analyzed after pre-column derivatization as PITC amino acids on a Supelco LC-18DB column (250 × 4 mm, 5 μm) at 245 nm (M. Boni, BioChem ImmunoSystems, Montreal, Quebec). Molecular weights of the peptides were determined by FAB mass spectrometry on a MS-50 HMTCTA mass spectrometer interfaced with a DS-90 data system (Drs. M. Evans and M. Bertrand, Department of Chemistry, University of Montreal). Proton NMR spectra of the purified peptides were recorded in DMSO-*d*<sub>6</sub> solution at 308 K a Varian VXR-400S spectrometer equipped with a Sun workstation. For all proton spectra nondegassed samples in 5 mm tubes were

used. Resonance assignments were made by analysis of the 1-D <sup>1</sup>H and 2-D H,H-COSY spectra (34).

**Peptide synthesis and purification.** Tic was synthesized as described elsewhere in detail (16). Boc-amino acids were purchased from Bachem Bioscience, Philadelphia, PA, and Sigma, St. Louis, MO. All solvents were of analytical grade and were used without further purification.

Peptide synthesis was performed by the manual solid-phase technique using a *p*-methylbenzhydrylamine resin (1% crosslinked, 100–200 mesh, 0.69 meq/g resin) obtained from Peninsula, Belmont, CA. The first Boc-amino acid was coupled to the neutralized resin using diisopropylcarbodiimide (DIC). All other Boc-protected amino acids were coupled with DIC and 1-hydroxybenzotriazole (HOBt) as coupling reagents. Side-chain protecting groups were Cl<sub>2</sub>-Bzl (Tyr) and O-benzyl (Ser).

The following steps were performed in each cycle: (1) addition of Boc-amino acid (2.5 equiv.) in CH<sub>2</sub>Cl<sub>2</sub>, (2) addition of HOBt (2.5 equiv.) and mixing for 1 min, (3) addition of DIC (2.5 equiv.) and mixing for 2–3 h, (4) washing alternately with CH<sub>2</sub>Cl<sub>2</sub> and DMF (4 × 2 min), (5) washing with EtOH (2 min), (6) monitoring completion of the reaction with the KAISER test, (7) Boc deprotection with 50% (v/v) TFA in CH<sub>2</sub>Cl<sub>2</sub> (30 min), (8) washing alternately with CH<sub>2</sub>Cl<sub>2</sub> and DMF (6 × 2 min), (9) neutralization with 10% (v/v) DIEA in CH<sub>2</sub>Cl<sub>2</sub> (2 × 5 min), (10) washing with CH<sub>2</sub>Cl<sub>2</sub> (3 × 2 min), EtOH (2 min) and CH<sub>2</sub>Cl<sub>2</sub> (2 × 2 min). Double-coupling of the tyrosine residue was necessary in case of the Tic containing analogues.

After final coupling of the *N*-terminal amino acid, steps (7)–(10) were carried out, followed by washings with MeOH and subsequent drying of the resin *in vacuo*. Peptides were cleaved from the resin by treatment with HF for 1 h at 0°C (20 mL HF plus 1 mL anisole/g resin). After evaporation of the HF, the resin was extracted three times with Et<sub>2</sub>O and, subsequently, with 7% acetic acid. The crude peptides were then obtained in solid form through lyophilization of the acetic acid extracts. The yields ranged between 60 and 70% (calculated on the basis of the initial resin capacity).

The crude peptides were desalted and purified by low-pressure reversed-phase chromatography (17) on LiChroprep RP-18 (40–63 μm particle size) (E. Merck, Darmstadt, Germany), using a linear gradient from 20–50% MeOH in 0.1% TFA (water). If necessary, further purification to homogeneity was achieved by semipreparative HPLC, as described in the General Section. Final products were obtained as lyophilisates. Homogeneity of the peptides was established by TLC in three different solvent systems, and by analytical HPLC under conditions identical with those described above (Table 1). The spectral analysis between 200 and 350 nm and the integration of the HPLC chromatograms observed at 215 and 280 nm indicated that the purity of

R. Schmidt *et al.*

all peptides was at least 98%. The structural identity of the purified peptides was confirmed by amino acid analysis, FAB mass spectrometry and  $^1\text{H}$ -NMR spectroscopy.

**Chromatographic studies.** The low-temperature HPLC studies were performed on an HP-1090 liquid chromatograph (Hewlett-Packard, Palo Alto, CA) equipped with a diode array detector and an autosampler. The column was thermostatted by using a Lauda K-2/RD constant temperature bath (Brinkmann, Westbury, NY). Chromatographic experiments were performed isocratically using 0.05 M  $\text{KH}_2\text{PO}_4$  (pH 2.5, adjusted with 60% orthophosphoric acid) as the mobile phase with varying amounts of methanol on porous octadecyl silica of 5  $\mu\text{m}$  particle size (Ultrapure ODS, Beckman, Fullerton, CA, and LiChrospher RP-18, E. Merck, Darmstadt, Germany, 250  $\times$  4.6 mm) and on columns (30, 50 or 105  $\times$  4.6 mm) packed with nonporous micropellicular octadecyl silica of 2  $\mu\text{m}$  particle size (29, 30). The normal-phase chromatography was performed on a silica gel column (50  $\times$  4.6 mm, 3  $\mu\text{m}$  particle size, Phase Separations Inc., Norwalk, CT), using isocratic mixtures of hexane/dichloromethane or chloroform at  $-10^\circ\text{C}$ . The solvent was filtered and degassed by helium purging. Samples were dissolved in water or the eluent and 20  $\mu\text{L}$  samples were injected. The column effluent went directly into the diode array detector without passing through the heat exchanger.

**Receptor binding assays and bioassays.** The opioid receptor binding assays were performed as reported in detail elsewhere (35). Binding affinities for the  $\mu$ - and  $\delta$ -opioid receptors were determined by displacing, respectively, [ $^3\text{H}$ ]DAMGO (Amersham) and [ $^3\text{H}$ ]DSLET (New England Nuclear) from rat brain membrane preparations. Incubations were performed for 2 h at  $0^\circ\text{C}$  with [ $^3\text{H}$ ]DAMGO and [ $^3\text{H}$ ]DSLET, at respective concentrations of 0.72 and 0.78 nM.  $\text{IC}_{50}$  values were obtained from the log dose-displacement curves, and  $K_i$ -values were calculated from the  $\text{IC}_{50}$  values by means of the equation of Cheng & Prusoff (36), using values of 1.3 and 2.6 nM for the dissociation constants of [ $^3\text{H}$ ]DAMGO and [ $^3\text{H}$ ]DSLET, respectively.

*In vitro* opioid activities of the compounds were tested in the GPI (37) and MVD (38) bioassays, as reported in detail elsewhere (35, 39). A log dose-response curve was determined with [Leu $^5$ ]enkephalin as standard for each ileum and vas preparation, and  $\text{IC}_{50}$  values of the compounds being tested were normalized according to a published procedure (40).  $K_e$ -values for the antagonists were determined from the ratio of  $\text{IC}_{50}$  values obtained in the presence and absence of a fixed antagonist concentration, as described in the literature (41). Antagonist concentrations used were as follows: naloxone, 5 nM; compound 7, 200 nM; compound 8, 1000 nM; (GPI assay), 10 nM (MVD assay); TIPP, 30 nM.

## ACKNOWLEDGMENT

This work was supported by operating grants from the Medical Research Council of Canada (Grant MT-5655), the National Institute on Drug Abuse (Grant DA-04443), the National Institutes of Health (Grant GM 20993), the US Public Health Service and the National Science Foundation (Grant BCS-9014119).

## REFERENCES

- DeCastiglione, R., Faoro, F., Piani, S., Perseo, G. & Piani, G. (1981) *Int. J. Peptide Protein Res.* **17**, 263-272
- Broccardo, M., Erspamer, V., Falconieri-Erspamer, G., Improta, G., Linari, G., Melchiorri, P. & Montecuccchi, P.C. (1981) *Br. J. Pharmacol.* **73**, 625-631
- Erspamer, V., Melchiorri, P., Falconieri-Erspamer, G., Negri, L., Corsi, R., Severini, C., Barra, D., Simmaco, M. & Kreil, G. (1989) *Proc. Natl. Acad. Sci. USA* **86**, 5188-5192
- Mor, A., Delfour, A., Sagan, S., Amiche, M., Pradelles, J., Rossier, J. & Nicolas, P. (1989) *FEBS Lett.* **255**, 269-274
- Chang, K.-J., Killian, A., Hazum, E. & Cuatrecasas, P. (1981) *Science* **212**, 75-77
- Amiche, M., Delfour, A. & Nicolas, P. (1988) *Int. J. Peptide Protein Res.* **32**, 28-34
- Giagoni, G., Mennuni, L., Pecora, N., Basilico, L., Parolaro, D. & Gori, E. (1987) *Pharmacol. Res. Commun.* **19**, 173-181
- Yamazaki, T., Ro, S. & Goodman, M. (1991) *Biochem. Biophys. Res. Commun.* **181**, 664-670
- Yamazaki, T., Pröbstl, A., Schiller, P.W. & Goodman, M. (1991) *Int. J. Peptide Protein Res.* **37**, 364-381
- Yamazaki, T., Ro, S., Goodman, M., Chung, N.N. & Schiller, P.W. (1993) *J. Med. Chem.* **39**, 708-719
- Jacobson, J., Melander, W., Vaisnys, G. & Horváth, C. (1984) *J. Phys. Chem.* **88**, 4536-4542
- Henderson, D.E. & Horváth, C. (1986) *J. Chromatogr.* **368**, 203-213
- Gesquiere, J.C. & Diesis, E. (1989) *J. Chromatogr.* **478**, 121-129
- Henderson, D.E. & Mello, J.A. (1990) *J. Chromatogr.* **499**, 79-88
- Dalaet, N., Elseviers, M., Tourwé, D. & Van Binst, G. (1990) in *Innovations and Perspectives in Solid Phase Synthesis* (Epton, R., ed.) pp. 472-480, SPCC, Birmingham.
- Schiller, P.W., Weltrowska, G., Nguyen, T.M.-D., Lemieux, C., Chung, N.N., Marsden, B.J. & Wilkes, B.C. (1991) *J. Med. Chem.* **34**, 3125-3132
- Böhlen, P., Castillo, F., Ling, N. & Guillemin, R. (1980) *Int. J. Peptide Protein Res.* **16**, 306-310
- Schiller, P.W., Nguyen, T.M.-D., Weltrowska, G., Wilkes, B.C., Marsden, B.J., Lemieux, C. & Chung, N.N. (1992) *Proc. Natl. Acad. Sci. USA* **89**, 11871-11875
- Lord, J.A.H., Waterfield, A.A., Hughes, J. & Kosterlitz, H.W. (1977) *Nature (London)* **267**, 495-499
- Liebmann, C., Schnittler, M., Hartrodt, B., Born, I. & Neubert, K. (1991) *Pharmazie* **46**, 345-351
- Charpentier, S., Sagan, S., Delfour, A. & Nicolas, P. (1991) *Biochem. Biophys. Res. Commun.* **179**, 1161-1168
- Brandt, W., Barth, A. & Hölte, H.-D. (1994) In  *$\beta$ -Casomorphins and Related Peptides: Recent Developments* (Brantl, V.J. & Teschemacher, H., eds.) pp. 93-105, VCH Publishers, Weinheim
- Schmidt, R., Chung, N.N., Lemieux, C. & Schiller, P.W. (1994) *Regulatory Peptides* **54**, 259-260
- Tancredi, T., Salvadori, S., Amodeo, P., Picone, D., Lazarus, L.H., Bryant, S.D., Guerrini, R., Marzola, G. & Temussi, P.A. (1994) *Eur. J. Biochem.* **224**, 241-247

## Dermorphin analogues

25. Schmidt, R., Vogel, D., Mrestani-Klaus, C., Brandt, W., Neubert, K., Chung, N.N., Lemieux, C. & Schiller, P.W. (1994) *J. Med. Chem.* **37**, 1136-1144
26. Sagan, S., Amiche, M., Delfour, A., Camus, A., Mor, A. & Nicolas, P. (1989) *Biochem. Biophys. Res. Commun.* **163**, 726-732
27. Schiller, P.W., Nguyen, T.M.-D., Chung, N.N. & Lemieux, C. (1989) *J. Med. Chem.* **32**, 698-703
28. Schiller, P.W., Nguyen, T.M.-D., Berezowska, I., Weltrowska, G., Schmidt, R., Marsden, B.J., Wilkes, B.C., Lemieux, C. & Chung, N.N. (1993) In *Peptide Chemistry 1992 (Proc. 2nd Jpn. Symp. Peptide Chem.)* (Sakakibara, S., ed.) pp. 337-340, ESCOM Science Publishers, Leiden, The Netherlands
29. Khaghatgi, K. & Horváth, C. (1988) *J. Chromatogr.* **443**, 343-354
30. Khaghatgi, K. (1990) *J. Chromatogr.* **499**, 267-278
31. Goodman, M. & Mierke, D.F. (1989) *J. Am. Chem. Soc.* **111**, 3489-3496
32. Delaet, N.C.J., Verheyen, P.M.F., Tourwé, D. & Van Binst, G. (1991) *Biopolymers* **31**, 1409-1417
33. Wilkes, B.C. & Schiller, P.W. (1994) *Biopolymers*, **34**, 1213-1219
34. Aue, W.P., Bartholdi, E. & Ernst, R.R. (1976) *J. Chem. Phys.* **64**, 2229-2246
35. Schiller, P.W., Lipton, A., Horrobin, D.F. & Bodanszky, M. (1978) *Biochem. Biophys. Res. Commun.* **85**, 1332-1338
36. Cheng, Y.C. & Prusoff, W.H. (1973) *Biochem. Pharmacol.* **22**, 3099-3102
37. Paton, W.D.M. (1957) *Br. J. Pharmacol.* **12**, 119-127
38. Henderson, G., Hughes, J. & Kosterlitz, H.W. (1972) *Br. J. Pharmacol.* **46**, 764-766
39. DiMaio, J., Nguyen, T.M.-D., Lemieux, C. & Schiller, P.W. (1982) *J. Med. Chem.* **25**, 1432-1438
40. Waterfield, A.A., Leslie, F.M., Lord, J.A.H., Ling, N. & Kosterlitz, H.W. (1979) *Eur. J. Pharmacol.* **58**, 11-18
41. Kosterlitz, H.W. & Watt, A.J. (1968) *Br. J. Pharmacol.* **33**, 266-276

## Address:

Dr. Peter W. Schiller  
Laboratory of Chemical Biology and Peptide Research  
Clinical Research Institute of Montreal  
110 Pine Avenue, West  
Montreal, Quebec  
Canada H2W 1R7

**THIS PAGE BLANK (USPTO)**

**This Page is Inserted by IFW Indexing and Scanning  
Operations and is not part of the Official Record**

**BEST AVAILABLE IMAGES**

Defective images within this document are accurate representations of the original documents submitted by the applicant.

Defects in the images include but are not limited to the items checked:

☒ **BLACK BORDERS**

☐ **IMAGE CUT OFF AT TOP, BOTTOM OR SIDES**

☐ **FADED TEXT OR DRAWING**

☐ **BLURRED OR ILLEGIBLE TEXT OR DRAWING**

☐ **SKEWED/SLANTED IMAGES**

☐ **COLOR OR BLACK AND WHITE PHOTOGRAPHS**

☐ **GRAY SCALE DOCUMENTS**

☐ **LINES OR MARKS ON ORIGINAL DOCUMENT**

☐ **REFERENCE(S) OR EXHIBIT(S) SUBMITTED ARE POOR QUALITY**

☐ **OTHER:** \_\_\_\_\_

**IMAGES ARE BEST AVAILABLE COPY.**

**As rescanning these documents will not correct the image problems checked, please do not report these problems to the IFW Image Problem Mailbox.**